

10th INTERNATIONAL
100% RENEWABLE
ENERGY CONFERENCE



IRENEC 2020
PROCEEDINGS
4 - 6 JUNE 2020

RENEWABLE ENERGY
ASSOCIATION



Editors

Tanay Sıdkı Uyar

Alper Saydam

Publishing Date July 2020

ISBN 978-605-62511-6-0

Copyright © 2020 Renewable Energy Association of Turkey (EUROSOLAR Turkey)

All rights reserved. No part of this book may be reproduced in any form or by any electronic or mechanical means, including information storage and retrieval systems, without permission in writing from the publisher.

No responsibility is assumed by the publisher for any injury and/or damage to persons or property as a matter of products liability, negligence or otherwise or from any use or operation of methods, products, instructions or ideas contained in the material here in.

Dear Participants,

In our journey of promoting 100% Renewable Energy, we have arrived the 10th stop where we shall again share our research results and other achievements.

Every day we are discovering and practicing the good quality of renewable energies. The genie is out of the bottle. It is time to use the good quality of human beings to guide this opportunity effectively to the destination. The qualities of human beings can play its role if the individuals and countries talk together and define problems correctly and find solutions that can be implemented.

Renewable energy resources at each corner of the atmosphere are ready to be converted to electricity and process heat locally when needed. Kinetic energy of the moving air, chemical energy stored in biomass, heat and light of the sun and geothermal resources are available all over our planet earth free of charge. As the main energy source of living space on earth, sun and its derivatives were available before, are available today and will be available in the future.

Global support provided for the renewable energy made the market penetration of renewables possible. Today wind and solar energy became the cheapest way of producing electricity in many parts of the World.

Cities and countries who are trying to reach 100% renewable energy mix are working on preparing the infrastructure necessary to be able to supply more renewable energy for industry, transportation and buildings by smart grids and renewable energy storage systems.

Since renewable energy is available at every corner of our atmosphere, Community Power (the involvement of the local people individually or through their cooperatives and municipalities in the decision making process and ownership of their energy production facilities) is becoming the most effective approach for transition to 100% renewable energy future.

During IRENEC 2020 we shall share and learn from the global experiences on difficulties, barriers, opportunities and solutions for transition to 100 % renewable energy societies and make our contribution to Global Transition to 100% Renewable Energy.

Best Regards,

Tanay Sıdkı Uyar

Conference Chair, IRENEC 2020

President, Renewable Energy Association of Turkey

(EUROSOLAR Turkey)



Tanay Sıdkı Uyar

Conference Chair,
IRENEC 2020

**RENEWABLE ENERGY
ASSOCIATION**

**EURO
SOLAR** **EUROSOLAR
Turkey**

Organization

Organizing Committee

Conference Chair

Tanay Sıdkı Uyar

President, EUROSOLAR Turkey, TR

Conference Co-Chairs

İbrahim Dinçer

University of Ontario Institute of Technology, CA

Remigijus Lapinskas

President of World Bioenergy Association, LT

Wolfgang Palz

EU Commission Official (ret.)

Şener Oktik

ŞİŞECAM Chief Research & Technological Development Officer

Hasan Heperkan

Professor in Mechanical Engineering, İstanbul Aydın University, TR

Local Organizing Committee (Administrative)

Başak Gündüz

Serdar Tan

Işıl Uyar

Local Organizing Committee (Academic)

Alper Saydam

Doğancan Beşikci

Tanay Sıdkı Uyar

Program Committee (Research Papers)

Çetinkaya, Hasan Basri	Power System Consulting Senior Key Expert, Siemens, TR
Beşikci, Doğançan	Marmara University, TR
Yılmaz, Fatih	NDU Turkish Naval Academy, TR
Sarı, Alperen	Marmara University, TR
Köker, Utku	Suleyman Demirel University, TR
Leblebicioğlu, Emre	Marmara University, TR
Arıncı, Burak	Yildiz Technical University, TR
Karahan, Fahri	Queen Mary University, UK
Kon, Okan	Balikesir University, TR
Caner, İsmail	Balikesir University, TR
Adebayo, Victor Oluwatobi	Cyprus International University, CY
Öztaş, Hazal	Gazi University, TR
Şahin, Doğa	Gazi University, TR
Mert, Ülkem Onur	Cyprus International University, CY
Adun, Humphrey	Cyprus International University, CY
Akkaya, Mustafa Anıl	Yeditepe University, TR
Onat, Tuba Artan	Niğde Ömer Halisdemir University, TR
Şahin, Ali	Marmara University, TR

Scientific Advisory Committee

Andrew Lang	Senior Consultant, World Bioenergy Association
Assoc. Prof. Dr. Bilal Gümüş	Dicle University, Turkey
Assoc. Prof. Dr. Egemen Sulukan	National Defence University, Turkish Naval Academy
Stefan Gsänger	Secretary General, World Wind Energy Association
Prof. Dr. Hasan Heperkan	İstanbul Aydın University, Turkey
Dr. Yusuf Bicer	Hamad Bin Khalifa University, Qatar

Contents

Full Research Papers

Importance of Energy Storage Systems in Future Energy Infrastructure and Critical Application Areas	3
<i>Hasan Basri Cetinkaya, Panagiotis Stamoulis</i>	
Effects of 100% Renewable Implementation Costs and Energy in Burdur	12
<i>Doğancan Beşikci, Egemen Sulukan, Tanay Sıdkı Uyar</i>	
Energy System Analysis and Modeling of an Electric-Powered Ferry	20
<i>Fatih Yılmaz, Egemen Sulukan, Doğuş Özkan, Tanay Sıdkı Uyar</i>	
Calculation of Wind Turbine Installation on a University Campus via Windsim	27
<i>Alperen Sari, Egemen Sulukan, Doğuş Özkan, Tanay Sıdkı Uyar</i>	
Hourly Optimization of Electricity Generation in City Scale	39
<i>Utku Köker, Halil İbrahim Koruca, Egemen Sulukan, Tanay Sıdkı Uyar</i>	
An Onshore Wind Farm Design in Büyükada via WindSim	50
<i>Emre Leblebicioğlu, Tanay Sıdkı Uyar</i>	
Integrating Wind Energy to Smart Grids.....	61
<i>Burak Arıncı</i>	
Increasing of Binary ORC Geothermal Power Plant Efficiency by A Geothermal-Solar Hybrid Design	68
<i>Fahri Karahan, Füsün Tut Haklıdır</i>	
Investigation the Effects of Reducing Heat Transfer Coefficients of Building Envelope on Global Warming in Turkey	74
<i>Okan Kon, İsmail Caner</i>	
Renewable Energy Consumption Due to Internal Gas Gap Thickness in Buildings' Windows.....	94
<i>Okan Kon, İsmail Caner</i>	
An Approach to A Better Transition to Sustainable Transportation System: Case Study of Three Cities (Abuja, Kumasi & Erbil).....	110
<i>Victor Oluwatobi Adebayo, Prince Tettey, Nabaz Rasool, Tanay Sidki Uyar</i>	

Production of Hydrogen-Rich Syngas in a Fluidized Bed	133
<i>Hazal Öztan, Duygu Uysal Ziraman, Özkan Murat Doğan, Bekir Zühtü Uysal</i>	
Glycerin as a Heat Transfer Fluid in Solar-Organic Rankine Cycle	143
<i>Doğa Şahin, Duygu Uysal Ziraman, Özkan Murat Doğan, Bekir Zühtü Uysal</i>	
Integration of Renewables in Turkish Republic of Northern Cyprus.....	155
<i>Ülkem Onur Mert, Tanay Sıdkı Uyar</i>	
Multivariate Based Modelling of Solar Energy Growth: A Discussion of Relevant Factors Influencing African Solar Energy Development	163
<i>Humphrey Adun, Michael Adedeji, Tonderai Ruwa, and Mustafa Dagbasi</i>	
The Evolution of Feed in Tariff Mechanism Towards Feed in Premium Mecha- nism	177
<i>Mustafa Anıl Akkaya, Murat Onuk</i>	
The Effect of Molasses Concentration on Voltage Generation.....	184
<i>Tuba Artan Onat</i>	
The Wind Farm Design Optimizing for Pendik Sabiha Gokcen Region	195
<i>Ali Şahin, Tanay Sıdkı Uyar</i>	

Importance of Energy Storage Systems in Future Energy Infrastructure and Critical Application Areas

Hasan Basri Cetinkaya¹ and Panagiotis Stamoulis²

¹ Smart Infrastructure / Digital Grid, SIEMENS A.S, Istanbul, Turkey
hasan.cetinkaya@siemens.com

² Portfolio Professional, FLUENCE ENERGY, Erlangen, Germany
panagiotis.stamoulis@fluenceenergy.com

Abstract. Energy infrastructure will be transformed into a whole new order. The main reason for this new order is that climate change has reached a very dangerous level. This danger has made renewable energy a necessity, not a choice. In this arrangement, the existing control and protection structure will not be sufficient. Energy Storage Systems (ESS) will play a critical role in sustaining this new structure and providing a secure and economical energy. In recent years, reductions in the costs of energy storage systems have made it possible to use this technology. However, in a power system where wind and solar energy are integrated, energy storage will not be an option but will be a technical necessity. This requirement will manifest itself in every field. Energy storage systems have different uses in energy transmission systems, energy distribution systems and industry.

The purpose of this paper is to express the maximum benefit that energy storage systems can generate in related areas and in some cases, demonstrating this benefit with the help of power system analyses and site measurements. The results are clearly showing that Energy Storage systems will play a very critical role in transition to 100% Renewable Energy.

Keywords: Energy storage, power system analysis, measurements, transmission, distribution, industrial

1 Introduction

The transition of electrical energy to renewables continues rapidly. This transition causes different operational difficulties in energy generation, transmission and distribution, and requires faster and automatic control of energy quality. At this point, energy storage systems offer the technology that makes all these problems manageable. Just like in wind and solar power plants, it will be expected from the energy storage systems to have similar responses to conventional power plants. Depending on the bidirectional inverter system structures and fast response times, it is estimated that unique features will be expected from energy storage systems.

In the energy structure of the future, energy storage systems will not manifest themselves in just one area. They will be integrating to transmission system to com-

compensate rapid power and voltage changes that may occur in renewable energy integrations. They can also be used to help frequency regulation during severe faults. In distribution systems they can be used to regulate the fast and high voltage changes that will occur in high amount of renewable energy integration at the end of feeders, and to enable Microgrids for an uninterruptible supply. The industrial plants have goals of being a carbon neutral company. In order to achieve this goal and in order to contribute to clean energy, they are also planning to use storage systems together with renewables, in order to eliminate fluctuating power at point of coupling to the grid. For industrial plants, renewable may also be integrated without the necessity of meeting the grid regulations and can be within the framework of “Unlicensed Energy Generation Regulations”. In that case, all energy produced by renewables should be consumed in the plant.

The benefits of using energy storage systems for transmission and distribution systems have been investigated in many studies [1]. Since energy storage systems have the ability to reduce peak load, it is known that they can create significant decreases in energy costs. Especially for diesel generators used in the islands, they can be an excellent alternative with renewable energy systems [2, 3]. The price of lithium-ion batteries has fallen by about 80% over the past five years [4]. This puts energy storage systems in a feasible position. We can expect them to be included in our entire energy system at a rate similar to the integration speed that occurs in renewable energy. The cost of different type of storage systems and performance characterization are also investigated in some studies [5]. Energy storage systems provide tools to overcome the technical and economic obstacles pursued in the wide-ranging integration of sustainable energy sources [6].

2 Energy Storage Systems

Energy Storage Systems will have a very important role in the energy structure of the future. It can be considered as a large-scale battery with full control, with X MVA power, capable of providing X MW or X MVAR very quickly, with control modes that can vary according to requirements. It can address transmission, distribution system and industrial facilities. It is irreplaceable for more renewable integration. Compared to conventional generators, they offer a much wider range of working area for the same amount of power.

They have many critical application areas such as; Integration of renewables, offset-diesel generation & islands, T&D expansion deferral, frequency regulation, peak-load management, power quality and critical power for industrial plants. They have also additional benefits like; Maintaining adequate spinning reserve to ensure grid N-1 reliability, maximizing renewable generation with DC-coupled Energy Storage, ensuring digital inertia, minimizing energy costs and optimizing Microgrids.

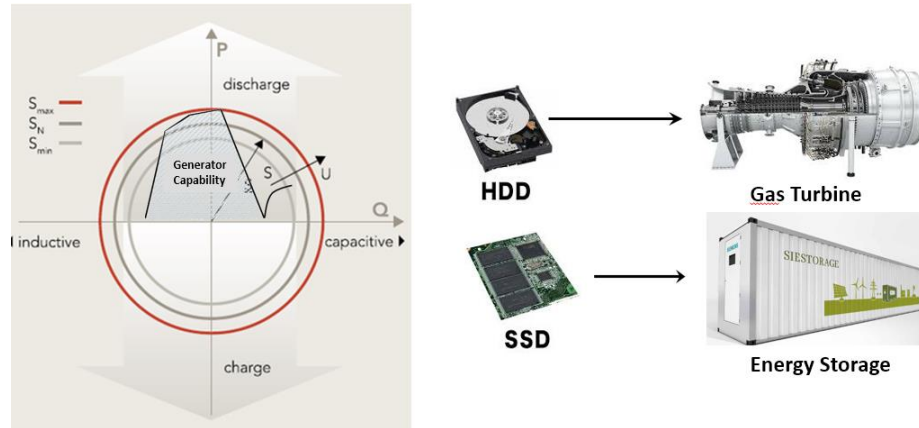


Fig. 1. Comparison of working structures and working area of Energy Storage Systems and Conventional Power Generation units.

3 Transmission System Applications

It is reported in the IEC documents that high capacity energy storage systems will be needed in the case of high integration of renewable energy [7]. Especially when replacing conventional power plants, because source is fluctuating, there will be more rapid changes in load flow. This impairs the smoothness of the power. Energy Storage systems will be compulsory system component to increase harmony and smoothness with renewable energy generation.

Beside this, the grid function can be better if you take a leading-edge resource like battery-based energy storage and make it 60 times for responsive than current standard and 2000 times more responsive than traditional flexible power generation [8]. This is what today's advanced energy storage systems can do. This is also a requirement and not a choice, since grids are increasingly dominated by renewables with fluctuating outputs. The response time may reach to 150 ms [9]. The human eye takes around 300-400 ms to blink, meaning this response is unusually fast, even for batteries – quite literally addressing a drop in frequency faster than the blink of an eye.

Many TSOs are already experiencing curtailment of solar and/or wind generation in part because of a lack of system stability. In transmission systems an electrical storage system can be used in many ways like, fast frequency response, primary operating reserve, secondary operating reserve, steady state reactive power, fast reactive power support. Batteries can be 'turned up' when needed. By responding more aggressively to faults, and at full power output, batteries reduce curtailment – allowing renewable generation to replace more conventional generation.

There exist numerous examples for Energy Storage Plan in Transmission Systems. One of the large capacity examples is called "Grid Booster" in Germany (TransnetBW). Large amounts of renewable electricity must be transmitted from the north and east to the south and west. If the generated electricity exceeds line capacities, the four German transmission system operators (TSOs) have to perform costly redispatch measures. The grid infrastructure clearly needs expansion, for which the four German transmission system operators (TSOs) have conceived the "Network Development Plan (NDP) 2030 [9]. To minimize the need for grid exten-

sion and cut redispatch costs, the NDP includes innovations that could result from technological progress in the coming years. In addition to Power-to-X and monitoring systems, prototypes of so-called grid boosters are also considered. The concept includes a fast power source in the shape of a large battery at the end of a line section that is subject to frequent strain and overload. The booster battery can supply energy within a few seconds. In periods of high grid load, the booster is intended to relieve the system in case of disturbances until the bottleneck can be eliminated in a targeted manner by the system management [9].

In transmission systems, large centralized power plants may need to have faster ramp rates, lower minimum generation levels, and fewer starts and stops. They will also require grid services such as spinning reserve and frequency regulation to stabilize the grid. Black start in the event of a grid failure is also crucial. Lower emissions rates, reduced balance of plant, interconnection, and operating and maintenance costs are also required. These all can be achievable with Energy Storage Systems. Energy Storage Systems can also create Synthetic (Digital) Inertia which improves frequency response or Rate of Change response or a combination of both forms (step response). In 2016, the System Operators (SOs) in the Island of Ireland (Eirgrid and SONI) undertook a major study reviewing the ability of synthetic inertia to help keep RoCoF within manageable levels. Their report outlined key requirements for synthetic inertia providers. QUB's research and international operational battery experience demonstrates that batteries can meet all requirements which include fast response, fast ramp-up and smooth recovery. Batteries can be 'turned up' when needed. By responding more aggressively to faults, and at full power output, batteries reduce curtailment and allowing renewable generation to replace more conventional generation. In an environment where renewable energy is highly integrated, energy storage will not be an option, but a necessity

4 Distribution System Applications

In distribution grid, significant amount of distributed generation is expected to be integrated in upcoming years. Distribution networks are not designed with these generation units in mind. It is known that these generation will create serious fluctuations in voltage according to the maximum power values, the line cross section and the distance to which related power is transmitted. In addition, this can possibly create serious flicker issues in the system. Therefore, stabilizing the power on the source side will solve many problems. This can be possible with the use of Energy Storage Systems together.

A renewable generation, together with an ESS will have a smoother generation profile, less oscillation and less negative impact. The ESS can also be used as a fast acting reactive power source in order to prevent voltage limits from being exceeded [10].

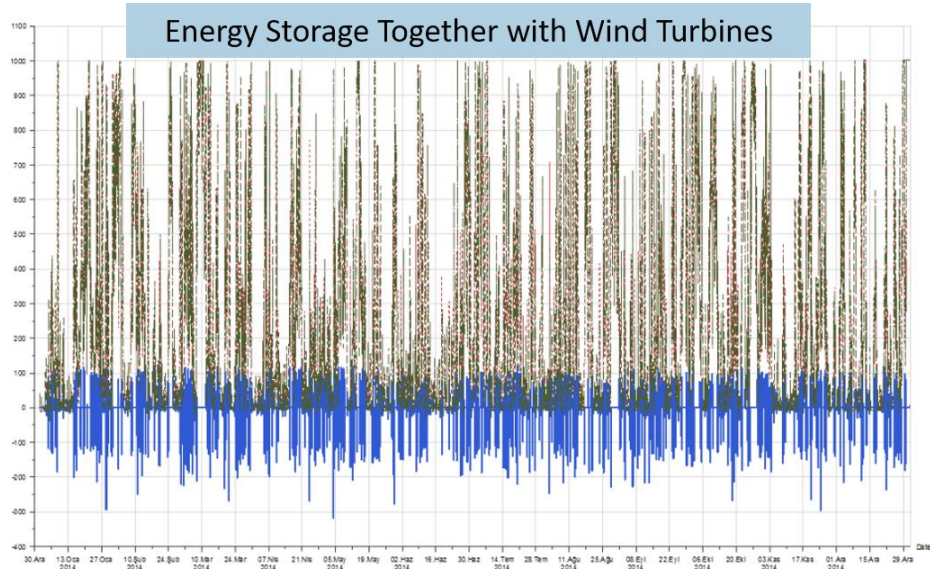


Fig. 2. Power variations in the use of the energy storage system (20%) with renewable energy generation (Blue lines are showing charging and discharging of energy storage system)

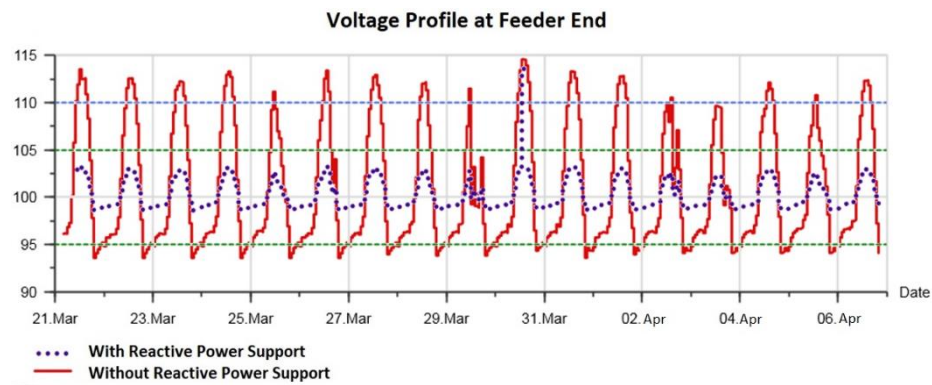


Fig. 3. Voltage profile of a feeder where a large amount of distributed generation is connected

5 Island Applications

Energy storage systems are unrivaled in terms of cost with their applications on the islands. Mainly, diesel generators are used for electricity on islands that are not connected to the national grid. Their operating efficiency are low, fuel costs are high. Optimum economy can be achieved when energy storage systems are used together with diesel generator sets and renewable energy. In that case, there will be less curtailment in renewable generation, costs will be reduced (reducing diesel generator sets usage) and more clean energy can be used. When engines can operate steadily at maximum power, the operating efficiency can be maximized and CO₂ and No_x emissions can be reduced. The measurements taken in the installed systems reveal that this type of structure is more successful in frequency and voltage stability during severe conditions (see Fig. 4) [11].

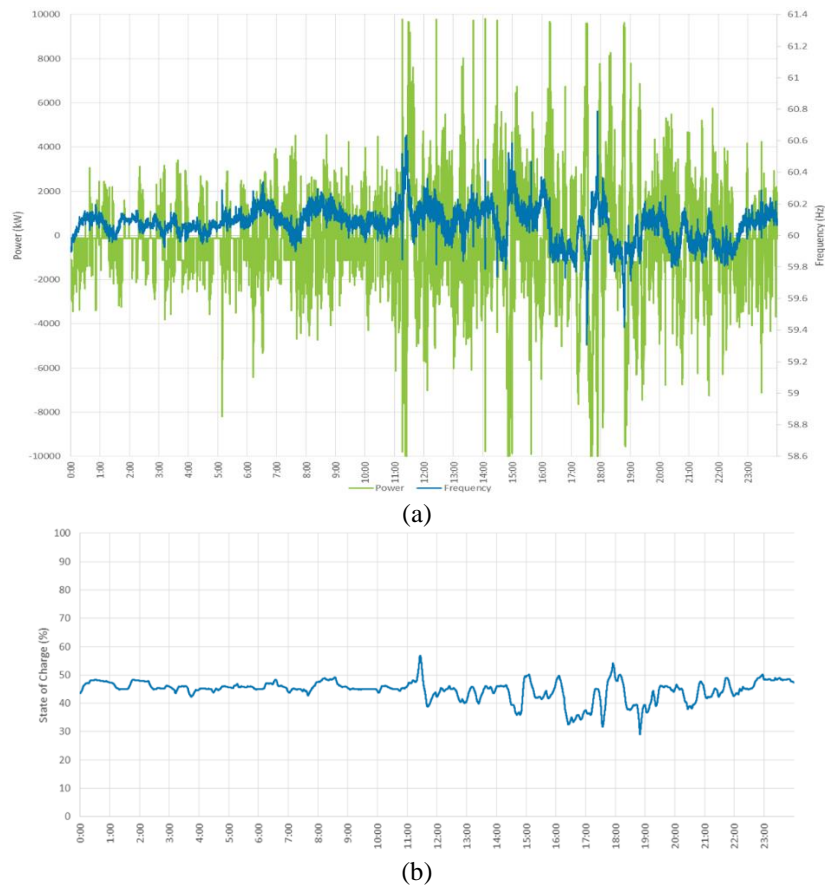


Fig. 4. (a) Power and frequency deviations of island grid, (b) charging & discharging actions of an ESS during Hurricane Irma

6 Industrial Applications

For an industrial facility, energy storage can mean a lot. These benefits include, critical power, volt-var, frequency stabilizing and black-start supports. In order not to facing a complete shutdown of a critical plant, a storage system can be a very good source of power to feed the critical processes during a severe fault. Because energy storage systems do not have a rotating element, there will be no mechanical strains during and after a fault. Energy storage systems can support voltage during faults in addition to conventional generators. They can also support motor startups with its fast-activated reactive power output. At the time of a conventional generator loss, they can support frequency recovery, they can give more time to load shedding to activate, even in some cases eliminating load shedding. Energy storage systems can make a quick start during a black-start procedure and they may eliminate production loss and speed up the entire proses start action.

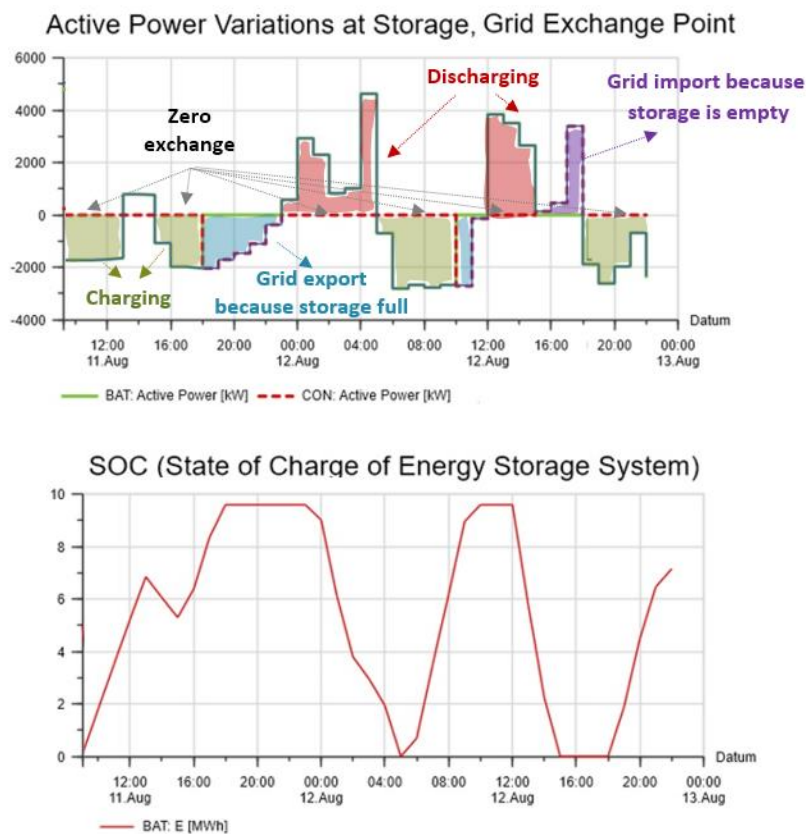


Fig. 5. Energy storage system operation & state of charge level in an industrial facility targeting zero power exchange at the point of coupling

Industrial plants would also like to integrate renewables without the necessity of meeting the grid regulation and will be within the framework of the unlicensed generation regulation. In that case, all the energy generated from renewables should be consumed in the plant. The structure should be configured according to that principle [12]. A philosophy should be established such that the power exchange with the grid is "0" at the relevant location, or no power flow to the grid side at all (see Fig.5) [12].

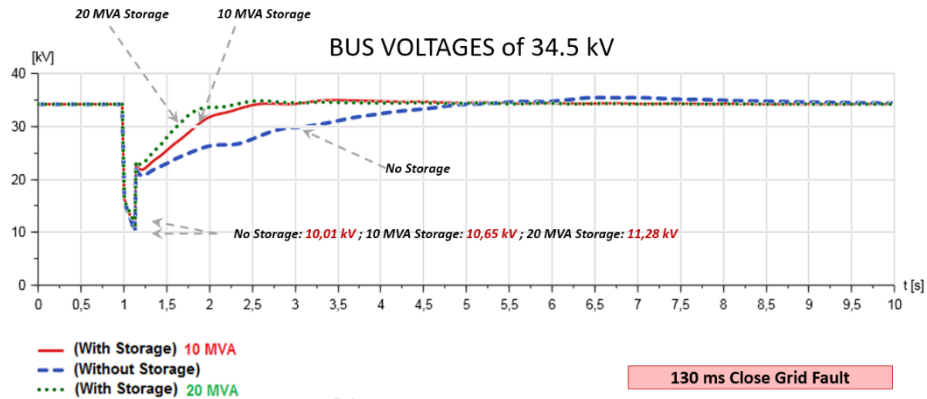


Fig. 6. Voltage recovery after a fault w/wo energy storage in an industrial facility

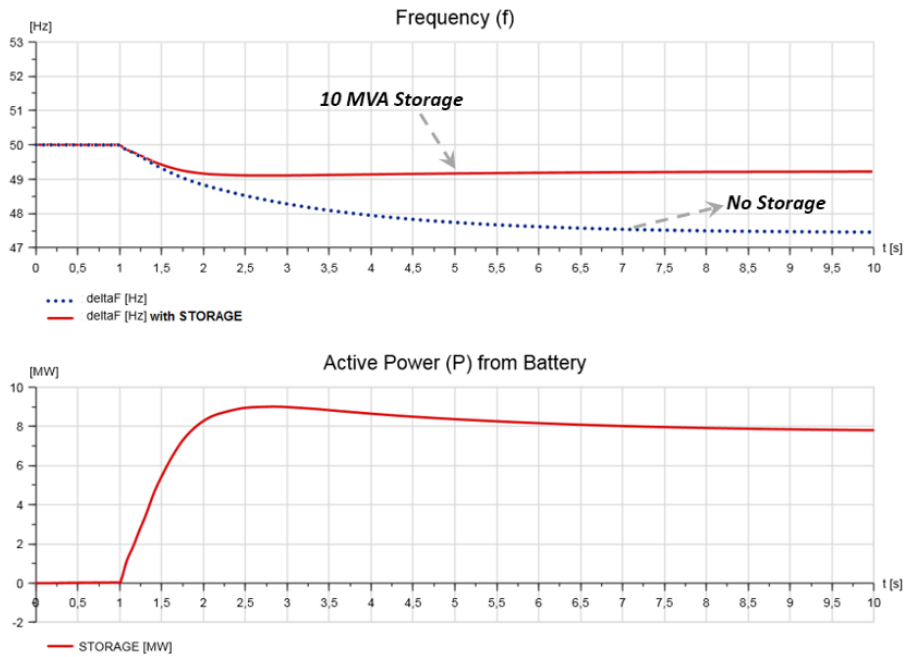


Fig. 7. Frequency recovery after a generator trip in an industrial plant in island mode

7 Conclusion

In this study, the benefits of energy storage systems have been examined and these benefits have been tried to be revealed by field measurements and power system analysis. It is clear that, energy storage systems will play a crucial role in the entire energy structure of the future for economical optimization and eliminating the negative effects of renewable energy integrations. Energy storage seems to be not an option, but a technical necessity.

References

1. M.Z. Erel, E. Bektas, Y.Yalman, K.Bayindir, "A Review of Battery Energy Storage Applications for Transmission and Distributed Grids", II.International Scientific and Vocational Studies Congress, BILMESS, October (2018).
2. P.Blechingner, R.Seguín, C.Cader, P.Bertheau, Ch.Breyer, "Assesment of the Global Potential for Renewable Energy Storage Systems on Small Islands", 8th International Renewable Energy Storage Conference and Exhibition, IRES 2013, Energy Procedia 46 (2014) 325 – 331, ScienceDirect, DOI:10.1016/j.egypro.2015.01.071, Published by Elsevier Ltd. (2013)
3. IRENA, Electricity Storage and Renewables for Island Power – A guide for desicion makers, May (2012).
4. <https://www.nrel.gov/news/features/2020/declining-renewable-costs-drive-focus-on-energy-storage.html>, 02 Jan (2020), last accessed 2020/06/01
5. Energy Storage Technology and Cost Characterization Report, July 2019, HydroWires, U.S Department of energy (2019)
6. Nynke Verhaegh, Petra de Boer, "Growders: Demonstration of Grid Connected Electricity Storage Systems, January (2011)
7. IEC Whitepaper, "Grid integration of large-capacity Renewable Energy sources and use of large-capacity Electrical Energy Storage", (2011)
8. White Paper by FLUENCE, "The Need for Speed – Supporting Rapid Decarbonization with the World's Fastest Grid-Scale Battery", WP-007-01-EN, (2020)
9. <https://www.tscnet.eu/transnetbws-grid-booster-confirmed/> 22 Dec (2019), last accessed 2020/06/01
10. H. B. Cetinkaya, Energy Market Regulatory Authority (EMRA) / Research and Development Project - Determination of Connection Criteria of Generation Facilities to Distribution Network (2018)
11. Case Study, Storm Resilience, "Energy Storage Provides Grid Resilience During Severe Storm Conditions in the Dominican Republic", Fluence Energy, (2018).
12. H. B. Cetinkaya, B. Kurucay, P. Stamoulis, O. Erisik, T.Turhan, M.Ozkan, E.Ozderli, "A Case Study on the use of Energy Storage in Industrial Plants with a Renewable Energy Plan", ICEEE 2020, 7th International Conference On Electrical And Electronics Engineering, (2020)

Effects of 100% Renewable Implementation Costs and Energy in Burdur

Doğancan Beşikci¹, Egemen Sulukan², Tanay Sıdkı Uyar³

¹Friterm A.Ş., Tuzla, İstanbul

² Mechanical Engineering Department/ National Defence University
Tuzla-Istanbul, 34942, Turkey.

³ Mechanical Engineering Department/ Marmara University
Kadıköy-Istanbul, 34722, Turkey

dogancanbesikci@friterm.com, esulukan@dho.edu.tr,
tanayuyar@marmara.edu.tr

Abstract. The transformation from fossil to renewable in energy production is increasing every year, accelerating with technological developments and the damage caused by the changing climate. This transformation, which is carried out by energy producing companies, has started to be included in the countries' own road maps. Thus, in this renewable energy-centered transformation, countries include these resources in their long-term strategic plans. Thus, they first contribute to preventing climate change and then reducing their countries' dependence on foreign energy. Countries use current scientific methods to determine road maps. One of the most important methods in this process is the energy modeling system. In this system, countries or local governments can measure the impact of beneficial technologies such as renewable or harmful technologies such as fossil by revealing their energy equivalence with a mathematical model. This method allows to see the behavior of the system without technological investment yet. In this study, with the help of Answer-TIMES model, which is one of the energy modeling methods, it was aimed to extract the energy balance between the years of 2016-2031 in Burdur. In the second stage, it is aimed to determine the potential of all renewable resources in Burdur and to apply the technological, economic and ecological effects to the city in the medium term by applying these resources to the model. According to the baseline scenario, Burdur's electricity consumption is projected as 1.95-5.15 PJ between 2016-2031. The potential of solar, biomass and wind applied in alternative scenarios was put into operation in 2019 and showed that the city can meet all electricity needs in the period until 2031. The application of renewable resources has also been observed to dramatically reduce electricity imports and carbon emissions produced by the city.

Keywords: Renewable energy, energy modeling, Answer-TIMES

1 Introduction

For tens of years' countries are investing renewable technologies for making sustainable communities. Completely sustainable societies limited by both efficient wise and investment cost wise of these renewable technologies. But today, each renewable technology proved themselves and used by entire world. Even, some of the major cities, publishing their 100% renewable road maps for 2050 and so on.

For example, Barcelona wants to become energy independent self-sustainable city by 2050 with their 1.6 million citizens. To make this target possible, they determined a starting point and approach to reach energy independency. And they want to become self-sustainable for both urban and rural areas. Another example is Frankfurt. They want to be a 100% renewable community with 50% energy saving in end of 2050 for their 717 thousand citizens. City Frederikshavn in Denmark, Geneva-France and Malmö-Sweden are the other cities that want to become a self-sustainable or 100% renewable communities [1].

In this context, this study aims to find economic, technology and ecological effects of 100% renewable electricity production scenario of Burdur, Turkey. The model established between 2016-2031. 2016 is the base year and data has been acquired from Turkish Statistical Institute (TURKSTAT) and Energy Market Regulatory Authority (EPDK). Future years forecasted by national growth rates and energy demand increases. In the last sections, 100% renewable energy scenario will show the effects of such investment.

Additional to cities, lots of academic studies also published in this area. Pless, Billman and Wallach published a paper about Greensburg, Kansas. Greensburg hit by a tornado in 2007 and 90% of their structures destroyed in this disaster. The study discussed the rebuilding efforts of Greenburg. According the study, in three years, half of the building have been built and reached to 40% energy saving. And all the city-owned structures rebuilt by LEED gold and platinum standards. To satisfy the electricity need, 12.5 MW wind farm also implemented to city [2].

Another study made by Morel, Obara and Morizane in Japan. They want to find best possible operation method for 100% renewable energy in Kitami-Japan. According to paper, while finding the strategy, they also want to reach zero CO₂ emission. In the results, they suggest using digital simulation on hourly level to find demand for a year. And the simulations show that, it is possible to achieve 100% renewable with zero CO₂ emissions while keeping the grid quality within allowed limits [3].

In a paper that made by Kartite and Cherkaoui, presents a methodology to find 100% renewable electricity generation of city located west of Morocco. They used hybrid PV/Wind system with battery storage while finding objective function by Improved Search Algorithm (IBSA). According to results, IBSA shows the effectiveness of this methodology [4].

The paper will present the material and methodology in next sections and will end with results section.

2 Material and Methodology

Answer-TIMES modelling software were used to establish mathematical model. TIMES is the optimization method that uses energy-economy-ecology-engineering background.

TIMES energy model structure is designed by the modeler and then respective energy carriers, technologies, environmental emissions, and demands are specified with relevant qualitative and quantitative data input for each separate region. The specified items characterize both currently exists in the energy system and the future candidates within the specified time horizon. Specified time-series and time-independent data contain the economic and technology-based policy assumptions over the identified region and time horizon. Reference year is set on a past year and the statistical values are fixed on this year by the modeler.

2.1 Objective Function

Below functions shows the backbone of TIMES method. Objective function aims to minimize the total cost of system and find least cost solutions between constraints. Therefore:

$$1. NPV = \sum_{r=1}^R \sum_{YEARS} (1 + d_{r,y})^{REFYR-y} x ANNCOST(r, y) \quad (1)$$

In equation (1), NPV (Net Present Value) of the model describes the net cost of the system. ANNCOST refers to the annual cost. The general discount rate is shown by "d". REFYR is the reference year for discounting, YEARS is the number of years in each period "t" and the letter "R" is the number of regions.

$$2. VAR_OBJ_{(z)} = \sum_{r \in REG} REG_OBJ(z, r) \quad (2)$$

The equation (2) represents the overall objective function of each region defined in model. The model can calculate both single and multi-regional structures.

$$3. REG_OBJ_{(z,r)} = \sum_{y \in (-\infty, +\infty)} DISC(y, z) x \{ INVCOST(y) + INVTAXSUB(y) + INVDECOM(y) + FIXCOST(y) + FIXTAXSUB(y) + VARCOST(y) + ELASTCOST(y) - LATEREVENUES(y) - SALVAGE(z) \} \quad (3)$$

where;

$O(z)$: Total system cost, discounted to the beginning of year z,

$VAR_O(z)$: Total cost of all regions, discounted to year z,

$REG_O(z, r)$: Total cost of the region r, discounted to year z.

$INVCO(y)$: It is the investment cost,

$INVTAXS(y)$: The tax and subsidy costs,

$INVDEC(y)$: Decommissioning capital costs,

$FIXCO(y)$: It is the fixed annual cost,

$FIXTAXS(y)$: Fixed annual tax and subsidy,

$VARCO(y)$: All variable costs (proportional to some activity),

ELASTCO (y) : Cost incurred when demand is reduced due to price elasticity,
 LATEREVENU(y): Revenue accounts for commodity recycling occurring after the end of horizon,
 SALVAGE (z) : Salvage value of all capital costs of technologies whole life extends beyond the end of horizon [5].

2.2 Reference Energy System and Database

Reference energy system (RES) is the main structure that shows the energy flow in analyzed system. Also shows the import, export and mining processes. Basically, represents the supply and demand chain of the domain. Figure 1 shows the reference energy system of Burdur.

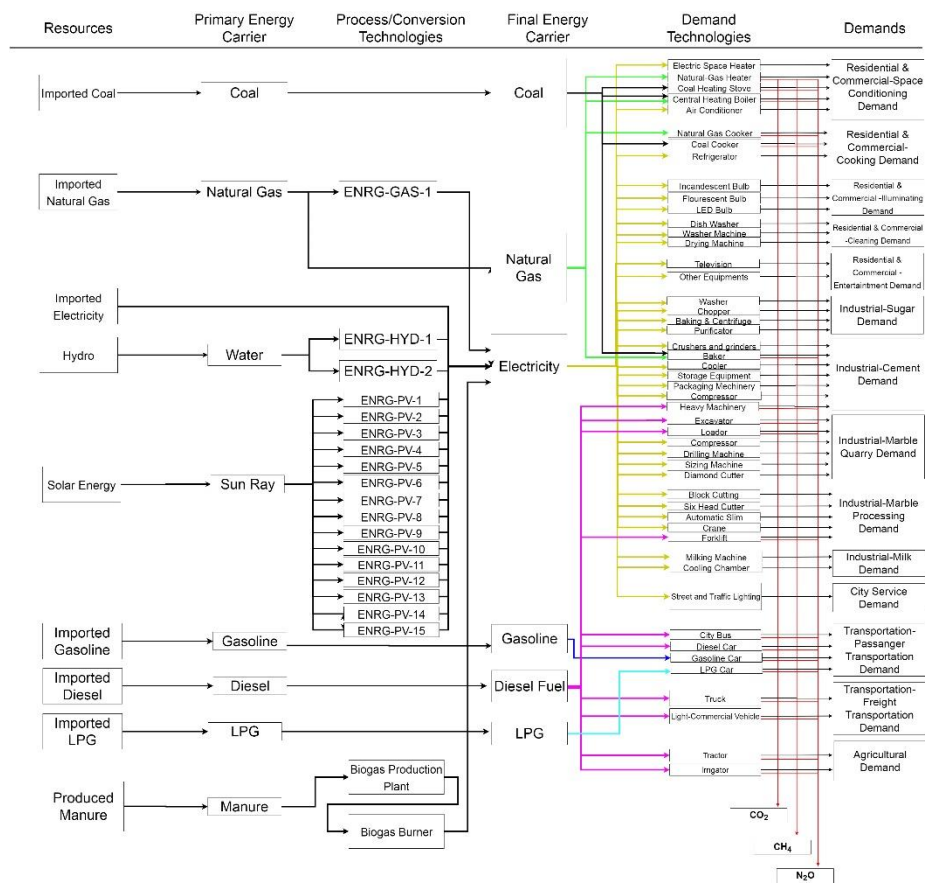


Fig. 8. Reference energy system of Burdur.

RES diagram has six columns. Resources column shows import, export and mining processes. According to figure 1, Burdur has no mining process. It is mainly import-

ing the energy needs. Second and fourth columns are showing the energy carriers. Third column represents the process and conversion technologies. Fifth and sixth columns are showing the demand technologies and demands. Demands are divided to 5 sub section: Residential and commercial, industrial, city service, transportation and agriculture.

After establishing the reference energy system, second step is to calculate data of the technologies. In this paper, all related data collected from face-to-face meeting with experts in Burdur, TURKSTAT and EPDK annual reports [6][7]. All emission factors calculated by Intergovernmental Panel on Climate Change (IPCC) and National greenhouse has emission reports [8].

All demand side data can be seen in Table 1. Future years has been projected according to national growth rate and demand increase forecasts.

Table 1. Demand needs and future projections (PJ).

	Commodity	2016	2021	2026	2031
Residential and Commercial Demands	CLEANING.DEMAND	0,130	0,162	0,202	0,252
	COOKNG.DEMAND	0,401	0,499	0,622	0,775
	ENTERTAINMENT.DMN	0,130	0,162	0,202	0,252
	ILLUMINATION.DEMAND	0,035	0,044	0,055	0,068
	SPC.CONDITIONING.DMND	1,244	1,551	1,933	2,408
Industrial Demands	CEMENT.DEMAND	0,668	0,832	1,037	1,292
	MARBLE.PROCESSING.DEMAND	0,682	0,850	1,059	1,320
	MARBLE.QUARRY.DEMAND	0,343	0,428	0,533	0,664
	MILKING.DEMAND	0,177	0,221	0,275	0,343
	SUGAR.DEMAND	0,041	0,050	0,063	0,078
City Service Demand	SERV-DEMAND	0,016	0,020	0,025	0,032
Transportation	FREIGHT.TRNSPORT.DEMAND	3,631	4,525	5,639	7,027
	PASSANGER.TRNSPORTATION	0,911	1,135	1,415	1,763
Agricultural Demand	AGRI-DEMAND	0,107	0,133	0,166	0,207

2.3 100% Renewable Energy Scenario

With 100% renewable scenario, we aimed to find economic, environmental and energy wise effects of renewable investment to Burdur. Investments implemented between 2020-2031 equally. Three different renewable technology evaluated within this scenario. According to Renewable Energy Directorate, Burdur has 58.16 MW of wind potential and 1.6 PJ electricity can be generated via biomass.

Solar potential is quite high when compared with biomass and wind. Therefore, wind and biomass potential implemented completely. Rest of the electricity need will be considered from solar-based generation.

3 Results

Biomass investment results shown in Table 2. According to table, investment starts at 2020 with 0.78 PJ electricity. Last year of the time horizon, electricity generation reached to full potential with 1.26 PJ. To invest such technology, 22.81 mil\$ dollar need to be invested in 2020 and this numbers reaches to 36.53 mil\$ in 2031. Even thought, there is no significant fossil-based power plant in Burdur, it prevents to invest equal fossil-based power plant in other regions of Turkey. According to this concept, 97.97 kT of CO₂ emissions prevented.

Table 2. Biomass investment results.

Parameter	Units	2016	2019	2020	2025	2030	2031
Total Levelized Cost	2000\$USm	0	0	22.8112	28.2468	35.0006	36.5359
Total Electricity Generation	PJ	0	0	0.7866	0.974	1.2069	1.2599
Emission Mitigation	kt-CO ₂	0	0	-61.17	-75.75	-93.86	-97.97
Total Installed Capacity	GW	0	0	0.0312	0.0386	0.0478	0.0499

Another result is addressed in wind investments. The related data is shown in Table 3. Similar to biomass results, the investment begins in 2020 and ends in 2031. Total of 58 MW installed capacity implemented in time horizon. Investment and fixed operation cost also presented in table 3. 58 MW wind installation prevents 42.79 kT CO₂ emission in every year after 2031.

Table 3. Wind based electricity generation results.

Parameter	2020	2023	2026	2029	2031
Fixed O&M Costs (Mil US \$)	0.2301	0.9203	1.6105	2.3007	2.7609
Investment Costs (Mil US \$)	1.1643	4.6569	8.1495	11.6421	13.9704
Installed Capacity (GW)	0.0048	0.0194	0.0339	0.0485	0.0582
Electricity Generation (PJ)	0.0459	0.1834	0.321	0.4585	0.5502
Co ₂ Mitigation (kt)	-3.566	-14.264	-24.962	-35.66	-42.792

Last results are the solar investments and shown in table 4. As mentioned before, rest of the capacity need will be covered by solar photovoltaic investments. Therefore, 308 MW additional capacity implemented to system between 2020 to 2031 equally. Investment cost reaches to 68 mil\$ cumulatively in 2031. And to maintain such technology, 6.8 mil\$ needs to spend for fixed operation and maintenance costs. Last result is CO₂ emission mitigation. 308 MW solar photovoltaic power plant will prevent 260 kT CO₂ every year after 2031.

Table 4. Results of solar investments.

Parameter	2020	2023	2026	2029	2031
Fixed O&M Costs (Mil Us \$)	0.557	2.2278	3.8987	5.5696	6.6835
Investment Costs (Mil Us \$)	5.6704	22.682	39.6936	56.7051	68.046
Electricity Generation (PJ)	0.2794	1.1177	1.956	2.7943	3.3532
Installed Capacity (GW)	0.0253	0.1013	0.1772	0.2532	0.3038
Co ₂ Mitigation (Kt)	-21.7313	-86.9253	-152.119	-217.313	-260.776

4 Conclusion

It is possible to build 100% renewable, environment friendly, cost-effective and self-sufficient cities with today's renewable technology. We can solve the electricity dependency and emission problem by investing 100% renewable politics by using every possible renewable potential in our geography.

In this paper, 100% renewable potential evaluated to see the results in environmental, technological and economical level. In this context, Burdur selected as a case city and reference energy system developed between 2016-2031. Total investment costs of three different technology vary between 30 to 124 mil\$. This potential can mitigate 85 kT CO₂ in 2020 and 400 kT CO₂ in 2031 by itself.

References

1. Brinhault, A., Eisermann, M., Lacassagne, S., Cities heading towards 100% renewable energy by controlling their consumption. CLER, November 2016.
2. Pless, S., Billman, L., Wallach, D. From tragedy to triumph: Rebuilding Greensburg, Kansas to be a 100% Renewable Energy City. ACEEE Summer Study, 2010.
3. Morel, J., Obara, S., Morizane, Y. Operation strategy for a power grid by 100% renewable energy at a cold region in Japan. Journal of Sustainable Development of Energy, Water and Environment Systems. Vol. 2, No. 3, 2014
4. Kartite, J., Cherkaoui, M. Towards 100% renewable production: Dakhla smart city electrification. Third International Conference on Smart City Applications. Edition 2, PP 1146-1156, 2019
5. Loulou R, Lehtila A, Kanudia A, Remme U, Goldstein G. Documentation for the TIMES Model Part 2. 2016.
6. <http://www.tuik.gov.tr>. Accessed 04.12.2020
7. <http://www.epdk.gov.tr>. Accessed 15.03.2020
8. https://www.ipcc-nggip.iges.or.jp/EFDB/find_ef.php?ipcc_code=2.A.2&ipcc_level=2. Accessed 06.11.2018

Energy System Analysis and Modeling of an Electric-Powered Ferry

Fatih Yılmaz¹, Egemen Sulukan², Dođuş Özkan², Tanay Sıdkı Uyar³

¹ Barbaros Institute of Naval Sciences and Engineering, National Defence University
34942 Tuzla, İstanbul, Turkey

² Mechanical Engineering Department National Defence University Turkish Naval Academy
34942 Tuzla, İstanbul, Turkey

³ Department of Mechanical Engineering Marmara University Göztepe, İstanbul, Turkey

yilmazf58@gmail.com, esulukan@dho.edu.tr
dozkan@dho.edu.tr, tanayuyar@outlook.com

Abstract. In parallel with the increasing sensitivity of the international community in recent years on that harmful greenhouse gas emissions causing global warming and climate change should be reduced and the United Nations (UN) Framework Convention on Climate Change and Paris Agreement on Climate Change, International Maritime Organization (IMO) that is the UN specialized agency with responsibility for the safety and security of shipping and the prevention of marine and atmospheric pollution by ships has also increased its efforts in order to reduce emissions from international shipping in recent years. IMO that in particular aims to reduce carbon dioxide (CO₂) emissions from maritime transportation by 50% until 2030 and by 70% until 2050, compared with 2008, has established very important regulations during the last 15 years. Briefly, these regulations are related with Energy Efficiency Design Index (EEDI) for reducing CO₂ emissions of new ships, Ship Energy Efficiency Management Plan (SEEMP) and Data Collection System (DCS) for Ship Fuel Consumption for existing ships, Sulfur (S) content limits for marine fuel oil, Azoth oxide (NO_x) emission limits for internal combustion marine engines and Emission Control Areas (ECA) in terms of NO_x and Sulfur oxide (SO_x) for the different sea areas of the world. All of those regulations and therefore additional costs have accelerated the maritime industry's efforts to make more use of the alternative/renewable energy sources onboard ships and at ports. Especially in Northern European countries, which are prominent with their fjords within the ECAs, the use of all-electric or hybrid ferries with energy storage technology in Li-ion batteries has started to become widespread instead of using fossil-based fuels in the maritime transportation. In accordance with 11th Development Plan of Turkey, it is envisaged that the use of the electric-powered ferries for passenger and car transportation in short-distance will also become widespread in the near future of Turkey. In this study, the objective is to analyze and model the energy system of an electric-powered ferry using for maritime transportation. With this aim, a Reference Energy System (RES) for a diesel electric-powered ferry, which consists of resources, conversion process & technologies, final energy carriers, demand technologies & sectors, has been established and analyzed.

Keywords: All-electric Ships, Hybrid Ships, Energy Efficiency.

1 Introduction

Today, about 85% of the world trade is transported by sea. In this context, maritime transportation by ships has a strategic importance for the world economy, trade and logistics activities. The maritime transport is very important not only for economy and trade but also for public transportation between countries or cities, including inland passenger and vehicle transportation.

On the other hand, maritime transportation activities have also various environmental impacts from ports and ships for air, water, soil/sediments and ecosystem. The most important one of those impacts is the air pollution from ships, including passenger ships and ferries. The international community is fighting against the global climate change due to greenhouse gases (GHG) produced by different sectors, including maritime which is also producing GHG from ships. IMO makes effort to reduce it.

2 IMO's Environmental Safety Regulations and Significance of Ship Energy System Analysis

The IMO aims to reduce carbon dioxide (CO₂) emissions from maritime transportation by 50% until 2030 and by 70% until 2050, compared with 2008. For this aim, many regulations such as Energy Efficiency Design Index (EEDI) for reducing CO₂ emissions of new ships, Ship Energy Efficiency Management Plan (SEEMP) and Data Collection System (DCS) for Ship Fuel Consumption for existing ships, Sulfur (S) content limits for marine fuel oil, Azoth oxide (NO_x) emission limits for internal combustion marine engines and Emission Control Areas (ECA) in terms of NO_x and Sulfur oxide (SO_x) for the different sea areas of the world were adopted in the last 15 years.

All of those international regulations have forced the shipowners and ship management companies to analyze the energy efficiency of their ships due to heavy costs and penalties for violations. Application of those environmental regulations to inland passenger and vehicle transportation depends on the relevant Coastal states.

The energy system analysis of a ship ensures the lower fuel consumption and emissions by more effective energy management, in compliance with the IMO's targets on reducing the GHG emissions from shipping [1].

3 Reference Energy System (RES) Concept

The Reference Energy System (RES) is a set of parameters that reveals the characteristics of technologies and resources used to provide energy balance and is a network of all technological activities required for energy supply and end-use activities. There are usually five main components of a typical RES model which are primary energy sources (SCR), energy conversion technologies (CON), energy processing (PRC), energy end uses (DMD) and demands (DM) (see Fig.1) [2].

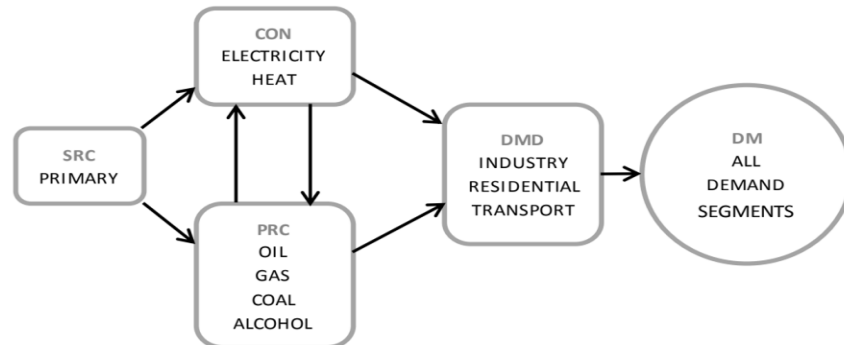


Fig. 1. Main Components of a Typical RES Model (Simplified illustration)

4 Literature Review

In the relevant literature, there are some studies which are specifically related with analysis and modelling of a RES for ships. For example, Sulukan at al. (2018) studied a RES of a generic ship to evaluate the energy consumption characteristics and energy demand segments of a generic ship by energy system analysis approach and simplified energy network [2]. Benli at al. (2019) studied for developing the RES of a generic frigate [1]. Yılmaz at al. (2018) studied a RES design for a crude oil tanker to indicate interrelations and connections between the energy carriers, respective technologies, and the determined demands [3]. Yan at al. (2019) studied to establish the structure of a cruise ship's energy system with multiple facilities such as an internal combustion engine, gas turbine, dual fuel engine, pv panels, and the wind turbine [4].

Majority of other studies related with RES modelling are related with different issues and sectors. For example, Scapino at al. (2020) investigated the sorption thermal energy storage potential in a reference energy system interacting with different energy markets [5]. There are also various studies in the literature related with energy system analysis and planning of different countries such as France [6], Denmark [7], Turkey [8-9], Ireland [10], Colombia [11], Iran [12].

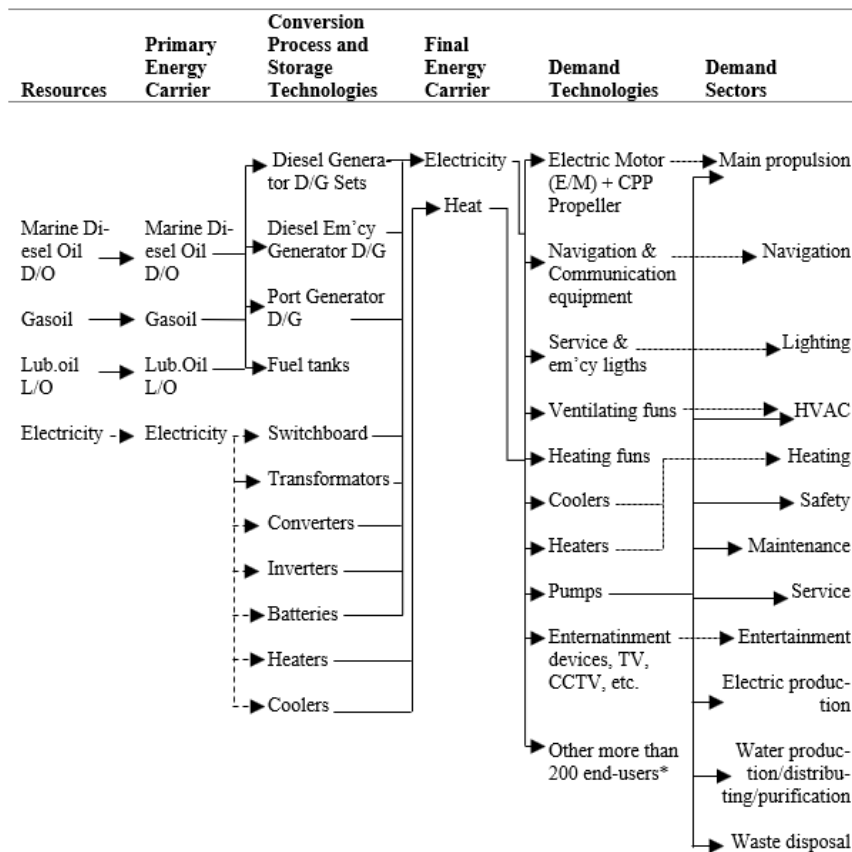
5 RES Modelling of a Diesel Electric-Powered Ferry

In this study, the objective is to analyze and model the energy system of an electric-powered ferry using for maritime transportation. With this aim, a Reference Energy System (RES) for an electric-powered ferry, which consists of resources, conversion process & technologies, final energy carriers, demand technologies & sectors, are established and analyzed. The RES of a ship shows us the general structure of the energy follows from the resources to the demands throughout conversion process and end-use technologies. The technical particulars of the diesel electric-powered ferry, which has been investigated in scope of this study, are shown from the Table 1 as below.

Table 5. Technical Particulars of the Diesel Electric-Powered Ferry Investigated

Type	Vehicle & Passenger Ferry
Length (m)	64
Breadth (m)	18
Draught (m)	3,3
Speed (knot)	12-13
Vehicle capacity	80
Passenger capacity	590
Propulsion System	Electric Motor + Controlled Pitch-Propeller (CPP)
Main Energy System	Diesel Electric (4 x 570 KWh)

The RES model of the ferry is shown from the Fig. 2 as below. This model has been established by considering the current energy system the ferry.



* Other more than 200 end-users belong to each of demand sectors.

Fig. 2. RES Model for the Diesel Electric-Powered Ferry Investigated

5.1 Resource Technologies (Import-Export)

The fuel is the main energy resource of the ferry. The fuel is only used to produce electricity by four diesel generators with internal combustion diesel engines on board ferry. The main types of fuel used are marine diesel oil, lubricating oil and gasoline while the ferry is sailing and maneuvering. The electricity is also imported from the shore and is used while the ferry is berthed.

5.2 Primary Energy Carriers

The main primary energy carriers are the electricity imported from the shore as well as the marine diesel oil, the lubricating oil and the gasoline.

5.3 Conversion Technologies

In general, the conversion technologies are converting the primary energy carriers to final energy carriers such as electricity or heat. The main conversion technologies for the ferry are the diesel generators with internal combustion diesel engines, heaters and coolers onboard.

5.4 Process Technologies

In general, the process technologies are changing the form, characteristic or location of the energy. The main process technologies for the ferry are frequency converters, transformers, converters, inverters and rectifiers.

5.5 Storage Technologies

The main storage technologies are the storage tanks for different kinds of the fuels and conventional batteries for the storage of electricity in case of emergency.

5.6 Final Energy Carriers

The final energy carriers are described as electricity and heat.

5.7 Demand Technologies

During this study, more than 220 demand technologies including pumps, ventilation fans and electrical devices under 12 different demand sectors have been detected for the ferry.

5.8 Demands

The main demand sectors for the ferry are described as main propulsion, safety, electric propulsion, HVAC, service, heating, waste disposal, lighting, water production/distributing/purification, maintenance, navigation and entertainment. Fig.3 shows the distribution of hourly energy load (KW/h) by demand sectors of the ferry. This figure has been created in accordance with full electricity loading analysis of the fer-

ry, so it does not include utilization and availability parameters of the demand technologies.

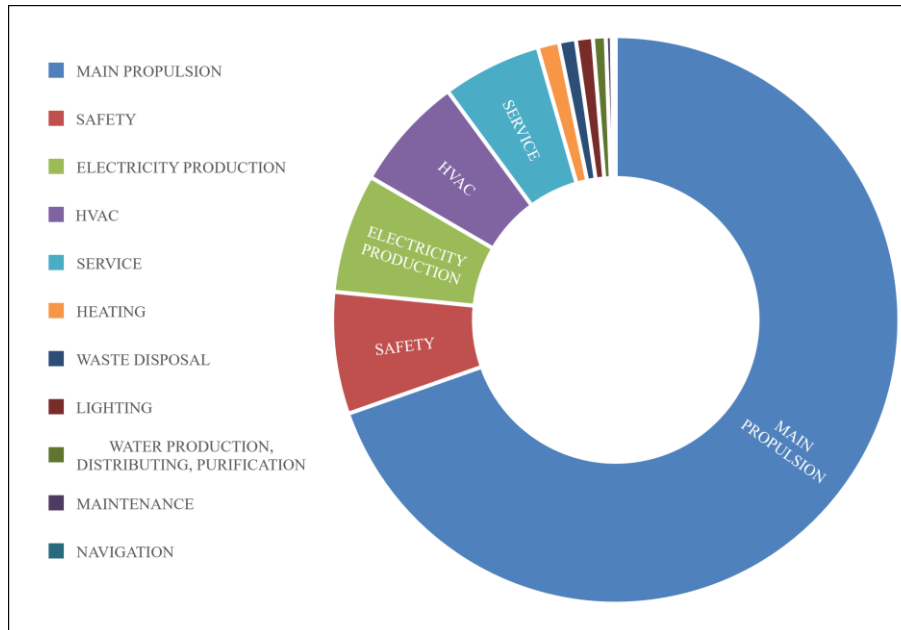


Fig. 3. Distribution of hourly full energy load (kW/h) by demand sectors of the ferry

6 Results

The ferry investigated has currently a diesel electric energy system. Total amount of approximately 2400 KW/h energy needs of the demand technologies and demand sectors of the ferry are currently provided by four diesel generators, each of which has an electricity production capacity of approximately 570 KWh. The propulsion system with frequency converters and Voith system is a substantial demand sector of the ferry, with a share of about 70% for full electricity loading condition of the ferry.

It may be planned to convert to a hybrid energy system by adding a few sets of lithium batteries, thus reducing the emissions by using fewer diesel generators. For example, two sets of lithium batteries with adequate electricity production capacity for each of aft and forward may be replaced with two sets of diesel generators. Of course, environmental aspects and costs of this conversation should be considered as well.

Another alternative may be to convert to all-electric energy system. But, it has been observed that there are some constraints at this stage related with insufficient lithium battery energy storage capacity for long-distance, insufficient infrastructure onshore for high voltage electricity supply, emergency situations at sea, high cost of lithium battery equipment investment and high price of onshore electricity in current.

7 Conclusion and Remarks

In scope of this study, the energy system of a diesel electric-powered ferry using for maritime transportation has been analyzed and modeled by establishing its Reference Energy System (RES) based on design full loading electricity analysis. However, further study is needed to develop the RES model of the ferry for a reference year, which should be included utilization and availability parameters for each of demand technologies during the reference year. This study is ongoing in scope of thesis study.

References

1. Benli, İ.T., Sulkan, E., Alkan, A.D. A. Developing the Reference Energy System of a Generic Frigate. *Journal of Naval Sciences and Engineering*, 15 (1), 1-20, (2019).
2. Sulukan, E, Özkan D., Sarı, A. Reference Energy System Analysis of a Generic Ship. *Journal of Clean Energy Technologies*, 6 (5), 371-376, (2018).
3. Yılmaz, M.A., Sulkan, E., Özkan, D, Uyar, T.S. A. Reference Energy System Design for a Crude Oil Tanker. *International 100% Renewable Energy Conference (IRENEC) Proceedings Book*. 50-55, (2018).
4. Yan, Y., Zhang.H., Long, Y., Wang, Y., Liang, Y., Song, X., Yu, J.J.Q., Multi-objective Design Optimization of Combined Cooling, Heating and Power System for Cruise Ship Application. *Journal of Cleaner Production*, 233, 264-279 (2019).
5. Scapino, L., Servi, D., Zondag, H.A., Driken, J., Rindt, C.C.M., Sciacovelli, A. Techno-Economic Optimization of an Energy System with Sorption Thermal Energy Storage in Different Energy Markets. *Applied Energy*, 258. (2020). <https://doi.org/10.1016/j.apenergy.2019.114063>
6. Seck, G.S., Karakowski, V., Assoumou, E., Maizi, N., Mazaauric, V. Embedding Power System's Reliability within a Long-Term Energy System Optimization Model: Linking high renewable energy integration and future grid stability for France by 2050. *Applied Energy*, 257. (2020). <https://doi.org/10.1016/j.apenergy.2019.114037>
7. Hagos, D.A. and Ahlgren, E.O. Exploring Cost-Effective Transitions to Fossil Independent Transportation in the Future Energy System of Denmark. *Applied Energy*, 261. (2020). <https://doi.org/10.1016/j.apenergy.2019.114389>
8. Mutluel, F. and Sulukan, E. Reference Energy System Development for Turkish Residential Sector. *IRENEC 2014 Conference Proceedings Book*, 179-186. (2014).
9. E. Sulukan, M. Sağlam, T.S. Uyar, M. Kırıldıoğ. Determining Optimum Energy Strategies for Turkey by MARKAL Model. *Journal of Naval Science and Engineering*, 6(1), 27-38. (2010).
10. Glynn, J., Gargiulo, M., Chiodi, A., Deane, P., Rogan, F. Zero Carbon Energy System Pathways for Ireland Consistent with the Paris Agreement. *Climate Policy*, 19(1), 30-42. (2019).
11. Roncallo, O.P, Campillo, J., Ingham, D., Hughes, K., Pourkashanian, M. Large Scale Integration of Renewable Energy Sources (RES) in the Future Colombian Energy System. *Energy*, 186. (2019). <https://doi.org/10.1016/j.energy.2019.07.135>
12. Ahmadi, S., Fakehi, A.H., Vakili, A., Aghtaie, M.M. An Optimization Model for the Long-Term Energy Planning Based on Useful Energy, Economic and Environmental Pollution Reduction in Residential Sector: A case of Iran. *Journal of Building Engineering*, 30. (2020). <https://doi.org/10.1016/j.jobbe.2020.101247>

Calculation of Wind Turbine Installation on a University Campus via Windsim

Alperen Sarı¹, Egemen Sulukan², Dođuş Özkan², Tanay Sıdkı Uyar¹

¹ Mechanical Engineering Department/ Marmara University
Kadıköy-Istanbul, 34722, Turkey

² Mechanical Engineering Department/ National Defence University/ Turkish Naval Academy
Tuzla-Istanbul, 34942, Turkey.

alperensari@gmail.com, esulukan@dho.edu.tr, dozkan@dho.edu.tr,
tanayuyar@marmara.edu.tr

Abstract. As well as the negative effects of climate change being felt throughout the world, increasing global energy demand and variable costs force people to find clean, sustainable and low-cost energy alternatives. Renewable energy, which is the energy obtained from the energy flow that exists in the continuous natural processes, stands out because it is sustainable, it provides locality, and it is economical and environmentally friendly. In recent years, solar and wind energy has come to the fore with a serious decrease in energy production costs and installation, and the share of production has increased worldwide. Technologies that generate electricity from renewable energy are preferred not merely because of their low cost, but also because of their contribution to combating climate change and sustainable development goals. In this context; The purpose of this study is to examine the wind power plant installation by calculating the location of wind turbines through windsim, which will meet the electricity demand of a university campus in Istanbul, which uses wind energy as a source. The location of the wind turbines that can be installed in the Turkish Naval Academy of National Defence University was calculated through the Windsim software based on wind intensity and direction data for seven months obtained from the Kartal Meteorology Regional Directorate. As a result, it was evaluated that the proposed system could provide additional income by meeting more than the amount required by the installation of two wind turbines, and would be a cost-effective and environmentally friendly application for the Naval Academy campus by reducing the total greenhouse gas emission.

Keywords: Wind Power Plant, Renewable Energy, Windsim, Clean Energy, Wind Turbine.

1 Introduction

Energy demands have tended to increase due to population growth, industrialization, developing technologies, and increasing consumption over the last decade. Countries need to consume an increasing amount of energy to be able to industrialize and develop in an industrial and economic sense. In this context, competition between countries has increased on industrialization and economic growth, and it is necessary to control energy resources to come to fore in this fight. However, as it is well known, the energy resources are not only limited but also not distributed equally to every region in the world [1]. The depletion of fossil fuel resources in the world and the energy production based on fossil fuels are one of the main sources of military and political problems among countries. Furthermore, an increase in environmental awareness in developed countries forces governments to find alternative environmentally friendly energy production. Therefore, these situations direct countries to new, clean, and renewable energy sources [2].

Energy sources such as solar, wind, geothermal, biomass, and wave are called new clean or renewable energy sources and they have been highly used in recent years because of their less environmental and climatic problems encountered during the production and conversion of energy [3]. Wind and solar energy technologies and installation costs have decreased significantly among renewable energy sources as a result of technological developments over the past decade. Thus, the usage areas and rates of wind and solar power plants have increased more than other renewable energy applications. Nowadays, wind energy is becoming one of the most important renewable energy sources with technological developments, and applications have been developed rapidly. Additionally, their economic benefits have become competitive with conventional energy sources [4]. In this study, a wind power plant was investigated whether it can be the main energy source and can meet the annual energy demand of the university campus via Windsim simulation tool. It has been calculated that the proposed wind power plant installation can meet the self-consumption of the campus by this system.

2 Wind Energy

The wind is originated from the curvature of the earth, slope of the axis of rotation, the inhomogeneous nature of the earth's surface, the air movement caused by the pressure differences as a result of the warming and cooling of the earth. The sun heats the ground surfaces differently, which changes air temperature, pressure, and humidity. The movement of the air is the reason for the pressure deviation and movement from high pressure to low pressure creates the wind [5]. Wind energy consists of moving air masses that meeting different surface heat.

There are some advantages of wind energy such as it is a natural, clean, infinite power and renewable energy source. It also does not need to transport and does not require very high technology for energy production. In addition, this energy source is free and abundant in the atmosphere and has not hazardous outputs or residues to the

environment as its source is the sun [6]. Therefore, wind energy should be converted to another form of energy such as electricity by transforming mechanical energy into electrical energy. For this conversion wind turbines are used which consist of a rotor, generator and surrounding structure as seen in Figure 1 [7].

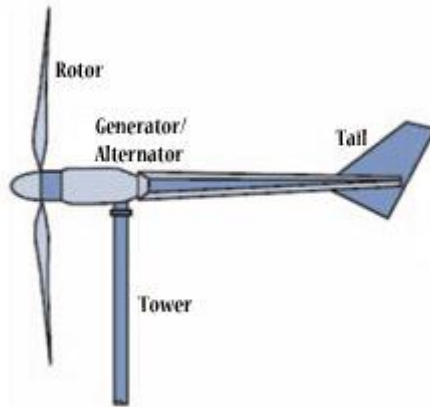


Fig. 1. A Wind Turbine Components [7].

The wind is preferred more with advantages such as wind speed, reliability, independence from fuel and disassembly costs among the renewable energy sources. Moreover, developments in turbine technology have contributed greatly to the increasing wind energy production in recent years. On the other hand, the new developments in composite materials, the rapid development of aerodynamic and mechanical structures minimize noise and magnetic pollution that enabled high-power turbines to operate. Thus, the unit cost of energy production has been reduced highly and this situation has increased the utilization rate of wind energy when compared to other energy productions in the last twenty years [8].

3 Wind Energy Potential and Application In The World and In Turkey

Since the end of the last century, the total installed electricity generation capacity from wind energy has increased quickly worldwide. There are more than 100 countries producing electricity with wind energy in the world.

When we consider it regionally, the place where wind energy is most commonly used is Pacific with % 44.1. Europe is followed by % 32.1 and Americas with % 16. When looking at the countries with the highest installed wind power, China, the United States and Germany have been in the top 3 for a long time. As seen in Figure 2, India and Spain also followed these three countries in 2019 [10].

When evaluated in terms of total installed wind power in 2018, China alone accounts for 35.7 percent of the total installed power in the world. America and Germa-

ny follow China with 16,3 percent and 10 percent, respectively [9]. Considering the newly established capacities in 2018, China, America and Germany are in the top three ranks, respectively.

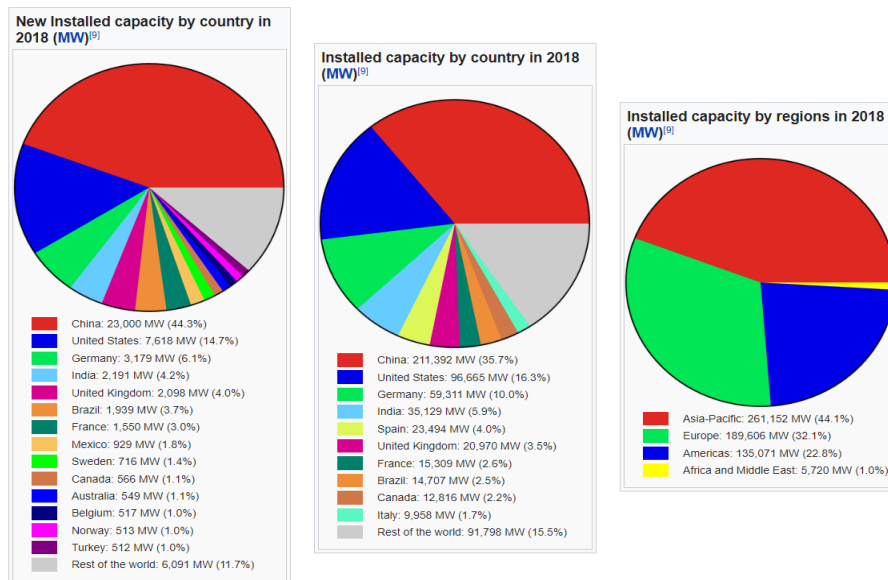


Fig. 2. Wind Energy Statistics in 2018 [9].

RENEWABLE ENERGY INDICATORS 2018

		2017	2018
INVESTMENT			
New investment (annual) in renewable power and fuels ¹	billion USD	326	289
POWER			
Renewable power capacity (including hydropower)	GW	2,197	2,378
Renewable power capacity (not including hydropower)	GW	1,081	1,246
Hydropower capacity ²	GW	1,112	1,132
Wind power capacity	GW	540	591
Solar PV capacity ³	GW	405	505
Bio-power capacity	GW	121	130
Geothermal power capacity	GW	12.8	13.3
Concentrating solar thermal power (CSP) capacity	GW	4.9	5.5
Ocean power capacity	GW	0.5	0.5
Bioelectricity generation (annual)	TWh	532	581

Fig. 3. Renewable Energy Indicators in 2018 [10].

When evaluated in terms of total installed wind power in 2018, China alone accounts for 35.7 percent of the total installed power in the world. America and Germany fol-

low China with 16,3 percent and 10 percent, respectively [9]. Considering the newly established capacities in 2018, China, America and Germany are in the top three ranks, respectively.

While the installed power of wind energy in the world was 540 MW in 2017, it increased to 591 MW in 2018 can be seen in Figure 3 [10].

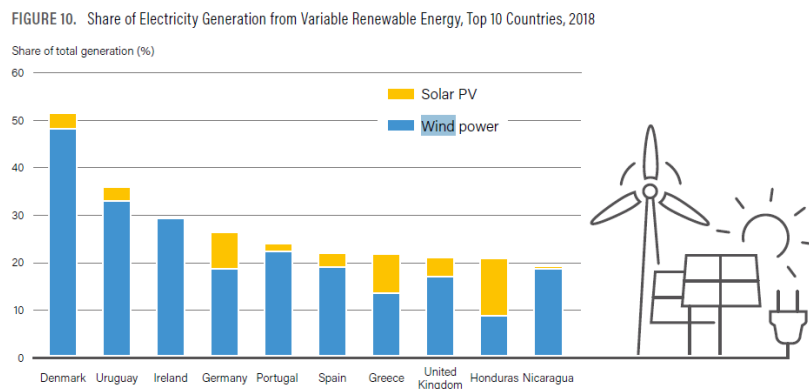


Fig. 4. Share of Electricity Generation from VRE, Top 10 Countries [10].

According to the Shares of Electricity Production from Variable Renewable Energy shown in Figure 4, the leading country in the world stands out as Denmark. While Denmark generates more than half of its electricity from renewable energy, it achieves most of it with wind energy. Uruguay, Ireland and Germany follow Denmark, and all three countries produce most of their energy from renewable energy from wind energy.

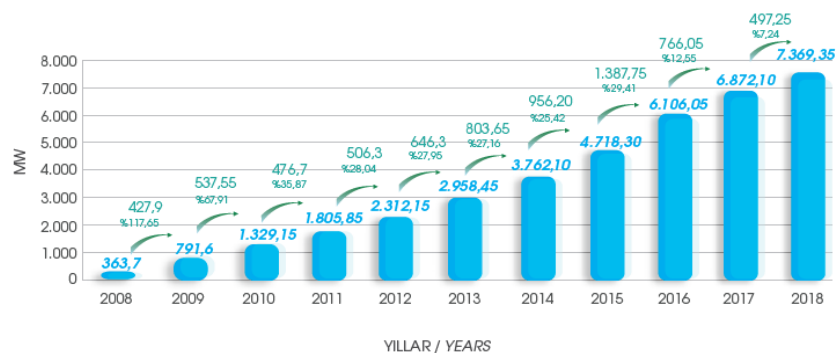


Fig. 5. Cumulative Installations for Wind Power Plants in Turkey [12].

Turkey ranks seventh in Europe and 12th in the world in wind farm installations [10]. When considering all renewable energies, wind energy is considered to have more

potential than other renewable energy sources in Turkey [11]. Installation of wind power plant in Turkey is increasing every year. The biggest increase was experienced in 2016 with 1387,75 MW shown in Figure 5. Turkey Wind Energy Association in 2018, according to a report released in six months brought to life with 497 MW installed power of 650 million dollar investment. Turkey's total wind installed capacity reached 7369 MW. [12].

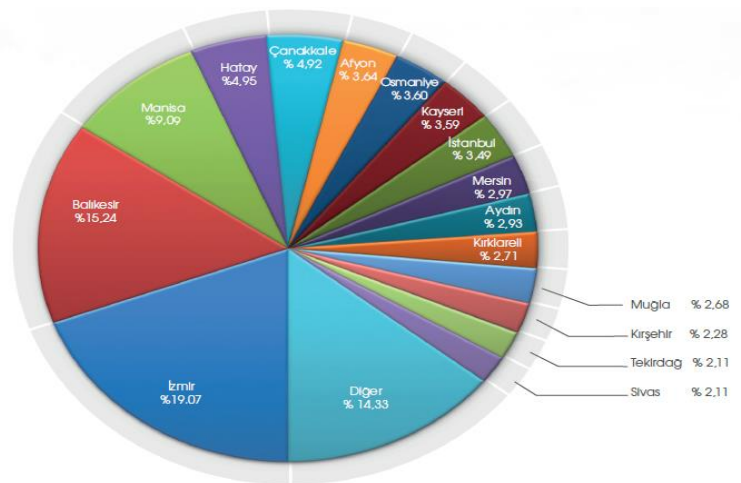


Fig. 6. Operational WPP's According to Cities [12].

While there was an increase of 7.24 percent compared to the previous year, the number of projects in the business increased from 164 to 180. When we look at the ranking by provinces, İzmir takes the first place with 1405 MW. İzmir is province that ranks first not only in terms of wind investments, but also in terms of wind industry. Balıkesir is among the provinces with the highest wind power plants with 1123 MW, Manisa 669 MW, Hatay 364 MW and Çanakkale 362 MW installed power. More than half of the installed wind power is in these five provinces.

4 Wind Power Plant Feasibility Study

The Naval Academy campus is located in Tuzla district of Istanbul, on the Tuzburnu peninsula. The location, on which the meteorological data is based, is 40.51 ° N latitude, 29.15 ° E longitude and 7 m height. The Naval Academy is located at a latitude of 40.8 ° N, longitude of 29.3 ° E and approximately at sea level [13].



Fig. 7. Satellite image of the Turkish Naval Academy campus

On the campus of the Naval Academy, there is an academic complex with administrative buildings, service buildings, modern sports facilities, a fully equipped marina and harbor, and classrooms, amplifiers and laboratories where engineering education is provided. These structures are seen in the satellite image given in Figure 7.

4.1 Windsim

Firstly, Windsim software which will be used in turbine design calculations is introduced. Secondly, the parameters to be used in the setup and calculation of the Turkish Naval Academy wind turbine were determined and defined in windsim software tool. Finally, the energy production amount of the wind power plant designed within the Turkish Naval Academy is calculated in one year and the results are evaluated.

WindSim offers simulation software and consultancy services that allow you to design and operate efficient and high-return wind power plants. It is headquartered in Norway and provides software products and consultancy services on a global scale [14]. Windsim, a modern and advanced wind power plant design software, offers computational fluid dynamics-based (CFD) advanced processing power with a user-friendly interface specially developed for modeling 3D visuals and wind power plants. The calculation steps of Windsim software is shown in Fig.8 . In windsim

software meteorological data, roughness map and terrain data are defined as inputs. Then, the Reynolds Averaged Navier-Stokes equations of the Atmospheric Boundary Layer is used by windsim software to analyze according to the CFD method.

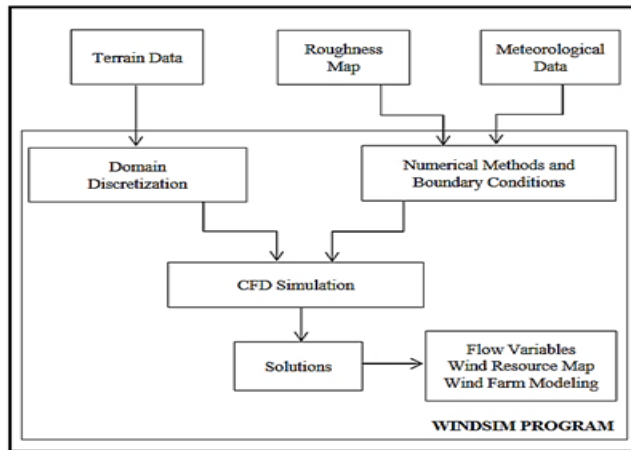


Fig. 8. Basic flowchart of wind resource assessment by Windsim [14]

4.2 Wind Turbine Installation on a University Campus via Windsim

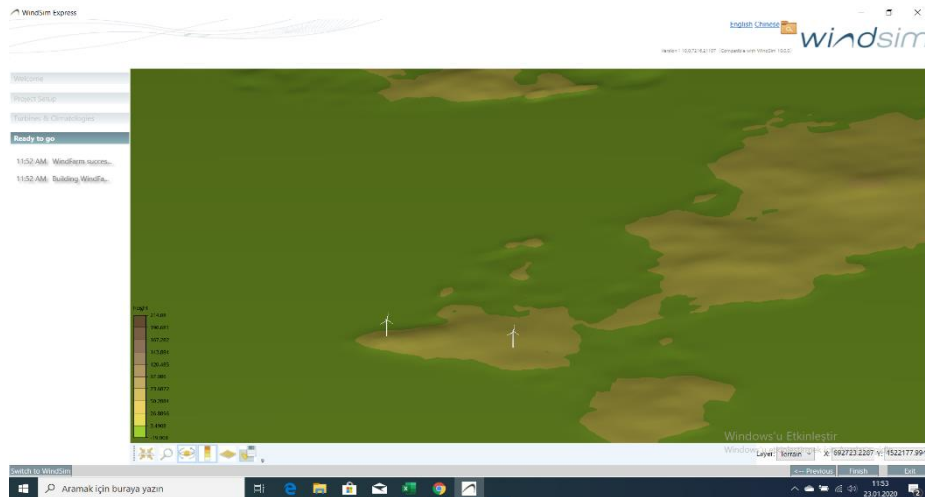


Fig. 9. Wind turbine locations.

In this study, it was evaluated that the annual maximum energy consumption of the Naval Academy Campus would be 5000 MW and accordingly, Gamesa 52 wind tur-

bine, whose values were defined in Windsim Express, was preferred by calculating that two wind turbines could meet the needs. We preferred to use two Gamesa G52 wind turbines which locations are shown in figure 9 in this study for numerical analysis.

The results module enables the user to examine the results from the Wind fields calculations. Variables such as wind speed, wind direction, turbulence intensity and wind shear exponent can be examined. This module can provide a useful analysis of the results from the Wind fields but any information generated here is not used in any other modules.

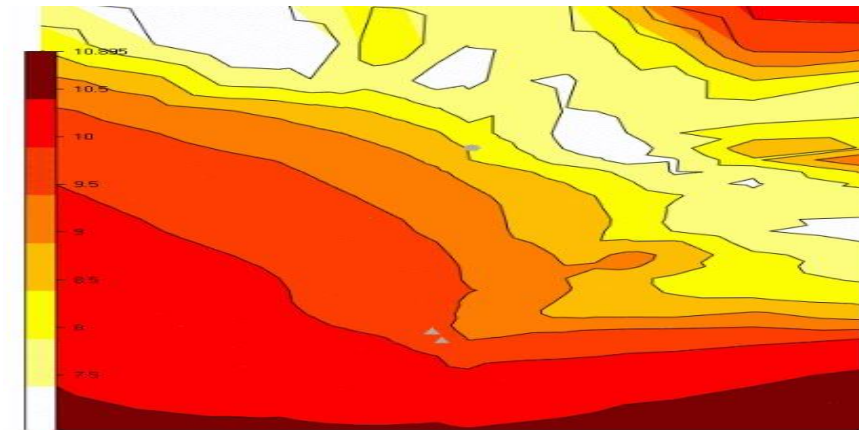


Fig. 10. Turbulence intensity from results module

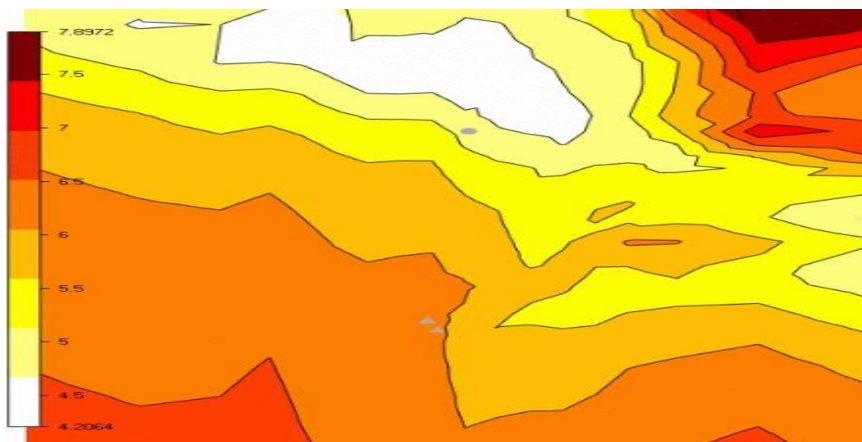


Fig. 11. The wind resource map with average wind speed (m/s) at a hub height of 65 meters.

The average wind speed of the region where the wind turbine is planned to be installed was calculated by CFD analysis by Windsim software. It is shown in figure 10 that the average wind speed is determined as 9.5 m / s at a height of 65 m. It has been observed that wind source map data are compatible with wind atlas data.

Energy analysis of the wind power plant, which was planned to be established in Tuzla Naval Academy, was carried out according to the change in air density at the determined height. According to the results of the analysis given in Table I, the annual power generation (AEP) of the designed wind farm is determined as 6595,5 MWh / y.

Table 6. Energy Production Based on the Frequency Table.

name	power	hub height	density	wind speed	wind speed including wake losses	power density	gross AEP	AEP with wake losses	wake loss	full load hours
	(kW)	(m)	(kg/m ³)	(m/s)	(m/s)	(W/m ²)	(MWh/y)	(MWh/y)	(%)	(h)
wecs1	850	65.0	1.225	10.15	10.15	1872.0	3301.8	-	-	3884.5
wecs2	850	65.0	1.225	10.21	10.21	1930.7	3293.7	-	-	3874.9
All	1700	-	-	-	-	-	6595.5	-	-	3879.7
Mean	-	-	1.225	10.18	10.18	1901.3	-	-	-	-
Reference production at climatology position: DHO_DENEME_7m										
ref..	850	80.0	1.225	9.31	-	1388.7	3053.9	-	-	3592.8
ref..	850	7.0	1.225	7.04	-	614.8	2119.6	-	-	2493.6

Table 1. Energy production based on the frequency table.

The annual maximum energy consumption of the Naval Academy Campus would be around 5000 MWh/y. So we can understand that the proposed wind power plant installation can meet the self-consumption of the campus by this system.

For Turkish Naval Academy we chose two Gamesa G52 wind turbines to meet the energy demand. Surplus energy is generated by DHO is given to Tuzla and Pendik districts not only to meet the energy demand of these area but also can provide an income for school. This also mitigate the environmental pollution too.

5 Results and Conclusion

Turkey is one of the developing countries, so energy demand of the countries continues to increase day by day. Situated in a difficult geography, Turkey has realized the need to reduce dependence on foreign energy to ensure the continuity of production. Turkey wants to meet their energy demands via local and national capabilities, and so increase incentives for investment in renewable energy systems. Thanks to its geographical location, Turkey is a country with a very significant wind energy potential. Wind energy is one of the cheapest and most common energy sources to install among renewable energy sources around the world. When all this is taken into consideration wind energy is vital for Turkey to compete with other countries. If the country takes advantage of this extraordinary resource efficiently, energy management can achieve its goals and objectives.

In this study, the installation of a system consisting of wind turbines that use wind energy as a source, which will meet the demand of the Naval Academy campus in Istanbul, has been examined. In these analyzes, Windsim simulation tool has been used and it has been calculated that the proposed wind power plant installation can meet the self-consumption of the campus by this system. According to feasibility study, investment of a WPP which has 6595.5 MWh/y AEP is feasible by 2 number of commercial Gamesa G52 wind turbine. However, cost analysis of the designed WPP was not considered in this study. Also, we make only one analysis to forecast the economical aspect of the WPP. More reliable results can be got if cost analysis is performed and the number of analysis is increased.

The results obtained by the analysis “provide adequate, reliable and economic energy resources to support economic and social development; ensuring energy supply security; to give priority to combating climate change; support adequate investment to meet growing energy demand, "the force's priorities shows full compliance with the official energy policy of Turkey.

References

1. H. SOYDAL, Z. MIZRAK and M. ÇETİNKAYA, "MAKRO EKONOMİK AÇIDAN TÜRKİYE'NİN ALTERNATİF ENERJİ.," Pamukkale Üniversitesi Sosyal Bilimler Enstitüsü Dergisi., no. 11, pp. 117-137, 2012.
2. İ. ÇOLAK, R. BAYINDIR, İ. SEFA, Ş. DEMİRBAŞ and H. ERGEN., "ALTERNATİF ENERJİ KAYNAKLARININ KULLANIMI," in III. Yenilenebilir Enerji Kaynakları Sempozyumu ve Sergisi, MERSİN, 2005.
3. İ. ÇOLAK and M. DEMİRTAŞ, "Rüzgâr Enerjisinden Elektrik Üretiminin Türkiye'deki Gelişimi.," TÜBAV Bilim Dergisi, vol. 1, no. 2, pp. 55-62, 2008.
4. K. B. POTUK, "RÜZGAR TÜRBİNİ KANAT TASARIMI VE ANALİZİ.," Dokuz Eylül Üniversitesi, İzmir, 2015.
5. E. KOÇ and M. C. ŞENEL, "DÜNYADA VE TÜRKİYE'DE ENERJİ DURUMU -," Mühendis ve Makina, vol. 54, no. 639, pp. 32-44, 2013.
6. M. C. ŞENEL and E. KOÇ, "DÜNYADA VE TÜRKİYE'DE RÜZGÂR ENERJİSİ DURUMU-GENEL DEĞERLENDİRME," Mühendis ve Makina, vol. 56, no. 663, pp. 47-56, 2015.
7. WindSolarUSA, "Wind Turbine Components," 2017. [Online]. Available: <http://www.windsolarusa.com/wind/wind-turbine-components/>. [Accessed 10 05 2020].
8. H. R. (. SEZER, "YENİLENEBİLİR ENERJİ KAYNAKLARININ TÜRKİYE ELEKTRİK SİSTEMİNE TEKNİK VE EKONOMİK ETKİLERİ VE AB UYGULAMALARI.," in III. YENİLENEBİLİR ENERJİ KAYNAKLARI SEMPOZYUMU BİLDİRİLERİ, MERSİN, 2005.
9. K. & C. G. W. E. Ohlenforst, "Global Wind Report 2018.," Global Wind Energy Council, 2019.
10. H. E. e. a. Murdock, "Renewables 2019 Global Status Report.," REN21, 2019.

11. E. S. a. T. S. UYAR, "A Comparative Wind Power Plant Feasibility Study for Gökçeada, Turkey," *Journal of Naval Sciences and Engineering*, vol. 3, no. 5, pp. 55-63, 2009.
12. Türkiye Rüzgar Enerjisi Birliği, "Türkiye Rüzgar Enerjisi İstatistik Raporu," 2019.
13. E. SULUKAN, "İstanbul'da Bir Fotovoltaik Sistemin Tekno-Ekonomik ve Çevresel Analizi," *Pamukkale Üniversitesi Mühendislik Bilimleri Dergisi*, vol. 1, no. 26, pp. 127-132, 2020.
14. [Online]. Available: <https://www.windsim.com/about.aspx>.

Hourly Optimization of Electricity Generation in City Scale

Utku Köker¹[0000-0001-7165-777X], Halil İbrahim Kuruca¹[0000-0002-2448-1772],

Egemen Sulukan²[0000-0003-1138-2465], Tanay Sıdkı Uyar³[0000-0002-0960-1203]

¹ Industrial Engineering Department, Süleyman Demirel University, Isparta, Turkey

² Mechanical Engineering Department, National Defence University, Turkish Naval Academy, Istanbul, Turkey

³ Mechanical Engineering Department, Marmara University, Istanbul, Turkey

utku.koker@afad.gov.tr, halilkoruca@sdu.edu.tr,
esulkan@dho.edu.tr, tanayuyar@marmara.edu.tr

Abstract. The demand figures for electrical energy consistently increase, and this causes stress on local/national agencies to answer it as economically as possible. Somehow, various technologies exist in the energy supply side, and almost all of them are competent in the market today. This work presents a 16-year electrical energy scenario developed with the Answer-TIMES model generator for Uşak, a small province in the Internal Aegean Region of Turkey. A “business-as-usual what-if scenario” is built to evaluate the self-sustainability of the city through electrical energy generation if energy importation policy is discarded and changed with energy generation. The electrical energy demands of residential, industrial, service and other sectors are fed to the model as a single energy demand unit in PJ to obtain the “hourly optimum electrical energy production” with the least possible cost. In particular, the study underscores the importance of hourly optimization in achieving the local supply targets as well as underlining the environmental aspects of building a self-sustainable energy generation infrastructure in Uşak. The work provides valuable information to local and national decision-makers by estimating the cost of upgrading the energy structure generation system of Uşak annually to a self-sustainable energy grid in exchange for the amount of emission to be caused. As a result, annual investments on a combination of various power plants are shown by the TIMES generator to give the optimum cost figures according to the scenario.

Keywords: Energy Optimization, TIMES Optimization, Emissions, Energy Costs, Regional Energy Modeling.

1 Introduction

Energy is the most critical asset in the development of technology since the beginning of humanity. Fossil fuels dominated the most significant portion of the inputs of the energy systems in every decade. However, some adverse effects of this energy generation method became visible in the last century. Reports began to rise in number identifying the environmental externalities to air pollution issues of fossil fuels after the 1950s. The petrol crisis and international affairs made the problems bigger in the procurement of fossil fuels from both economic and political points of view.

Energy generating methods from fossil fuels were warning the governments to find solutions to input problems. Even though advances in natural gas and coal power plants were significant, renewable energy methods became the focus of many environments since the primary inputs, wind, and sun were assumed to be infinite. In the same era, two important milestones are critically important, Rio and Kyoto declarations. Rio Declaration is the first international step in history to fight with the emissions since the World Climate Conference, which was held in 1979.

United Nations Framework Convention on Climate Change (UNFCCC) was a real success just following the Rio Declaration. One hundred eighty-four countries ratified the Convention in 1994. This strong environmental stance continued with the Kyoto Protocol in 1997 that forced the countries to reduce greenhouse gases by an average of %5 below their 1990 levels in the 2008-2012 time span [1]. Kyoto protocol is followed by many other Conference of Parties (COP) until today to maintain and empower the frame of limiting and reducing GHG emissions. The Endorsement of Turkey's Ratification of the Kyoto Protocol was adopted in the General Assembly of the Turkish Grand National Assembly on February 5, 2009, and by Article 25, Turkey joined the party of official members of the Protocol (GEF Country Portfolio Evaluation Turkey (1992-2009) [2].

Today the renewable electricity generation methods are already competitive in the energy markets, and the efficiencies of these methods are increasing every year, threatening the market share of the old conventional energy generation techniques.

The supply security of energy is critically important for modern countries to manage sustainable growth and other macro indicators. From this perspective, countries prefer to supply their energy or primary energy resources from various vendors to reduce the dependency on a single or a few groups. Renewable energy power plants are the right answers to this need with various generation methods, from geothermal to landfill or wind energy generation. As their cost figures dropped down in the last ten years, these power plants gained significant importance in modern countries.

Energy supply security has two dimensions, national and regional levels. Building international energy hubs is a complex problem, including an integrated energy grid programming of all the participant countries' energy grids with an extensive amount of primary energy inputs and various suppliers under different legislation procedures of more than one country. Providing security in the country level may be maintained by having energy supply secured provinces. Today, initiations like Covenant of Mayors pay attention to local plans like the reduction of CO₂ emissions from local transport and energy generation processes [3].

Uşak is a province in the Internal Aegean Region of Turkey with a population of 370 509 [4] in 2019. A summary of the electrical energy consumption of the sectors in Uşak in 2016 is given in Table 1.

Table 1. Electricity Consumption in Uşak in the reference year

	Lighting	Residential	Industry	Agriculture	Commercial	Total
2016	21687,27	195075,55	826647,22	16519,47	405486,77	1465416,28

This paper studies the electrical energy generation system of Uşak in the period of 2016-2031. The business as usual model of the city is formed and optimized on annual basis while the electrical energy import from the primary grid is nullified. This new state is a “what if “analysis and shows the optimum portfolio of energy technologies to be engaged at the beginning of each year to answer the annual demand.

Existing energy generation technologies in Uşak are listed in Table 2 in megawatts. The productions of Alperteks (4.29 MW Natural Gas Power Plant) and Uşak Çöp Fabrikası (1,2 MW Landfill PP) data can not be found in Energy Exchange Istanbul Transparency Platform (EXIST) of EPIAŞ which means that those firms directly consume the generated electricity or there is no production in the given period. Since no production exists in the given period, related installed power values are not included and written in parenthesis.

Table 2. Installed Power Capacities of Uşak in the Reference Year

Technologies	Uşak (MW)
Solar Power Plants (PP)	2,85
Wind PP	54
Landfill PP	0 (1,2)
Nat Gas PP	18,45 (4,29)
Coal PP	3,72

Energy Flow Optimization Model (EFOM) was the primary tool in energy sector modeling in the mid-70s [5]. During the 80s, the MARKet ALlocation model (MARKAL) was introduced. In the year 90s and 2000s, the dominant sides of the two tools were combined in the TIMES model family. All of the three programs enabled the users to make single/multi-sector models, including long periods with their compelling annual programming logic. These programs were used successfully in various energy analyses from testing the "80% greenhouse gas reduction" target feasibility of California with CA_TIMES [6] to the MARKAL Model of Turkey [7].

Somehow, researchers would insist on working more precisely and demand the addition of seasonal data to their models. This weakness was solved by advanced MARKAL versions [8]. This high-level intra-annual time-slicing methodology was initially implemented in the United Kingdom energy model [9]. However, a more complicated time slicing, allowing to build an hourly model, was still not an option in MARKAL. TIMES solved this conflict, and users could make hourly dispatch models

that could only be simulated before. Kannan and Turton developed an hourly model of "Swiss TIMES Electricity Systems (STEM-E) Model" to analyze the differences in the outputs with the eight season based classical TIMES model (four seasonal, two diurnal (day/night) [10].

All the above-mentioned references are on the national scale. On the other hand, the small models of specific regions such as provinces or cities also exist in the energy literature. Almost all these related models are prepared on an annual basis, including one single season rather than an hourly high-level structure. This paper processes the hourly data of Uşak to obtain the results of a what-if analysis, which tests the feasibility of energy-self-sustainable province in our case. While some of the papers in Turkish energy literature [11-12] puts the city in the core of the analysis, none of these papers have analyzed the "overall electrical energy system" of the city in a proper time interval by using a decision support tool i.e. TIMES or an alternative program. This paper aims to fill this void by improving the logic to an hourly basis.

The following parts of the paper are organized as follows. In the second section, a brief description of the TIMES model is given. The analysis of the model is presented in the third section. GM, pGM(1,1), and pGMar(1,1) methods are applied to historical data of Turkey in Section 3. A brief review of the paper and the future research are in Section 4.

2 High-Level Time Resolution Model of Uşak

2.1 TIMES Model and Objective Function

TIMES model generator and GAMS package are used in this work. TIMES is an energy optimization suit taking into account environmental, financial, and technical aspects. The electrical energy generation system of Uşak is optimized with required data of energy supply, consumption, and demand-side with technical, environmental, and economic inputs over a multiperiod horizon at hourly resolution in a single region model.

TIMES optimizes the energy system by giving the least cost under the given constraints with the objection function:

$$NPV = \sum_{r=1}^R \sum_{y \in YEARS} (1 + d_{r,y})^{REFYR-y} * ANNCOST(r, y)$$

The objective function can be given in another form where all regional objectives are summed up:

$$VAR_OBJ(z) = \sum_{r=1}^R REG_OBJ(z, r)$$

$$REG_OBJ(z) = \sum_{y \in (-\infty, +\infty)}^R DISC(y, z) * \left\{ \begin{array}{l} INVCOST(y) + INVTAXSUB(y) + \\ INVDECOM(y) + FIXCOST(y) + \\ FIXTAXSUB(y) + SURVCOST(y) + \\ VARCOST(y) + VARTAXSUB(y) + \\ ELASTCOST(y) - LATEREVENUES(y) \end{array} \right\} - SALVAGECOST(z)$$

where:

NPV	net present value of the total cost for all regions (the TIMES objective function).
ANNCOST(r,y)	is the total annual cost in region r and year y.
d(r,y)	is the general discount rate.
REFYR	is the reference year for discounting.
YEARS	is the set of years for which there are costs, including all years in the horizon, plus past years (before the initial period) if costs have been defined for past investments, plus several years after EOH where some investment and dismantling costs are still being incurred, as well as the Salvage Value and
R	is the set of regions in the area of study.
INVCOST(y)	is the total investment cost in year y.
INVTAXSUB(y)	is the total taxes and subsidies on investments in year y.
INVDECOM(y)	is the total decommissioning cost in year y.
FIXCOST(y)	is the total fixed annual cost in year y.
FIXTAXSUB(y)	is the total annual fixed taxes/subsidies on capacity in year y.
SURVCOST(y)	is the total fixed annual cost in DLAG state in year y.
VARCOST(y)	is the total variable annual cost in year y.
VARTAXSUB(y)	is the total annual variable taxes/subsidies on capacity in year y.
ELASTCOST(y)	is the total cost of demand reductions in year y.
LATEREVENUES(y)	is the lump sum discounted to the user-selected base year.
SALVAGECOST(z)	is salvage cost.

The model is built on the following assumptions:

- New investments in power plant capacities are planned annually. Construction and the engagement of the power plants to the grid would be ready at the beginning of the given year.
- Seven different energy generation technologies are used as alternative technology investments in the model. One or more of these technologies are chosen by the model for each investment period according to the energy demand. Alternative

power plant types are solar power plants, onshore wind power plants, geothermal power plants, natural gas power plants, combined-cycle natural gas power plants, lignite power plants in the model.

- The fuel, operations & maintenance, and investment cost datasets are taken from IEA [13] and presented in Table 3.

Table 3. Installed Cost Figures per kWh for 2016

TECHNOLOGY	Investment	Cost	Fixed Cost	Variable Cost
GY	\$/kW	\$/kWh	\$/kWh	\$/MWh
Nat Gas PP	708		34	0
Nat Gas CC	1021		30,5	2,5
Geothermal	1493		100	0
Wind PP	1667		21,3	0
PV PP	1555		30,0	4,70
Biogas	4447		100	0
Coal PP	2080		37,8	3,8

- CO₂ emission factors of photovoltaic and onshore wind power plants are assumed to be zero in the model. Emission values of natural gas, coal, biogas, and geothermal power plants are obtained from various resources [14-15].
- Due to the problems in the Energy Exchange Istanbul Transparency Platform (EXIST) of EPIAŞ database related to 2015, electricity demand of the base year and the availability factors of geothermal, solar and wind power plants are taken from 2012 Turkey Energy Model found in the EnergyPLAN official web site [16].
- Purchase prices and transportation fees of coal are obtained from a specialist in the sector, while natural gas prices are taken from a report (including the BOTAŞ figures) on the official site of TMMOB [17].
- The high-resolution model of Uşak is based on the least cost option as mentioned previously. As a result, it provides the electricity via the local grid by looking at the optimum cost figures unlikely to the real spot electricity market mechanism that takes intraday and day-ahead markets
- Even though the advances in energy markets result in lower-cost energy generators every coming year, the model assumes the technology prices steady over the years for the sake of simplicity.
- Cost, efficiency, and availability factors, as well as the hourly demand figures, are assumed to be steady over the years to provide a basis for comparison in the model.

MARKAL and TIMES programs offer a time slice solution as a midcourse to the short-long term algorithms. Most MARKAL models use annual time slices; however, a flexible time-slicing was embedded in the later applications of MARKAL. Uşak

high-resolution TIMES model is designed in an hourly manner to solve hourly peak and deep demand problems. Annual models take the average of the whole year, which disables the system to diagnose instantaneous peak and deeps in the given time span. In another way, annual models assume that the (average) demand value of the models behaves as if the pattern is viable in the whole duration equalizing the 24-hour demand to a constant value and setting it as the representative throughout the year.

On the other hand, the demand pattern changes every hour and even every minute, which makes it almost impossible to analyze. Due to this conflict, analysts take the demand figure as an average value, which constitutes one of the main assumptions of all MARKAL/TIMES models. Uşak high-resolution TIMES model is an hourly model that can handle this problem and provides the researcher with valuable insight into how the energy generation system answers the instantaneous changes in the local energy demand. From this point of view, the paper adds a significant contribution to energy literature, especially for regional modeling cases.

3 Analysis of Scenario Results

The total primary energy supply of the region is almost multiplied by two from 17,4 to 30.92 PJ between 2016-2031, giving 5,28 to 10.42 PJ as the final electrical energy output. An increase in input energy is found as %78, while the output increase has geared up to %97,3 during the period. Output electrical energy has a tendency to pass the annual demand slightly some of the given years, which alerts the analysts for a possible grid stabilization problem. The mechanism of answering the hourly demand is prone to errors due to its nature. Some of the power plants are run as much as they can produce since the YEKDEM subsidy finances those assets with significant amounts and pre guaranteed purchase agreements. On the other hand, coal and natural gas power plants do not have pre guaranteed purchase agreements similar to YEKDEM. As a result, these plants can only answer the demand amount (if exists) after the YEKDEM power plant output is subtracted from the overall demand. If the amount of YEKDEM subsidized power plants' output surpasses the overall hourly demand, generators do not stop and keep up working at full capacity, causing an electrical energy amount to occur at that given hour for exportation purposes. This amount of energy is the direct cause of the positive difference between the hourly electricity generation and the hourly demand in the export positive years. If the energy generated by YEKDEM subsidized power plants is insufficient and extra energy is required, then the unsubsidized power plants are expected to be engaged in the system in the given hour to answer that remaining demand part. As a general rule, as high the renewable power plant capacity is, that hard it is to balance the grid.

The model outputs show that a lignite power plant is an optimum solution for electricity generation in the period. The installed power bars of the given technologies favor the investment on the lignite power plant in the region since the green bar steadily rises throughout the years in Fig. 1. However, this can be slightly decisive. The amount of renewable energy investments in the region is limited to a certain extent. Wind power capacity of Uşak is 0.057 GW and 0.054 GW of this capacity is already

utilized by 2015. 0.003 GW, which is the only capacity to be used, is also evaluated by the model at the beginning and added to the existing capacity reaching full wind capacity in 2016. Similarly, solar, biomass, and geothermal capacities are bounded to 0.05 GW maximum potential capacities, and all of these capacities are utilized in the same year, reaching full capacity in all renewable assets. Just after these capacity investments, no further improvement is possible as renewable capacity development in the region and GAMS optimizer uses fossil technologies to answer the remaining electricity demand with the least cost finalizing the deal with the coal power plant. The program chooses the lignite power plant as the best option in a feasible fossil power plant portfolio and uses this technology until 2031 to match the demand figures. A very small amount of combined-cycle natural gas power plant is invested in small amounts every year too. So briefly, the model increases the installed capacity of the lignite and combined-cycle natural power plants every year because of the insufficiency in renewable power potential of the city after 2016.

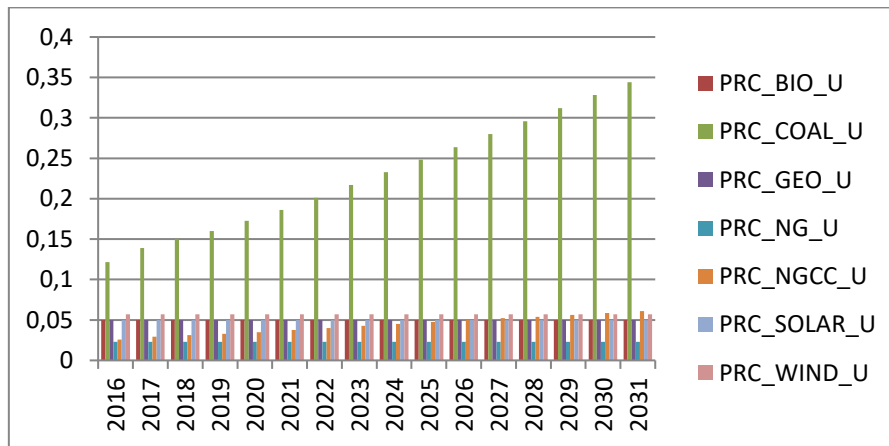


Fig. 1. Installed power figures of Uşak in the optimized plan

The environmental outcome of the base scenario is charted out in Fig. 2 below. %65 emission increase is recorded in 2031 when compared to the reference values of 2016. The investments on the lignite power plant directly affected the emission rates in the given era.

Using the advantage of the regulations on the subsidization of the renewables, Turkey has invested heavily in renewables in the last ten years. On the other hand, the model presented in this paper excludes the subsidy and market interrelations for the sake of simplicity, and instead, the least cost logic is applied in the scenario. The market price of the energy generated by the renewables is constant under RERSM. As the amount of energy increases from these assets, the amount of financial burden caused by RERSM also increases. This tradeoff caused a series of debates in the energy environments in Turkey since the subsidy was first initiated.

New capacity investment costs are excluded in the base model. This cost item is different for each sort of energy generation technology and shows great variation

from 500 to 4500 m\$/GW. The return on investment values of each power plant is viable in the power plant useful life periods. As a result, including the investment cost with the given variation would be unfair and wrong for the optimization process. Since these costs are not included an extra spreadsheet work would be needed for the calculation of the financial perspective of the base scenario. Calculations show that the existing power plant payments cost 195,6 million US dollars until 2031. The new investments for a self-sustainable energy system in Uşak need an additional 1329,3 M US dollars in the same time-span.

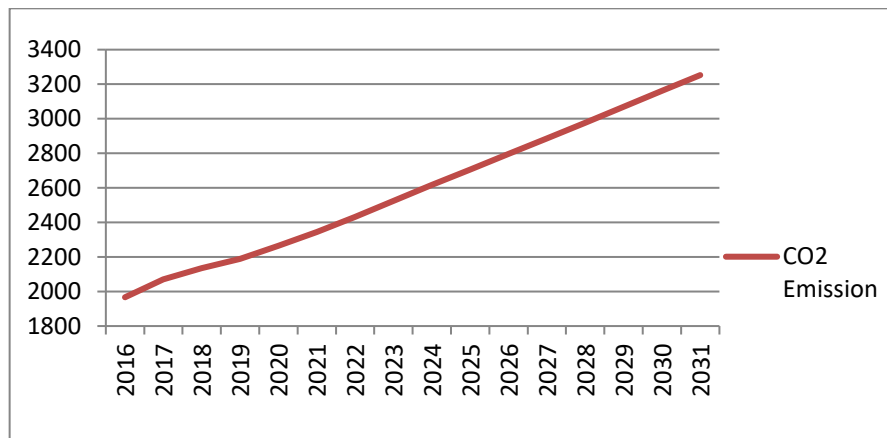


Fig. 2. CO2 Emission values of the optimum plan

4 Conclusion

TIMES is a flexible tool for researchers who want to work on annual and even hourly analysis. This paper presented a BAU what-if scenario, which may be a valuable base for further works. As a next step, various scenarios can be developed for the Uşak region by applying additional required constraints in some energy technologies according to the desired purposes. Current personal computers are capable of handling hundreds of operations in single seconds, and personal laptops can process not only annual models but hourly models like the model included in this study. From this point on, new and more detailed regional and national studies should be expected to be published soon.

This study presents the technological and environmental outcomes of the self-sustainable Uşak scenario. Unlike most studies, the model was designed in an hourly manner, and this feature lets the researchers include the deep and peak energy states of the region in high time resolution, which cannot be done at the annual level.

Outcomes of the base scenario utilized all the available renewable potential in the region, and as the demand grew bigger, fossil supplies are significantly financed. An excess amount of energy tends to occur during the hourly utilization, and the amount of this excess capacity should be an interesting topic for decision-makers. Electric

vehicles are expected to be insignificant numbers shortly. So charging the batteries of these vehicles and charging needs of other assets emerge as a big problem before the energy supply sector. Neatly designed scenarios on finding the optimum costs of these charging needs in well-chosen periods is an important working area currently, which demands interdisciplinary studies. The excess energy of the hourly base scenario in renewable energy-rich provinces is a strong candidate to be analyzed for related purposes due to stabilizing problems.

Hourly optimization analysis is so few in energy literature. Further scenarios can be developed in this study to provide more in-depth knowledge to decision-makers. A base scenario is developed in this paper which constitutes a basis for comparison with alternative scenarios to be built. As the cost of renewable energy technologies decreases significantly over the years, cheaper PV or wind energy scenarios can be developed to see financial and environmental differences with the base model presented here. In this respect, new hourly models and scenarios will be highly valuable for decision-makers and local authorities as well as the national policymakers.

Acknowledgments

The findings in this paper result from a research project with project number FDK-2019-6839 and is supported by the Scientific Research Projects Coordination Unit of Süleyman Demirel University, Turkey.

References

1. Sulukan E., Sağlam M., Uyar T. S., Kırılıdoğ M.: Determining Optimum Energy Strategies for Turkey by MARKAL Model, *Journal of Naval Science and Engineering*, 6:27-38,2010.
2. Eo, G. GEF Country Portfolio Evaluation: Turkey (1992–2009). Global Environment Facility Evaluation Office, Washington, (2011).
3. Köker U., Koruca H.İ., Sulukan E., Uyar T.S., Calculating the Levelized Cost of Electricity by an Urban Scaled Simulation Approach, 9th International 100% Renewable Energy Conference, 24-26 April 2019, İstanbul, Turkey.
4. 17. Turkish Statistical Institute, 2019 Population of Uşak, <http://www.tuik.gov.tr/>
5. Rahimi, A., Deroover, M., & Jimenez, I. (1989, August). Electric power system planning in the framework of the overall energy system. In *Proceedings of the 24th Intersociety Energy Conversion Engineering Conference* (pp. 2943-2948). IEEE.
6. Yang, C., Yeh, S., Zakerinia, S., Ramea, K., & McCollum, D. (2015). Achieving California's 80% greenhouse gas reduction target in 2050: Technology, policy and scenario analysis using CA-TIMES energy economic systems model. *Energy Policy*, 77, 118-130.
7. Sulukan E., Sağlam M., Uyar T. S., Kırılıdoğ M.: A Preliminary Study for Post-Kyoto Period for Turkey by MARKAL Model, 5th International Ege Energy Symposium and Exhibition, 27-30 June 2010 Pamukkale University, Denizli, Turkey.
8. Noble, K. (2006). Enhanced timeslices, technology filters and ADRATIO Rules, MARKAL/ANSWER updates (15 August 2006). Australia: Noble-Soft Systems Pty Ltd.
9. Kannan, R. (2011). The development and application of a temporal MARKAL energy system model using flexible time slicing. *Applied Energy*, 88(6), 2261-2272.
10. Kannan R., Turton H.: A Long-Term Electricity Dispatch Model with the TIMES Framework, *Environmental Modelling and Assessment*, 18:325-343, 2013.
11. Taktak, F., & Mehmet, I. L. I. (2018). Güneş Enerji Santrali (GES) Geliştirme: Uşak Örneği. *Geomatik*, 3(1), 1-21.
12. Aydin, N. Y., Kentel, E., & Duzgun, S. (2010). GIS-based environmental assessment of wind energy systems for spatial planning: A case study from Western Turkey. *Renewable and Sustainable Energy Reviews*, 14(1), 364-373.
13. International Energy Agency, Nuclear Energy Agency (2015). *Projected Costs of Generating Electricity 2015 Edition*.
14. United States Environmental Protection Agency, *Direct Emissions from Stationary Combustion Sources*, January 2016.
15. Official Site of Zorlu Enerji, <https://www.zorluenerji.com.tr/fileuploads/kizildere/teknik-olmayan-ozet-tr.pdf>, last accessed 2020/03/20.
16. Official Site of EnergyPLAN, https://www.energyplan.eu/useful_resources/existingcountrymodels/, last accessed 2020/03/20.
17. TMMOB Makine Mühendisleri Odası Enerji Çalışma Grubu, Elektrik ve Doğal Gaz Fiyatlarına Yapılan Son Zamların Analizi, https://www.tmmob.org.tr/sites/default/files/elektrik_dgaz_zam_analizi.pdf, 13.08.2

An Onshore Wind Farm Design in Büyükada via WindSim

Emre Leblebicioğlu¹, Tanay Sıdkı Uyar¹

¹Department of Mechanical Engineering, Marmara University, Eğitim Mahallesi, Fahrettin Kerim Gökay Cd., Istanbul, 34722, Turkey

leblebicioglu.emre@gmail.com

Abstract. Electricity generation by wind farms plays a key role in the clean energy transition, such that wind energy leads the renewable electricity production together with solar energy (except hydropower) in the whole world. Hence, wind farms that have a high capacity factor are significant to accelerate the transition from carbon-based energy production to the clean energy. Therefore, well-designed wind power plants or wind farms is a necessity to use the selected wind farm field efficiently and to obtain a high capacity factor. Although there are a lot of designing parameters of WFs, some software programs guide us to design WFs. In this study, optimal WFs design for Büyükada was carried out by using WindSim software program.

Keywords: Wind Farm, Wind Power Plant, Wind Energy, WindSim, Büyükada

1 Introduction

Nowadays, all world is facing a serious problem known as global warming which threatens all living beings on the Earth. Energy generation by fossil fuels plays one of the main roles to increase carbon emissions that cause climate change together with fossil fuel-based vehicles, growing population and industrialization. Thus, the decreasing carbon footprint is significant to deal with the climate change. The Paris Agreement's long-term temperature goal is to keep the increase in global average temperature to well below 2 °C above pre-industrial levels and to pursue efforts to limit the increase to 1.5 °C, recognizing that this would reduce the risks and impacts of climate change.

Renewable energy systems lead the clean electricity generation zero carbon emission implementations. Furthermore, a total of 181 GW renewable power was added in

2018. Also installed renewable power capacity reached 2378 GW, according to REN 21 Global Status Report [1]. Even though progress in the renewable energy industry, the all-world is still not far away to meet the targets of the Paris Agreement. Since global energy-related carbon dioxide emissions went up an estimated 1.7 % in 2018 because of increased fossil fuel consumption in the industry and transportation.

Wind energy has a critical role in the clean energy transition such that wind power capacity accounts for more or less 25 % of renewable power capacity. Wind energy is commonly used to produce electricity nowadays. There are a lot of wind farms that are spread to various terrains even on the sea or ocean in the whole world. The global installed capacity of wind power plants is nearly 591 GW worldwide. [1]

Turkey has a huge amount of energy demand as a developing country and this demand is increasing day by day. Turkey has a dependency on foreign-sources to generate electricity. Because domestic fossil fuel reserves are inadequate to supply the energy demand. Turkey needs to increase its renewable energy capacity to reduce foreign-source dependency. Thanks to Turkey's geographical position, renewable energy capacity in Turkey is huge.

It is undeniable the fact that wind power is important for the deployment of renewable power capacity. Especially developing countries that have an immense wind potential like Turkey have increased their investments in the wind energy sector. A total installed capacity of wind power plants (WPPs) in Turkey reached 7.369 MW in 2018. [1]

As shown in Fig.1, installed wind power capacity has been increasing each passing year.

According to Turkey's development plan, Turkey aims to increase rapidly its wind power capacity next years.



Fig. 1. The capacity of Cumulative Installed Wind Power Plants in Turkey by years [3]

Raising the capacity of wind farms (WFs) shows the importance of designing WFs over a limited area. Wind turbines (WTs) should be well-installed on a selected area to get the most efficient electricity production during a year. Designing a wind farm (WF) is implemented to compute the optimal placement of each WT over the terrain.

However, a lot of wind power plants are installed with many failures due to lack of efficient wind turbine placement over the terrain, site analyzing, wind source estimation etc. [2]

In this article, designing of a WF was successfully done for Büyükada. The main purpose of this study is to show the annual wind power generation capacity of planned WF.

2 Material and Methods

The selected area for the wind farm is Büyükada which is an island on the Marmara Sea. Although, this island is not far away from the nearest coastal, electricity is one of the biggest problems. Approximately 7500 people live on the island and this population increases especially in the summertime due to foreign and domestic tourists. Hence, the energy demand of Büyükada shows changes during the year. Estimated annual average electricity consumption is roughly 3.65 GWh. The size of Büyükada is 5.461 km² and this is relatively small. Thus, the placement wind turbines on a limited area is important. Overview of Büyükada is shown in Fig.2 below.

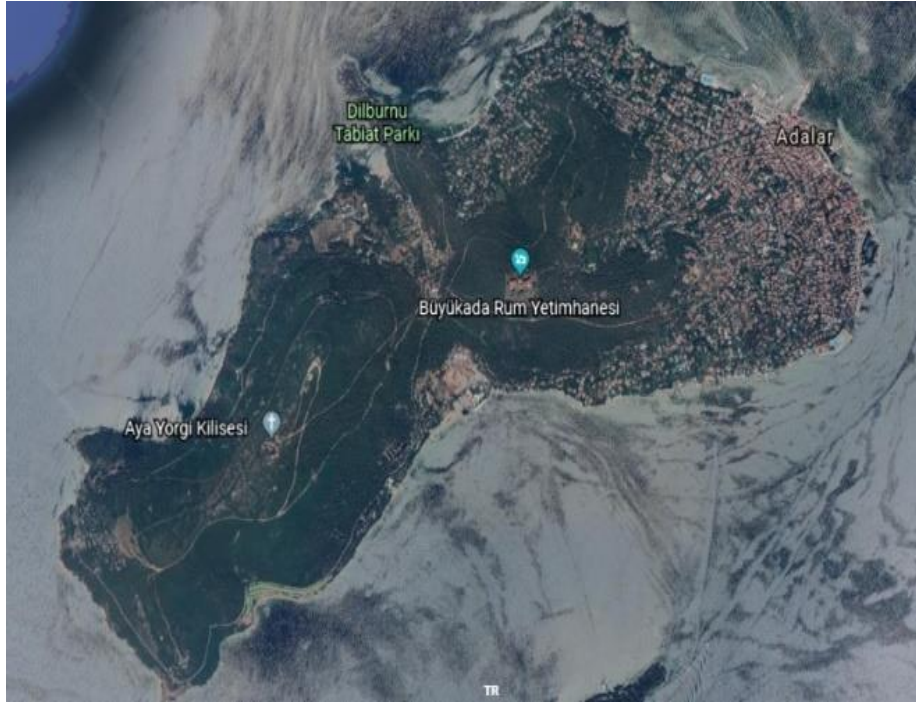


Fig. 2. Overview of Büyükada

There are various parameters to design a WF, such as wind speed, wind direction, surface roughness, location of the selected area etc. Maximum capacity factor is obtained only with decent wind analysis and well-designed power plant. In the first step of this study, Büyükada wind potential which contains hourly wind speed and wind direction data during a year were evaluated. Secondly, the estimated annual electricity consumption of Büyükada was obtained to determine the capacity of wind turbines. Thirdly, optimal specific locations were determined to place selected wind turbines on the area. Lastly, all the information was inserted to WindSim software to compute results. There are also different steps to get the right results in WindSim.

WindSim is a modern Wind Farm Design Tool (WFDT). WindSim is used to optimize the energy generation of the wind power plant while at the same time keeping the turbine loads within acceptable limits. This is achieved by calculating numerical wind fields over a digitalized terrain. In the wind energy sector, this is called micro-siting⁴. WindSim designs the wind farm with 6 modules. These are Terrain, Wind Fields, Objects, Results, Wind Resources and Energy.

Energy module of WindSim is the most important part for the feasibility of the wind farm. The result of this module gives the estimated annual electricity production for WF.

3 Designing Wind Farm by WindSim

3.1 Terrain

The first step of flow field simulation is the generation of a 3D model of the selected area for the WF design. This is carried out in the Terrain module in WindSim. but first, .gws file which is a special file format of WindSim, is obtained by WindSim Express tool that is a file generation for WindSim. [4]

Digital terrain model is obtained as Fig. 3 by the coordinates of Büyükada. Moreover, digital roughness map is created as shown in Fig. 4.

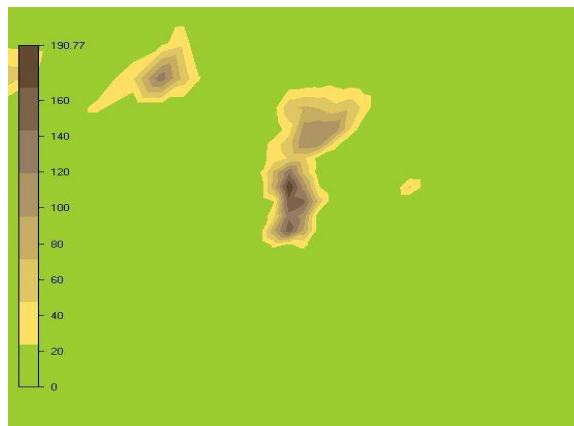


Fig. 3. Digital terrain model - Elevation (m)

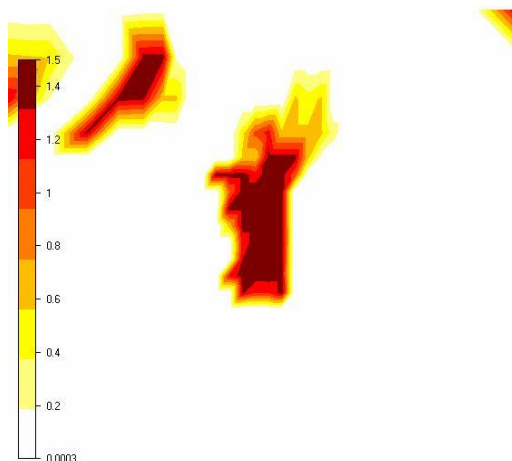


Fig. 4. Digital terrain model - Roughness height (m).

3.2 Wind Fields

The Wind Fields module is based on the computation of Reynolds Averaged Navier-Stokes equations (RANS). Moreover, the standard k-epsilon model is applied as a turbulence closure. According to the results of the 3D model in the Terrain module, the simulation of the Wind Fields module can be started. The solution procedure is iterative since the equations are non-linear. By using the initial conditions, the solution is progressively resolved by iteration until a converged result is obtained. [4]

Wind Speed 3D (u,v,z) on the terrain is as shown in Fig 5 below.

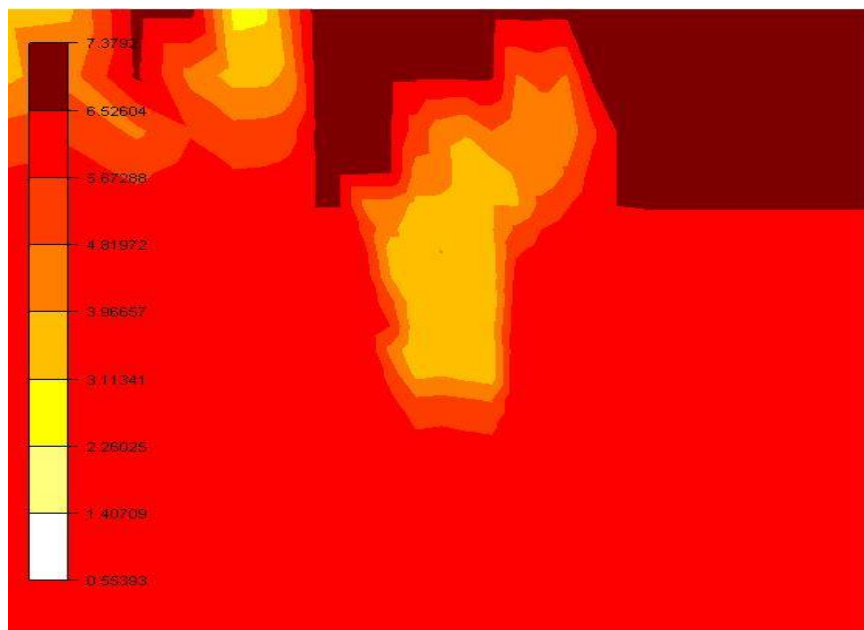


Fig. 5. Convergence monitoring: Wind speed 3D (u,v,w)

3.3 Objects

The Objects module is used to position turbines and to process the climatology file. For visualization purposes, various geometrical objects can also be placed within the 3D terrain model. The exported wind turbines and climatology files by WindSim Express is imported to the WindSim software in this module. [4]

Wind turbine model of this project is Gamesa G90 2 MW. Two of these turbines were placed on the terrain by the Object module, considering parameters such as surface roughness and elevation values that affect the efficiency and capacity factor of the WF.



Fig. 6. Park Layout of Wind Farm

3.4 Results

The results of the wind field simulations are stored in a reduced database covering the vertical extension from the ground up to the "Height of reduced wind database" as specified in the Wind Field module. The Result module extracts 2D horizontal planes from this database. [4]

To sum up, this module shows us the result of climatology data on the selected area unlike Wind Fields module. Also, the module illustrates data that is imported to the software.

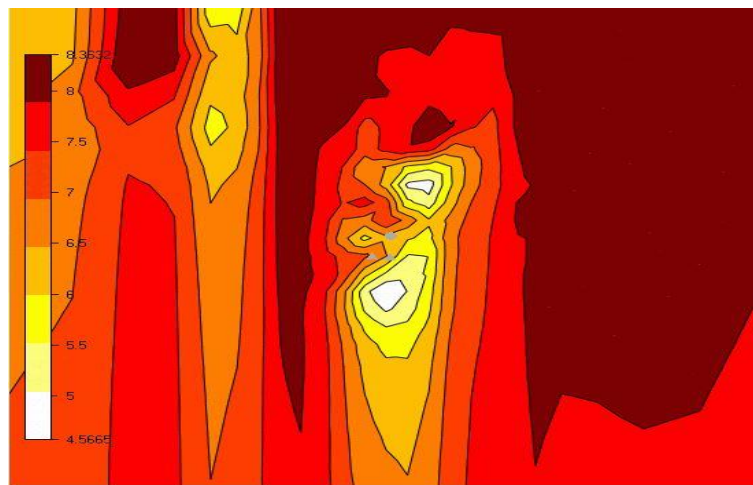


Fig. 7. Wind speed 3D (u,v,w), Not Normalized

3.5 Wind Resources

The Wind Resource module contains a tool for area classification. Finding high speed connected areas where the areas are grouped according to the wind speed and size. The possible power production in the area is also estimated. [4]

Wind speed 3D is shown in Fig. 8 and power density is shown Fig.9 below. This module is the result of wind blockages, elevation, roughness and turbulent areas on the field.

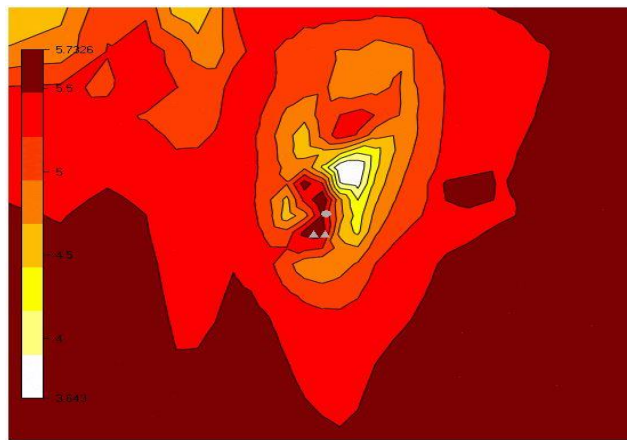


Fig. 8. Wind speed 3D (u,v,w), Not Normalized

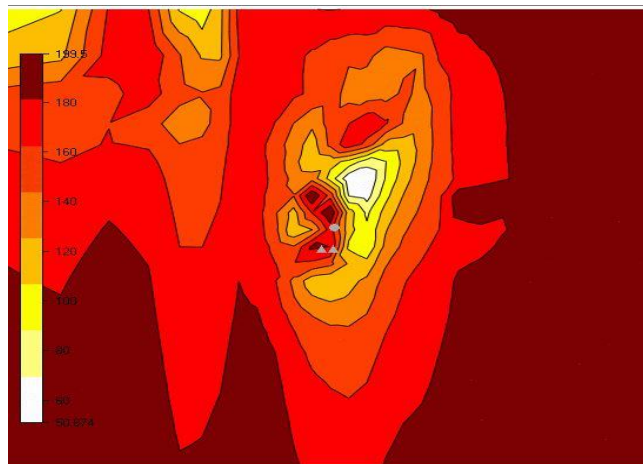


Fig. 9. Power Density (W/m²)

3.6 Energy

The annual energy production (AEP) is calculated for all visible Turbine objects that are placed on the field. If several climatology objects are available, the AEP based on each climatology is calculated separately. Any discrepancies between the AEP's based on different climatology are easily accessible.

A climatology is given by its frequency distribution and presented graphically in the wind rose. Additionally, a climatology is given by its Weibull distribution. The AEP is calculated for both representations.

name	power (kW)	hub height (m)	density (kg/m ³)	wind speed (m/s)	wind speed including wake losses (m/s)	power density (W/m ²)	gross AEP (MWh/y)	AEP with wake losses (MWh/y)	wake loss (%)	full load hours (h)
wecs1	2000	100.0	1.225	6.20	6.20	250.3	4146.5	-	-	2073.2
wecs2	2000	100.0	1.225	6.27	6.27	262.7	4261.2	-	-	2130.6
All	4000	-	-	-	-	-	8407.7	-	-	2101.9
Mean	-	-	1.225	6.23	6.23	256.5	-	-	-	-
Reference production at climatology position: vortex_time_series_80m										
ref..	2000	100.0	1.225	6.21	-	251.8	4152.3	-	-	2076.1
ref..	2000	80.0	1.225	6.02	-	226.8	3846.5	-	-	1923.2

Table 1. Energy production based on the frequency table.

As can be seen in Table 1, each turbine has the potential to produce about 4200 MWh per year. Also, the total annual electricity generation is roughly 8400 MW.

Memorize that estimated annual electricity consumption of Büyükada is 3650 MWh. Thus, wind turbines can be able to supply this electricity demand and excess electricity can be exported to the other region in Istanbul.

Capacity factor of this WF is calculated as shown below.

$$\text{Capacity Factor} = \frac{8,4 \text{ MWh/y}}{(24 \text{ hours/day}) * (365 \text{ days}) * 4 \text{ MW}} * 100 = 24 \%$$

Average capacity factor of onshore WFs is between 25 % and 35 %. In this project, the estimated capacity factor was calculated as 24%. In this project, the optimal wind farm was designed by considering environmental effects and the limited available area. WF was not placed close to residential zone, instead, it was located in a field where surface roughness is high. For these reasons, the estimated capacity factor of WF is lower than average.

4 Conclusion

In this study, the most realistic results were obtained by the advanced software for the planned wind farm in Büyükada. According to these results, a wind farm can supply electricity demand of Büyükada. But, in this study, initial, maintenance and operational costs were not considered. Since Büyükada is an island, it is obvious that an initial cost of WF can be close to offshore WF. Off-shore WF was not designed and considered in this study but this option should also be examined for designing a WF for islands. The focus of this study was to design onshore WF for an island using WindSim.

There are also more things that can be considered to design a WF such as the distance between turbines and electrical grid (transformer) and transportation of wind turbine components (Nacelle, Tower and Blades). Because the selected area is the island, transportation is a tough challenge to deal with. In this study, the main focus was micrositing and power production capacity of WF on the selected area.

As a result, Windsim and similar wind analysis software are significant for pre-installation of a wind farm. These type of software tools must be used for designing wind power plants. This study is now a unique example for designing onshore WF in an island using WindSim.

References

1. Renewables 2019 Global Status Report. Ren21
2. Büşra Yakşı, Semih Akın, Yusuf A. Kara. A Wind Power Plant Feasibility Study For Bursa, Gemlik Region In Turkey By Windsim Software. International Journal of Energy Applications and Technologies Vol. 3, Issue 2, pp. 72 – 76, 2016
3. Turkish Wind Energy Statistic Report 2019. Turkish Wind Energy Association
4. Dr. Catherine Meissner. WindSim Getting Started 11th Edition. December 2017.

Integrating Wind Energy to Smart Grids

Burak Arıncı

Yıldız Technical University, Davutpaşa, ISTANBUL 34220, TURKEY

burakarinci333@hotmail.com

Abstract. Today, the fact the most people consider is that energy is the most critical and significant subject for surviving our mankind. This paper illustrates the importance of smart grids to distribute electric energy systems for a better future and also shows the effects of renewable energy on it. Although it is a new issue, smart grid is far better and more productive than classical Electricity Transmission and Distribution Systems. The efficiency of this system can be picked up and surged by utilizing Renewable Energy Sources. The research which we worked on it, gives examples and explanations about integrating renewable energy sources to smart grid systems, especially wind turbines with different types of generators. By using method of comparisons through generators' efficiency with the perscrutation on the flexibility and effects of wind turbines in the context of smart grids.

Keywords: Wind power, Smart grids, Power quality, ETDS, Wind turbine, Renewable energy, DFIG, SCIG, PMSG

1 Introduction

The conventional wisdom is that, one of the greatest trouble for future's Energy Transmission and Distrubition Systems is efficiency. Not only leading the electric energy effectively but also draining away the traditional fuel supplies have put us for researching new areas such as renewable sources and developing new methods like smart grid. Despite being novice, wind energy takes a large place for increasing smart grids's efficiency in a very good way. Analyzing the areas of integrating this alternating source by using different types of generators and effects to the smart grids, it is showed clearly the significant value of wind energy. The integration of wind turbines into intelligent networks is a revolution in both the future electricity market and all energy sectors. In addition to the fact that wind energy is a very clean energy type and also the maintenance costs are very low, the great efficiency provided for the Smart Grid Systems has inevitably been used in Smart Grids. The use of wind energy in Intelligent Network Systems which has an interactive relationship between demand side power generation is a great revolution of our time and also great opportunity for the electricity sector.

2 Smart Grid

2.1 History of Smart Grid

Clean and controllable energy thought led the Smart Grids to pop-up by dedicated engineers. In 2003, the term of Smart Grid has been announced as a word. Smart Grid is the way which is monitored through power generation, transmission and distribution by a central system. This long-term change in the process of electrical engineering, has created new areas such as T&D technologies, automation and controlling programmes, intelligent sensors, smart meters etc.

2.2 Main Motivations of Smart Grid

Losses in the classical Electricity Transmission and Distribution System are one the greatest motivations for advancing the infrastructure of ETDS. On the other hand, Carbon Emission is a critical case for this new area. Moreover, aging factor is also significant issue for shifting to the old infrastructure of renewed Electricity Transmission and Distribution System. Whole these reasons above have been set up onto thinking of future's Smart Grid development.

The desire to balance produced and consumed electricity has been one of the main motivations for the adapting of intelligent networks to old lines. However, there are many different types of little motivations, the focus on leveraging the distribution grid management and transmission systems take a very large place within that advancement. Among all these motivations, renewable energies are the most important structure that can provide all these possibilities. In this work, we will try to examine the most important of these renewable energies, namely the integration of wind energy into intelligent networks.

Table I. Comparison between smart and current grid [1]

	Current Grid	Smart Grid
Communications	None or one-way	Two-way, real-time(fast)
Customer Instruction	None or limited	Extensive
Operation & Maintenance	Manual, time-based	Remote monitoring and diagnostics, predictive
Generation	Centralized	Centralized and distributed, substantial renewable resources, energy storage
Power Flow Control	Limited	More extensive
Reliability	Based on static, off- line models and simulations	Proactive, real-time predictions, more actual system data
Restoration	Manual	Self-healing
Topology	Mainly radial	More network

3 Wind Energy

Despite being important, defining most of the advancements in smart grid technology within its one aspect, smart meters which can interconnect both providers and customers, is not enough to get the importance of this new area. Necessity of not only better standards of serving electricity or more reliable system, but also a cleaner environment and budget friendly power. Being cost-competitive with other sources, offering different job opportunities, existing as an inexhaustible way of energy, requiring less maintenance and operating costs have given a vital role to wind turbine energy in the scale of smart grid progress.

3.1 Wind Energy In Smart Grid Context

Lots of advancements in smart grid usually called as its one aspect "smart meters" but this technology not only offers a better reliable electricity system but also looks for a cleaner environment and lower costs. On contrary, being kinda expensive, renewable energy systems are good for cleaner environment. Environmental, economical and maturity factors are really important for preferring renewable energies to integrate smart grid systems. Although the economical benefits of wind energy is a contradictory case, the wind technologies are still in its newly stages. It is believed that in the long view, optimizations of wind energy systems will have been enhanced.

3.2 Wind Turbine Generators

In the past, there were two types of wind turbines which are fixed speed and the variable speed. But at the present time, with new challenges in use which is defined the variable speed wind turbine is a bit different. The main purpose of this to enhance maximum aerodynamic efficiency with a very big scale of wind speed. Generally it is utilized with three rotor blades, horizontal axis design and a generator which is placed in the nacelle. Three types of different generators are used and they are; Doubly Fed Induction Generators(DFIG), Squirrel Cage Induction Generators(SCIG) and Permanent Magnet Synchronous Generators(PMSG).

3.3 Comparison of Three Types of Generators

- Despite being simpler than other generator types, rugged and brushless, reaching to about %30 of synchronous speed, compensating reactive power and ensuring smooth grid integration and considering high efficiency and yield, DFIG still includes some problems just like gearbox which causes bearing malfunctions and also some difficulties related in complying with grid fault ride-through.
- On the other hand, having a huge popularity of its mechanical simplicity and robust constructions moreover, with a rotor bars which are very well resistant to vibrations and dirt, SCIG types require two full scale converters and do not function as a multi-pole direct drive mode without gearbox.

- There are great advantages of PMSG such as lower maintenance cost due to elimination of gearbox, developed reliability and longevity appears with the absence of the gears and bearings which are by themselves the main reason of faults in the generators. Furthermore, lower weight, high efficiency and yield are perfect benefits of PMSG. However, using permanent magnet brings unignorable cost and it is almost twice size of that of the conventional geared- drive SCIG, by the way being a new technology names it as low maturity. All of these reasons cause a mass and weight that can reach to critical proportions especially for above 3MW.

Table II. Annual energy yield / total cost of three different wind generator systems. [3]

COST (EURO)	Generator Types		
	SCIG	DFIG	PMSG
Gearbox	220	220	-
Converter	120	40	120
Generator cost	287	320	432
Total cost with margin for company costs	1837	1870	1982
Annual energy yield MWh	6705	7690	7890
Annual energy yield/total cost	3.63	4.11	3.98

3.4 The Future of Wind Generators

In overall, reliability, efficiency and availability are significant requirements, so that the direct-drive PMSG comes into play because of ignoring the gearbox, that is very important to increase its usability especially in off-shore applications. PMSG are usually big but there is no problem of land and space hindrance for off-shore systems. It is expected that with a conceivable economical optimization, PMSG highly possible to will have seen in a large scale of wind industry area more than other types of generators.

4 Wind Energy Against The Backdrop Of Smart Grids

4.1 The Economy of Wind Energy

Although the economy of wind energy systems is still a controversial topic, it is a new field and is believed to develop. Despite there is no fuel need, wind turbines come at cost that is still on the same line with classical energy sources. Expectations about wind energy's future mostly searching new areas which reduce these highest costs, there are a lot of initial factors to eliminate it such as omitting gearbox and utilizing much cheaper power electronics circuits to connect the grid- side.

4.2 Adaptation of Wind Energy Through Smart Grids

The environmental aspect of wind power is very clear. There is no pollution by bringing almost zero environmental impact (birds, noise etc.) which make wind one of the greatest choices to use in this new term, in smart grid technologies.

To control whole electrical system in the context of smart grid such an important case. Hence, the predictivity shines out right over there. Calculating all power generations and knowing the demand side through customers and matching them perfectly are one of the main subjects of smart grid technologies, indeed, the wind is variable and generally predictions of weather patterns are only good for just 48-72 hours, still the wind energy is very electable cause the loads are also very variable and the study of smart grid technologies is matching these variabilities voluminously.

Thus, if a smart grid would optimize the fluctuations in the wind and match them with the load, constantly adjusting the distribution of the load to the wind turbines able to generate power, the penetration of the wind in the system can rise up.

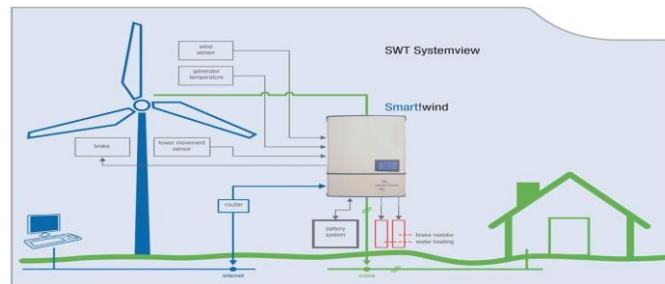


Fig. 1. The connection between a wind turbine and a household in the context of smart grids. [4]

4.3 Intelligent Wind Converters

If we consider that main generators which used in wind energy systems are PMSG and DFIG. Both requires power electronics circuits to connect grid-side. Hence, the importance of converters which generally AC to DC then AC again, pops up. Through years, the expectation of the advance in power electronics may have changed the way of integration the wind energy to smart grid systems. And also, to control reactive power and harmonics of the grid are problems which appear in a large scale. In DFIG, to supply variable frequency while wind turbine rotating in a variable speed, it is used partial converters. In spite of that, PMSG need full-scale converters, for growing off-shore systems where low-maintenance is one of the critical issues, PM machines are selected ones. With whole integrations combined, off-shore systems, partial load applications, high rated power and low maintenance costs call for medium voltage(MV).

Reactive power compensation, power factor improvement, and dynamic var support become more important than ever due to the continuing efforts to improve the voltage profile, power quality, and to reduce power losses. Smart grids will require the energy sources, like wind turbines to provide them with full var management, from leading to lagging power factors, dynamically, with fast response times.

4.4 Interconnection Wind Power to Grid

It is of utmost importance that the alternating current systems are installed close to the transformer centers in the applications of terrestrial wind turbines. However, switching power AC converters from AC to DC and then back to AC is a very important application for reactive power compensation and control of harmonics. The demand side control, despite the variable speed, to properly adjust the rotor and grid-side frequencies has a critical position in adapting the wind turbines to the smart grid. Advanced wind energy technology with commercially available network management systems, power electronics, medium voltage switchgear, network interconnect solutions, cable technologies and Energy Storage features developed for wind farm applications, efficient, reliable and environmentally friendly smarter network operation. Over the years, as the permanent magnet synchronous generators become more economical, wind turbine systems will become more economical, more beneficial and more advanced to the environment. The developments in the power electronics industry will undoubtedly facilitate the integration of the wind power into the network.

5 Conclusions

In this paper, the importance of wind power and wind turbines have been analyzed in terms of its different generator types and their efficiency and flexibility on smart grid systems. It is believed that by developing technology and smart power electronics' systems, wind turbines would take a large place within new smart grid technologies. When the economical problems of wind turbines disappears, their usability is going to rise up day by day.

In this context of wind energy and smart grids, it has been seen that for providing more flexibility and a safer potentiality to control the whole electricity grid, will be an initial case for the future's new technological systems. Renewable energy sources could easily supported by smart grids to control and make them more beneficial. Further studies will show us their benefits for sure.

References

1. Mietek Glinkowski, Jonathan Hou, Gary Rackliffe.: Advances in Wind Energy Technologies in the Context of Smart Grid. Journal 99(6), (2011).
2. RedE.E.,http://www.ree.es/sites/default/files/11_PUBLICACIONES/Documentos/Renewable-2016.pdf
3. H. Polinder, F. F. A. van der Pijl, G.-J. de Vilder, P. Tavner.: Comparison of direct-drive and geared generator concepts for wind turbines. CONFERENCE 2005, in Proc. IEEE, pp. 543–550.
4. Smart Power Electronics, <http://www.smart-power-electronics.de/cms/en/products/smart-wind>
5. G. Köktürk, A. Tokuç.: Vision for wind energy with a smart grid in Izmir, July(2017)
6. A.Beainy, C.Maatouk, N.Moubayed, F.Kaddah.: Comparison of Different Types of Generator for Wind Energy Conversion System Topologies. CONFERENCE 2016, in Proc. IEEE, 13-15 July (2016).
7. A.Slimen, H.Tlijani, M.Dhaoui, R.B.Younes.: Intelligent Control of Wind Pump Based on PMSG Using Pitch Control, CONFERENCE 2017, in Proc. IEEE, **INSPEC Accession Number:** 17415423, Marrekech(2017)
8. S.Paul, S. Rahman, A.Rahman.: Wind Energy Integration in Smart Grid, International Journal of Scientific & Engineering Research, Volume 5, Issue 11, November(2014)

Increasing of Binary ORC Geothermal Power Plant Efficiency by A Geothermal-Solar Hybrid Design

Fahri Karahan¹ and Füsün Tut Haklıdır ²[0000-0002-9469-8870]

¹ Sustainable Energy Systems Engineering, Queen Mary University, London, UK

² Energy Systems Engineering, Istanbul Bilgi University, Eyup, Istanbul, Turkey

fusun.tut@bilgi.edu.tr

Abstract: Geothermal energy is one of the most sustainable and renewable energy options. The selection of the geothermal power cycle technologies directly depends on the geothermal reservoir temperature, geothermal reservoir type and non-condensable gas amounts. Binary ORC is the most used technology in geothermal power industry. However, like any other renewable energy systems, ORC cycles have also some challenges during the operational phase of a geothermal power plant such as; high ambient temperature, medium reservoir temperature and scaling in heat exchangers. To handle the challenges, the solar- geothermal hybrid systems with thermal energy storage unit is one of the most promising solutions. Geothermal-solar hybrid systems with TES have a positive effect on the main overall system efficiency.

Turkey has great geothermal power capacities in the Western Anatolia (WA). However, most of companies prefer to install binary ORC type geothermal power plants. These are compact and generally small size power systems and the reservoir temperatures under 200 °C supports to use ORC technologies at the most of geothermal fields in the WA. However, it is known that the ambient temperature can reach to 40 °C in the WA in summer periods and the efficiency of the ORC plants may reduce up to 40 % due to air cooled condenser systems.

In this study, Gümüşköy GPP is selected as a case study which has medium temperature reservoir. To increase fluid temperature, solar collectors are added as the auxiliary heat source. In this study, it is recommended that residual heat which is collected by solar collector must be stored in the TES which phase change material to minimize heat loss. In this design, the stored heat is added to the fluid when solar radiation is no more available to collect by the collectors.

Keywords: Geothermal energy, ORC, Solar, Thermal energy storage, Western Anatolia

1 Introduction

Geothermal energy is one of the renewable, sustainable, and environmentally friendly source and good choice with the high capacity factors for electricity production. Turkey is an important player for geothermal power production; in 2020, it had more than 1.5 GWe installed capacities at geothermal power market and the Turkish government has declared that the geothermal power target will be 4 GWe for 2030 (Haklıdır Tut and Şengün, 2020).

Between 1984–2019 period, around 50 numbers geothermal power plants were installed along the Büyük Menderes Graben and Gediz Graben in Western Anatolia. Most of the power plants are located at between Denizli (Kızıldere town), Aydın (Germencik, Salavatlı, Köşk, Pamukören towns) and Manisa (Alaşehir, Salihli towns) provinces. In Turkey, most of the geothermal power plants utilize an ORC binary cycle system while a few using flash and advanced geothermal systems for power production (Fig.1).

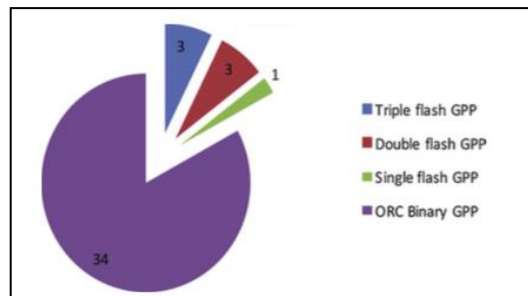


Fig.1. Number of geothermal power plants, by type, in Turkey (Haklıdır Tut and Balaban Özen, 2019).

Although geothermal power production is a one of the green option and between 70-95 % capacity factor values based on the cycle types, the operational periods of them are critical to achieve the installed capacities of these power plants. Thermodynamic changes on geothermal fluids based on pressure and temperature from the deep zones of geothermal reservoirs to surface conditions may cause serious problems like mineral scaling, corrosion or steam quality, and discharge of non-condensable gases during the power plant operations at water-dominated systems (Haklıdır Tut and Balaban Özen, 2019). One other common problem has been identified as cooling systems of ORC binary cycles, which mostly use air-cooled systems in Western Anatolia also (Fig.2). Using air-cooled condenser system can reduce energy production of ORC binary geothermal systems especially in summer times. The outside temperature at air-cooled system has affected the performance of the ORC type power plant. Be-

cause, they are generally designed based on the average outside air temperature and when the outside air temperature is higher than the average value, energy production in the power plant has a lower than its actual design condition (Demirdağ et al., 2017). The second problem is lower reservoir temperatures than expected values in some geothermal fields.

In this study, one concept study is examined to use solar-geothermal binary ORC hybrid power system to increase energy production in Western Anatolia especially summer times.



Fig.2. An example for air-cooled type ORC binary power plant in Western Anatolia (Source: ORMAT website).

2 Solar-ORC Binary Hybrid System Possibility in Western Anatolia

Due to increasing of energy efficiency of the power plant there are several methods can be used. One of the method is to use different two energy sources in a one system such as called; hybrid energy system.

Most of the geothermal systems which of them are suitable for the power production have been located in Western Anatolia. However, some of the medium enthalpy geothermal reservoirs are not suitable to efficient power generation in Western Anatolia. Hybrid energy systems can contribute to these geothermal reservoirs to produce more energy. The main problem in medium enthalpy reservoirs is; geothermal fluid is not hot enough to produce steam from the source. If an additional heat source can be added to steam production systems, these wells will be able to produce steam from these

wells. Main problem is to add that additional heat source without of any fuel cost. Hybrid energy systems, which will use renewable sources, can apply that heat without of any fuel cost.

2.1 Revised Design for Solar-ORC Binary System in the Western Anatolia

In this concept study, an existing ORC binary geothermal power plant is selected to integration of hybrid system in Aydın province at Western Anatolia. The plant has been started to produce energy in 2013 and after a while, it is noticed that the plant could not to reach the installed capacity due to insufficient reservoir temperature condition in the field. The main problem was incoherence between the turbine design temperature and measured wellhead temperature. Because of the higher design temperature, there was a power out problem in the ORC-binary power plant.

The operator company was decided to install parabolic solar collectors to the existing geothermal system to increase steam temperature to generate more energy in the system. Geothermal fluid transfers to working fluid of ORC by the help of geothermal heat exchanger. After working fluid of ORC (R-134a) reaches to solar thermal heat exchanger by the heat of therminol-62 are transferred to R134-a by the helping of solar heat exchanger and temperature of steam reaches to better condition to produce more energy.

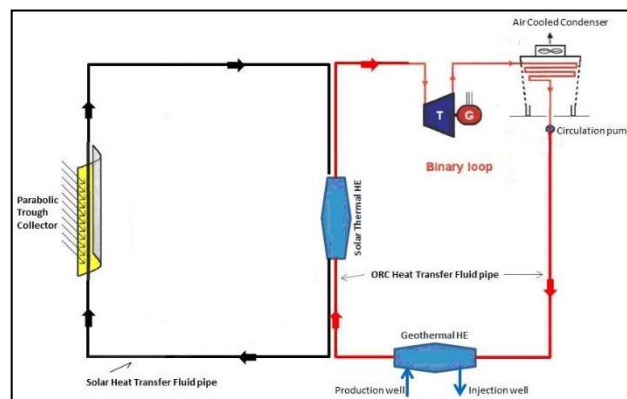


Fig.3. The revised hybrid design of the existing ORC power plant (Kuyumcu et al., 2012)

2.2 The Proposed Design of Solar-ORC Binary System in the Western Anatolia

In some geothermal fields, because of the climate and ambient temperature, air-cooled

cooling systems can reduce efficiency of the system. For example, in Stillwater hybrid power plant one of the important reasons for low efficiency is ambient temperature. Because of the ambient temperature, air cooled system cannot reduce temperature of working fluid and it reduce heat transfer ratio between geothermal fluid and R-134a. Moreover, solar collectors cannot generate heat at nights in a solar-geothermal hybrid power plant. To solve all these problems, thermal energy storage (TES) system is good option like in Stillwater power plant. By the help of thermal energy storage system, it will be able to use additional heat at nights. TES system consists of two main tanks (Fig.4). These are called cold and hot tanks. In the cold tank, the working fluid of solar cycle is stored and the fluid gains heat in solar system. After the solar system, if temperature of fluid is not in desired temperature for system, fluid is sent to the cold tank again to be heated again by solar collector. If the solar collector provides the desired temperature, it is stored in the hot tank. By the help of this system heat transfer between hot and cold working fluid is prevented and the system have access to hot working fluid in night time. It is the best way to store heat without using any fuel consumption.

Our recommendation to increase efficiency of the system is using by TES. The reason of the usage of TES is to provide energy all day long. Because, the solar collectors can only work during the daytime. In this study, it is thought that to provide depreciation of the system on time, the operator company should be used TES for the power plant system. Existing geo-solar hybrid system will not be able to work with full performance, because of inefficient additional heat source. TES will be able to increase temperature of geothermal brine also at night times.

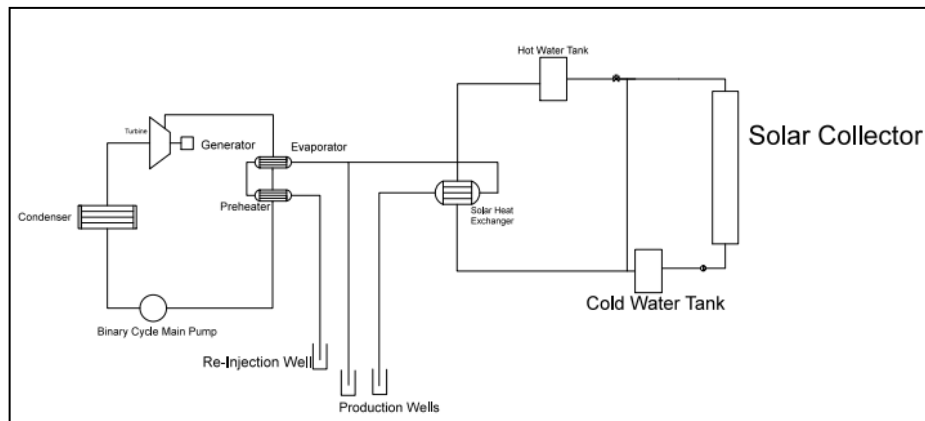


Fig.4. Geothermal ORC- solar hybrid and TES system (Karahana, 2018; Bassetti et al. 2018)

3 Conclusion

In this study, the ways of increasing the efficiency of geothermal hybrid power plants have been investigated. The study is focused on geothermal power plants, which use medium enthalpy geothermal reservoirs. It is concluded that geothermal-solar system can increase the energy output, while thermal energy storage provides continually energy production in the system. This hybrid and energy storage concept has been more reliable and suitable for the Western Anatolia ORC-binary geothermal power systems.

References

1. Haklıdır Tut, F.S., Şengün, R. 2020. Hydrogeochemical similarities and differences between high temperature geothermal systems with similar geologic settings in the Büyük Menderes and Gediz Grabens of Turkey” *Geothermics*, v. 83.
2. Haklıdır Tut, F.S., Özen Balaban, T. 2019. A review of mineral precipitation and effective scale inhibition methods at geothermal power plants in West Anatolia (Turkey). *Geothermics* 80, 103-118.
3. Demirdağ, E., Haklıdır Tut, F.S., Bilge, A.N. 2017. The Lifetime Extension Methods of Binary Type Geothermal Power Plants”, *International Energy Law Materials and Energy Summit, Istanbul-Turkey, 27-30 September 2017*.
4. Kuyumcu, Ö. C., Solaroğlu, U.D., Akar, S., Serin, O. 2012. Hybrid geothermal and solar thermal power plant case study: Gümüşköy GEPP. *Transactions, Geothermal Resources Council* 36:1091-1096.
5. Karahan, F. 2018. Geothermal- Solar Hybrid Thermal Power Plant Design with Case Study of Gümüşköy Hybrid Power Plant in Western Anatolia-Turkey. BsC thesis, Istanbul Bilgi University, Department of Energy Systems Engineering, 56 p.
6. Bassetti, M.C., Consoli, D., Manente, G., Lazzaretto, A. 2018. Design and off-design models of a hybrid geothermal-solar power plant enhanced by a thermal storage. *Renewable Energy*, V. 128,460-472.

Investigation the Effects of Reducing Heat Transfer Coefficients of Building Envelope on Global Warming in Turkey

Okan Kon¹[0000-0002-5166-0258] İsmail Caner²[0000-0003-1232-649X]

^{1,2}Balikesir University, Engineering Faculty, Mechanical Engineering Department,
Cagis Campus, 10145, Cagis/Balikesir, Turkey

ismail@balikesir.edu.tr

Abstract. In this study, the change in the emission reduction was investigated due to the decrease in the heat transfer coefficients of the building envelope such as external walls, ceilings, and floors for five climate zones according to TS 825 (Turkish Insulation Standard) which were renewed in December 2013. Emission changes were investigated for the five provinces which have the highest heating degree-day (HDD) value and the five provinces which have the highest total area of the building envelope heated. For this purpose, a 1%, 2, 5, 10, and 25% reduction in heat transfer coefficients for the external wall, ceiling, and floor were taken into account. Fuel consumption values per unit area were determined for the heating period of these ten provinces. Consequently, Turkey's general area of the building envelope for heating was used to calculate the total emissions for 2018. It is assumed that coal and natural gas were used as fuel. Combustion equations of fuels and CO₂ and SO₂ emissions were examined in calculations.

Keywords: Global Warming, Fuel Emissions, Heat Transfer Coefficient.

1 Introduction

The aim of the study is examine the change in CO₂ and SO₂ emissions related to fuel consumption for five province which has the highest heating degree-day value and five heated province which has the highest building envelope area due to the decrease in the heat transfer coefficients of the building envelope such as external walls, ceilings, and floors which recommended according to TS 825 (Turkish Insulation Standard) for five climate zones. The provinces with the highest heating degree-day value are determined as Ardahan, Erzurum, Kars, Agri, and Bayburt. The provinces with the highest total external wall, floor, and ceiling area are determined as Istanbul, Ankara, Izmir, Bursa, and Antalya. Here, a 1, 2, 5, 10, and 25% reduction in the thermal transfer coefficients for the external wall, ceiling, and floor was taken into account. Coal and natural gas were accepted as fuel. The degree-day method has been taken into account while finding the amount of fuel consumption per unit area. In the calculations, the combustion equations of the fuels are examined.

2 Methodology

2.1 Heating Degree-Day Calculation

The concept of heating degree-day is calculated based on the basic temperatures that are accepted for heating on cold days, taking into account the daily maximum and minimum temperatures for many years (more than 10 years).

According to the 21-year data, heating degree-day values were determined according to the calculation method given below by using the daily maximum (t_{max}), daily minimum (t_{min}) and basic temperature (t_b). Heating degree-day value was found for 19.5 °C basic temperature [1]. Heating degree-day value;

$$\text{If } t_{max} > t_b, t_{min} < t_b \text{ ve } (t_{max} - t_b) < (t_b - t_{min}), \text{ HDD}_{day} = 0.5(t_b - t_{min}) - 0.25(t_{max} - t_b) \quad (1)$$

$$\text{If } t_{max} > t_b, t_{min} < t_b \text{ ve } (t_{max} - t_b) > (t_b - t_{min}), \text{ HDD}_{day} = 0.5(t_b - t_{min}) - 0.25(t_{max} - t_b) \quad (2)$$

$$\text{If } t_{max} < t_b, t_{min} < t_b \text{ ise } \text{HDD}_{day} = t_b - 0.5(t_b + t_{min}) \quad (3)$$

$$\text{HDD}_{year} = \sum_{\text{günler}} \text{HDD}_{gün} \quad (4)$$

$$\text{HDD} = \frac{\sum_{21 \text{ year}} \text{HDD}_{year}}{21} \quad (5)$$

2.2 Fuel Consumption and Emission Calculation

In the study, coal and natural gas were accepted as fuel. Equation (15) is used when finding fuel consumption per unit area. Using the combustion equation (6), CO₂ and SO₂ emission values for coal and CO₂ for natural gas were calculated using equation (10) and equation (11). Finally, with the help of equation (12), (13) and (14), the CO₂ and SO₂ emissions of fuels per unit area were determined with the help of equation (15), where we found the fuel consumption per unit area. The heat transfer coefficients recommended separately for the five climatic zones in TS 825 for the external wall, floor, and ceiling given in Table 3 were used in the fuel consumption calculations. Chemical formulas of fuels are given in Table 1. Table 2 shows the heating system efficiency and lower heating values of the fuels used in calculations. In Table 3, the heating degree-day values for all cities in Turkey and the value of the heat transfer coefficient for the external wall, floor, and ceiling were given. In Table 4, the total surface area of the buildings in Turkey 2018 (exterior walls, floors and ceilings of total) and the cities with the highest value of the heating degree-days are shown. In Table 4, using natural gas and coal as fuel, for the five cities with the highest surface area data were taken from Turkey Statistical Institute data for 2018. The reason for the absence of 2019 is due to the large contraction in the construction industry.

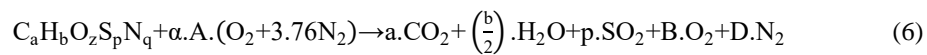
Table 1. Chemical Formulas of Fuels [2]

Fuel	Chemical Formula (C _a H _b O _z S _p N _q)
Coal	C _{7.078} H _{5.149} O _{0.517} S _{0.01} N _{0.086}
Natural gas	C _{1.05} H ₄ O _{0.034} N _{0.022}

Table 2. Fuels and properties [3]

Fuel	Lower Heating Value H _u	Efficiency of Heating System η _{H,s} (%)
Natural gas	34.485.10 ⁶ J/m ³	93
Coal	25.080×10 ⁶ J/kg	65

General chemical formula of fuel combustion equation [4,5,6];



Here, $O_2 + 3.76 N_2$ shows the air is dry. With the equalisation of Oxygen for A, B and D;

$$A = \left(a + \frac{b}{4} + p - \frac{z}{2}\right) \quad (7)$$

$$B = (\alpha - 1) \cdot \left(a + \frac{b}{4} + p - \frac{z}{2}\right) \quad (8)$$

$$D = 3.76 \cdot \alpha \cdot \left(a + \frac{b}{4} + p - \frac{z}{2}\right) + \frac{q}{2} \quad (9)$$

Here, CO and NO_x emissions are neglected. Combustion emission rates produced by combustion of 1 kg of fuel are given below;

$$M_{CO_2} = \frac{a \cdot CO_2}{M} \quad (\text{kg } CO_2 / \text{kg fuel}) \quad (10)$$

$$M_{SO_2} = \frac{p \cdot SO_2}{M} \quad (\text{kg } SO_2 / \text{kg fuel}) \quad (11)$$

If the amount of the total fuel burned to the right of the above equations are derived by writing M_f , the total emissions of CO_2 and SO_2 are found as follows;

$$M_{\text{CO}_2} = \frac{44.a}{M} \cdot M_f \quad (\text{kg} / \text{m}^2 \text{ year}) \quad (12)$$

$$M_{\text{SO}_2} = \frac{64.p}{M} \cdot M_f \quad (\text{kg} / \text{m}^2 \text{ year}) \quad (13)$$

M is the molar weight of the fuel and is found as follows [4,5,6]. Here, the sub-indices a , b , z , p , q are combinations of the elements in the chemical formula of fuels.

$$M = 12.a + b + 16.z + 32.p + 14.q \quad (\text{kg} / \text{kmol}) \quad (14)$$

amount of heating fuel consumed annually [4,5,6],

$$M_f = \frac{86,400.U.HDD}{H_u.\eta_{H,s}} \quad (15)$$

Here, U is the heat transfer coefficient of the external wall, floor or ceiling. H_U indicates the lower heating value of the fuel used and $\eta_{H,s}$ indicates the efficiency of the heating system. The value of 86400 ($24 * 60 * 60$) is the equivalent of a day in seconds and multiplied by density ($0.76 \text{ kg} / \text{m}^3$) to detect natural gas consumption in kg. [7].

Table 3. Heating degree day (HDD) and heat transfer coefficient values of external walls (U_w), floor (U_f) and ceiling (U_c) in all cities in Turkey [1,8]

Province	External wall (U_w)	Floor (U_f)	Ceiling (U_c)	Climate zone	Heating degree-day (HDD)	Province	External wall (U_w)	Floor (U_f)	Ceiling (U_c)	Climate Zone	Heating degree-day (HDD)	Province	External wall (U_w)	Floor (U_f)	Ceiling (U_c)	Climate Zone	Heating degree-day (HDD)
Adana	0.66	0.66	0.43	1	1244	Duzce	0.57	0.57	0.38	2	2463	Manisa	0.57	0.57	0.38	2	1888
Adiyaman	0.57	0.57	0.38	2	2016	Edirne	0.57	0.57	0.38	2	2558	Mardin	0.57	0.57	0.38	2	2287
Afyonkarahisar	0.48	0.43	0.28	3	3102	Elazig	0.48	0.43	0.28	3	3004	Mersin	0.66	0.66	0.43	1	1109
Agri	0.36	0.36	0.21	5	4686	Erzincan	0.38	0.38	0.23	4	3348	Mugla	0.57	0.57	0.38	2	2215
Aksaray	0.48	0.43	0.28	3	2946	Erzurum	0.36	0.36	0.21	5	4934	Muş	0.38	0.38	0.23	4	3903
Amasya	0.57	0.57	0.38	2	2576	Eskişehir	0.48	0.43	0.28	3	3239	Neşehir	0.48	0.43	0.28	3	3246
Ankara	0.48	0.43	0.28	3	2960	Gaziantep	0.57	0.57	0.38	2	2326	Nigde	0.48	0.43	0.28	3	3142
Antakya	0.66	0.66	0.43	1	1416	Giresun	0.57	0.57	0.38	2	2079	Ordu	0.57	0.57	0.38	2	2118
Antalya	0.66	0.66	0.43	1	1361	Gumüşhane	0.38	0.38	0.23	4	3488	Osmaniye	0.57	0.57	0.38	2	1341
Ardahan	0.36	0.36	0.21	5	5059	Hakkari	0.38	0.38	0.23	4	3716	Rize	0.57	0.57	0.38	2	2125
Artvin	0.48	0.43	0.28	3	2713	Iğdır	0.48	0.43	0.28	3	3050	Sakarya	0.57	0.57	0.38	2	2154
Aydın	0.57	0.57	0.38	2	1572	Isparta	0.48	0.43	0.28	3	2911	Samsun	0.57	0.57	0.38	2	2148
Balıkesir	0.57	0.57	0.38	2	2312	İstanbul	0.57	0.57	0.38	2	2188	Sanlıurfa	0.57	0.57	0.38	2	1758
Bartın	0.57	0.57	0.38	2	2537	İzmir	0.66	0.66	0.43	1	1480	Siirt	0.57	0.57	0.38	2	2270
Batman	0.57	0.57	0.38	2	2126	Kahramanmaraş	0.57	0.57	0.38	2	1983	Sinop	0.57	0.57	0.38	2	2191
Bayburt	0.38	0.38	0.23	4	4236	Karaman	0.48	0.43	0.28	3	3054	Sivas	0.38	0.38	0.23	4	3643
Bilecik	0.48	0.43	0.28	3	2689	Kars	0.36	0.36	0.21	5	4770	Tekirdag	0.57	0.57	0.38	2	2349
Bingöl	0.48	0.43	0.28	3	3193	Kastamonu	0.38	0.38	0.23	4	3350	Tokat	0.48	0.43	0.28	3	2728
Bitlis	0.38	0.38	0.23	4	3616	Kayseri	0.38	0.38	0.23	4	3336	Trabzon	0.57	0.57	0.38	2	2025
Bolu	0.48	0.43	0.28	3	3050	Kilis	0.57	0.57	0.38	2	1865	Tunceli	0.48	0.43	0.28	3	3056
Burdur	0.48	0.43	0.28	3	2702	Kirikkale	0.48	0.43	0.28	3	2844	Uşak	0.48	0.43	0.28	3	2749
Bursa	0.57	0.57	0.38	2	2272	Kirklareli	0.48	0.43	0.28	3	2578	Van	0.38	0.38	0.23	4	3617
Canakkale	0.57	0.57	0.38	2	2106	Kırşehir	0.48	0.43	0.28	3	3126	Yalova	0.57	0.57	0.38	2	2150
Cankiri	0.48	0.43	0.28	3	3162	Kocaeli	0.57	0.57	0.38	2	2098	Yozgat	0.38	0.38	0.23	4	3550
Corum	0.48	0.43	0.28	3	3219	Konya	0.48	0.43	0.28	3	3162	Zonguldak	0.57	0.57	0.38	2	2305
Denizli	0.57	0.57	0.38	2	1958	Kutahya	0.48	0.43	0.28	3	3131						
Diyarbakır	0.57	0.57	0.38	2	2528	Malatya	0.48	0.43	0.28	3	2800						

Table 4. The highest total heating surface area in Turkey for permission to use the structure of residential areas in 2018 (external walls, floors and ceilings of the total), and cities with the highest heating degree-day value [1,9]

Province	Total Heating Surface Area (Total external walls, floors and ceilings (m ²))	Heating Degree- day Value (HDD)
The provinces with the highest heating degree-day value		
Ardahan	17,117	5059
Erzurum	624,823	4934
Kars	340,769	4770
Agri	1,415	4686
Bayburt	104,829	4236
The provinces with the highest heating surface area		
Istanbul	28,059,644	2188
Ankara	13,925,246	2960
Izmir	4,091,531	1480
Bursa	7,007,832	2272
Antalya	84,338	1361
Turkey	Using Natural Gas	2713
	120,635,372	(Turkey avg.)
	Using Coal	
	32,193,958	
		Average
Zone 1		1322
Zone 2		2148
Zone 3		2983
Zone 4		3618
Zone 5		4862

3 Result and Discussion

3.1 Amount of The Fuel Consumption

Total natural gas consumption per unit area (sum of fuel consumption per unit area for external wall, floor, and ceiling) depending on the heat transfer coefficients which recommended in TS 825 for building envelope calculated between 12.660 to 11.284 m³/m² for the five provinces which has the highest heating degree-day value. When the heat transfer coefficient is reduced by 1%, it is calculated between 12.533 to 11.171, when it is decreased by 2%, it is calculated between 12.407 to 11.059 when it is decreased by 5%, it is calculated between 12.027 to 10.720 when it is decreased by 10%, between 11.394 to 10.156 and when it was reduced 25%, it was calculated between 9.495 to 8.463 m³/m². For provinces with the highest total area of the building envelope (total external wall, floor and ceiling areas), these values are between 9.478 to 6.409 m³/m² depending on the recommended heat transfer coefficients in TS 825. It is calculated between 9.383 to 6.345 when decreased by 1%, between 9.289 to 6.281 when decreased by 2%, between 9.004 to 6.088, when decreased by 5%, it is founded

between 8.530 to 5.768, when decreased by 10% and it is calculated between 7.109 to 4.807 m^3/m^2 when decreased by 25%.

Total coal consumption per unit area (sum of fuel consumption per unit area for external wall, floor, and ceiling) depending on the recommended heat transfer coefficients in TS 825 for the external wall, floor, and ceiling; it is calculated between 21.348 to 19.028 kg/m^2 for the five provinces which has the highest heating degree-day. Total coal consumption was calculated between 21.134 to 18.838 when the heat transfer coefficient was reduced by 1%, between 20.921 to 18.648 when decreased by 2%, between 20.280 to 18.077 when decreased by 5%, between 19.213 to 17.125 when decreased by 10% and between 16.011 to 14.271 kg/m^2 when decreased by 25%. For provinces with the highest total area of the building envelope (total external wall, floor, and ceiling areas), these values are between 15.983 to 10.807 kg/m^2 per unit area depending on the recommended heat transfer coefficients in TS 825. When the heat transfer coefficient was reduced by 1%, it is calculated between 15.823 to 10.699, it was reduced by 2%, calculated between 15.663 to 10.591, it was reduced 5%, calculated between 15.183 to 10.267, it was reduced 10%, between 14.384 to 9.726 and it was reduced 25%, between 11.987 to 8.105 kg/m^2 .

Figure 1 shows the change in natural gas consumption for the coldest five provinces (heating degree-day value is the highest) depending on the reduction in heat transfer coefficient on the external wall, floor, and ceiling. In Figure 2, the change of natural gas consumption for five provinces with the highest heating surface area is shown depending on the reduction in heat transfer coefficient on the external wall, floor, and ceiling. Figure 3 shows the change in coal consumption for the five coldest provinces (heating degree-day value is the highest) depending on the reduction in heat transfer coefficient on the external wall, floor, and ceiling. In Figure 4, the change of coal consumption for the provinces with the five highest heating surface areas is shown depending on the reduction in heat transfer coefficient on the external wall, floor, and ceiling. In Table 5, the average fuel consumption in Turkey and in general change was explained according to the change of the heat transfer coefficient of the external walls, floor, and ceiling.

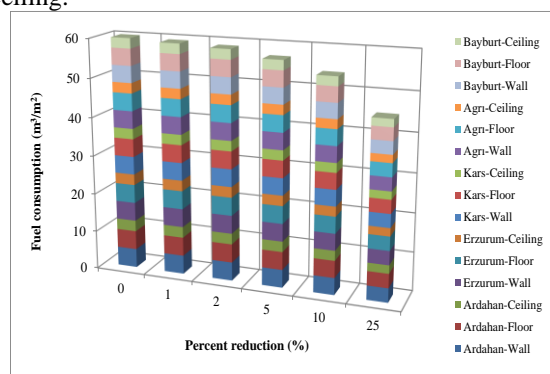


Fig. 1. The reduction in natural gas consumption for the five coldest provinces in Turkey (heating degree-day value is the highest) depending on the change of heat transfer coefficient of the external wall, floor, and ceiling

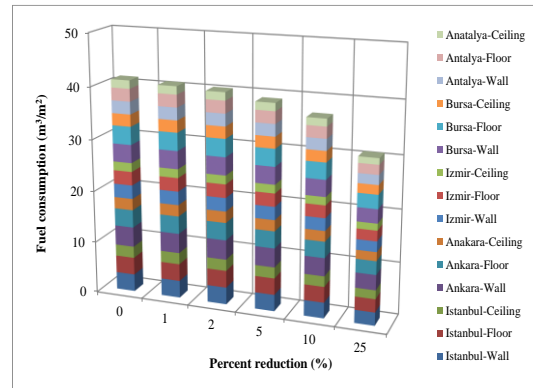


Fig. 2. The reduction in natural gas consumption for the provinces with the five highest heating surface area depending on the change of heat transfer coefficient of the external wall, floor, and ceiling

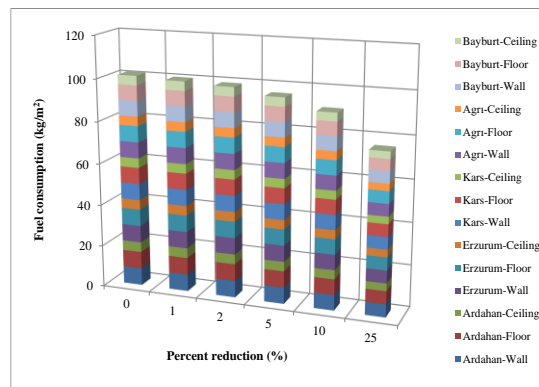


Fig. 3. The reduction in coal consumption for the five coldest provinces in Turkey (heating degree-day value is the highest) depends on the change of heat transfer coefficient of external wall, floor, and ceiling.

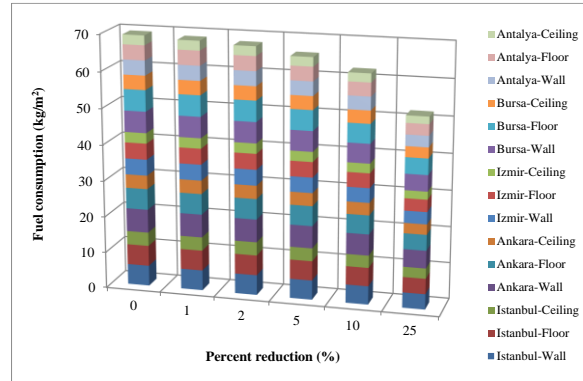


Fig. 4. The reduction in coal consumption for five provinces with the highest heating surface area depending on the change of heat transfer coefficient of the external wall, floor, and ceiling.

Table 5. Average per unit area fuel consumption change due to percent reduction of heat transfer coefficients of the external wall, floor, and ceilings in Turkey.

Parameter	Percent reduction of heat transfer coefficients (%)					
	0	1	2	5	10	25
NATURAL GAS						
Natural gas consumption according to external wall unit area (m³/m²)						
Average	3.546	3.511	3.476	3.369	3.192	2.660
Natural gas consumption according to floor unit area (m³/m²)						
Average	3.414	3.380	3.346	3.244	3.073	2.561
Natural gas consumption according to ceiling unit area (m³/m²)						
Average	2.205	2.183	2.161	2.095	1.984	1.654
Natural gas consumption according to total surface unit area (m³/m²)						
General Average	9.166	9.074	8.982	8.708	8.249	6.874
COAL						
Coal consumption according to external wall unit area (kg/m²)						
Average	5.980	5.920	5.861	5.681	5.382	4.485
Coal consumption according to floor unit area (kg/m²)						
Average	5.758	5.700	5.642	5.470	5.182	4.318
Coal consumption according to ceiling unit area (kg/m²)						
Average	3.718	3.681	3.644	3.532	3.346	2.789
Coal consumption according to total surface unit area (kg/m²)						
General Average	15.456	15.301	15.147	14.683	13.910	11.592

Turkeys' average natural gas consumption per unit area (total fuel consumption per unit area for exterior wall, floor, and ceiling) depending on the heat transfer coefficients recommended in TS 825 for external wall, floor and ceiling were calculated as 9.166 m³/m², when the heat transfer coefficient is reduced by 1%, it is calculated as 9.074 m³/m², when reduced 2%, it is calculated as 8.982 m³/m², when 5% reduced it is calculated 8.708 m³/m², when reduced by 10%, it is calculated as 8.249 m³/m² and when 25% reduced it is calculated as 6.874 m³/m².

Turkeys' average coal consumption per unit area (total fuel consumption per unit area for exterior wall, floor, and ceiling) depending on the heat transfer coefficients recommended in TS 825 for external wall, floor and ceiling were calculated as 15.456 kg/m², when the heat transfer coefficient is reduced by 1%, it is calculated as 15.301, when reduced 2%, it is calculated as 15.147, when 5% reduced it is calculated 14.683, when reduced by 10%, it is calculated as 13.910 and when 25% reduced it is calculated as 11.592 kg/m².

3.2 Amount of Emission Related to Fuel Consumption

CO₂ emission related to total natural gas consumption per unit area (total CO₂ emission per unit area for external wall, floor, and ceiling) depending on the heat transfer coefficients recommended in TS 825; were calculated between 176.200 to 157.054 kg/m² for the five provinces which have highest heating degree-day values. When the heat transfer coefficient was decreased by 1%, It was calculated between 174.438 to 155.484, when it was decreased by 2%, between 172.676 to 153.913, when it was decreased by 5%, between 177.390 to 149.202, when it was decreased by 10%, it was calculated between 158.580 to 141.349 and when it was decreased by 25%, it is calculated between 132.150 to 117.791 kg/m². For provinces with the highest total area of the building envelope (total external wall, floor, and ceiling areas), these values are calculated between 131.916 to 89.198 kg/m² per unit area depending on the recommended heat transfer coefficients in TS 825. When the heat transfer coefficient was decreased by 1%, it is calculated between 130.597 to 88.306, reduced by 2%, between 129.278 to 87.414, reduced by 5%, between 125.320 to 84.738, decreased by 10%, between 118.725 to 80.278, and decreased by 25%, calculated between 98.937 to 66.899 kg/m².

CO₂ emission related to total coal consumption per unit area (total CO₂ emission per unit area for external wall, floor, and ceiling) depending on the heat transfer coefficients recommended in TS 825; were calculated between 72.574 to 64.688 kg/m² for the five provinces which have highest heating degree-day values. When the heat transfer coefficient was decreased by 1%, It was calculated between 71.848 to 64.041, when it was decreased by 2%, between 71.122 to 63.394, when it was decreased by 5%, between 68.945 to 61.454, when it was decreased by 10%, it was calculated between 65.316 to 58.219 and when it was decreased by 25%, it is calculated between 54.430 to 48.516 kg/m². For provinces with the highest total area of the building envelope (total external wall, floor, and ceiling areas), these values are calculated between 54.334 to 36.739 kg/m² per unit area depending on the recommended heat transfer coefficients in TS 825. When the heat transfer coefficient was decreased by 1%, it is calculated between 53.791 to 36.372, reduced by 2%, between 53.247 to 36.004, reduced by 5%, between 51.617 to 34.902, decreased by 10%, between 48.900 to 33.065, and decreased by 25%, calculated between 40.750 to 27.554 kg/m².

SO₂ emission related to total coal consumption per unit area (total SO₂ emission per unit area for external wall, floor, and ceiling) depending on the heat transfer coefficients recommended in TS 825; were calculated between 0.149 to 0.133 kg/m² for the five provinces which have highest heating degree-day values. When the heat

transfer coefficient was decreased by 1%, It was calculated between 0.148 to 0.132, when it was decreased by 2%, between 0.146 to 0.130, when it was decreased by 5%, between 0.142 to 0.126, when it was decreased by 10%, it was calculated between 0.134 to 0.120 and when it was decreased by 25%, it is calculated between 0.112 to 0.100 kg/m². For provinces with the highest total area of the building envelope (total external wall, floor, and ceiling areas), these values are calculated between 0.112 to 0.075 kg/m² per unit area depending on the recommended heat transfer coefficients in TS 825. When the heat transfer coefficient was decreased by 1%, it is calculated between 0.111 to 0.075, reduced by 2%, between 0.109 to 0.074, reduced by 5%, between 0.106 to 0.072, decreased by 10%, between 0.100 to 0.068, and decreased by 25%, calculated between 0.084 to 0.057kg/m².

In Figure 5, the CO₂ emissions change graph according to natural gas consumption and due to the reduction in heat transfer coefficient was given for five coldest provinces (heating degree-day value is the highest). In Figure 6, the CO₂ emissions change graph according to natural gas consumption and due to the reduction in heat transfer coefficient (external wall, floor, and ceiling) were given for the provinces with five highest heating unit surface area. In Figure 7, the CO₂ emissions change graph according to coal consumption and due to the reduction in heat transfer coefficient was given for five coldest provinces (heating degree-day value is the highest). In Figure 8, the CO₂ emissions change graph according to coal consumption and due to the reduction in heat transfer coefficient (external wall, floor, and ceiling) were given for the provinces with five highest heating unit surface area. In Figure 9, the SO₂ emissions change graph according to coal consumption and due to the reduction in heat transfer coefficient was given for five coldest provinces (heating degree-day value is the highest). In Figure 10, the SO₂ emissions change graph according to coal consumption and due to the reduction in heat transfer coefficient (external wall, floor, and ceiling) were given for five provinces with the highest heating unit surface area. In Table 6, the average emission change in Turkey according to the percent reduction of heat transfer coefficients (external wall, floor, and ceiling) were given.

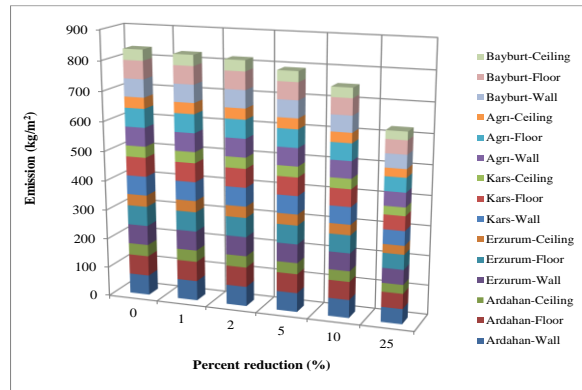


Fig. 5. The change of CO₂ emission according to natural gas consumption and a decrease in the heat transfer coefficient of external walls, floors, and ceiling for five coldest (heating degree-day value is the highest) provinces in Turkey.

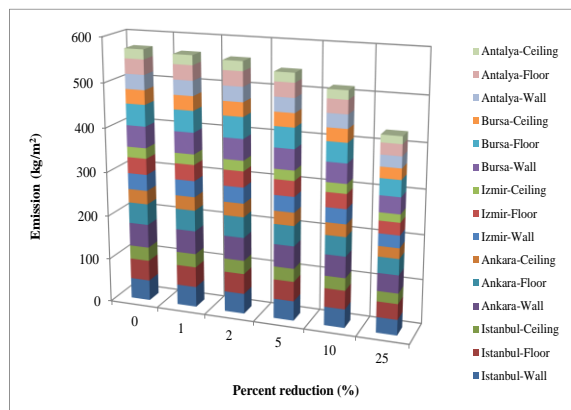


Fig. 6. The change of CO₂ emission according to natural gas consumption and a decrease in the heat transfer coefficient of external walls, floors, and ceiling for the provinces with five highest heating surface areas in Turkey.

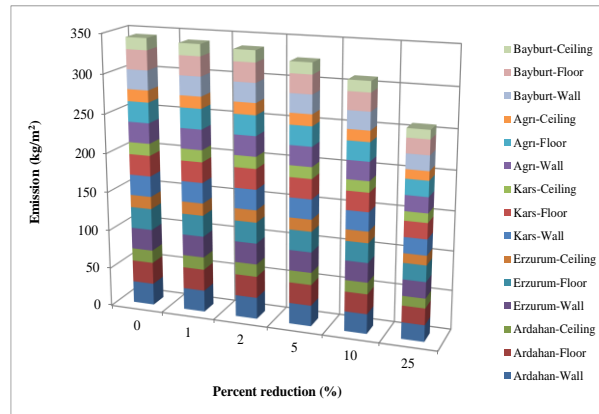


Fig. 7. The change of CO₂ emission according to coal consumption and a decrease in the heat transfer coefficient of external walls, floors, and ceiling for five coldest provinces which has highest heating degree-day in Turkey.

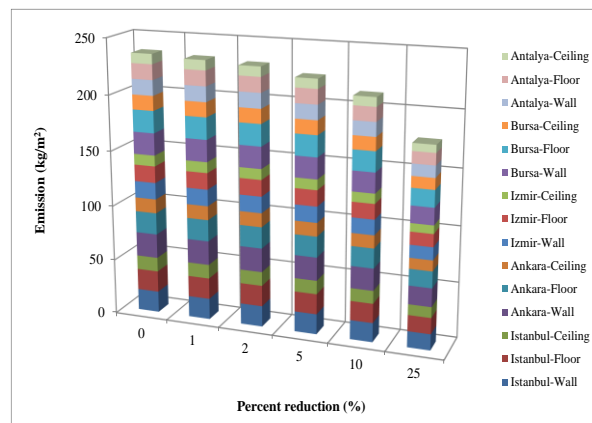


Fig. 8. The change of CO₂ emission according to coal consumption and a decrease in the heat transfer coefficient of external walls, floors, and ceiling for the provinces with five highest heating surface areas in Turkey.

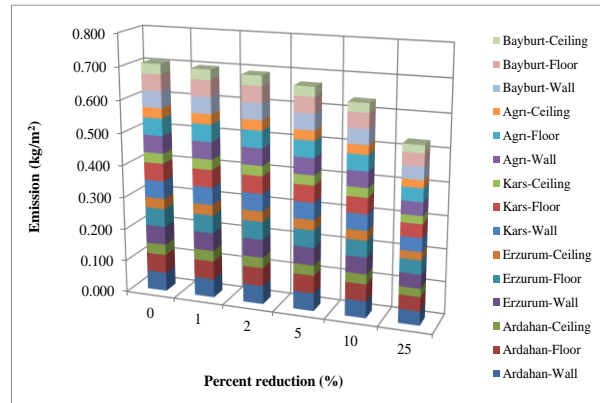


Fig. 9. The change of SO₂ emission according to coal consumption and a decrease in the heat transfer coefficient of external walls, floors, and ceiling for five coldest provinces which has the highest heating degree-day in Turkey.

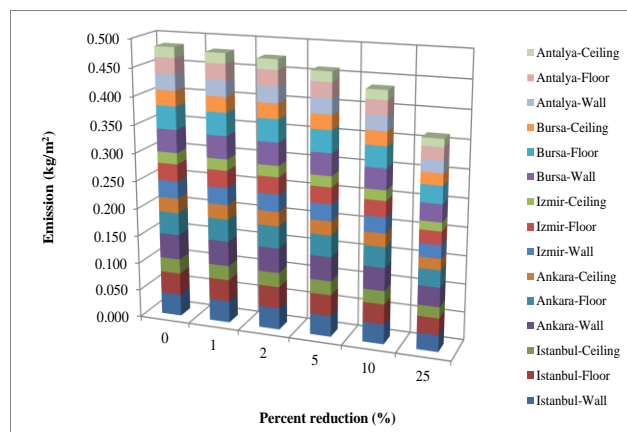


Fig. 10. The change of SO₂ emission according to coal consumption and a decrease in the heat transfer coefficient of external walls, floors, and ceiling for the provinces with five highest heating surface areas in Turkey.

Table 6. Average and general total emission change depending on the percent reduction in heat transfer coefficient of the external wall, floor, and ceiling in Turkey unit area

Parameter	The percent reduction in heat transfer coefficient (%)					
	0	1	2	5	10	25
NATURAL GAS						
CO₂ emission for external wall unit area according to natural gas consumption (kg/m²)						
Average	49.360	48.866	48.373	46.892	44.424	37.020
CO₂ emission for floor unit area according to natural gas consumption (kg/m²)						
Average	47.522	47.046	46.571	45.145	42.769	35.641
CO₂ emission for ceiling unit area according to natural gas consumption (kg/m²)						
Average	30.688	30.381	30.074	29.153	27.619	23.016
CO₂ emission for total surface unit area according to Turkey's natural gas consumption (kg/m²)						
General Average	127.569	126.293	125.018	121.191	114.812	95.677
COAL						
CO₂ emission for external wall unit area according to coal consumption (kg/m²)						
Average	20.330	20.127	19.924	19.314	18.297	15.248
CO₂ emission for floor unit area according to coal consumption (kg/m²)						
Average	19.573	19.378	19.182	18.595	17.616	14.680
CO₂ emission for ceiling unit area according to coal consumption (kg/m²)						
Average	12.640	12.513	12.387	12.008	11.376	9.480
CO₂ emission for total surface unit area according to Turkey's coal consumption (kg/m²)						
General Average	52.543	52.018	51.493	49.916	47.289	39.408
SO₂ emission for external wall unit area according to coal consumption (kg/m²)						
Average	0.042	0.041	0.041	0.040	0.038	0.031
SO₂ emission for floor unit area according to coal consumption (kg/m²)						
Average	0.040	0.040	0.039	0.038	0.036	0.030
SO₂ emission for ceiling unit area according to coal consumption (kg/m²)						
Average	0.026	0.026	0.025	0.025	0.023	0.019
SO₂ emission for total surface unit area according to Turkey's coal consumption (kg/m²)						
General Average	0.108	0.107	0.106	0.103	0.097	0.081

Turkey CO₂ emission average due to total natural gas consumption per unit area (total fuel consumption per unit area for external wall, floor, and ceiling) depending on the heat transfer coefficients recommended in TS 825 was calculated as 127.569 kg/m². When the heat transfer coefficient was decreased by 1%, it was calculated as 126.293 kg/m², when decreased by 2%, 125.018 kg/m², when decreased by 5%, 121.191 kg/m², when decreased by 10%, 114.812 kg/m², when decreased by 25%, it was calculated as 95.677 kg/m².

Turkey's average CO₂ emission due to total coal consumption per unit area (total fuel consumption per unit area for external wall, floor, and ceiling) depending on the heat transfer coefficients recommended in TS 825 was calculated as 52.543 kg/m². When the heat transfer coefficient was decreased by 1%, it was calculated as 52.018 kg/m², when decreased by 2%, 51.493 kg/m², when decreased by 5%, 49.916 kg/m², when decreased by 10%, 47.289 kg/m², when decreased by 25%, it was calculated as 39.408 kg/m².

Turkey's average SO₂ emission due to total coal consumption per unit area (total fuel consumption per unit area for external wall, floor, and ceiling) depending on the heat transfer coefficients recommended in TS 825 was calculated as 0.108 kg/m². When the heat transfer coefficient was decreased by 1%, it was calculated as 0.107 kg/m², when decreased by 2%, 0.106 kg/m², when decreased by 5%, 0.103 kg/m², when decreased by 10%, 0.097 kg/m², when decreased by 25%, it was calculated as 0.081 kg/m².

3.3 Total Emission Change for the Provinces with the Highest Heating Surface Area and Highest Heating Degree-Day Values

CO₂ emission for the provinces with the highest heating degree-day values due to total natural gas consumption for the total surface area (total CO₂ emission dependent on the total of the external wall, floor and ceiling area) related to the heat transfer coefficients recommended in TS 825 was calculated between 107,373.790 to 230.941 tone/year. When the heat transfer coefficient is reduced by 1%, it was calculated between 106,300.052 to 228.631, when reduced by 2%, between 105,226.314 to 226.322, when reduced by 5%, between 102,005.100 to 219.394, when reduced by 10%, between 96,636.411 to 207.847, when reduced by 25%, it was calculated between 80,530.342 to 173.206 tone/year. For provinces with the highest total area of the building envelope (total external wall, floor, and ceiling areas), these values calculated between 3,494,879.790 to 7522.785 tone/year. When the heat transfer coefficient was decreased by 1%, it was calculated between 3,459,930.992 to 7,447.557, when decreased 2%, between 3,424,982.195 to 7,372.329, when reduced 5%, between 3,320,135.801 to 7,146.646, when decreased by 10%, between 3,145,391.811 to 6,770.507 and when decreased 25%, it was calculated between 2,621,159.843 to 5,642.089 tone/year.

CO₂ emission for the provinces with the highest heating degree-day values due to total coal consumption for the total surface area (total CO₂ emission dependent on the total of the external wall, floor and ceiling area) related to the heat transfer coefficients recommended in TS 825 was calculated between 25,716.118 to 293.053 tone/year. When the heat transfer coefficient is reduced by 1%, it was calculated between 25,458.957 to 290.122, when reduced by 2%, between 25,201.796 to 287.192, when reduced by 5%, between 24,430.312 to 278.400, when reduced by 10%, between 23,144.506 to 263.748, when reduced by 25%, it was calculated between 19287.089 to 219.790 tone/year. For provinces with the highest total area of the building envelope (total external wall, floor, and ceiling areas), these values calculated between 78,986.946 to 5,744.544 tone/year. When the heat transfer coefficient was decreased by 1%, it was calculated between 78,197.077 to 5,687.099, when decreased 2%, between 77,407.207 to 5,629.653, when reduced 5%, between 75,037.599 to 5,457.317, when decreased by 10%, between 71,088.252 to 5,170.090 and when decreased 25%, it was calculated between 59,240.210 to 4,308.408 tone/year.

SO₂ emission for the provinces with the highest heating degree-day values due to total coal consumption for the total surface area (total SO₂ emission dependent on the total of the external wall, floor and ceiling area) related to the heat transfer coeffi-

cients recommended in TS 825 was calculated between 52.847 to 0.602 tone/year. When the heat transfer coefficient is reduced by 1%, it was calculated between 52.319 to 0.596, when reduced by 2%, between 51.790 to 0.590, when reduced by 5%, between 50.205 to 0.572, when reduced by 10%, between 47.562 to 0.542, when reduced by 25%, it was calculated between 39.635 to 0.452 tone/year. For provinces with the highest total area of the building envelope (total external wall, floor, and ceiling areas), these values calculated between 162.320 to 11.805 tone/year. When the heat transfer coefficient was decreased by 1%, it was calculated between 160.697 to 11.687, when decreased 2%, between 159.074 to 11.569, when reduced 5%, between 154.204 to 11.215, when decreased by 10%, between 146.088 to 10.625 and when decreased 25%, it was calculated between 121.740 to 8.854 tone/year.

In Figure 11, the graph of total CO₂ emission change is given for provinces with the highest heating degree-day value and highest total heating surface area that will occur with natural gas consumption and a decrease in heat transfer coefficients. In Figure 12, the graph of total CO₂ emission change is given for provinces with the highest heating degree-day value and highest total heating surface area that will occur with coal consumption and a decrease in heat transfer coefficients. In Figure 13, the graph of total SO₂ emission change is given for provinces with the highest heating degree-day value and highest total heating surface area that will occur with coal consumption and a decrease in heat transfer coefficients. In Table 7, the average emissions change in Turkey depends on the percent reduction in the heat transfer coefficient of external walls, floor, and ceiling were given.

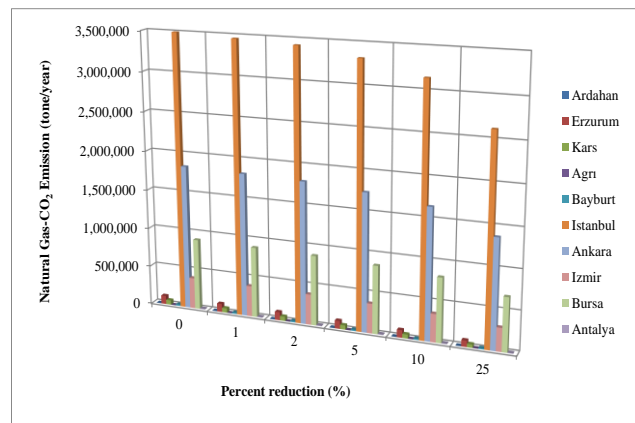


Fig. 11. Total CO₂ emission change graph for provinces with the highest heating degree-day value and highest total heating surface area depend on the natural gas consumption and a decrease in heat transfer coefficients.

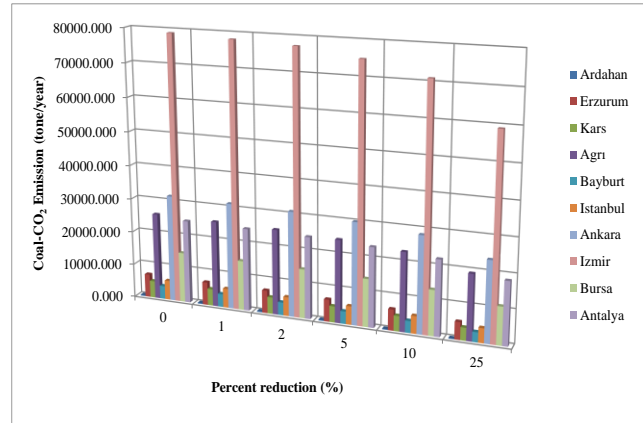


Fig. 12. Total CO₂ emission change graph for provinces with the highest heating degree-day value and highest total heating surface area depend on the coal consumption and a decrease in heat transfer coefficients.

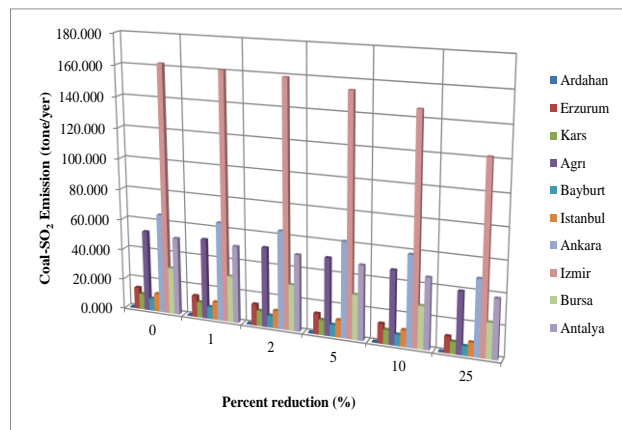


Fig. 13. Total SO₂ emission change graph for provinces with the highest heating degree-day value and highest total heating surface area depend on the coal consumption and a decrease in heat transfer coefficients.

Table 7. The average and general total emissions change table in Turkey depends on the percent reduction in the heat transfer coefficient of external walls, floor, and ceiling.

Province	Reduction in the heat transfer coefficient (%)					
	0	1	2	5	10	25
NATURAL GAS						
Turkeys' general CO₂ emission according to natural gas consumption for the total surface area (tone/year)						
Ardahan	3,016.022	2,985.861	2,955.701	2,865.221	2,714.420	2,262.016
Erzurum	107,373.790	106,300.052	105,226.314	102,005.100	96,636.411	80,530.342
Kars	56,613.576	56,047.440	55,481.304	53,782.897	50,952.218	42,460.182
Ağrı	230.941	228.631	226.322	219.394	207.847	173.206
Bayburt	16,463.864	16,299.225	16,134.587	15,640.671	14,817.478	1,2347.898
İstanbul	3,494,879.790	3,459,930.992	3,424,982.195	3,320,135.801	314,5391.811	2,621,159.843
Ankara	1,836,964.352	1,818,594.709	1,800,225.065	1,745,116.135	1,653,267.917	1,377,723.264
İzmir	396,866.819	392,898.151	388,929.483	377,023.478	357,180.137	297,650.114
Bursa	90,6347.575	897,284.099	888,220.623	861,030.196	815,712.817	679,760.681
Antalya	7522.785	7,447.557	7,372.329	7,146.646	6,770.507	5,642.089
Total	15,389,334	15,235,403	15,081,593	14,619,921	13,850,388	11,542,030
COAL						
Turkeys' general CO₂ emission according to coal consumption for the total surface area (tone/year)						
Ardahan	293.053	290.122	287.192	278.400	263.748	219.790
Erzurum	6,904.079	6,835.038	6,765.997	6,558.875	6,213.671	5,178.059
Kars	5,028.288	4,978.006	4,927.723	4,776.874	4,525.460	3,771.216
Ağrı	25,716.118	25,458.957	25,201.796	24,430.312	23,144.506	19,287.089
Bayburt	3,913.230	3,874.098	3,834.966	3,717.569	3,521.907	2,934.923
İstanbul	5,744.544	5,687.099	5,629.653	5,457.317	5,170.090	4,308.408
Ankara	31,654.696	31,338.149	31,021.602	30,071.961	28,489.226	23,741.022
İzmir	78,986.946	78,197.077	77,407.207	75,037.599	71,088.252	59,240.210
Bursa	14,867.005	14,718.335	14,569.665	14,123.655	13,380.305	11,150.254
Antalya	24,702.101	24,455.080	24,208.059	23,466.996	22,231.891	18,526.576
Total	1,691,567	1,674,665	1,657,763	1,606,994	1,522,420	1,268,699
Turkeys' general SO₂ emission according to coal consumption for the total surface area (tone/year)						
Ardahan	0.602	0.596	0.590	0.572	0.542	0.452
Erzurum	14.188	14.046	13.904	13.479	12.769	10.641
Kars	10.333	10.230	10.127	9.817	9.300	7.750
Ağrı	52.847	52.319	51.790	50.205	47.562	39.635
Bayburt	8.042	7.961	7.881	7.640	7.238	6.031
İstanbul	11.805	11.687	11.569	11.215	10.625	8.854
Ankara	65.051	64.401	63.750	61.799	58.546	48.788
İzmir	162.320	160.697	159.074	154.204	146.088	121.740
Bursa	30.552	30.247	29.941	29.024	27.497	22.914
Antalya	50.763	50.256	49.748	48.225	45.687	38.073
Total	3,477	3,445	3,413	3,316	3,123	2,608

4 Conclusions

When the results obtained from the calculations in the study are examined,

Ardahan is the province with the highest heating degree-day (HDD) value with 5059 in Turkey. Mersin has the lowest heating degree-day (HDD) value with 1109. According to Turkey Statistics Institution data, buildings take a building use permit for 2018 is Istanbul which has the highest population density in Turkey and has the highest heating surface area in Turkey. The second is Ankara, the third is Izmir, the fourth is Bursa and the fifth is Antalya.

Ardahan which is the coldest area in Turkey and has the highest heating degree-day value has the highest fuel consumption per unit area and highest CO₂ and SO₂ emissions. It was observed that the highest amount of fuel consumption and CO₂ and

SO₂ emissions per unit area occurred in Ankara province, depending on the area where the highest heating surface area (total external wall, floor and ceiling) for 2018. The reason for this is that Ankara has a higher heating degree-day (HDD) value and colder climate compared to the other four provinces.

When considering the total heating area for natural gas consumption and CO₂ emissions for Turkey 2018 data, Istanbul is the highest province. The reason for this is the city with the highest number of houses using natural gas. The province with the highest coal consumption and associated CO₂ and SO₂ emissions is İzmir. İzmir is the province with the highest number of houses using coal. Considering the total heating area for the five provinces with the highest heating degree-day value, the province with the lowest natural gas consumption and CO₂ emission is Ağrı. The reason for this, Ağrı has the lowest number of natural gas used houses compared to the other four. Ardahan is the province with the lowest coal consumption and associated CO₂ and SO₂ emissions. Ardahan province is the province with the lowest total area of heating connected with coal compared to the other four.

Finally, the recommended heat transfer coefficients for the external wall, floor, and ceiling in TS 825, depending on the entire area (the sum of the external wall, floor and ceiling area) in Turkey, CO₂ emission is calculated as 11,542,030 tone/year when decreased 25%, it is calculated as 15,389,334 tone/year. CO₂ emissions depend on the total coal consumption in Turkey was calculated as 1,691,567 tones/year when were decreased by 25%, it is calculated as 1,268,699 tone/year. SO₂ emissions depend on the total coal consumption in Turkey is calculated as 3,477 tones/year, when heat transfer coefficients were decreased by 25%, it is found as 2,608 tone/year.

References

1. Dombaycı, Ö. A.: Degree-days maps of Turkey for various base temperatures, *Energy*, 34 (11), 1807-1812(2009)
2. Keçebaş, A.: Determination of optimum insulation thickness in pipe for exergetic life cycle assessment, *Energy Conversion and Management*, 105, 826-835(2015).
3. Kurekçi, N. A.: Determination of optimum insulation thickness for building walls by using heating and cooling degree-day values of all Turkey's provincial centers, *Energy and Buildings* 118, 197-213(2016).
4. Çomaklı, K., Yüksel, B.: Environmental impact of thermal insulation thickness in buildings, *Applied Thermal Engineering*, 24 (5-6), 933-940(2004).
5. Kon, O.: Determining Theoretically And Practically The Optimum Insulation Thickness Of Buildings Used For Different Purposes According To Heating And Cooling Loads, Ph.D. Thesis, Balıkesir University, Institute of Science, Balıkesir, Turkey (2014).
6. Kon, O.: Calculation of fuel consumption and emissions in buildings based on external walls and windows using economic optimization, *Journal of the Faculty of Engineering and Architecture of Gazi University* 33(1),101-113(2018).
7. Doğal Gaz-LPG Tesisatı ve Bacalar ISISAN Yayınları No:345
8. TS 825: Thermal insulation requirements for buildings, Turkish Standard, December 2013.
9. Turkey Statistical Institute Housing Data (TUIK)

Renewable Energy Consumption Due to Internal Gas Gap Thickness in Buildings' Windows

Okan Kon¹[0000-0002-5166-0258], İsmail Caner²[0000-0003-1232-649X]

^{1,2}Balikesir University Engineering Faculty Mechanical Engineering Department Cagis Campus
10145 Cagis/Balikesir-Turkey

ismail@balikesir.edu.tr

Abstract. In this study, the change in the consumption of renewable energy sources such as olive cake (as a biomass) and geothermal energy depending on the internal gap thickness of the building windows in Balikesir province was investigated. Gonen district in Balikesir is the city where the first application of the geothermal district heating system used. In addition, geothermal district heating systems are applied in districts such as Bigadiç, Edremit, Güre and Sındırgı. Besides, in the districts such as Edremit, Burhaniye, Havran, Gömeç, Ayvalık, which are close to the Aegean Sea and have coasts, are produced olive and olive cake as a biomass. In this study, heat transfer coefficients were calculated in two glazed windows with 3, 6, 9, 12, 15 and 18 mm air gap thickness. Fuel and energy consumptions related to heat transfer coefficients were determined. In fuel and energy consumption calculations, heating degree-day values of Balikesir province for different base temperatures were used. In addition, the chemical formula for olive cake, depending on its chemical composition, has been determined. CO₂ and SO₂ emissions of the olive cake were calculated using the chemical formula and with the help of combustion equations.

Keywords: Olive Cake, Geothermal Energy, Air Gap Thickness, Window Heat Transfer Coefficient

1 Introduction

Balikesir province is very rich in terms of geothermal resources. Balikesir ranking is 4th at the geothermal energy potential in Turkey. In Balikesir, 7 geothermal areas were determined at 30 ° C and higher temperatures. These are Balikesir-Pamukcu, Balya-Dag Hot Spring, Bigadic-Hisarköy, Sındırgı-Hisaralan, Edremit-Derman, Gure, Manyas-Serpin, Kepekler, Gonen and Susurluk-Yildiz regions which are very important hot water sources from geothermal energy. The Bigadic geothermal district heating system which started its operations in 2004 to heat 3,000 residences uses the energy produced in Hisarköy geothermal area in residential heating. Sındırgı geothermal district heating system which is planned to heat 3,000 residences for Sındırgı district, has been designed. Edremit geothermal district heating system was put into operation in the region in order to heat the Edremit district center in 2003 and it was designed to respond to a total capacity of 7,500 residences. Gure geothermal district

heating system was put into operation in 2004, and 589 residences were heated in the system as of December 2011. The first geothermal district heating system in Turkey put into operation in 1987 for 600 residences in Gonen. The number of houses heated by 1,600 houses added to the system in 1995 reached 2,200. As of December 2009, the number of subscribers in the system reached 2,636 and the equivalent of 2,993 residences was realized [1].

In agriculture, especially in the production of olive oil; Balikesir ranks 5th with a capacity of 120,369 tons /year in Turkey. In olive production; Edremit, Burhaniye, Havran, Gomec, Ayvalik are the leading regions. Of the agricultural waste, olive cake is the solid waste left by the processing of olives into oil. It contains some oil and high humidity. Olive cake is extracted in oil factories and its moisture is reduced and it becomes a fuel. It gives very high efficiency in industrial boilers and stoker floor heating boilers. Due to the high lignin content, it has been determined that it is more appropriate to obtain activated carbon by pyrolysis compared to other biomass. In Turkey, 1 million tons of olives enter olive oil production annually and approximately 450,000 tons of olive cake is obtained following Spain, Italy and Greece olive oil production. Olive cake can be used as fuel alone or it can be burned with other fuels such as low-calorie lignite coal. An average of 42,951 tons/year dry olive cake is obtained in Balikesir province. The average thermal capacity of this is 743,052 GJ/year, and if biogas is obtained, its average biogas capacity is 7,645,100 m³/year [1].

The aim of the study is to investigate the change in the use of renewable energy sources such as biomass (olive cake) and geothermal energy depending on the thickness of the internal gap in the windows of the buildings in Balikesir. Firstly, heating degree-day (HDD) values were calculated for different base temperatures (15.5, 17.5, 19.5, 21 and 23) of Balikesir province. Secondly; calculations were made for the uncoated glazed window with 0.89 emissivity value given the standard of TS 2164 (Principles for the preparation of the projects of the central heating systems) and the coated glazed window with the lowest emissivity value of 0.05. Besides, the gap thickness of 3, 6, 9, 12, 15, 18 mm given in the same standard was taken into account [2]. Heat transfer coefficients in double-layered windows with air gap are calculated. Fuel and energy consumption based on heat transfer coefficients were determined. Finally, as biomass, the chemical formula for olive cake depending on its chemical composition has been determined. CO₂ and SO₂ emissions of the olive cake were calculated by using the chemical formula and with the help of combustion equations. Outdoor temperature was taken from the external data for the General Directorate of Meteorology, Balikesir, as (-7.7) °C for 11 January and wind speed as 9.5 m/s for the coldest day of 2017 [3].

2 Material and Method

2.1 Heating degree-day calculation

The concept of heating degree-day is calculated based on the basic temperatures that are accepted for heating on cold days, taking into account the daily maximum and minimum temperatures for many years (more than 10 years).

According to the 21-year data, heating degree-day values were determined according to the calculation method given below by using the daily maximum (t_{max}), daily minimum (t_{min}) and base temperature (t_b). Heating degree-day value was found for 19.5 °C basic temperature [4]. Heating degree-day value;

$$\text{If } t_{max} > t_b, t_{min} < t_b \text{ ve } (t_{max} - t_b) < (t_b - t_{min}), \text{HDD}_{day} = 0.5(t_b - t_{min}) - 0.25(t_{max} - t_b) \quad (1)$$

$$\text{If } t_{max} > t_b, t_{min} < t_b \text{ ve } (t_{max} - t_b) > (t_b - t_{min}), \text{HDD}_{day} = 0.5(t_b - t_{min}) - 0.25(t_{max} - t_b) \quad (2)$$

$$\text{If } t_{max} < t_b, t_{min} < t_b \text{ ise } \text{HDD}_{day} = t_b - 0.5(t_b + t_{min}) \quad (3)$$

$$\text{HDD}_{year} = \sum_{\text{days}} \text{HDD}_{day} \quad (4)$$

$$\text{HDD} = \frac{\sum_{21 \text{ year}} \text{HDD}_{year}}{21} \quad (5)$$

2.2 Calculation of heat transfer coefficient of windows

In the vertical position, the air trapped between the two glass layers rises through the hot surface (internal glass layer) and falls through the cold surface (external glass layer), and the cycle starts depending on the Nusselt number of the fluid. If the number of Nusselt is 1, the air is motionless and it performs heat transfer by conduction, and if Nusselt is greater than 1, heat transfer is performed with the natural convection. Convection heat transfer is only as rigid as the Nu number of heat transfer through conduction. When the Rayleigh number is less than 1708, conduction heat transfer takes place, since buoyancy cannot overcome fluid resistance. When the Rayleigh number is greater than 1708, buoyancy overcomes fluid resistance and convection heat transfer takes place, as laminar flow, called Bernard cells, appears to be in the form of octagonal cells. [5]. The structure of the window used in calculations is given in Figure 1.

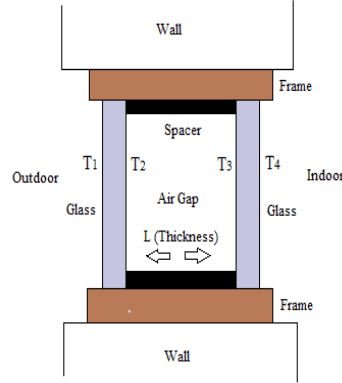


Fig. 1. Windows structure

General heat transfer coefficient for multi-glazed windows [6,7],

$$U = \frac{1}{\frac{1}{h_i A} + \frac{c}{k_{cam} A} + \frac{1}{(U_{2-3,con} + U_{2-3,rad})} + \frac{c}{k_{cam} A} + \frac{1}{h_o A}} \quad (6)$$

Here, the internal layer of the external window $U_{2-3,con}$ conduction and $U_{2-3,rad}$ is radiation heat transfer coefficient;

$$U_{2-3,con} = \frac{1}{\frac{L}{A k_{hava}} + (n-2) \left(\frac{c}{A k_{cam}} + \frac{L}{A k_{hava}} \right)} \quad (7)$$

$$U_{2-3,rad} = \frac{1}{\frac{2(1-\varepsilon)}{(A\varepsilon)} + \frac{2(n-1)(1-\varepsilon)}{(A\varepsilon)} + \frac{(n-1)}{(F_{ij}A)}} \cdot \frac{\sigma(T_2^4 - T_3^4)}{(T_2 - T_3)} \quad (8)$$

Here, n is the number of layers, L is air gap thickness, A is a surface area, ε is emissivity, σ is Stefan-Boltzman constant, h_o and h_i are internal and external convection heat transfer coefficients, k_{glass} is heat conduction coefficient of glass ($k_{glass} = 0.92$ W/mK). The $(1-\varepsilon)/(\varepsilon A)$ and $1/F_{ij}$ are the surface and area the radiation resistance, respectively. F_{ij} appearance factor was taken as 1. Glass thickness (c) is accepted as 4 mm [6,7].

h_i is the internal convection heat transfer coefficient and it is equal to the sum of indoor radiation and convection heat transfer coefficient.

$$h_i = h_r + h_c \quad (9)$$

The internal radiation heat transfer coefficient, h_r was taken as 4.4 W/m²K for uncoated windows, for coated windows, h_r was taken as $(4.4 * \varepsilon / 0.837)$, and h_c convection value was taken as 3.6 W/m².K. These values standardized according to EN 673.

Here, ε is emissivity and v is wind speed (m/s). External convection heat transfer coefficient according to ASHRAE is given below [8].

$$h_0 = 7.1 + 3.42.v \quad (10)$$

2.3 Calculation of fuel consumption

Annual fuel consumption for heating for multi-glazed windows [9,10]

$$M_{FH} = \frac{86.400.U_T.HDD}{\eta_H.H_u} \quad (11)$$

Here, HDD is heating degree-day value, U ($W/m^2.K$) is heat transfer coefficient of windows, H_u is lower heat value and η_H is heating system efficiency.

2.4 Chemical formula of olive cake

The total mass of a mixture of N mixtures, m_T , is the sum of the individual masses of the mixes. The total mole amount of the mixture is n_T , the sum of the individual molar amounts of the mixtures. [11].

$$m_T = \sum_{i=1}^N m_i \quad (12)$$

$$n_T = \sum_{i=1}^N n_i \quad (13)$$

The molar ratio of the mixture to the total molar ratio of the mixture (y_n) is the molar ratio.

$$y_n = \frac{n_i}{n} \quad (14)$$

Sum of the mass ratio (y_m) and mole ratio (y_n) is one.

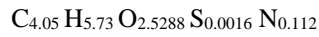
$$\sum_1^N y_{m_i} = 1 \quad (15)$$

$$\sum_1^N y_{n_i} = 1 \quad (16)$$

The mass of a substance is equal to the molar quantity (n) of the substance multiplied by the molar mass (M). [11].

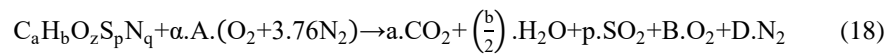
$$m=n.M \quad (17)$$

Chemical formula of olive cake is given below;



2.5. Combustion equations and emission calculation

General chemical formula of fuel combustion equation [7,12,13];



Here, $O_2 + 3.76 N_2$ shows the air is dry. With the equalisation of Oxygen for A, B and D;

$$A = \left(a + \frac{b}{4} + p - \frac{z}{2}\right) \quad (19)$$

$$B = (\alpha - 1) \cdot \left(a + \frac{b}{4} + p - \frac{z}{2}\right) \quad (20)$$

$$D = 3.76 \cdot \alpha \cdot \left(a + \frac{b}{4} + p - \frac{z}{2}\right) + \frac{q}{2} \quad (21)$$

Here, CO and NO_x emissions are neglected. Combustion emission rates produced by combustion of 1 kg of fuel are given below;

$$M_{CO_2} = \frac{a.CO_2}{M} \quad (\text{kg CO}_2/\text{kg fuel}) \quad (22)$$

$$M_{SO_2} = \frac{p.SO_2}{M} \quad (\text{kg SO}_2/\text{kg fuel}) \quad (23)$$

If the amount of the total fuel burned to the right of the above equations is derived by writing M_f , the total emissions of CO₂ and SO₂ are found as follows;

$$M_{CO_2} = \frac{44.a}{M} \cdot M_f \quad (\text{kg/m}^2 \text{ year}) \quad (24)$$

$$M_{SO_2} = \frac{64.p}{M} \cdot M_f \quad (\text{kg/m}^2 \text{ year}) \quad (25)$$

M is the molar weight of the fuel and is found as follows. Here, the sub-indices a, b, z, p, q are combinations of the elements in the chemical formula of fuels.

$$M=12.a+b+16.z+32.p+14.q \quad (\text{kg/kmol}) \quad (26)$$

amount of heating fuel consumed annually [7,12,13].

3 Result and Discussion

3.1 The values used in calculations

Energy sources and their properties used for heating are given in Table 1. In Table 2, heating degree-day (HDD) values of Balikesir province for different basic temperatures are shown. The chemical composition of olive cake as biomass is given in Table 3. Table 4 shows the windows internal surface temperatures depending on the air gap thickness for uncoated windows with 0.89 emissivity value and coated with 0.05 emissivity value. In Table 5, the window heat transfer coefficients equations based on the air gap thickness were obtained for coated and uncoated windows with emissivity 0.05 and 0.89, respectively. Table 6 shows window heat transfer coefficients depending on the air gap thickness for uncoated and coated windows. Figure 2 shows the windows internal surface temperatures depending on the air gap thickness for uncoated windows with 0.89 emissivity value. In Figure 3, windows internal surface temperatures depending on the air gap thickness are given for coated glass window with 0.05 emissivity value. Figure 4 shows heat transfer coefficients depending on air gap thickness for uncoated glass windows with 0.89 emissivity value. In figure 5, heat transfer coefficients based on air gap thickness are given for coated glass window with 0.05 emissivity value.

Table 1. Energy sources and their properties used for heating [14, 15]

Fuel	Lower heating value	Efficiency
	H_u (J/kg)	η_H (%)
Geothermal energy	$36.000 \cdot 10^6$	98
Olive cake energy (Biomass)	$20.934 \cdot 10^6$	87

Table 2. Heating degree-day (HDD) values of Balikesir province for different base temperatures

Province	Base temperature (T_b)				
	15.5	17.5	19.5	21	23
Balikesir	1510	1895	2312	2641	3095

Table 3. Chemical composition of olive cake as biomass [16]

Ingredient	Percentage Mass (%)
Carbon (C)	48.59
Hydrogen (H)	5.73
Nitrogen (N)	1.57
Oxygen (O)	40.46
Sulphur (S)	0.05
Ash	3.60

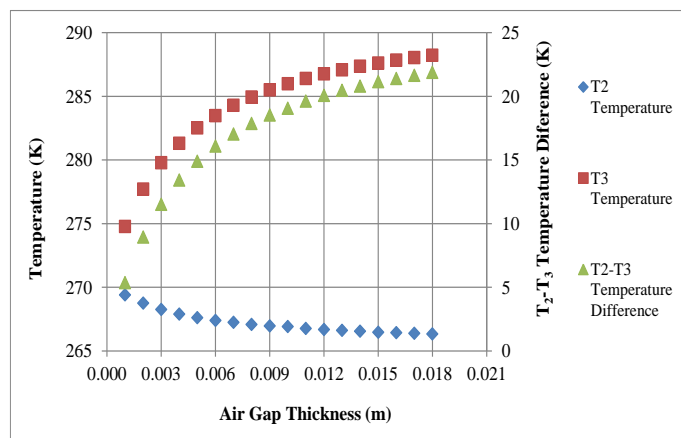
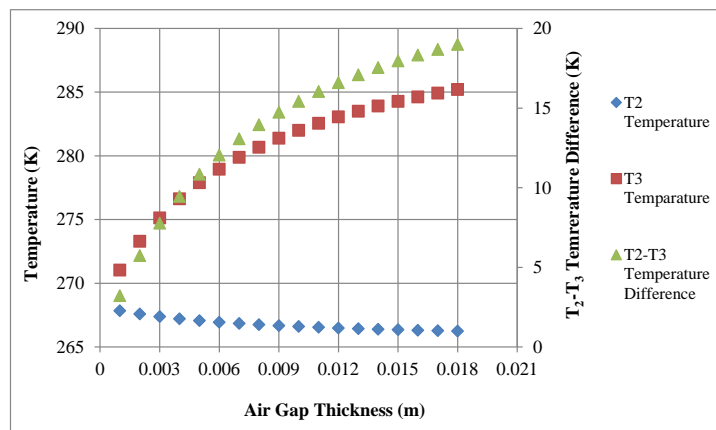
**Fig. 2.** The windows internal surface temperatures depending on the air gap thickness for uncoated windows with 0.89 emissivity value**Fig. 3.** The windows internal surface temperatures depending on the air gap thickness for coated glass window with 0.05 emissivity value

Table 4. The windows internal surface temperatures depending on the air gap thickness for uncoated windows with 0.89 emissivity value and coated with 0.05 emissivity value

Air Gap Thickness (m)	Uncoated windows with 0.89 emissivity value			Coated windows with 0.05 emissivity value		
	T ₂ Temperature (K)	T ₃ Temperature (K)	T ₃ -T ₂ Temperature Difference (K)	T ₂ Temperature (K)	T ₃ Temperature (K)	T ₃ -T ₂ Temperature Difference (K)
0.003	268.26	279.78	11.52	267.36	275.12	7.76
0.006	267.39	283.48	16.09	266.93	278.95	12.03
0.009	266.97	285.50	18.53	266.66	281.38	14.73
0.012	266.69	286.75	20.06	266.47	283.05	16.58
0.015	266.46	287.60	21.14	266.33	284.28	17.94
0.018	266.34	288.22	21.88	266.23	285.21	18.98

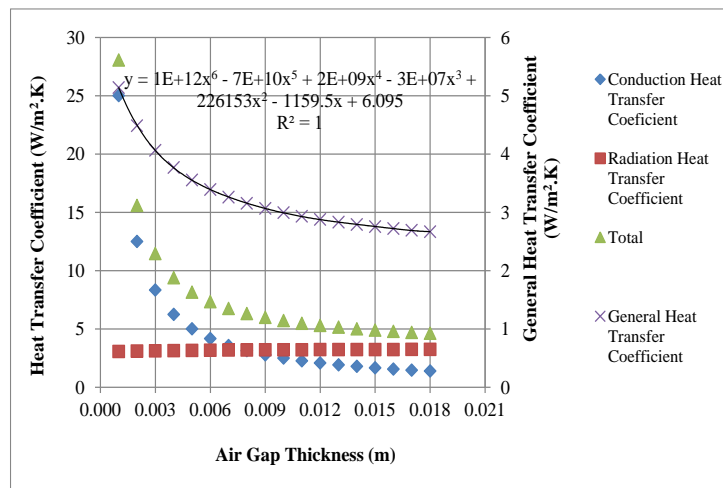


Fig. 4. Heat transfer coefficients depending on air gap thickness for uncoated glass windows with 0.89 emissivity value

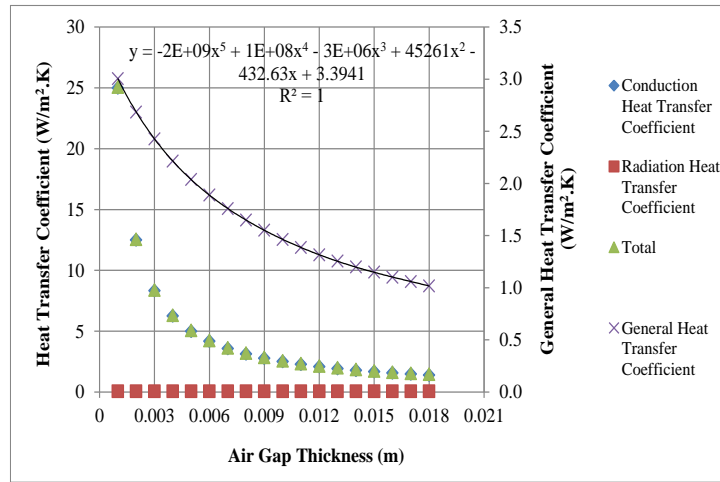


Fig. 5. Heat transfer coefficients based on air gap thickness are given for coated glass window with 0.05 emissivity value

Table 5. The window heat transfer coefficients equations based on the air gap thickness for coated and uncoated windows with emissivity 0.05 and 0.89

Parameter	Equation	Regression coefficient (R ²)
Uncoated windows with 0.89 emissivity value	$U_T = 1E+12L^6 - 7E+10L^5 + 2E+9L^4 - 3E+7L^3 + 226153L^2 - 1159L + 6.095$	1
Coated windows with 0.05 emissivity value	$U_T = -2E+9L^5 + 1E+8L^4 - 3E+6L^3 + 45261L^2 - 432.63L + 3.3941$	1

Table 6. The window heat transfer coefficients depending on the air gap thickness for uncoated and coated windows

Air Gap Thickness (m)	Uncoated windows with 0.89 emissivity value				Coated windows with 0.05 emissivity value			
	Conduction Heat Transfer Coefficient (W/m ² .K)	Radiation Heat Transfer Coefficient (W/m ² .K)	Total (W/m ² .K)	General Heat Transfer Coefficient (W/m ² .K)	Conduction Heat Transfer Coefficient (W/m ² .K)	Radiation Heat Transfer Coefficient (W/m ² .K)	Total (W/m ² .K)	General Heat Transfer Coefficient (W/m ² .K)
	U _{cond.}	U _{rad.}	U _{cond.+Urad.}	U _T	U _{cond.}	U _{rad.}	U _{cond.+Urad.}	U _T
0.003	8.333	3.123	11.456	4.062	8.330	0.059	8.389	2.427
0.006	4.170	3.173	7.343	3.389	4.170	0.060	4.230	1.889
0.009	2.780	3.202	5.982	3.067	2.780	0.061	2.841	1.551
0.012	2.080	3.219	5.299	2.877	2.080	0.061	2.141	1.316
0.015	1.670	3.231	4.901	2.755	1.670	0.062	1.732	1.149
0.018	1.389	3.240	4.629	2.667	1.389	0.062	1.451	1.018

For the uncoated window with emissivity 0.89, the air gap thickness between 0.003 to 0.018 m and the temperature difference within the window varied between 11.52 to 21.88 K. Conduction heat transfer coefficient has been calculated between 8.333 to 1.389 W/m².K for the gap thickness between 0.003-0.018 m. Radiation heat transfer coefficient has been found between 3.123 to 3.240 W/m².K. General heat transfer coefficient has been determined between 4.062 to 2.667 W/m².K.

For the coated window with emissivity 0.05, the air gap thickness between 0.003 to 0.018 m and the temperature difference within the window varied between 7.76 to 18.98 K. Conduction heat transfer coefficient has been calculated between 8.333 to 1.389 W/m².K for the gap thickness between 0.003-0.018 m. Radiation heat transfer coefficient has been found between 0.059 to 0.062 W/m².K. General heat transfer coefficient has been determined between 2.427 to 1.018 W/m².K.

3.2 Calculated energy consumption and emission values

In Table 7, geothermal and biomass (olive cake) energy consumption depending on the air gap thickness is given for the uncoated window with emissivity 0.89. Table 8 shows the geothermal and biomass (olive cake) energy consumption depending on the air gap thickness for the coated window with emissivity 0.05. In Table 9, biomass (olive cake) emission values depending on the air gap thickness are given for uncoated and coated windows.

Table 7. Geothermal and biomass (olive cake) energy consumption depending on the air gap thickness for the uncoated window with emissivity 0.89

Geothermal Energy Consumption (kg/m²)						
Air Gap Thickness (m)	General Heat Transfer Coefficient (W/m².K) U_T	Base temperature (T_b)				
		15.5	17.5	19.5	21	23
0.003	4.062	15.021	18.851	22.999	26.272	30.788
0.006	3.389	12.532	15.728	19.187	21.919	25.687
0.009	3.067	11.342	14.233	17.365	19.837	23.267
0.012	2.877	10.639	13.352	16.290	18.608	21.807
0.015	2.755	10.188	12.785	15.599	17.819	20.882
0.018	2.667	9.863	12.377	15.101	17.250	20.215
Biomass (Olive Cake) Energy Consumption (kg/m²)						
0.003	4.062	29.098	36.517	44.552	50.892	59.641
0.006	3.389	24.277	30.467	37.171	42.460	49.759
0.009	3.067	21.970	27.572	33.639	38.426	45.032
0.012	2.877	20.609	25.864	31.555	36.045	42.242
0.015	2.755	19.735	24.767	30.217	34.517	40.451
0.018	2.667	19.105	23.976	29.252	33.414	39.159

Table 8. Geothermal and biomass (olive cake) energy consumption depending on the air gap thickness for the coated window with emissivity 0.05

Geothermal Energy Consumption (kg/m²)						
Air Gap Thickness (m)	General Heat Transfer Coefficient (W/m².K) U_T	Base temperature (T_b)				
		15.5	17.5	19.5	21	23
0.003	2.427	8.975	11.263	13.742	15.697	18.396
0.006	1.889	6.985	8.767	10.696	12.218	14.318
0.009	1.551	5.736	7.198	8.782	10.032	11.756
0.012	1.316	4.867	6.107	7.451	8.512	9.975
0.015	1.149	4.249	5.332	6.506	7.432	8.709
0.018	1.018	3.764	4.724	5.764	6.584	7.716
Biomass (Olive Cake) Energy Consumption (kg/m²)						
0.003	2.427	17.386	21.818	26.620	30.408	35.635
0.006	1.889	13.532	16.982	20.719	23.667	27.735
0.009	1.551	11.110	13.943	17.012	19.432	22.773
0.012	1.316	9.427	11.831	14.434	16.488	19.322
0.015	1.149	8.231	10.329	12.602	14.396	16.870
0.018	1.018	7.292	9.152	11.166	12.754	14.947

Table 9. Biomass (olive cake) emission values depending on the air gap thickness for uncoated and coated windows.

Air Gap Thickness (m)	Base temperature (T _b)									
	15.5	17.5	19.5	21	23	15.5	17.5	19.5	21	23
Emission values depending on the uncoated windows with 0.89 emissivity										
	CO₂ Emission (kg/m²)					SO₂ Emission (kg/m²)				
0.003	53.782	67.494	82.345	94.064	110.234	0.032	0.040	0.049	0.056	0.066
0.006	44.871	56.312	68.703	78.479	91.970	0.027	0.034	0.041	0.047	0.055
0.009	40.607	50.961	62.175	71.023	83.233	0.024	0.030	0.037	0.042	0.050
0.012	38.092	47.804	58.323	66.622	78.076	0.023	0.028	0.035	0.040	0.046
0.015	36.476	45.777	55.850	63.798	74.766	0.022	0.027	0.033	0.038	0.044
0.018	35.312	44.315	54.066	61.759	72.378	0.021	0.026	0.032	0.037	0.043
Emission values depending on the coated windows with 0.05 emissivity										
	CO₂ Emission (kg/m²)					SO₂ Emission (kg/m²)				
0.003	32.135	40.326	49.202	56.203	65.864	0.019	0.024	0.029	0.033	0.039
0.006	25.011	31.388	38.295	43.744	51.263	0.015	0.019	0.023	0.026	0.031
0.009	20.535	25.771	31.443	35.916	42.091	0.012	0.015	0.019	0.021	0.025
0.012	17.424	21.867	26.678	30.475	35.713	0.010	0.013	0.016	0.018	0.021
0.015	15.213	19.091	23.292	26.608	31.181	0.009	0.011	0.014	0.016	0.019
0.018	13.478	16.916	20.638	23.573	27.627	0.008	0.010	0.012	0.014	0.016

For uncoated windows with emissivity 0.89, it is calculated that the geothermal energy consumption varies between 9.863 to 30.788 kg/m² for air gap thickness between 0.003-0.018 m and heating degree-day values between 15.5-23⁰C basic temperatures. Olive cake consumption was found between 19.105 to 59.641 kg/m². By burning the olive cake, CO₂ emission was determined between 35.312 to 110.234 kg/m² and SO₂ emission between 0.021 to 0.066 kg/m².

For coated windows with emissivity 0.05, it is calculated that the geothermal energy consumption varies between 3.764 to 18.396 kg/m² for air gap thickness between 0.003-0.018 m and heating degree-day values between 15.5-23⁰C basic temperatures. Olive cake consumption was found between 7.292 to 35.635 kg/m². By burning the olive cake, CO₂ emission was determined between 13.478 to 65.864 kg/m² and SO₂ emission between 0.008 to 0.039 kg/m².

4 Conclusions

As the air gap of the window increases, the temperature difference inside the window increases. Conduction heat transfer coefficient decreases, Radiation heat transfer coefficient increases and General heat transfer coefficient decreases.

For the uncoated windows with emissivity 0.89 and coated window with emissivity 0.05 given at the standard of TS 2164, Principles for the preparation of the projects of the central heating systems, the internal window temperature difference for the coated window is higher than the uncoated window. While the conduction heat transfer coefficient is unchanged in the coated and uncoated glass windows, the radiation heat transfer coefficient is also higher in the uncoated glass window. This is because the glass is coated and the low emissivity value is effective.

Heating base-day values increase with the increase of base temperature. This is because of the increase in the difference between the base temperature and the outdoor temperature and increase of the sum of these differences. With the increase in the air gap thickness at any base temperature, the fuel consumption and emission values associated with the consumption of olive cake decrease for the unit area.

For uncoated glazed windows with emissivity 0.89, the energy consumption for both geothermal and olive cake varies between 16.6 to 3.2% with every 3 mm increase in air gap thickness. This percentage was calculated between 22.2 to 11.4% for coated windows with emissivity 0.05. The percentage change rate decreases with every 3 mm increase. This is due to the decrease in the value of general heat transfer coefficient every 3 mm increase.

The emission values for the olive cake with the lowest energy consumption were calculated at 15.5 °C base temperature and 18 mm air gap thickness, and the highest energy consumption and emission values were calculated at 23 °C base temperature and 3 mm air gap thickness.

References

1. T22 Güney Marmara Bölgesi Yenilenebilir Enerji Araştırması Sonuç Raporu. (South Marmara Region Renewable Energy Research Final Report)
2. TS 2164 Turk standard, Principles for the preparation of the projects of the central heating systems (2000)
3. Data of General Directorate of Meteorology
4. Dombaycı, Ö., A.: Degree-days maps of Turkey for various base temperatures, Energy, 34 (11), 1807-1812 (2009).
5. Pul., H., Ertürk, M., Keçebaş, A., Uygunoğlu, T., Daşdemir, A.: İl bazında çift ve üç camlı pencereler için optimum hava tabakası kalınlığı analizi, Tesisat Mühendisliği, 151, 5-13 (2016).
6. Karabay, H., Arıcı, M.: Multiple pane window applications in various climatic regions of Turkey, Energy and Buildings, 45, 67-71 (2012).

7. Kon, O.: Calculation of fuel consumption and emissions in buildings based on external walls and windows using economic optimization, *Journal of the Faculty of Engineering and Architecture of Gazi University* 33 (1), 101-113 (2018).
8. Maçka, S.: Türkiye iklim bölgelerine göre enerji etkin pencere türlerinin belirlenmesi, M Sc. Thesis, Institute of Science, Karadeniz Technical University, Trabzon, Turkey (2008).
9. Uçar, A., Balo, F. : Determination of the energy savings and the optimum insulation thickness in the four different insulated exterior walls, *Renewable Energy*, 35(1), 88-94 (2010).
10. Kaynaklı, Ö., Mutlu, M., Kılıç, M.: bina duvarlarına uygulanan ısı yalıtım kalınlığının enerji maliyeti odaklı optimizasyonu, *Tesisat Mühendisliği*, 126, 48-54 (2012).
11. Çengel, Y., Boles M., A.: Mühendislik yaklaşımı ile termodinamik, McGraw-Hill, Literatür yayıncılık, Çeviri Dertbentli, T., (1996).
12. Çomaklı, K., Yüksel, B.: Environmental impact of thermal insulation thickness in buildings, *Applied Thermal Engineering*, 24 (5-6), 933-940 (2004).
13. Kon, O.: Determining Theoretically And Practically The optimum insulation thickness of buildings used for different purposes according to heating and cooling loads, Ph.D. Thesis, Balıkesir University, Institute of Science, Balıkesir, Turkey (2014).
14. Aslan, A.: Investigation of energy and thermoeconomic efficiency of Gonen geothermal district heating system. Ph.D. Thesis, Balıkesir University, Institute of Science, Balıkesir, Turkey, (2010).
15. Doğuş Pirina. <http://www.doguspirina.com.tr> (November 2015).
16. Michopoulos, A., Skoulou, V., Voulgari, V., Tsikaloudaki A., Kyriakis, N., A.: The exploitation of biomass for building space heating in Greece: Energy, environmental and economic considerations, *Energy Conversion and Management*, 78, 276–285 (2014).

An Approach to A Better Transition to Sustainable Transportation System: Case Study of Three Cities (Abuja, Kumasi & Erbil)

Victor Oluwatobi Adebayo¹, Prince Tettey¹, Nabaz Rasool¹, Tanay Sidki Uyar²

¹Energy systems Engineering Department, Cyprus International University, TRNC, Mersin 10, Turkey.

²Marmara University Faculty of Engineering, Turkey.

`captainaero@yahoo.com, kojotey@yahoo.com,
nabaz.mahamadd@gmail.com, tanaysidkiuyar@outlook.com`

Abstract. Sustainable transportation is viewed as one of the key components in building sustainable cities. On the other hand, the economic, environmental and societal effects of transport are described as serious issues that can threaten the sustainability of cities. This article provides an elucidative review of the relationship between transportation (precisely road transportation) and sustainability. Firstly, the article provides a brief review about the conventional energy systems which are the main causes of unsustainability. Secondly, the paper gives a review about the situation of transportation today, transportation and energy, the effects of transportation, sustainable transportation and its implication and the options of renewables in transportation. The report further seeks to describe the challenges that need to be tackled in order to achieve a sustainable transport network in three different cities (Abuja, Kumasi & Erbil). This is accomplished by recognizing the current system and developments in urbanization and motorization in each individual city and their effects on the environment as well as mobility. In conclusion, the report discusses initiatives or routes that each city government can take to help tackle sustainability problems relating to transportation

Keywords: Sustainability, Transportation, Environment, Urbanization, Cities

1 Introduction

Conventional energy sources, for example, petroleum gas, oil, coal, or nuclear are dominating and not surprisingly, hold most of the energy usage. However, sustainable energy sources like wind energy, sunlight based, biogas/biomass, tidal, geothermal, and so forth are free of charge and are always available whenever humans are ready to utilize them. Sustainable energy is clean energy and it is always accessible without exhausting. Whenever a sustainable energy source is utilized, there is always the same available energy, with the same quality as the previously used one. This empowers sustainable energy sources to reach potentials which makes them compete enough with the conventional energy sources (Kaushika et al, 2016).

Many years ago, humans lived in harmony with nature, without any detrimental effects on the environment. Various activities of humans did not adversely affect nature with regards to energy usage. Nature and humans were at peace with each other until the emergence of cities, which required the use of more energy. This constituted the industrial revolution, and humans had to turn and attend to other ways of obtaining energy, in order to meet the energy demand. The mining and burning of coal became eminent as the technology capable of meeting the increasing demand of energy. However, detrimental issues owing to the use of this technology had to be addressed. A typical example being the London case, where a group of miners were burnt to death in their quest to mine coal for energy use. The industrialized countries now realized the existence of several disadvantages of the coal technology and so later resorted to petroleum. Similarly, in 1976, the petroleum crisis emerged and consequently these industrialized countries realized petroleum was not the best possible solution to this global menace. Nuclear energy, which is now obsolete, emerged between 1973 and 1978 to help solve the increasing adverse effects of coal and petroleum technologies. The problem was institutionalized and the industrialized countries then resorted to exportation of these obsolete technologies to developing countries as they immensely search for better ways of tackling the energy menace.

Presently, most energy frameworks are dominantly founded on fossil fuels, yet this needs to change later on. The explanation that more and more renewable energy is being implemented into the electricity system is to save fuel mainly fossil fuels and nuclear energy, when considering certain explicit situations. In a long period of time bioenergy will turn into the key issue, as biomass is a constrained asset that cannot be relied upon to supplant every single fossil fuel that is currently being used (Lund, 2000). Apart from the activities of humans that results in CO₂ emissions from the burning of fossil fuels and the specifications with reference to sustainable usage of biomass, there are a few different purposes behind why this change is significant: Security of supply and geopolitical issues, health dangers associated with burning of fossil fuels, socio-economic outcomes of the energy blends, possession and democracy, while business advancement and employment creation are other significant segments of the energy framework that have had immense attention for a considerable length of time (Lund and Hvelplund, 2012).

Fossil fuels have a significant impact in these issues and an unsustainable utilization of bioenergy may cause comparative difficulties later on. In current fossil-based frameworks, the adaptability depends on the fuels used in power plants, boilers and vehicles in fluid and solid form. Modern energy frameworks depend on infrastructure and storage facilities that can respond to the demands by means of moving fossil fuels to different parts of the world in ships and pipelines on the worldwide level, to national or regional energy infrastructure for example, coal, gas and oil storage facilities. Thus, a worldwide framework depends on enormous scale reserve of energy-dense fossil fuels that typically can deftly fulfil the needs at the perfect time and place (Connolly and Mathiesen, 2014). While this reality has already been established for the fossil-fuel based energy framework, the test currently is to make a similarly or progressively flexible energy provisions with increasing demand in the use of renewable energy. In addition, some studies have also looked at more sectors as a major aspect

of the way towards 100% renewable energy systems, including electricity, heat and transport (Connolly et al., 2011).

There is as yet a dominating sector of core interest; explicitly, on the best way to incorporate fluctuating resources into the electricity sector. Significant spotlight is being put on energy efficiency and conservation, sources of renewable energy and the handling of intermittent nature of renewable energy sources. While campaigns on electricity conservation ought to be intense, more attention is put around the combination of fluctuating renewable energy into the electricity framework to bring down emissions (Ryu et al, 2014). A typical example being the strong advocacy on the use of the following accessories: ICT, smart meters and smart grids associated with existing electricity demands, EV's and individual heating innovations, adaptable interest, storages and electricity distribution, power- to-gas and transmission (Debnath et al, 2015). A few authors are likewise linking the smart grids to the idea of smart cities, but continue to pay attention to the electricity grid only and /or on individual structures. Without a doubt, not many authors consider the transition as a total overhaul of the entire energy system (Orecchini and Santiangeli, 2011).

The great challenge has to do with the sector which deals with conveying goods and people from one place to another, and no single innovation or technology can find a convenient solution to this transportation menace. Additionally, the present utilization of biofuels is intensely discussed and the biomass use is disputable, even with new bio-refining innovations also utilizing waste biomass items, because of the association with the manufacturing of food and land use. Simultaneously a lot of bioenergy should be utilized in the heat, power and mechanical segments later on, and requests from all areas, including transport, is as a matter of fact on the ascendancy. At the end of the day, renewable energy system is essentially needed to tackle every one of the issues related with all the energy segments, particularly the transportation sector (Eickhout et al., 2008). This makes the integration of renewable transportation systems into conventional transportation systems to achieve sustainable transportation system will be a salient topic for discussion.

2 Transportation Today

Prior to the 19th century, travelling was a laborious venture especially with the involvement of manufactured goods and agricultural produce. Movement of goods were major herculean tasks for passengers of all kinds. The most radical changes notable in the speed and experience of traveling came into existence with the establishments of transportation technologies such as the steamboats, building of canals and rail tracks. Use of waterways such as the canals and inland rivers helped in managing barriers mostly associated with distance and cost while the mechanized transport systems aided the movement of both goods and humans making journeyings quite faster and less perilous. Road transport began to surface in the mid-nineties and attained superiority over the rail transport in the early 20th century.

The efficiencies of mechanized and automobile road transport systems soon birthed the idea of Air transport with significant concerns over extremely long routes, controlling notably the speed and time taken in arriving such destinations. However, ocean freight still maintained top place in the movement of goods and materials (Gilbert & Perl 2018).

Consistent improvement on transportation technologies over the centuries have significantly revamped the scale of movements socio-economically (Geels 2002). Shipping, railways, motor vehicles and airplanes have in one way or the other had a vital noticeable impact on social and economic progress (Cowie 2010). The resultant changes in the means and the speed of movement have also been pushed by and have also pushed for changes in systems of production and consumption we now see nowadays.

3 Transport and Energy

Transportation and energy are standard physical applications where giving momentum to a mass (passengers, vehicles, freight, etc.) requires a proportionate amount of energy. The matter is how effectively this energy is collected for efficient use, which is defined as a strong modal function (Rodrigue, 2020).

Petroleum oil commodities are very much used in today's transport to the extent that it is more than 50 per cent of the oil ever consumed from 1983. We can assume that more than 95 percent of the overall oil consumed worldwide happened before the inception of the Second World War (Gilbert et al, 2018).

Considering transport and energy, a huge percentage of the fuel utilized in carrying goods and people from one place to another is derived from crude oil. Around the world, transport efficiency was equitably distributed between petroleum (gas), and also heavy fuels comprising of diesel fuel and jet fuel. There were solid regional contrasts. There has been an increment in the utilisation of oil for conveying people than the utilization of oil for different reasons. The major inquiry, nonetheless, is not who will be answerable for the development in the utilisation of oil for conveying goods and people however, it is about finding out if the predictable development can occur in the earliest place. According to Gilbert et al (2018), three elements can thwart the development, these include the absence of oil, activity to control the consumption of oil in light of its ecological effects, and monetary deterioration or possibly interruption.

4 Effects of Transportation

The transport sector is the one of the major sectors which has contributed to the contamination of the air in the world, as it releases nearly a fourth of all the greenhouse gas (GHG) emissions. There has been a decline in the emissions since 2007, but they keep increasing more than in 1990. Road transport, specifically, was viewed as behind over 70% of GHG emissions from the transport division in 2014 (European commis-

sion, 2016). There has been a rise in CO₂ emissions by the transportation sector and again the road transportation represents around 74 % of the aggregate as appeared in (figure: 2).

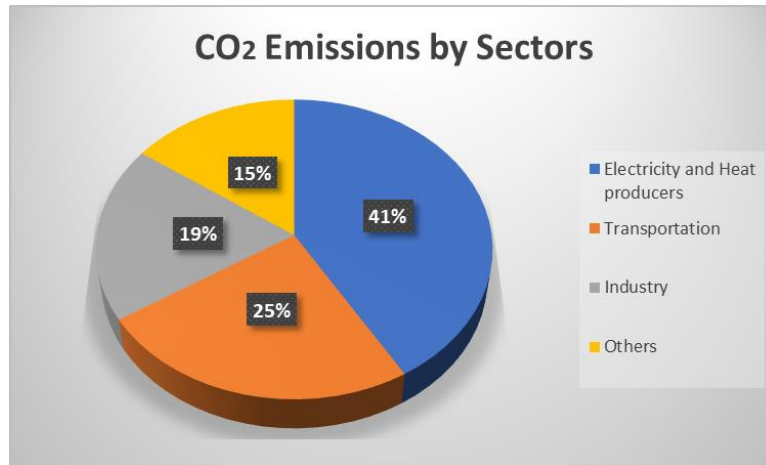


Fig. 9. CO₂ emissions by the various energy segments in 2017 (IEA, 2019)

In December 2015, 195 states including Canada consented to the Paris Agreement, an extra international action put in place to raise the eagerness to tackle climate change through a decline in worldwide GHG emissions, and limitation of the worldwide average temperatures to fall beneath 2°C. As indicated by the Intergovernmental Panel on Climate Change, this depends on understanding that 2°C is the most extreme permissible emissions limit, after which irreversible there would be the occurrence of climate destructions. All efforts should thus be on board to bring down GHG emissions so as to stay away from unsustainable climate conditions from happening (Dean and Green, 2017). Taking into account that countries have various sectors adding to their individual GHG emission profiles, each is foreseen to achieve its task by engaging various methods. For instance, Canada signed an official commitment in April 2016 to diminish its GHGs by thirty percent beneath 2005 levels by 2030, and this goes to decreasing emissions somewhere in the range of 200 and 300 mega tons from anticipated levels (Cunliffe et al, 2019).

5 Understanding sustainable transportation and its implication

Transportation frameworks have been portrayed as the “backbone” of urban areas in acknowledgment of this crucial job (Vučić, 2009). Along these lines, tenable improvement and transport are connected. On the other hand, the social, financial, and ecological effects of transport are encircled as urgently important concerns which are capable of disputing the feasibility of urban areas and locales. A viable transportation chain is a vital accelerator for the financial and social improvement of a city.

The improvement of tenable vehicle frameworks is one of the Global aims for Sustainable Development and is the first concern of the Pan-European Program on Transport, Environment and Health (the PEP), that is centered around protective, productive, available, moderate, comprehensive, green and sound portability and transport (Barrette et al, 2015). Portability and transport are still a genuine test for practical urban advancement.

The designing of cities and peri-urban areas as per blended-application and intelligent development plan standards should be a portion of a prospective tenable transportation system. City advancement together with these standards is capable of helping to bring down reliance on private cars and rather encourage the patronage community transport services and non-mechanized transport for not so long intervals and day to day drives (Un-Habitat, 2013). Concurrently, transport services inside urban areas are getting perpetually difficult to anticipate and to oversee. A few urban areas have just started to incorporate advanced mechanizations into their transport framework.

5.1 Strategies to increase sustainability of Urban Mobility

Conservation of urban areas need a maintainable mode of transport and movement, hence the need to investigate and change to new sustainable methods of transportation. Existing modes of transportation have undesirable effects on the environment (pollution) consequently making the cities less habitable. The aim of sustainable urban mobility is to upgrade all means of transportation that will have less negative impact on the communities and cities at large. These include the promotion of movement such as walking, cycling and sharing of auto mobile by individuals and households. Integrating the use of contemporary technology for all motorized transport. Implementations of such policies necessitates vigorous Research and Development (R& D), regularity in plans and policies and consistent communication. According to Makarova et. al., (2017) a form of unified methodology to these strategies is of utmost importance as transport infrastructure may have a ripple effect on other environmental and social issues and the overall development of a city.

Assmann et. al., (2006) reported that high emissions levels in developing countries come from use of second hand cars, poor maintenance and poorly worked on engines. A solution advocated by (GTZ, 2003) is regular inspection and maintenance. Others could be introduction of European standards backed by sturdy government and upgrading fuel quality. All these if not properly managed by regular inspection and good maintenance culture will be a thing of the past (Aßmann & Sieber, 2005).

5.2 Facing the Ownership and Usage of Private Vehicles

The need for personal vehicles is universal and important. Private vehicles, from scooters to large-scale cars, offer a high level of access to goods, services and activities, as well as immense freedom and flexibility. Cars and light trucks are also regarded for many as symbols of rank and as a safe and convenient means of travel. Such vehicles are an effective way for companies to increase their productivity. Every-

where in the world, vehicle ownership, size, use and energy consumption are increasing (Schipper & Lewis-Davis, 1999).

Car ownership per 1 000 inhabitants is projected to grow continuously, and most countries are experiencing significant increases in the rate of driving license. The average annual distance traveled by passenger car is also rising, resulting in a large increase in the total annual mileage driven. The use of policy initiatives such as fuel taxes, vehicle taxes based on fuel efficiency and road pricing will, however, reduce this expected growth by reducing overall demand and promoting the transition to more fuel-efficient / low-emission vehicles (OECD, 2002).

It has been argued that different behavioural changes may be needed to achieve stable transportation, including driving style changes, mode choices, car ownership, and location choices changes. Both adjustments are correlated with various behavioural costs which may vary with different travel purposes. For example, traveling by public transport instead of a car may be more feasible for some trips (e.g., commuting) than for other trips (e.g., shopping), and it may be easier to change travel time for some journeys, but not for others. In general, behavioral changes should take place according to a general cost-minimization rule, first choosing the less costly adaptation alternatives (Loukopoulos, Jakobsson, Gärling, Schneider, & Fujii, 2004).

Transport policies would strive not only to minimize the attractiveness of automobile usage, but also to raise the attractiveness of other modes of transport, so that car use can be modified efficiently.

5.3 Options for Renewable Energies in Transport

The transport industry is one of the main sources of significant energy use and carbon emissions in urban areas. While diesel and gasoline are the main forms of energy used in urban transportation, alternative and additional energy sources have been introduced. Electricity (used in hybrid, electric and fuel cell vehicles) is an effective and transformative energy source, gaseous fuels, biofuels, from other sources (natural gas, hydrogen, and liquefied petroleum gas) alcohols and ethers. As these sources are renewable and have a lower impact on the environment than diesel and petrol, alternative and intermediate energy sources can be used to facilitate the development of sustainable transport systems. (Li & Loo, 2014).

Replacing diesel and gasoline in both private and public vehicles with renewable and transitional energy sources is complex because it involves multiple challenges. The challenges include not only the technological complexities of vehicle construction and design of infrastructure, but also the lack of political and public support. It was stated that only when alternative sources of power compete with fossil fuel efficiency in all aspects, such as cost, convenience and reliability (Vimmerstedt et al., 2012).

In urban transport, the main alternative and transitional energy source is electricity, biofuels (e.g. biodiesel and vegetable oil), other gaseous fuels (hydrogen, natural gas and LPG), alcohols (ethanol and methanol) and ethers. (Fig. 4) (Ramadhas, 2016). Since the global energy crisis of the 1970s, there has been a lot of attention given to alternative and transitional energy sources. These include the rapid increase in the use

of natural gas in forms such as compressed natural gas (CNG) and LPG in the last decades (Bechtold, 2002).

Most of the recent findings concentrate on electricity and biofuels, which can become the largest long-term renewable sources of energy for urban transport. With regard to the use of hydrogen, alcohols and ethers, the new trend is to use them in fuel cell vehicles instead of as primary fuels or to combine them with fossil fuels (Bechtold, 2002). One of the applications of electricity in urban transport is plug-in hybrid EVs (PHEVs), battery EVs (BEVs), and fuel cell EVs (FCEVs). PHEVs rely on diesel / gasoline and electricity which have been used for about half a century; most recently, more attention has been paid to BEVs and FCEVs. In 2012, the global EV inventory reached 180,000, representing just 0.02% of total passenger cars, but by 2020, the figure is projected to be 2% (Ministerial, 2013).

Methanol can be produced from wood, cellulose or natural gas, and it is expected that it has strong impacts in GHG emissions, once it is produced from biomass. However, there is a prediction that the price of methanol will be compared to that of traditional fuels in the future. For hydrogen, it can only be a source of transportation energy to reduce GHG emissions if it is been produced from renewables. Even though it has a promising potential because it is proved to be environmentally friendly, the hydrogen technology is not presently developed sufficiently for a wide spread.

Fuel cells also have great effects on GHG emissions if the fuels are also produced from renewable energy. For now, the technologies are not developed sufficiently enough for use in large scale. Electric vehicles also have strong impacts on CO₂ emissions, this also depends on the way the electricity is been produced. They operate with less noise and do not produce emissions. The drawback is just the limited range of the vehicles, which needs frequent fuelling.

The greatest drawbacks of the widespread use of alternative energy sources in the transport sector is the high cost of new technologies and technological immaturity. Such complex issues include not only the construction of engines and cars, but also the creation of fuel storage facilities, charging and refuelling infrastructures. Different types of alternative energy sources also have different technological obstacles. For instance, for electric vehicles, the obstacles might be battery performance and re-charging systems (Kamimura, Kuboyama, & Yamamoto, 2012; Krutilla & Graham, 2012; Pasaoglu, Honselaar, & Thiel, 2012).

6 Abuja City

In the same way as other developing urban cities, Abuja is encountering a cosmic pace of population growth. Without a doubt, its urbanization rate of 8.32% yearly makes it the fastest developing city in Africa (Myers, 2011).

Abuja is not just a state-of-the-art hub of Nigeria. It is a city where Elites who desire to realize their modernist vision of a systematic and delightful city and the poor who try to make ends meet are in a contest. Abuja is also the destination city with countless number of unemployed people commuting to the city in search of supposed job prospects and also for those seeing the city as a much safer place than other parts

of the country. In this context, together with the limitation of resources, the municipal government is struggling to meet the rising demands of providing basic public services, housing and an effective transportation system (Abubakar, 2014).

6.1 Abuja Transportation System

The present transport systems in Nigeria depend solely on the use of internal combustion engines which run on fossil fuels, this leads to a resultant rise to pollution, global warming and also climate change; whereas the adaptation of renewable energy in the transportation sector could meaningfully reduce greenhouse gas emissions and air pollution. The amount of petrol consumed in road transportation is the largest source of CO₂ emissions (Sperling & Cannon, 2009) which accounts for about 23% of worldwide CO₂ emissions (Saboori et al., 2014) in Nigeria about 59.5% of CO₂ comes from road transport (Tajudeen, 2015)

Throughout Abuja city and satellite cities, the bulk of movements are by private vehicles and taxis. Private cars are mostly used to satisfy the Abuja residents' regular mobility needs. According to Femi (2012), out of approximately 600,000 vehicles running daily on Abuja highways, some 520,000 are private vehicles. The procurement of various mass transit buses used as public transport is also distinguished by private ownership. Such popularly known as 'Kabu-Kabu' or 'Danfo' public transport media are mostly scrapped craps or imported second-hand cars, which easily become old and rickety with many tendencies to break down and smoke regularly. Such private vehicles make up the bulk of the unregulated public transportation vehicles in most of Abuja. We are then accompanied by motorcycles that were barred several years ago from the city after their problems rose to an unacceptable level that was very high. Then these motorcycles were replaced by so many tricycles in the city (Femi, 2012).

Therefore, in order to limit traffic congestion in the city of Abuja, the Abuja Master Project proposal recommended that so many expressways and major roads be built, light rail and bus transport networks in order to connect numerous district centers and also connect the major city with satellite settlements such as Gwagwalada, Kubwa, Lugbe, Karu, Suleja, Nyanya, Bwari, as shown in Figure 2. Today, Abuja stands out for its high-quality expressway among other African cities. But driving through the city and satellite traveling is still a frustrating experience, especially during peak hours. (Abubakar, 2014).

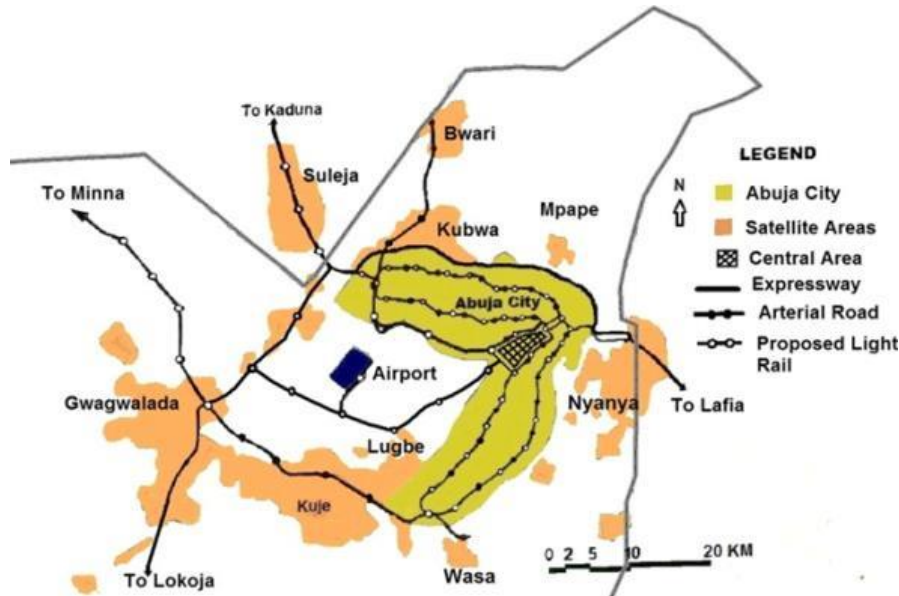


Fig. 10. Transport network of Abuja city. Source: Abubakar, 2014

In order to improve the transport system in Abuja, expanding highway lanes from three to five as is currently being done by the city administration will not be enough, but will also have to introduce a very efficient public transport system. The public transport busses now run by the city are not enough, rickety busses are used and are overcrowded most of the time (Abubakar, 2014).

6.2 Suggested Pathways/routes to achieve sustainable transportation in Abuja City

There are many modes and types of vehicles for transportation, using a wide range of fuel types and qualities for different applications. Therefore, the energy needs of the transportation sector are complex compared to other sectors, requiring solutions tailored to each application for renewable energy. Renewables, though, may play a role in all various transport types. Other modes of transportation to achieve sustainability is also discussed in this section.

There are three possible routes suggested in this paper for the achievement of sustainable transportation in Abuja city:

- using electric or hybrid electric vehicles and the use of light rail running on electricity is the first route.
- the second route is to encourage cycling and walking
- the last route is the use of biofuels produced from biomass to substitute fuels from fossil fuels or be blended with fossil fuels to be first used in public transport buses.

First Route

In building a smarter, cleaner and more sustainable future, cities, governments and businesses have to recognize the value of the use of Electric Vehicles (EVs).

What seemed to be one of the biggest setbacks faced by Nigeria's electric vehicle (EV) industry in April 2019, the bill by Senator Ben Murray-Bruce – seeking to phase out petrol vehicles – came to an end. 2035 was rejected by the Senate. Senator Ben stated that the EVs could assist in clearing up the issues of ozone depletion and also promote health (Ally, 2019).

Nigus Enfinity, brought up in Nigeria, plans to make EVs increasingly alluring to motorist in Nigeria, with plans to assemble the cars locally by year 2020. Ado-Ibrahim, the CEO of Nigus Enfinity said his firm is right now raising 100-megawatt solar power plant in Katsina state. It also of late united with a Chinese company with the expectation of importing electric vehicles that are affordable (Ally, 2019).

Sirienco, Slovak company, is also making arrangements to set up an assembly plant in Nigeria, where it will be assembling EVs. The plant is intended to be situated in Cross River state with the Cross-River State government proposing to support and render assistance. The project is intended to be a boom for the local economy (Akpan, 2019).

Abuja has an annual average solar (clearness level and normal radiation) of 5.45 kWh / m²/d (Anayochukwu Ani, Ndubueze Nzeako & Chigbo Obianuko, 2012). This value shows good prospects in Abuja for PV application. The authors believe there should be installation of charging stations in the city of Abuja, with installation of solar photovoltaic systems will be help promote the use of EVs in the city and the country at large, due to the fact that the city has a large number of elites who will be interested in trying out the electric vehicles. Therefore, the vehicles could be brought in from Cross River and Katsina states.

Despite the fact that the bill by Senator Ben Murray-Bruce's to make Nigeria a nation free from petrol vehicles by 2035 has been disenchanting, the country is still slowly moving forward, as private enterprise is leading the way.

To relieve the congestion in Abuja's transit, the municipal government should have a relationship with the private sector to complete the remaining phases of the railway network that would provide the city and its satellite settlements with transportation facilities. This will make travelling much more quick, comfortable, and less expensive and also pressure on existing roads will also decrease.

The Abuja Light Rail System is a key part of the Abuja Rail Mass Transit System and the FCT Master Plan. The project is being carried out in six lots. A dedicated overhead contact line system will provide electricity required for operation of the system. A line voltage of 1,500V DC is required for the seamless operation of the light train fleet ("Abuja Light Rail System, Abuja, Nigeria", 2019)

The authors suggest that this electricity should be provided by solar energy. Installation of Solar PV panels and batteries for storage will go a long way in providing constant electricity for the system due to the epileptic nature of the power system.

Second Route

As mentioned earlier, Abuja city relies heavily on road use by private cars and public buses. With population growth, poor road maintenance, poor car maintenance, insufficient public transport planning and weak pollution and climate change policies, roads are congested. It is therefore in this manner convenient to investigate possibilities for introducing cycling as a sustainable non-motorized transportation mode for Abuja city which also enhances mobility for the urban poor and increases interaction among nearly all groups. Engaging in cycling provides social, economic and environmental advantages to Abuja City as well as engaging in an accessible public transportation system.

Cycling and walking are almost unrecognized as there are only a few different road services for pedestrians (such as walkways, zebra crossings, footbridges, underpasses and signs) and bicycle lanes open. This has pedestrians and vehicles share the road. In the past when efforts have been made to provide these facilities, due to poor enforcement, many walkways are now been used as parking lots, trading and storage areas for abandoned material

Active travel facilities should therefore be integrated into the existing transport infrastructure in the city by the city's government through related agencies. Introducing and enforcing policies to reduce traffic and speed is very needful supported by appropriate infrastructure design criteria to create a low-risk and amenable environment for active travellers.

In addition, the provision of pedestrian paths along its roads and zebra crossings at major road intersections would encourage walking and improve road and passenger safety.

Bicycles are a convenient mode of transport for short journeys from one to three miles beyond walking distance. The authors suggest the integration of public transport networks and the cycle network, because they are complementary modes of transportation and they can be tied together in the form of a trip that looks like a door to door chain. The bicycle parking facilities at the train/ bus stations should meet the high-quality standards, and their design should accommodate smooth bicycle-train/ bus interchange, with very little time loss due to their interchange function. The parking facilities should be located on the cycling main access route, so that it will be easy for cyclists to park on their way to the station.

Third Route

It is suggested that fuel be switched to biofuels such as biodiesel and bioethanol for Nigeria's road transport sector, which currently runs entirely on diesel and petrol. The potential for biofuels that lead to sustainable production with greater environmental and socio-economic benefits cannot be overemphasized. Countries now allow conventional transport fuels to be mixed with 10% biofuels to ensure energy security and reduce emissions of greenhouse gases (Bindraban et al., 2009).

Sustainable processing of biofuels requires the use of crop residues, forest residues, and solid waste. Nigeria is a net transport importer of fuel oil, making it vulnerable to fluctuations in global fuel prices and dependent on foreign exchange to meet its do-

mestic energy needs. Consequently, the objective is to reduce the high reliance on imported petroleum by optimizing dominance.

While in Nigeria's low-carbon transition 'tale' other renewables such as solar and wind are needed, we suggest aggressive deployment of biofuels in the Nigerian energy system. In particular, we suggest the conversion of fuel to biofuels such as bio-diesel and bioethanol for Nigeria's road transport market

With the location of the current petroleum refineries in Nigeria's Delta region and the extensive biomass resources available in the same area, the Nigerian National Petroleum Corporation needs to consider, as part of its biofuels plan, whether it is better to produce finished biofuels in the new bio-refineries and transport them to the existing refineries for blending, or whether it is better to have an expansion of infrastructures in existing refineries to cater for the production of the biofuels.

It is possible to replace fossil fuel buses with an alternative (biofuel, fossil fuel / biofuel mixed) fuel bus for use in the public transport system of Abuja city if the proposed biofuel programme of the country works out. Most advanced and developed cities have experimented with alternative bus technologies that use bio-diesel, bio gas, bio ethanol.

The government of Abuja city can play a role here by providing subsidies for these energy-efficient vehicles. With respect to behavioural changes, the main objectives are to shift mode of transport from cars to buses, increase vehicle occupancy ratio, and telecommuting. This will, however, require the introduction of taxes on car owners and also the provision of huge incentives for bus operators. These actions would significantly reduce the demand for transport and, consequently, reduce the demand for energy.

7 Kumasi city

Road transport is the dominant mode of transportation in Ghana, having about ninety-four percent of cargo or freight and about ninety-eight percent of commuters utilizing transportation by road. In Ghana, private vehicle ownership is generally low, with public transport serving almost all or majority of the transportation needs of the population (Sam et al., 2014)

Kumasi is a city in Ghana, situated in the central part of the country, making it an important business and industrial area. This city is found in the Ashanti region of Ghana and has always had a relative advantage over other urban areas in the nation. Furthermore, Kumasi is a significant hub in the transportation framework of the entire country (Poku-Boansi and Adarkwa, 2013). The city is around two hundred and seventy kilometres north of the capital city of Ghana, known as Accra. Kumasi has an approximate land area of about 214.3 km² and possesses about 0.9 % of the Ashanti region's territorial area. The population of Kumasi is approximately 2,035,064 which comprises of 972,258 males and 1,062,806 females and this accounts for 36.2 % of the entire population of the Ashanti region. The predicted yearly population growth rate of the city is at 5.4 % and has resident density of about 9,434 individuals per km² (Ghana Statistical Service (GSS), 2010).

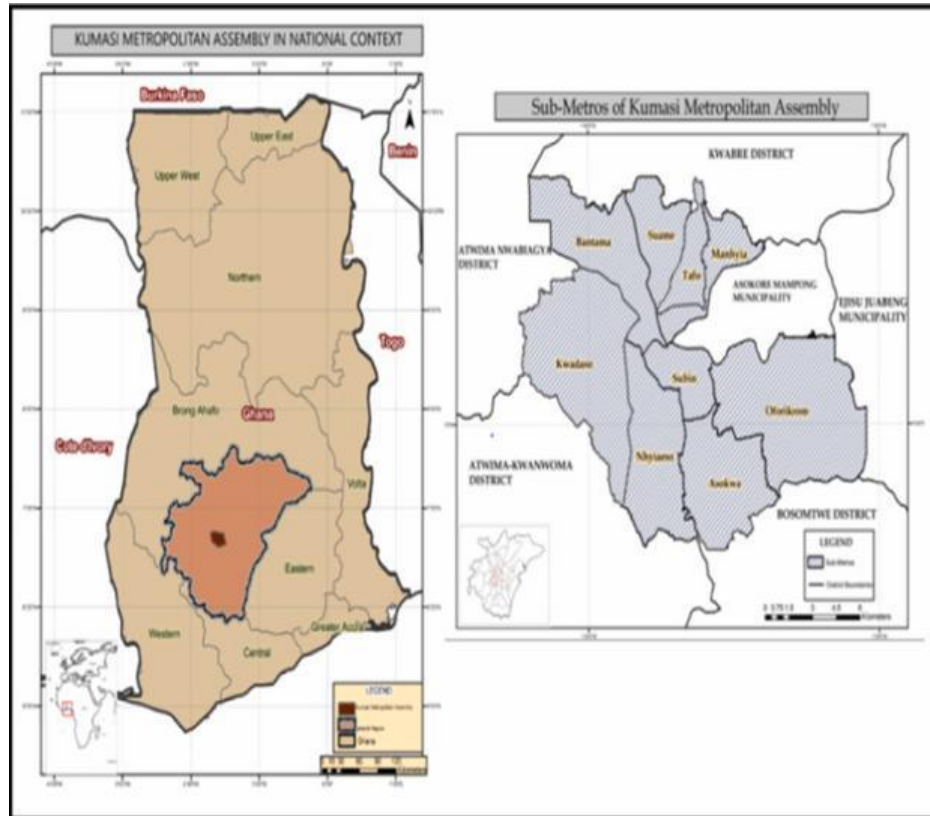


Fig. 11. Kumasi in national and regional context. Source: Kumasi Metropolitan Assembly, (KMA) 2014.

Some years back, the city was alluded to as “The Garden City” in the Western part of Africa because of its natural vegetation. The road structure of the city has a total road system of 1931.18 km, comprising of 136.4 km major roads connecting the city the surrounding urban communities, and 110.39 km of minor roads linking resident roads to the major roads.

The merchant roads which is 90.61 km connects the minor roads to the local roads. The road system of the city has its largest part being the local roads which occupies a total distance of 1593.78 km. The various housing areas are also being served by the local traffic system. Considering the total road system, about 62 % of the total road system are esteemed to be in motorable conditions (Poku-Boansi and Adarkwa, 2013).

Moreover, the physical structure of the city is spherical with a vibrant commercial area located in the central part. Almost 86 % of the city’s populace is monetarily dynamic and are occupied with the different parts of the economy. The administration related segments, utilizes about 72% of the city's dynamic working force (Kumasi Metropolitan Assembly, 2014).

The business and industrial nature of the city produces a great deal of mobility and thus transportation services demand is extensive. Considering Kumasi and Ghana at large, public mobility is predominantly by public transport which is usually provided by the private sector, owing to the impact of the nation's deregulation policy (Daniels et al., 2017). This city of Kumasi has large number of taxis, minibuses and buses operating as public transportation sources. This study however, focuses on the strategies to significantly integrate renewable energy systems into the existing transportation systems in the city of Kumasi. The various transportation modes are distributed as; 54.8 % of public transport, 19.6 % of private vehicles and 25.6 % of walking. The public transport holds the largest share of the transportation mode and has an average daily traffic of 6,225 taxis, 4,468 private cars, 8,091 small buses, 2,084 medium buses and 322 large buses (Borkloe et al., 2013).

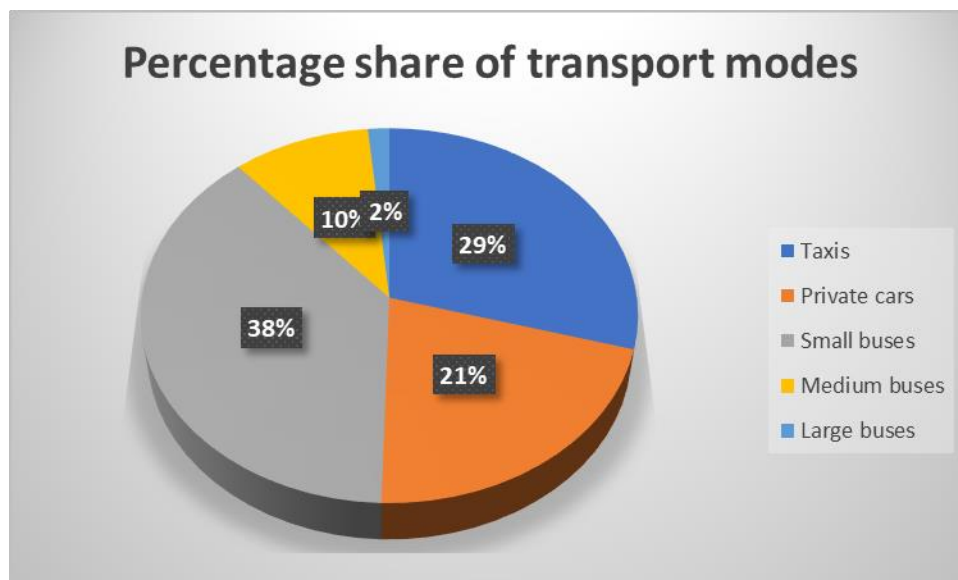


Fig. 12. Share of modes of transport in the town of Kumasi

It is very alarming to note that, all the vehicles available in the transport system in the city of Kumasi are ICEV's. These engines run on petroleum oil as fuel and the burning of these fuels has its own implications. The drastic increase in CO₂ emissions due to the combustion of these engines brings about a major menace. In 2005, the roads and transport department stated that public transport vehicles in the city of Kumasi possess average ages of about thirteen years (Quarshie, 2007). This again aggravates the emission of greenhouse gases since most of the engines at that age would not work at their optimum capacity. Air pollution is rising, culminating in excess of the national air quality standards and those approved by the World Health Organization in the city of Kumasi. Air pollution has significant effects on the health of citizens, disturbs vision and causes the distortion of buildings and local ecology, this goes a long way to reduce the quality of urban habitation.

Public transportation modes are the highest modes of transport in the city; however, all these vehicles are private owned. This usually results in a huge increase in the number of vehicles plying on the roads as public transport. Congestion is eminent, considering the increasing number of private owned commercial vehicles. Even though there exist an enormous number of commercial vehicles, pedestrians need to queue in order to get to their various destinations at peak hours.

These problems enumerated above makes the integration of renewable energy into the existing transportation system in the city of Kumasi very paramount. It is vivid that, when these problems are considered and addressed, Kumasi as a city would meet most of its goals of being a city worthy for habitation and development of citizens. There are several strategies to consider in order to integrate renewable energy transportation systems into the existing transport system of the city of Kumasi.

7.1 Strategies for Integration

The speedy development in demand for mobility, the surging in vehicle ownership and the ever-increasing cost of travelling imply that, pattern-based ideas of the future would not be able to obtain a viable answer to sustainable transportation system in the city of Kumasi. Scenarios enable ideas of the future to be portrayed within a particular system and under explicit assumptions. Scenarios go a long way to animate reasoning and prepare individuals into adapting to current situations. Within the background of the integration of sustainable transportation into the existing transportation system of the city of Kumasi, two clear pathways are proposed.

The eco-car

The building of eco-vehicles will be the significant to address the situation. This will primarily be used in the urban areas as a long-term solution. Despite the fact that renewable resources will still be required to develop the vehicle, hydrogen fuel cells would be used to power it. When considered, the vehicle will most likely be accessible within ten years, however, it is unlikely to attain a significant impact on the total stock of vehicles for a further ten years considering the current economic levels. Policies must address actions aiming at the facilitation of the research and development of the eco-car and also sending vivid indications to the car manufacturing industry to allocate resources in the building of small city-based vehicles.

The policies may include the following:

- increasing the budgets allocated to the research and development of the eco-car and its related technologies
- development and availability of supporting infrastructure for use when necessary
- provision of incentives for organizations to channel their investment in the suitable technology with the sole aim of getting to the production stage
- provision of disincentives for the acquisition of large inefficient cars to be used in the city

- subsidy being enjoyed by private cars should be phased out and the introduction of a scrappage programme to educate and encourage individuals to acquire the eco-car

In addition to the above proposal, the introduction of buses that run on biofuels will be the alternative approach to tackle this integration. Kumasi and its environs have a lot of vegetation and farmland such that, some of the farm produce go to waste. These excess farm produce can be utilised with a combination of the municipal sewage waste to produce enough biofuels to power buses. This can be related to the case of Kolkata a city in India where a bus fuelled by biogas from waste is under observation. The government of India is planning of introducing these types of buses if the results from the observation are viable. The main drivers accounting for this initiative is the low cost of biogas production in the city of Kolkata, which the city of Kumasi can also boast of possessing.

The reasons for these proposed actions will be the enormous impact in the reduction of GHG emissions, thereby reducing air pollution and global warming. The introduction of these policies and sustainable buses will also impact on congestion and the usage of space by traffic. However, other measures are also required to help in the integration of sustainable transportation systems.

Reduction in the Need to Travel

Regardless of whether the technology-based solutions are advanced, there still exist the noteworthy issue of increments in transport demands with leads to congestion. Supplementary actions are needed to lessen the need for individuals to travel before accessing services and facilities in the city. Supplementary actions can be in the form of technological advancements in information and communication systems, where telecommunication services create opportunities for advanced video-conferencing system and remote working. This is vital on the grounds that, advancements in transport technology alone is not enough to tackle the issue of sustainable transport integration. There will always exist a transition gap between the sustainable transport and the existing transportation system in Kumasi. This implies that, other correlative measures must be engaged to reduce drastically the traffic demands in the city.

The authorities of the city of Kumasi have a vital role to play in the provision and maintenance of accessibility and proximity of central business centre in the city. Sustainable living for most individuals involves sufficient size settlements, such that overall range of infrastructure and facilities are accessed within walking, cycling or public transport.

Finally, behavioural changes involving the reduction of private motor vehicle use, through highway charges and parking fees as well as behavioural changes that result from educating individuals on the paybacks that are associated with less motor vehicle usage. These proposed pathways will in the long run, improve the mobility in the city of Kumasi as sustainable transportation is integrated into the existing transportation system.

8 Erbil City

Hawler or Erbil is located in Kurdistan district and it is one of the fourth governorates, the capital of the district, Sulaymani, Halabja, and Duhok. The district is situated in the federal republic of Iraq in accordance with Iraqi establishment. Its area is round 15,074km² with 36.2° North latitude and 44.02° Longitude (NCCI, 2015). Erbil metropolis is confronted with ecological and biological problems, such as, wastewater remedy, water delivery, land safety, air contamination, noise contamination, and pollution due to the enormous increment in the number of vehicles, just as the large increment of open mills, which work in each authority of the municipal.

The road network of the Erbil city is commonly in satisfactory or deprived situations. The road system consists of main, minor and tertiary (local / metropolitan / rural) ways with a total network of approximately 23,400 kilometres. Nevertheless, the main roads involve about 5800 km, of which 1954 km are the main roads and 3854 km are the secondary roads and most of them remain on local streets. Nearly 60 percentage of the streets are not asphalted or in other words are not paved. About 98% of the roads have one lane in each direction and the remaining 2% (482 km) has two or more lanes on a two-lane road (World Bank, 2015).

A huge piece of the current street arrangement (15.480 km or 66%) is awful or basic (extremely terrible). The state of the street surface and pavement of the main and supplementary network are regularly in great condition or good, with 28% having feeble or horrible soils. The circumstance of extensions and other significant structures is of concern. Erbil city has 328 bridges, 95% of which require quick and urgent support and maintenance and/or adjustment (World Bank, 2015).

The degree and limit of the general population transport framework in Erbil is ruled by the utilization of cabs. No mass travel is available in Erbil urban communities, be it a customary intercity railroad, light rail travel, or transport fast travel. The quantity of traveller transports in Erbil in 2010 was 5,082 transports, of which 3,490 were intracity transports and 1,592 were intercity transports. The quantity of taxicabs was 55,331 of which 52,500 were intracity taxis and 2,831 were intercity taxis. The overall number of travellers utilizing these, was 5.13 million, most of whom (around 75 percent) were travellers of intracity taxis (World Bank, 2015).

8.1 Suggested Solutions

The transport segment is liable for 33% of worldwide energy request and one-sixth of worldwide ozone depleting substance discharges. It is also the part with the most minimal entrance of sustainable power source, such that, in 2016, just 4% of energy utilization in the vehicle sector originated from renewables (Hosseini and Wahid, 2016). In Iraq, likewise the energy utilization is high particularly for transportation in north of Iraq. It is obvious that a 100% inexhaustible economy would give an enduring answer for the difficulties raised by environmental change, sustainability, energy security, and contamination. Particularly for the locale, that faces challenges such as power generation issues, monetary emergency, and ecological difficulties.

There are two proposals in his paper for taking care of number of issues in this city they are:

Electric Vehicles

One of the best approaches to have reasonable transportation is moving the mobility portability framework to electricity power vehicles.

There is an engine system in an electric vehicle and this kind of car has at least one and response for moving the electricity vehicles. In general, electric cars exploit energy put away in battery-powered batteries. Essentially, there is a battery in an EV instead of a classic petroleum tank. The power obtained from its batteries controls the electric engine. They use 'clean energy' that limits natural effect.

EVs are additionally expected to assume a functioning role as energy stockpiling gadgets (power sources) in case of a calamity. For instance, during crises, for example, power blackouts because of a seismic tremor, where they can likewise use to move therapeutic hardware and different necessities. It implies that, alongside having an appropriate property of the vehicle, it needs a wellspring of intensity. For this reason, direct nearby planetary group class, and spotlight on sun powered Photovoltaic (PV) and wind power innovation become the central matters.

Considering solar PVs, information was acquired for Erbil city from a sun powered radiation database "PVGIS-CMSAF". The outcomes showed that the capability of Photovoltaic panel innovation to create power are distinctive as indicated by the time inside a day and the period inside a year (Azabany, et al., 2014). These gives a clear indication that Erbil city can benefit from the solar resource to power the electric vehicles.

Public Transportation

An alternative approach to have sustainable transportation is urging individuals to utilize public transportation rather than private vehicle, particularly by having a particular program and frameworks. In another words, systemize and database the outline of the specific scheme of transportation. For instance, most open vehicle suppliers have programs that enable managers to give limited or pre-charge passage cards to their workers. Notwithstanding making open vehicle less expensive for representatives, numerous businesses are capable of receiving charge rewards by partaking in these projects. Additionally, frequencies should be more than two times every hour, so as to make the waiting time not that much.

Moreover, fares should be sensible, in another word, city authorities must provide better transportation systems with affordable prices. In the event that travellers can drive their vehicles much less expensive than utilizing open travel, they would always opt for private rides rather than open travel.

Finally, it is prudent that, stakeholders in the Erbil city must ensure that all the said public modes of transport should utilize renewable energy sources as their sources of fuel.

9 Conclusion

Humans lived in harmony with nature without any issues concerning their immediate environment until the rise of the industrial age. This resulted in cities, indulging in various kinds of activities that went a long way to have detrimental effect on nature. Cities began to expand and the human populace also increased drastically which lead to the high demand for energy in all sectors including the transportation sector. The transportation sector is one sector that is needs immediate improvements in all forms to help the challenges being experienced in nature. This sector accounts for a significant amount of GHG emissions globally. The introduction of sustainable transportation systems has become eminent in addressing majority of the challenges being faced in the current transportation systems.

This paper takes a critical look at the current transportation system in three cities; Abuja, Kumasi and Erbil. The paper seeks to suggest pathways or route that would help these cities to integrate sustainable transportation system into their existing transportation system. These suggestions were based on the challenges and shortfalls in the existing transportation systems in the cities. In summary, it was suggested that, the eco-car and EV's are significant pathways to consider in these cities, since majority of the existing cars are private owned and household vehicles. However, institution of this pathway would have its own challenges. City authorities and the government at large must institute policies and regulations to assist the integration of this pathway.

Practical suggestions such as cycling and walking within realistic distances are also important when looking at integration of sustainable transportation. Buses being powered by biofuels are also suggested, especially in the cities of Abuja and Kumasi with vast farmlands and farm produce that often go waste. In addition, technological improvements in transport alone is not enough to curb the issue, but technological improvements in all sectors especially the communication and information sectors is necessary. Education on the need for sustainable transportation and behavioural changes of individuals in these cities are also important aspects of the integration. Finally, it is vivid that, when these suggested pathways are integrated into the existing transportation systems of these cities, challenges such as congestion, CO₂ emissions leading to air pollutions will be significantly improved.

References

1. Abubakar, I. R.: Abuja city profile. *Cities*, 41(PA), 81–91 (2014).
2. Abuja Light Rail System, Abuja, Nigeria. (2019). Retrieved 2 January 2020, from <https://www.railway-technology.com/projects/abuja-light-rail-system/>
3. Akpan, A. (2019). Retrieved 2 January 2020, from <https://guardian.ng/business-services/cross-river-slovak-firm-partner-on-electric-car-plant/>
4. Ally, C.: What is the future for electric vehicles in Nigeria? - EnviroNews Nigeria (2019)

5. Anayochukwu Ani, V., Ndubueze Nzeako, A., Chigbo Obianuko, J.: Energy Optimization at Datacenters in Two Different Locations of Nigeria. *International Journal Of Energy Engineering*, 2(4), 151-164 (2012).
6. Assmann, D., Laumanns, U., Uh, D.: Renewable energy: a global review of technologies, policies and markets. Routledge (2006).
7. Aßmann, D., Sieber, N.: Transport in developing countries: renewable energy versus energy reduction? *Transport Reviews*, 25(6), 719–738 (2005).
8. Azabany, A., Khan, K., Ahmed, W.: Solar Photovoltaic Generation Potential and Plant Capacity in Northern Iraq. *Asian Journal of Science and Technology*, 5(7), 423-426 (2014).
9. Barrette, J., Evelyne T., Saint-Pierre, F., Wetzell, S., Duchesne, I., Krigstin, S.: Dynamics of dead tree degradation and shelf-life following natural disturbances: can salvaged trees from boreal forests ‘fuel’ the forestry and bioenergy sectors? *Forestry: An International Journal of Forest Research* 88, no. 3 275-290 (2015).
10. Bechtold, R.: *Hydrogen*. SAE (2002).
11. Bindraban, P. S., Bulte, E. H., & Conijn, S. G.: Can large-scale biofuels production be sustainable by 2020?. *Agricultural Systems*, 101(3), 197-199 (2009).
12. Borkloe, J. K., Nyantakyi, E. K., Mohammed, G. A.: Capacity Analysis of Selected Intersections on Mampong Road, Kumasi-Ghana Using Micro Simulation Model. *International Journal of Structural and Civil Engineering Research (IJSCER)*, 2(3), 39-61 (2013).
13. Connolly, D., Lund, H., Mathiesen, B. V., Leahy, M.: The first step towards a 100% renewable energy-system for Ireland. *Applied Energy*, 88(2), 502-507 (2011).
14. Connolly, D., Mathiesen, B. V.: A technical and economic analysis of one potential pathway to a 100% renewable energy system. *International Journal of Sustainable Energy Planning and Management*, 1, 7-28 (2014).
15. Cowie, J.: The economics of transport: A theoretical and applied perspective. Routledge (2009).
16. Cunliffe, G., Christian H., Kennedy M., Pauw, W. P., Harald W.: Comparative Analysis of the NDCs of Canada, the European Union, Kenya and South Africa from an Equity Perspective: a research report funded by the Swedish Energy Agency. *Research report series* (2019).
17. Daniels, S., Hamidu, O., Sam, E. F.: SERVQUAL analysis of public bus transport services in Kumasi metropolis, Ghana: Core user perspectives. *Case Studies on Transport Policy*, 6(1), 25-31 (2018).
18. Dean, A., Green, D.: Climate Change, Air Pollution and Health in Australia. *Sydney, Australia: UNSW Sydney* (2017).
19. Debnath, U. K., Ahmad, I., Habibi, D., Saber, A. Y.: Energy storage model with gridable vehicles for economic load dispatch in the smart grid. *International Journal of Electrical Power & Energy Systems*, 64, 1017-1024 (2015).
20. Eickhout, B., van den Born, G. J., Notenboom, J., Oorschot, M. V., Ros, J. P. M., Van Vuuren, D. P., Westhoek, H. J.: Local and global consequences of the EU renewable directive for biofuels: Testing the sustainability criteria. *Local and global consequences of the EU renewable directive for biofuels: testing the sustainability criteria* (2008).
21. Femi, S. A. G.: Characterization of current transportation challenges in the federal capital territory, Nigeria. *Journal of Sustainable Development*, 5(12), 117 (2012). Ghana. Statistical Service. (2013). 2010 Population & housing census: National analytical report. Ghana Statistics Service.
22. Geels, F. W.: Technological transitions as evolutionary reconfiguration processes: a multi-level perspective and a case-study. *Research Policy*, 31(8–9), 1257–1274 (2012).

23. Gilbert, R., Perl, A.: Transport revolutions: moving people and freight without oil. Routledge (2018).
24. GTZ.: A Sourcebook for Policy-makers in Developing Cities. GTZ (2003).
25. Hosseini, S. E., Wahid, M. A.: Hydrogen production from renewable and sustainable energy resources: promising green energy carrier for clean development. *Renewable and Sustainable Energy Reviews*, 57, 850-866 (2016).
26. Kamimura, K., Kuboyama, H., Yamamoto, K.: Wood biomass supply costs and potential for biomass energy plants in Japan. *Biomass and Bioenergy*, 36, 107–115 (2012).
27. Kaushika, N. D., Reddy, K. S., Kaushik, K.: Conventional Energy and Power System. In *Sustainable Energy and the Environment: A Clean Technology Approach* (pp. 43-60). Springer, Cham (2016).
28. Krutilla, K., Graham, J. D.: Are Green Vehicles Worth the Extra Cost? The Case of Diesel-Electric Hybrid Technology for Urban Delivery Vehicles. *Journal of Policy Analysis and Management*, 31(3), 501–532 (2012).
29. Kumasi Metropolitan Assembly: The composite budget of the Kumasi metropolitan (2014).
30. Li, L., Loo, B. P. Y.: Alternative and transitional energy sources for urban transportation. *Current Sustainable/Renewable Energy Reports*, 1(1), 19–26 (2014).
31. Loukopoulos, P., Jakobsson, C., Gärling, T., Schneider, C. M., Fujii, S.: Car-user responses to travel demand management measures: goal setting and choice of adaptation alternatives. *Transportation Research Part D: Transport and Environment*, 9(4), 263–280 (2004).
32. Lund, H., Hvelplund, F.: The economic crisis and sustainable development: The design of job creation strategies by use of concrete institutional economics. *Energy*, 43(1), 192-200 (2012).
33. Lund, H.: Choice awareness: the development of technological and institutional choice in the public debate of Danish energy planning. *Journal of Environmental Policy and Planning*, 2(3), 249-259 (2000).
34. Makarova, I., Pashkevich, A., Shubenkova, K., Mukhametdinov, E.: Ways to increase population mobility through the transition to sustainable transport. *Procedia Engineering*, 187, 756–762 (2017).
35. Ministerial, C. E.: Electric Vehicle Initiative and International Energy Agency, Global EV Outlook-Understanding the Electric Vehicle Landscape to 2020, OECD/IEA: Paris, France (2013).
36. Myers, G.: African cities: alternative visions of urban theory and practice. Zed Books Ltd (2011).
37. NCCI (2015) Erbil Governorate Profile. [Online] Available at: ncci-raq.org/images/infobygov/NCCI_Erbil_Governorate_Profile.pdf [Accessed 1 January 2020].
38. OECD.: Strategies to Reduce Greenhouse Gas Emissions from Road Transport: Analytical Methods. Organisation for Economic Co-operation and Development (2002).
39. Orecchini, F., Santiangeli, A.: Beyond smart grids–The need of intelligent energy networks for a higher global efficiency through energy vectors integration. *International Journal of hydrogen energy*, 36(13), 8126-8133 (2011).
40. Pasaoglu, G., Honselaar, M., Thiel, C.: Potential vehicle fleet CO2 reductions and cost implications for various vehicle technology deployment scenarios in Europe. *Energy Policy*, 40, 404–421 (2012).
41. Poku-Boansi, M., Adarkwa, K. K.: The determinants of demand for public transport services in Kumasi, Ghana. *Journal of Science and Technology (Ghana)*, 33(3), 60-72 (2013).

42. Quarshie, M.: Integrating cycling in bus rapid transit system in Accra. In *Highway and Urban Environment* pp. 103-116. Springer, Dordrecht (2007).
43. Ramadhas, A. S.: *Alternative fuels for transportation*. CRC Press (2016).
44. Rodrigue, J., 2020. *Transportation And Energy*. [online] The Geography of Transport Systems. Available at: <https://transportgeography.org/?page_id=15592> [Accessed 24 May 2020].
45. Ryu, H., Dorjragchaa, S., Kim, Y., Kim, K.: Electricity-generation mix considering energy security and carbon emission mitigation: Case of Korea and Mongolia. *Energy*, *64*, 1071-1079 (2014).
46. Saboori, B., Sapri, M., bin Baba, M.: Economic growth, energy consumption and CO2 emissions in OECD (Organization for Economic Co-operation and Development)'s transport sector: A fully modified bi-directional relationship approach. *Energy*, *66*, 150-161 (2014).
47. Sam, E. F., Adu-Boahen, K., Kissah-Korsah, K.: Assessing the factors that influence public transport mode preference and patronage: Perspectives of students of University of Cape Coast (UCC), Ghana. *International journal of development and sustainability*, *3*(2), 323-335 (2014).
48. Schipper, L., Lewis-Davis, G.: Rapid Motorisation in the Largest Countries in Asia: Implication for Oil. *Carbon Dioxide and Transportation (Paris: International Energy Agency, 2001)* (1999)
49. Sperling, D., Cannon, J. S.: *Reducing climate impacts in the transportation sector*. Springer (2009).
50. Tajudeen, I. A.: Examining the role of energy efficiency and non-economic factors in energy demand and CO2 emissions in Nigeria: Policy implications. *Energy Policy*, *86*, 338-350 (2015).
51. Un-Habitat.: *Planning and design for sustainable urban mobility: Global report on human settlements* (2013).
52. Vimmerstedt, L., Brown, A., Heath, G., Mai, T., Ruth, M., Melaina, M., ... Bertram, K.: *High Penetration of Renewable Energy in the Transportation Sector: Scenarios, Barriers, and Enablers*. National Renewable Energy Lab.(NREL), Golden, CO (United States) (2012).
53. Vučić, I.: *Cooperation and Cluster Strategies Within and Between Technology-Intensive Organizations: How to Enhance Linkages among Firms in Techno-Parks*. PhD diss., M. Sc. thesis: Middle East Technical University. Ankara, 2009.
54. World Bank.: *The Kurdistan Region of Iraq: Assessing the Economic and Social Impact of the Syrian Conflict and ISIS* (2015).

Production of Hydrogen-Rich Syngas in a Fluidized Bed

Hazal Öztan^{1*}, Duygu Uysal Ziraman¹, Özkan Murat Doğan¹, Bekir Zühtü Uysal¹

¹ Gazi University, Faculty of Engineering, Chemical Engineering Department and Clean Energy Research and Application Center (CERAC), Maltepe 06570, Ankara, Turkey

*hazaloztan@gazi.edu.tr

Abstract. Syngas is the product of the gasification process. It includes combustible gases and hydrogen as an energy carrier. Syngas can be produced efficiently in fluidized beds. Biomass sources as well as coals with low carbon content can be easily used as the feed material for fluidized beds. The aim of this work is to produce hydrogen-rich syngas from olive kernel and Tunçbilek lignite. In the first part of the study, a theoretical kinetic model was developed to estimate the effects of steam/fuel ratio and temperature on syngas composition using Polymath program. It was found that the hydrogen content increased when the gasification temperature increased. In addition, a higher steam/fuel ratio was required to obtain hydrogen-rich syngas when the temperature was increased. In the second part, olive kernel and lignite were gasified experimentally in a laboratory scale fluidized bed. Steam was used as the fluidizing and gasification medium. The temperature was varied between 600-900°C. Olive kernel and lignite were fed to the column at a rate of 10 g/min by a screw feeder. The steam/fuel ratio was chosen as 0.7. The syngas thus produced was cooled, cleaned and then analyzed with a gas chromatography. The experimental results confirmed the theoretical finding that the percentage of hydrogen in the syngas increased with increasing temperature. At least 700 °C was required to produce syngas with an acceptable composition. H₂/CO ratio was greater than two for both fuels.

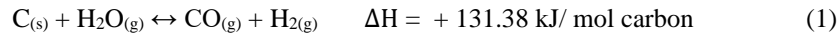
Keywords: gasification, fluidized bed, hydrogen, syngas

1 Introduction

Fossil fuels are on the top of producing energy in the world and energy demand is increasing day by day. There is a concern about the lifespan of fossil fuels since they are consumed rapidly. To meet the energy demand, coals that have low carbon content are utilized in thermochemical conversion processes. Coal is the longest-lived fossil fuels nowadays and lignite which is a type of low-rank coal is investigated to be utilized effectively in gasification processes. In addition to coals, biomass resources are preferred to be used in gasification as raw material due to their carbon content. Mediterranean countries where olive trees grow up have a lot of olive kernel because as a waste of high olive oil production. The olive kernel has a considerable amount of carbon. Thus, it can be used to produce energy in gasification or combustion processes. Gasification reactions are water gas, Boudouard, water gas shift and methanation

reactions. Water gas and Boudouard reactions are endothermic. Water gas shift and methanation reactions are exothermic reactions. Also, these reactions are equilibrium reactions. The reactions are given below.

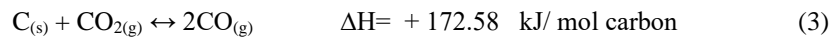
Water gas reaction



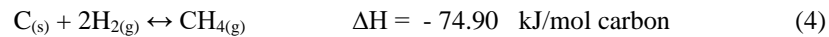
Water gas shift reaction



Boudouard reaction



Methanation reaction



Gasification enables producing syngas that is a combustible gas and it can be utilized in producing new chemicals such as ammonia, dimethyl ether, SNG. Syngas consists of hydrogen and carbon monoxide. While hydrogen itself is a promising energy carrier, when the ratio of hydrogen/carbon monoxide in syngas is about 2, it is possible to convert syngas into other hydrocarbons. Thus, syngas composition is the most important issue in gasification. In order to produce the desired syngas composition, operating conditions (temperature, the ratio of steam/fuel, the flow rate of gasifier agent, etc.) must be examined. In the literature, the effect of operating parameters has been studied. Especially, temperatures and steam/fuel ratio effects on gas composition have been investigated. There is a positive impact about hydrogen content in syngas if the gasifier temperature and steam/fuel ratio are increased. Velez et al. [1] have investigated the effect of the steam/fuel ratio on syngas composition. It has been reported that as the steam/fuel ratio is increased, the concentration of hydrogen in syngas increases. Feroso et al. [2] have shown that the temperature of gasification is the most important operating parameter and if it is increased, the hydrogen concentration in syngas also increases. Likewise, Hofbauer et al. [3] have claimed that temperature effects the syngas composition positively and hydrogen increases as temperature is increased. Also, they reported that the steam/fuel ratio affected the gas yield and decreased tar formation. Produced tar in gasifier is cracked by temperature and turns into combustible gases like methane.

In this study, syngas composition is investigated with a kinetic model. Temperature and steam/fuel ratio effects on syngas composition were determined by using Polymath. Also, Tunçbilek lignite and olive kernel were gasified experimentally in a laboratory-scale fluidized bed in the presence of steam. The influence of temperature on syngas composition was evaluated.

2 Materials and Methods

2.1 Fuels

Tunçbilek lignite and olive kernel were used separately as raw materials. Average particle diameters of lignite and olive kernel is 0.66 mm and 1.3 mm, respectively. Ultimate analyses are reported in Table 1.

Table 1. Ultimate analysis of fuels

Ultimate analysis (wt-%)		
	Tunçbilek lignite [5]	Olive kernel [4]
% C	56.89	50.5
% H	4.28	6.55
% O	7.97	32.33
% N	2.16	1.39
% S	1.47	0.21
% H ₂ O	13.51	5.86
% Ash	13.72	3.16

2.2 Procedure

Polymath Programming

Syngas compositions were estimated by Polymath program. Program inputs were written regarding the work of Basu [6] using nonlinear equations section. There were 7 nonlinear and 16 explicit equations for lignite gasification (Eq. 5-11). Temperatures and steam/fuel ratios were changed. Operating temperatures were selected as 700 °C, 800 °C and 900 °C. The ratios of steam/fuel were between 0.4-1. After all that Polymath program was executed. Syngas composition was obtained and effects of temperature-steam/fuel ratio were determined. Also, the same steps were followed for olive kernel gasification.

Balance of carbon

$$1.866 F_{XC} = V_{CO} + V_{CO_2} + V_{CH_4} \quad (5)$$

Balance of hydrogen

$$1.24 FS + (11.21F_{XH} + 1.24 FW) = V_{H_2} + V_{H_2O} + 2V_{CH_4} \quad (6)$$

Balance of oxygen

$$0.623 (FS + FW) + 0.701(F_{X_o} + FAO_a) = 0.5V_{CO} + V_{CO_2} + 0.5V_{H_2O} \quad (7)$$

Balance of nitrogen

$$0.8F_{XN} + 0.8F_{ANa} = V_{N_2} \quad (8)$$

Total of component's volume fractions

$$V_{CO} + V_{CO_2} + V_{H_2} + V_{CH_4} + V_{H_2O} + V_{N_2} = 1 \quad (9)$$

Equilibrium constant of Boudouard reaction

$$K_{pb} = \frac{P_{CO}^2}{P_{CO_2}} = \frac{V_{CO}^2 \cdot P}{V_{CO_2}} \quad (10)$$

Equilibrium constant of water gas reaction

$$K_{pw} = \frac{P_{H_2} P_{CO}}{P_{H_2O}} = V_{H_2} V_{CO} \frac{P}{V_{H_2O}} \quad (11)$$

Experimental

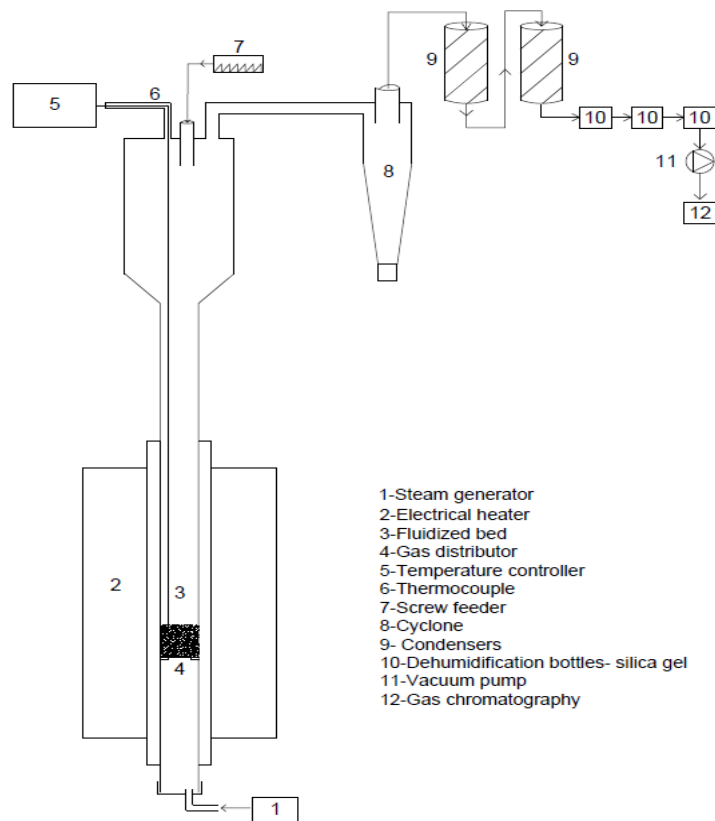


Fig. 13. Schematic diagram of fluidized bed reactor

Fig.1 shows the schematic diagram of the fluidized bed gasifier and its auxiliary equipments. The reactor (3) is made of quartz glass and it has an internal diameter of 5 cm and a height of 130 cm. The perforated plate (4) is located above 25 cm bottom of the column. The plate has 38 holes of 1.5 mm diameter. The column is covered by an electrical resistance (2) for temperature control. Silica sand, 310 μm in diameter, was used as bed material. Steam at 100 °C was produced with a steam generator (1) and was sent to the column. The reactor was equipped with a cyclone (8), temperature controller (5) and a thermocouple (6). There is a screw feeder (7) on the top of the column. To condensate the steam after the reactor there are two condensers (9) in the system and a vacuum pump (11) was used to get the gas sample. There are three gas cleaning bottles with silica gel (10). The analyses of the gas samples were done by a gas chromatography (12).

Gasification experiments of lignite and olive kernel were carried out separately in a fluidized bed. The column was heated to four different temperatures: 600 °C, 700°C, 800°C and 900 °C. The column temperature was controlled with the thermocouple. Steam was used as the fluidizing and gasifying medium. Steam was fed to the column at 100 °C. Fuels were fed to the column at a rate of 10 g/min by a screw feeder. The amount of feed was 6.6 % of the bed material. The steam/fuel ratio was chosen as 0.7 according to theoretical findings. Produced gas was cooled by condensers and cleaned by silica gels in bottles. Gas samples were collected in gas sampling bags. The gas was analyzed with gas chromatography in order to examine H_2 , CO , CO_2 , and CH_4 contents in the produced syngas.

3 Results and Discussion

3.1 Polymath Results

The written Polymath program was executed in order to obtain hydrogen-rich syngas composition. The effects of temperature and steam/fuel ratio on the hydrogen content were investigated. Tunçbilek lignite and the olive kernel were chosen the raw materials and gasification agent was steam. The effect of temperature on hydrogen in syngas is increasing due to gasification reactions being endothermic. Also, the optimum operating temperature interval for gasification processes is reported to be 600-1000 °C in Taba's study. Especially, water gas and Boudouard reactions are carried out at high temperatures. Water-gas reaction speeds up at high temperatures and produces hydrogen and carbon monoxide. Between 700-900 °C, both raw materials showed that when the gasification temperature was increased, hydrogen content in syngas increased. At constant steam/fuel ratio, temperature effects were presented in Fig 2 and Fig 3. The steam/fuel ratio affected the hydrogen content positively, too. At constant temperature, hydrogen content in syngas increased with increasing steam/fuel ratio. Hydrogen behavior has the same trend with olive kernel gasification. Hydrogen and carbon monoxide composition are presented in Fig 4 and Fig 5.

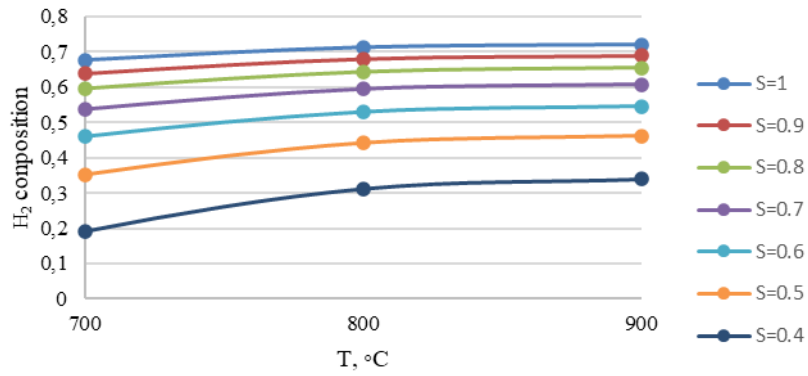


Fig.2. Effect of temperature on hydrogen in syngas for lignite

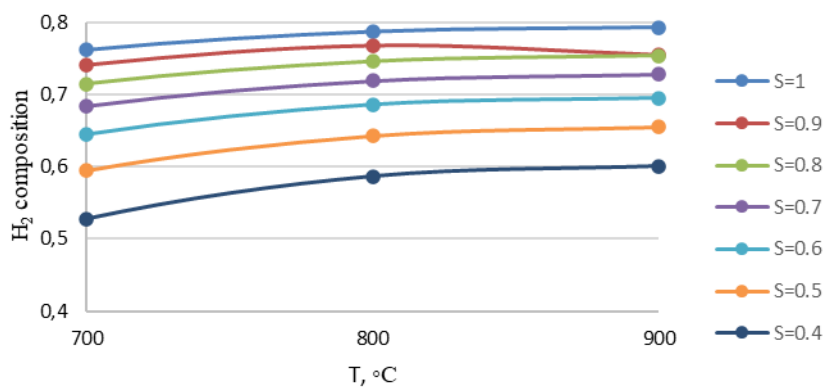


Fig.3. Effect of temperature on hydrogen in syngas for olive kernel

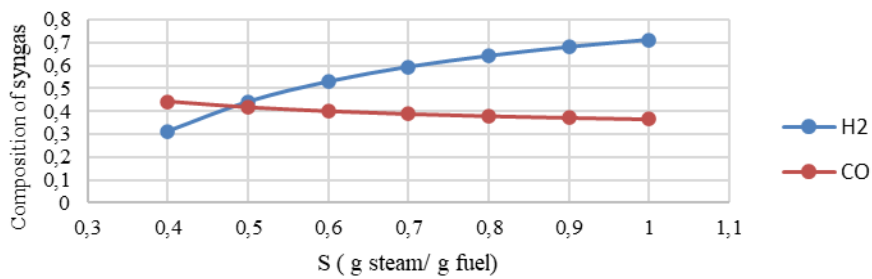


Fig. 4. Effect of steam/fuel ratio on syngas composition for lignite at 800 °C

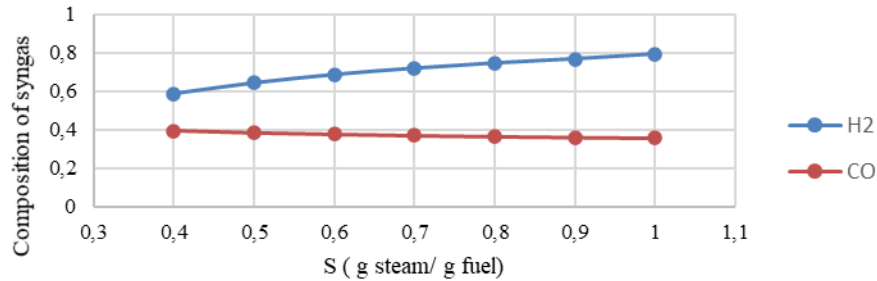


Fig. 5. Effect of steam/fuel ratio on syngas composition for olive kernel at 800 °C

3.2 Experimental Results

Gas composition and carbon conversion are affected by temperature. Hence, temperature is one of the most important operating parameters of gasification as stated before. Also, temperature affects gas and cold gas efficiency as well as char and tar conversion. This impact arises from the thermodynamic behaviors of gasification reactions and the equilibrium between them. Temperature limitations in gasification depend on the volatile matter of fuels, construction of gasifier, producing temperature of undesired components such as NO_x and melting temperature of ash. The temperature of coal gasification is limited between 750-1000 °C. Biomass gasification is the most effective and economic way to produce hydrogen. Temperature effects on biomass gasification is like that in coal gasification. As temperature increase, hydrogen content in syngas increases, too. Temperature limitation for biomass gasification is remarked in between 550°C and 900 °C [7].

In the experiments, lignite and olive kernel were gasified separately in the presence of steam in a fluidizing bed. Steam/fuel ratio was selected as 0.7 for both fuels to produce a hydrogen-rich syngas according to theoretical study. There is no need high steam/fuel ratio for lignite and olive kernel gasification. Because the selected ratio is enough to convert carbon content in fuels. Also, superficial velocity of steam is high in the column. It helps conversion of carbon with well solid-gas mixing. Syngas was effectively obtained from lignite and olive kernel in fluidized bed. Produced syngas has hydrogen, carbon monoxide, carbon dioxide and methane. The produced syngas composition is presented in Table 2 and 3. As temperature was increased, the hydrogen concentration in syngas increased. The effects of temperature on syngas compositions are presented in Fig 6 and Fig 7.

Table 2. Gas composition of syngas for lignite gasification

%	600 °C	700 °C	800 °C	900 °C
H₂	83.19	98.85	99.33	94.06
CH₄	0	0.18	0	0
CO	3.31	0	0.38	0.59
CO₂	13.50	0.96	0.27	5.34

Table 3. Gas composition of syngas for olive kernel gasification

%	600 °C	700 °C	800 °C	900 °C
H₂	40.67	64.76	97.55	95.33
CH₄	38.22	12.68	0.88	1.16
CO	21.12	13.40	1.58	3.51
CO₂	0	9.15	0	0

At high temperatures water gas reaction (Eq. 1) was very dominant and it produced high amount of hydrogen in syngas. Besides, water gas shift reaction (Eq. 2) supported the hydrogen production due to high steam velocity in the fluidized bed. The highest hydrogen content for lignite gasification was obtained as 99.3% at 800 °C. Also, the highest hydrogen composition for olive kernel gasification was 97.5% at 800 °C. Carbon content of fuels are different from each other. Amount of lignite's fixed carbon is higher than that of olive kernel. Thus, hydrogen content of syngas obtained from lignite is higher than that of obtained from olive kernel gasification.

Carbon monoxide and carbon dioxide relationship is quite complicated since equilibrium affects the syngas composition in gasifier related to operating conditions. At temperatures that are higher than 800 °C, Boudouard reaction (Eq. 3) dominating the reaction system and produced carbon monoxide by consuming carbon dioxide. Consuming carbon dioxide can be observed easily in lignite gasification results in Table 2. As the temperature was increased, carbon dioxide decreased. Farther, carbon monoxide and carbon dioxide contents depend on the volatiles and oxygen content of the fuels. Volatiles and oxygen contents of olive kernel is higher than that of the lignite. Oxygen reacted with carbon, carbon monoxide and volatiles. Hence, carbon monoxide and carbon dioxide contents increased in syngas. There was no methane in syngas (Table 2). The gasification temperatures for methane production (Eq. 4) are thermodynamically too high and produced methane by natural content of fuels in gasification of olive kernel is consumed by steam reforming reaction.

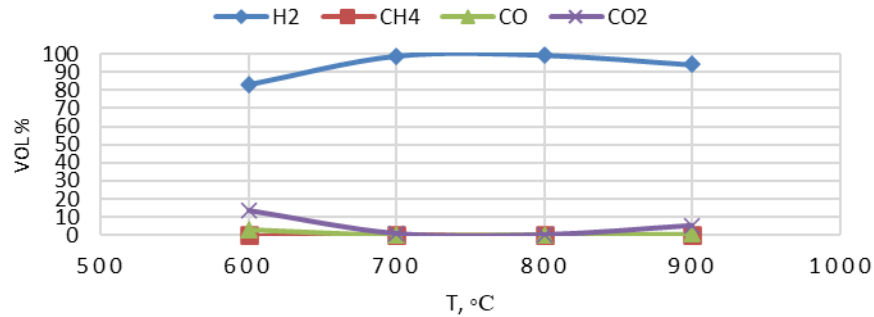


Fig.6. Effect of temperature on lignite gasification

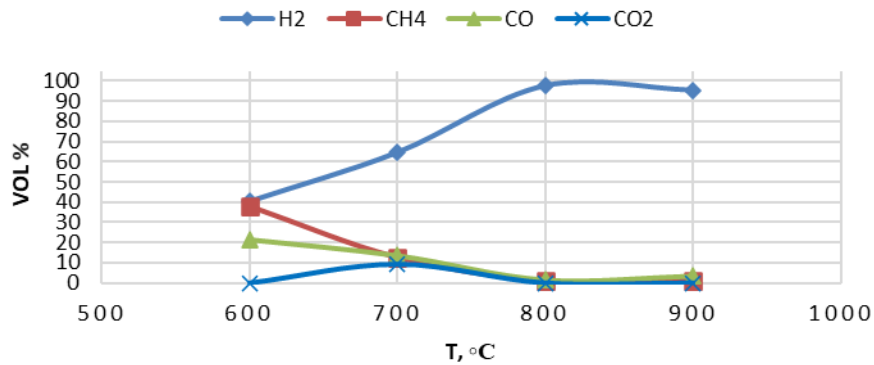


Fig.7. Effect of temperature on olive kernel gasification

4 Conclusion

Gasification of coal and biomass resources is an effective way to produce hydrogen-rich syngas. Temperature and steam/fuel ratio are important to produce a syngas with the desired composition. Therefore, the effects of these operating parameters have to be investigated carefully. In this study, hydrogen-rich syngas was aimed to produce experimentally from lignite and olive kernel in fluidized bed. The experimental finding showed that as the gasification temperature was increased, hydrogen composition in the syngas increased, too. Optimum gasification temperature for lignite and olive kernel gasification was 800 °C. At least 700 °C is required to produce syngas with an acceptable composition considering theoretical findings. As the steam/fuel ratio was increased, hydrogen production in syngas increased too. H₂/CO ratio was greater than 2 for both fuels. Thus, the syngas can be used to produce various chemicals. Although lignite and olive kernel have low carbon content, they can be gasified easily in fluid-

ized bed and hydrogen-rich syngas can be obtained. In this way, coals and biomass sources can be utilized in order to generate power.

Nomenclature

A:	air supply (kg dry air/kg dry fuel)
F:	amount of dry fuel (kg)
K_{pb} :	Boudouard reaction equilibrium constant
K_{pw} :	water gas reaction equilibrium constant
N_a :	mass fraction of nitrogen in air
O_a :	mass fraction of oxygen in air
P:	pressure of the reactor (Pa)
P_{H_2} :	partial pressure of hydrogen
P_{CO} :	partial pressure of carbon monoxide
P_{CO_2} :	partial pressure of carbon dioxide
P_{H_2O} :	partial pressure of steam
S:	total steam supplied (kg steam/kg dry fuel)
T:	temperature (°C)
V:	volumetric fraction of gas
W:	moisture content of fuel (kg water/ kg dry fuel)
w:	mass
X_C :	carbon content of the fuel (kg carbon/kg dry fuel)
X_H :	hydrogen content of the fuel (kg hydrogen/kg dry fuel)
X_N :	nitrogen content of the fuel (kg nitrogen/kg dry fuel)
X_O :	oxygen content of the fuel (kg oxygen/kg dry fuel)

References

1. Velez J and Chejne F.: Co-gasification of Colombian coal and biomass in fluidized bed: An experimental study, *Fuel*, 88, 424-430 (2009).
2. Feroso J and Arias B.: High pressure CO-gasification of coal with biomass and petroleum coke, *Fuel Processing Technology*, 90, 926-32 (2009).
3. Hofbauer, H and Rauch R.: Hydrogen rich gas from biomass steam gasification, 1st World Conference on Biomass for Energy and Industry, Sevilla- Spain (2001).
4. Hammad, A. E. A, Nadirov, E., Uysal, D., Doğan, Ö. M., Uysal, B.Z.: Pirinadan su buharı gazlaştırmasıyla sentez gazı üretimi, 12. Ulusal Kimya Mühendisliği Kongresi, İzmir (2016).
5. Uysal, D., Şahin, A., Genç, A., Doğan, Ö. M., Uysal, B.Z.: Kütahya- Tunçbilek linyitinin ve atık şlamın gazlaştırılması, 20. Ulusal Isı Bilimi ve Tekniği Kongresi, Balıkesir (2015).
6. Basu, P.: *Combustion and Gasification in Fluidized Bed*, Taylor and Francis Group, New York (2006).
7. Taba, L., E.: The effect of temperature on various parameters in coal, biomass and co-gasification, *Renewable and Sustainable Energy Reviews*, 16, 5584-5596 (2001).

Glycerin as a Heat Transfer Fluid in Solar-Organic Rankine Cycle

Doğa Şahin¹, Duygu Uysal Ziraman¹, Özkan Murat Doğan¹, Bekir Zühtü Uysal¹

¹ Gazi University, Faculty of Engineering, Chemical Engineering Department, and Clean Energy Research and Application Center (CERAC-TEMENAR) Ankara, 06570, Turkey

dogasahin@gazi.edu.tr

Abstract. Glycerin can be evaluated as a good heat transfer fluid with its high boiling point and heat transfer coefficient. Therefore, it is suitable for use as heat transfer fluid in solar energy systems. The aim of this work is to use glycerin as heat transfer fluid, with different flow rates, in parabolic trough solar collectors, and seeing how much energy can be produced with the Organic Rankine Cycle (ORC). In the first part of the study, the temperature of the glycerin at collector inlet and outlet at different flow rates were determined. Depending on this temperature difference and flow rate, thermal efficiencies were calculated. It was seen, when the flow rate increased, temperature difference decreased. According to this result, the optimum flow rate was determined according to this outcome. In the second part, the ORC system was simulated using the Chemcad program and used different working fluids. The work was calculated according to simulation results. When glycerin was fed to the collector with a 0.6 L/min flow rate, the calculated thermal efficiency was around 70%. The work was found 72 kW when R134a used as a working fluid in the ORC. Regarding the results, glycerin is a promising heat transfer fluid compared to water.

Keywords: parabolic trough solar collector, Organic Rankine Cycle, glycerin.

1 Introduction

The world has been facing a lot of environmental problems such as air pollution, global warming, mainly due to the emissions from increasing consumption of fossil fuels [1]. Increasing demands of energy from non-renewable sources remain unsustainable. Therefore, utilizing renewable energy sources as an alternative has been of great importance for domestic heating and electricity generation [2]. The classical methods for energy production are mostly harmful to the environment. Therefore, energy production by renewable energy sources is becoming a very important issue.

Interest in solar energy systems and studies on this topic is increasing. The reason for this increase, solar energy is all-natural, sustainable, and cheap. The average solar radiation falling on the earth, during the year is about 1361 W/m^2 . This average value varies according to the days of the year and where the rays reach the world.

The parabolic trough collector (PTC) type solar power system is one of the concentrated solar power systems and it is the most common solar system used for energy production in the world. The reason for this, these systems have low installation cost and works highly efficient. PTC heat the heat transfer fluid and this heated fluid can be a heat source in Organic Rankine Cycle. Thus, thermal energy can be produced from solar radiation.

Rankine cycle is generally used in power generation with the help of a heat source. The conventional Rankine Cycle is not an economic and efficient alternative for the conversion of heat to power from renewable energy sources [3]. A conventional Rankine Cycle using organic compounds rather than water is called the Organic Rankine Cycle (ORC) and it is the most accepted technology for converting low-grade heat energy sources into mechanical work [4]. There are many studies where PTC is used as a heat source for ORC. And there is a lot of study on the performance of systems with selected heat transfer fluids in the collector and working fluids in the cycle [4].

The heat transfer fluid should be classified based on the thermophysical properties in the working condition of PTC. The thermophysical properties of the heat transfer fluid (HTF) are specific heat capacity, enthalpy of phase change, thermal conductivity, viscosity, and melting point. However, the thermophysical properties like density, degradation temperature, thermal expansion coefficient, and thermal stability are necessary for selecting the heat transfer fluid. Specific heat capacity (C_p) is an important property that decides the suitability of HTF to be used as heat transfer or thermal energy storage material [6]. The melting point is directly related to the operational cost of the system because the solar area must be maintained above the freezing point even after sundown [7]. Therefore, the degradation temperature of HTF plays a key role in deciding the efficiency of the system [8]. The thermal conductivity of the heat transfer fluid is an important thermophysical property that influences the Nusselt number. Thermal conductivity and density of HTF are very sensitive to temperature. Therefore, it is recommended to measure these parameters in the working temperature range [9]. The pumping efficiency of the system depends on the dynamic viscosity and shear rates of the HTF. Another property required for the characterization of HTF is vapor pressure. Usually, in PTC, low vapor pressure is suitable because it shows the evaporation rate of the liquid [10].

In ORC, high molecular weight organic fluids are used instead of water to convert heat energy into electrical energy. Thus, the turbine turns more slowly. Since the turbine is the most expensive equipment of the system and with this slow rotation, the production efficiency is increased by preventing the metallic parts, rotary wings from being exposed to less pressure and corrosion [11,12]. The classic Rankine conversion at lower temperatures is less efficient and higher cost [13,14]. Some properties should be considered when choosing the working fluid. These properties; Thermodynamic and physical properties, the stability and compatibility of the fluid concerning the materials used, its safety, environmental compatibility, price, and availability should

be considered in working fluid selection [15]. High vapor density and low volumetric flow rate enable small equipment to use. Fluid viscosity should be low in the liquid phase and vapor phase so that the heat transfer coefficient is increased, and friction losses are reduced in heat exchangers [16]. High thermal conductivity causes a high heat transfer coefficient in the heat exchangers. The specific heat capacity of the fluid in the liquid phase does not directly affect the pump work or net work. But it is important for high net work [17]. The freezing point of the fluid must be lower than the lowest temperature of the cycle [18]. Since organic fluids will also decompose at high temperatures, it is important to use them by the working conditions [19]. Environmental compatibility should be evaluated both in terms of global warming potential (GWP) and ozone depletion potential (ODP) [20]. The security assessment should be done. Flammability, toxicity, corrosivity, explosion limit, and maximum allowable concentration values should be determined [21,22]. Three working fluids have been selected according to the properties determined in the selection of the working fluid and the information obtained from the literature. In ORC simulation studies, these working fluids have been tried to determine the suitable working fluid for the system.

In this study, the use of glycerin as a heat transfer fluid in a PTC was studied. Glycerin is a valuable chemical and the high boiling temperature of glycerin provides high-temperature steam and thus more thermal power can be produced. PTC is a medium temperature level system and it is seen that the glycerin degradation temperature is very high for these systems. When these properties are evaluated, glycerin seems like a promising heat transfer fluid, and the use of glycerin in the PTC system was investigated. This PTC system using glycerin as fluid was combined with an ORC system. Mathematical modeling and simulation programs were used to calculate thermal efficiency. The result of the simulation shows glycerin is suitable for that kind of s-ORC system.

2 Materials and Methods

In the solar Organic Rankine Cycle (s-ORC), the thermal energy production process is carried out with solar collectors. The thermal efficiency of the solar system is of great importance for energy to be produced. Therefore, the effect of the heat transfer fluid to be used on thermal efficiency must be considered. Glycerin was determined as the heat transfer fluid depending on the selection criteria. A two-step calculation procedure was carried out to determine the thermal efficiency to be obtained as a result of the use of glycerin in PTC. Firstly, thermal efficiency that can be obtained from the system used was calculated. Mathematical calculation was made using thermodynamic laws and heat transfer calculations. As a result of the calculations, thermal efficiency was calculated by using glycerin as a heat transfer fluid. To calculate the net work in ORC, an ORC system was simulated in the Chemcad program. Net work is calculated based on temperature changes obtained in PTC as well as selected working fluids.

The flow rate of the heat transfer fluid was calculated as follows. Theoretical heat calculation was made according to the incoming solar radiation, G_A (W/m^2) value and collector area, A (m^2) of the heat transfer fluid.

$$Q_{Theoretical} = G_A \cdot A \quad (4)$$

Useful heat is calculated by assuming that the current system operates with 85% efficiency. This assumption was made in the literature depending on the water used PTC systems [5].

$$Q_{useful} = Q_{Theoretical} \cdot 0.85 \quad (2)$$

The flow rate of the fluid in the collector was calculated as follows. Here, the temperature difference at the collector inlet and outlet is used.

$$Q_{useful} = m \cdot C_p \cdot \Delta T \quad (3)$$

There are three heat transfer types in PTC collector: conduction, convection, and radiation, which are based on the energy flow in and out of the collector, as indicated in Fig. 1.

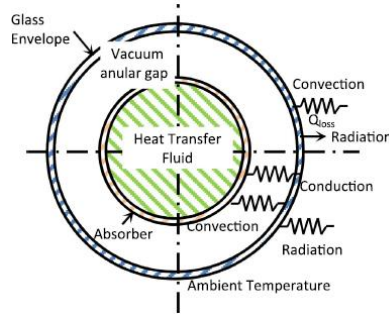


Fig. 1. Cross-sectional scheme of a PTC [25]

Q_{useful} , is the useful heat energy transferred from the sun rays. Q_{useful} is transferred from the absorber pipe to the liquid by conduction from the metal tube wall thickness and from the metal tube inner surface to the liquid.

$$Q_{useful} = h_i A_{mbi} (T_{mbi} - T_{av}) \quad (4)$$

$$Q_{useful} = \frac{\pi (d_{LM})_{mb} L k_{mb}}{\Delta x_{mb}} (T_{mbd} - T_{mbi}) \quad (5)$$

And if these equations are rearranged,

$$Q_{useful} = \frac{A_{mbi} (T_{mbi} - T_{av})}{\left[\frac{1}{h_i} + \frac{\Delta x_{mb}}{k_{mb}} \left(\frac{d_{mbi}}{(d_{LM})_{mb}} \right) \right]} \quad (6)$$

The heat transfer fluid transport coefficient, h_i , can be calculated according to the properties of the fluid at T_{av} , according to the Sieder-Tate equation for laminar flow [5].

$$Nu = \frac{h_i d_{mbi}}{k} \quad (7)$$

$$Nu = 1.86(RePr)^{1/3}(d/l)^{1/3}\left(\frac{\mu}{\mu_{wall}}\right)^{0.14} \quad (8)$$

$$Re = \frac{d_{mbd} \cdot v \cdot \rho}{\mu} \quad (9)$$

The mean bulk temperature, T_{mbi} and T_{mbd} calculated with these equations. To calculate the outside temperature of the glass tube, T_{cbd} , with the assumption of the outside temperature of the glass tube, radiation heat transfer coefficient $h_{d,r}$ is calculated from the glass tube to the environment [5].

$$h_{d,r} = \frac{\varepsilon_{cb}\sigma(T_{cbd}^4 - T_{Tank}^4)}{(T_{cbd} - T_{Tank})} \quad (10)$$

For the calculation of the heat transfer coefficient of the glass tube to the environment, $h_{d,t}$ following equation is used [5].

$$Nu = \frac{h_{d,t} d_{cbd}}{k_{air}} \quad (11)$$

$$Nu = 0,40 + 0,54Re^{0,52} \quad \text{for } 0.1 < Re < 1000 \quad [23] \quad (12)$$

$$Nu = 0,30Re^{0,6} \quad \text{for } 1000 < Re < 50000 \quad [23]$$

The thermal loss from the outer surface of the glass tube to the environment is expressed as,

$$Q_{loss,1} = A_{mbd} \left(\frac{d_{cbd}}{d_{mbd}}\right) [h_{d,t} + h_{d,r}] (T_{cbd} - T_{Tank}) \quad (13)$$

The glass tube inner surface temperature, T_{cbi} , is calculated from the conduction heat transfer equation, Eq. 14.

$$Q_{loss,1} = A_{mbd} \left(\frac{d_{cbd}}{d_{mbd}}\right) \frac{T_{cbi} - T_{cbd}}{R_{cb}} \quad (14)$$

And where, R_{CB} and X_{cb} is calculated by these equations,

$$R_{cb} = \frac{X_{cb} d_{cbd}}{k_{cb} - (d_{LM})_{cb}} \quad (15)$$

$$X_{cb} = \frac{d_{cbd} - d_{cbi}}{2} \quad (16)$$

The heat loss caused by convection and radiation between the absorber pipe outer surface and the glass tube is calculated by Eq. 17.

$$Q_{loss,2} = A_{mbd} [h_{ar,t} + h_{ar,r}] (T_{mbd} - T_{cbi}) \quad (17)$$

The heat transfer coefficient with convection in this equation, $h_{ar,t}$, is calculated by Eq.18.

$$h_{ar,t} = \frac{k_{eff}(d_{LM})_{ar}}{x_{ar}d_{mbd}} \quad (18)$$

The effective transfer coefficient, k_{eff} , calculated by Eq.19

$$\frac{k_{eff}}{k} = \max\left[1, 0.386\left(\frac{Pr \times Ra^*}{0.861 + Pr}\right)^{1/4}\right] \quad (19)$$

Thus, the heat transfer coefficient by convection, $h_{ar,t}$ is calculated. And the heat transfer coefficient by radiation, $h_{ar,r}$, calculated with the following equations [5].

$$h_{ar,r} = \frac{C_{ar}\sigma(T_{mcb}^4 - T_{cbl}^4)}{(T_{mcb} - T_{cbl})} \quad (20)$$

C_{ar} is calculated for the calculation of the heat transfer coefficient with radiation,

$$C_{ar} = \frac{1}{\frac{1}{\epsilon_{mb}} + \frac{1 - \epsilon_{cb}}{\epsilon_{cb}} \left(\frac{d_{mbd}}{d_{cbl}}\right)} \quad (21)$$

With all these equations, the amount of thermal loss, Q_{loss} , calculated with Eq.17. T_{cbd} the assumption is made until the amounts of heat loss calculated with Eq.13 and Eq.17 are equal. By this way T_{cbd} is calculated [5].

The overall heat transfer coefficient between the outer surface of the absorber pipe and the environment, U_{mbd} is calculated by Eq. 22.

$$U_{mbd} = \frac{1}{h_{ar,t} + h_{ar,r}} + \frac{1}{\left(\frac{d_{cbd}}{d_{mbd}}\right)R_{cb}} + \frac{1}{\left(\frac{d_{cbd}}{d_{mbd}}\right)(h_{d,t} + h_{d,r})} \quad (22)$$

The thermal loss between the absorber pipe and the environment is calculated with Eq. 23.

$$Q_{loss} = A_{mbd}U_{mbd}(T_{mbd} - T_d) \quad (23)$$

The available energy to the absorber pipe, Q_G , equal to the sum of the available energy to the heat transfer fluid, Q_{useful} , and the heat losses between the absorber pipe and the environment, Q_{loss} .

$$Q_G = Q_{loss} + Q_{useful} \quad (24)$$

The thermal efficiency of the system can be found by the ratio of the useful heat transferred to the heat transfer fluid to the useful energy to the absorber pipe [5,23].

$$\eta_{Thermal} = \frac{Q_{useful}}{Q_G} \times 100 \quad (25)$$

In the parabolic trough solar collector with a flow rate of 0.6 L/min of glycerine, the efficiency obtained is approximately 70% and the optical efficiency is about 35% when the temperature difference between inlet and outlet temperatures of the glycerine was about 30°C degrees.

2.1 Simulation Method

The ORC system is a very expensive system due to the equipment used. Besides the power they produce for large plants, this installation cost remains insignificant. However, in small applications, the use of the equipment and the right chemicals is of great importance. Chemcad simulation program simplifies the work of engineers with unique equipment and chemical options. The pump power required for a small-scale ORC system to be installed, turbine power and suitability of the fluid to be used can be seen with this simulation. For this reason, the necessary equipment values for power generation, which are of great importance in the continuation of this study, have been calculated with the help of this program and the network to be achieved has been calculated in this way. The heat transfer fluid heated by the effect of the sun rays is used to heat the working fluid used in the ORC. The working fluid to be used in the ORC is calculated according to these temperature values in the Chemcad simulation program and the network is calculated.

The ORC system in Chemcad simulation was showed in Fig. 2. Since PTC is used as a heat source and the maximum temperature that this system can output is determined, the steam temperature to the turbine was determined in this range. Superheated steam is fed to the turbine at 16 bar and 75°C. If the turbine operates with 85% efficiency, it is determined from the system that the pressure of saturated steam at the turbine outlet will drop to 6 bar. Thus, the work to be produced in the turbine is found. A condenser is used to condense the saturated steam to saturated liquid at the turbine. The work of this condenser has a negative impact on the system. The saturated liquid is pumped to the superheat pressure and thus the cycle is performed. Operating temperatures and values of the system are given in Table 1.

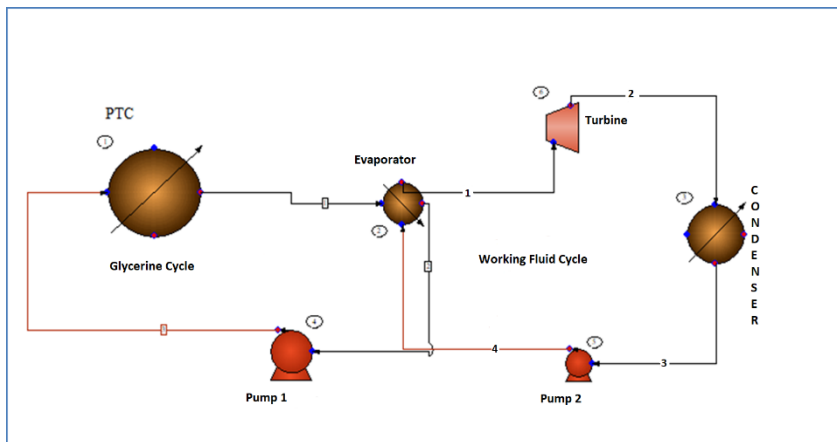


Fig. 2. Solar Organic Rankine Cycle (s-ORC) in Chemcad program

Table 1. Chemcad ORC simulation stream values

Stream Condition/ Stream number	Pressure, bar	Temperature, °C	Enthalpy, kJ/kg	Entropy, kJ/kg K
Superheated Steam, 1	16	75	447.37	1.76
Saturated Steam, 2	6	33.2	422.11	1.75
Saturated liquid, 3	6	20.7	228.56	1.09
Saturated liquid, 4	16	20	227.47	1.09

Some criteria for the selection of the working fluid to be used in ORC are determined and it was observed that the use of dry fluids should be preferred. It was emphasized that it should have high vapor density, low viscosity, easy to find, suitable for working conditions, compatible with the equipment, and have low global warming potential. With the literature review, the fluids used as working fluid in s-ORC that previously used PTC were determined. Three working fluids came to the fore with their suitability to all these features and their compliance with operating temperatures.

Three different working fluids are used in the simulation. These are R134a, pentane, and isopentane. According to Chemcad data, calculations of heat coming to the evaporator produced work in the turbine, the heat lost in the condenser, and pump work calculations were made. As a result of these calculations, net work to be obtained from working fluids have been determined.

According to the data obtained as a result of the simulation study, the net work to be obtained with R134a is higher than other working fluids. The working fluid to be used while installing the ORC system can be determined in this way and the experimental application stage can be started afterward.

3 Result and Discussion

In this study, which is related to the fact that thermal power generation from solar energy will be enough to meet energy needs, thermal efficiency and net work account can be obtained by combining PTC and ORC and using glycerin as a heat transfer fluid. For PTC the thermal efficiency to be obtained by using glycerin as heat transfer fluid was calculated.

The flow rate of the heat transfer fluid in the absorber pipe is of great importance for it to carry heat. As a result of the calculations, it was observed that the temperature difference between PTC inlet and outlet decreased as the flow rate was increased. Temperature difference increases as flow rate decreases but thermal efficiency decreases. To reach the highest thermal efficiency, an optimum flow rate value should be determined, and the system should be operated accordingly.

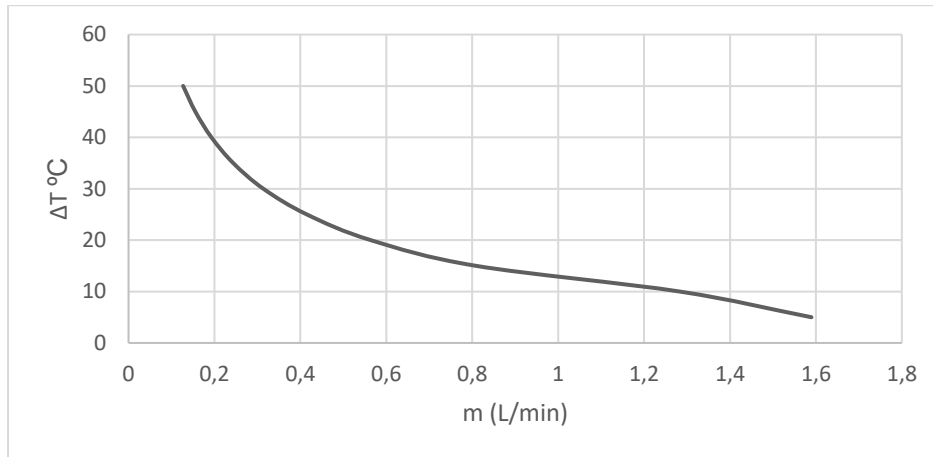


Fig. 3. The temperature difference in PTC according to the flow rate

As a result of the calculations, it was observed that the glycerin at the flow rate of 0.6 L/min reached a temperature difference of 30°C and obtaining the highest thermal efficiency value. This calculation made due to Section 2.1 and the results showed in Table 2.

This study aims to determine the net work to be obtained by using glycerin as heat transfer fluid in PTC and to calculate the net work that can be obtained in ORC accordingly. Since heat transfer fluid carries the heat obtained from the solar system, there are many factors to be considered when choosing. The high boiling point of the fluid increases the net work to be obtained from the ORC. Also, it should be able to work correctly with the equipment used in the system and should have a good heat transfer coefficient. To avoid any loss, the degradation temperature should be above the temperature range of the system under study. The viscosity of the fluid should be evaluated for easy pumping and a selection should be made accordingly. In terms of all these features, glycerin is a suitable working fluid for PTC. During the literature research, it was observed that there were many heat transfer fluids used in PTC, but there was no use of glycerin in pure form and this increased the importance and the originality of this study.

In ORC, where high molecular weight organic fluids are used as working fluids, the criteria considered in the selection of working fluids have been evaluated. In the selection of working fluid, the effect of vapor density on equipment size and viscosity effect on heat exchanger should be evaluated. Previously used working fluids in the literature were examined and some of those suitable for the working temperature of the current system was tested on the simulation program. ORC system created in Chemcad program and three of those working fluid tried. The thermal efficiency to be obtained by using glycerin as heat transfer fluid in PTC was calculated mathematically.

Table 2. The thermal efficiency calculation result of glycerin at a flow rate of 0.6 L/min

Calculated data	Unit	Value
Temperature difference, ΔT	°C	30
Average specific heat capacity, C_p	J/kgK	2799.14
Tank temperature, T_{tank}	°C	30
Solar radiation, G_A	W/m ²	1070.18
Flow rate, m	kg/s	0.01
Useful heat, Q_{useful}	W	1088.53
Average temperature, T_{av}	°C	113
Viscosity, μ	kg/ms	1.06
Absorber pipe outer surface area, A	m ²	0.26
Air flow rate, v	m/s	4.19
Reynold number, Re	-	138.59
Heat transfer coefficient of glycerin, $k_{glycerine}$	W/mK	0.30
Prandlt number, Pr	-	10185.4
Nusselt number, Nu	-	44.34
Thermal conductivity coefficient, h_i	W/m ² K	495.98
Absorber pipe inner area, A_{mbi}	m ²	0.25
Mean bulk temperature, T_{mbi}	°C	132
Glass tube outer temperature, T_{cbd}	°C	61.66
Radiation heat transfer coefficient, $h_{d,r}$	W/m ² K	6.63
Air temperature, T_{air}	°C	25
Viscosity of air, μ_{air}	kg/ms	1.8x10 ⁻⁴
Density of air, ρ_{air}	kg/m ³	1.2046
Heat transfer coefficient, $h_{d,t}$	W/m ² K	24.49
Total Heat loss, Q_{loss}	W	520.339
Glass tube inner temperature, T_{cbi}	°C	82.96
Temperature between absorber pipe and glass tube, $T_{mb,cb}$	°C	245.153
Inclination angle, β	-	4.04x10 ⁻³
Distance between absorber pipe and glass tube, l	m	0.01
Effective thermal conductivity of inert air in the space, k_{eff}	W/mK	4.28x10 ⁻²
Heat transfer coefficient between metal pipe and glass tube, $h_{ar,t}$	W/m ² K	5.22
Solar energy coming to absorber pipe, Q_G	W	1608.87
Thermal efficiency, $\eta_{thermal}$	-	67.65

Using these thermal efficiency values, a net work calculation was made with a simulation in the Chemcad program. In the Chemcad program, ORC was carried out with different working fluids and as a result, a net work value was obtained. The net work obtained with the working fluids R134a was observed as the highest value (Table 3).

Table 3. Calculated net work value for working fluids

Working Fluids	Calculated Net Work, kW
R134a	72.51
Pentane	70.14
Isopentane	65.74

Considering the previous studies in the literature, it is seen that water has been using as a heat transfer fluid in PTC. The heat transfer coefficient of water is higher than the glycerin. However, the boiling temperature of glycerin is higher than that of water. The high boiling temperature means that more thermal power can be produced from the system. Therefore, it can be evaluated that the use of pure glycerin as a heat transfer fluid is very efficient for this type of system. Since pure glycerin has a high viscosity, some problems may arise during the pumping process. In such cases, the difficulties in the system can be overcome by mixing glycerin-water with a mixture of high heat transfer coefficient and boiling point.

4 Conclusion

In this study, thermal efficiency and net work calculations to be obtained as a result of using glycerin as heat transfer fluid in PTC have been calculated. Therefore, a two-step calculation path was followed. Firstly, the thermal efficiency calculation was done by mathematical method. In the second part, a net work calculation was made with the help of the Chemcad simulation program. According to these calculations, it was determined that the thermal efficiency with a temperature difference of 30°C is 70%. As a result of this simulation, it was seen that 72-kW net work is obtained when R134a is used as a working fluid. And it was observed that the net work obtained by using glycerin as heat transfer fluid in the solar Organic Rankine Cycle is very promising compared to water.

References

1. Qiu G. Selection of working fluids for micro-CHP systems with ORC. *Renew Energy* 2012; 48:565–70

2. Boyle G, Everett B, Ramage J, University TO. Energy systems and Sustainability. Oxford: Oxford University Press; 2003.
3. Chen H, Goswami DY, Stefanakos EK. A review of thermodynamic cycles and working fluids for the conversion of low-grade heat. *Renew Sustain Energy Rev* 2010; 14:305967.
4. Roy J, Misra A. Parametric optimization and performance analysis of a regenerative Organic Rankine Cycle using R-123 for waste heat recovery. *Energy* 2012; 39:227–35.
5. Ciciyiyik, C.,” Parabolik oluk tipi güneş kolektörü ile enerji üretimi” Yüksek lisans Tezi, Gazi Üniversitesi Fen Bilimleri Enstitüsü, Ankara, (2012)
6. Y. Krishna, M. Faizal, and R. Saidur et al. /International Journal Of Heat and Mass Transfer 152 (2020) 11954.
7. R. Devaradjane, Utilization of molten nitrate salt nanomaterials for heat capacity enhancement in solar power applications, rc.library.uta.edu, 2013.
8. J.W. Raade, D. Padowitz, Development of molten salt heat transfer fluid with low melting point and high thermal stability, *J. Sol. Energy Eng.* 133 (3) (2011) 031013.
9. Q. Peng, J. Ding, X. Wei, J. Yang, X. Yang, The preparation and properties of multi-component molten salts, *Appl. Energy* 87 (9) (2010) 2812–2817.
10. R.H. Perry, D.W.G. (Eds.), *Perry’s Chemical Engineers’ Handbook*, Mc- Graw-Hill, 1997.
11. *Segur, J. B.; Oberstar, H. E. (1951). "Viscosity of Glycerol and Its Aqueous Solutions". Industrial & Engineering Chemistry. 43 (9): 2117–2120.*
12. Lide, D. R., ed. (1994). *CRC Handbook of Data on Organic Compounds (3rd ed.)*. Boca Raton, FL: CRC Press. p. 4386.
13. Özden, H., Paul D., “Organik Rankin Çevrim Teknolojisiyle Düşük Sıcaklıktaki Kaynaktan Faydalanılarak Elektrik Üretimi”, X. Ulusal Tesisat Mühendisliği Kongresi, İzmir (2011).
14. Twomey B, Jacobs PA, Gurgenci H. Dynamic Performance Estimation of small-scale solar cogeneration with an Organic Rankine Cycle using a scroll expander. *Appl Therm Eng* 2013; 51:1307-16.
15. Bertrant TF, Papadakis G, Lambrinos G, Author C. Criteria for working fluids selection in low-temperature solar Organic Rankine Cycles. In: *Proceedings of Eurosun 2008; 2008.Lisbon, Portugal p .1-8.*
16. Wang XD, Zhao L. Analysis of zeotropic mixtures used in low-temperature solar Rankine cycles for power generation. *Sol Energy* 2009; 83:605-13.
17. Mc Mahan AC. Design & optimization of Organic Rankine Cycle solar-thermal power plants. University of Wisconsin-Madison; 2006.
18. Quoilin S. Sustainable energy conversion using Organic Rankine Cycles for waste heat recovery and solar applications. University of Liège;2011.
19. Schuster A, Karl J, Karellas S. Simulation of an innovative stand-alone solar desalination system using an Organic Rankine Cycle. *Int J Thermodyn* 2007; 10:155–63.
20. Yang WJ, Kuo CH, Aydin O. A hybrid power generation system: solar-driven Rankine engine-hydrogen storage. *Int J Energy Res* 2001; 25:1107–25.
21. Aboelwafa O, A review of solar Rankine cycles: Working fluids, applications and cycle modifications, Environmental Engineering Program, Zewail City of Science and Technology,2018, Giza, Egypt.
22. Wu Z., Three-dimensional numerical study of heat transfer characteristics of parabolic trough receiver. *Appl Energy*2014; 113:902–11.
23. Duffie, J.A., Beckman W.A., “Solar engineering of thermal processes”, John Wiley & Sons Inc., Third edition, 2006.

Integration of Renewables in Turkish Republic of Northern Cyprus

Ülkem Onur Mert¹, Tanay Sıdkı Uyar¹

¹ Energy Systems Engineering, Cyprus International University

Haspolat, Nicosia, 99258, TRNC

ulkemonur@hotmail.com

Abstract. This paper is geared towards integration of different renewable sources of energy with the existing source of energy. The world tends towards having their systems energy efficient, at the same time cutting the carbon emission. In Europe for instance, many countries in the European Union are projected to adhere to the goal of ensuring there is 100% renewable consumption by 2050. Turkish Republic of Northern Cypress (TRNC), is such a country that has had a huge reliance on imported oil as their means electric generation and other uses. This has made the country spend a lot of money in sustaining development and looking at the well-being of its people. Looking at different renewable, TRNC has the capacity of achieving the goal of 100% renewable and spending less money on development, there are just needs to have some policies put across for these to happen.

Keywords: Renewable Energy, Energy Policy, Solar PV, Solar CSP, TRNC.

1 Introduction

In the past, there have been different fora, debates, and conferences regarding harnessing and how to collect electrical energy from different sources. The founding “fathers” of electricity gave us sources which were later discovered to non-renewable, or did not have any possibility of being replenished, and with the ever-growing electricity demand (going together with the growing population) these were found not to be sustainable. That is why renewable sources of energy have been found to be the answer to this, since they can be replenished and are obtained from natural sources, like the sun, wind, tides, geothermal etc. Efficiency in electrical energy distribution system in a power system, is achieved by optimization of energy consumption.

But more often than not, when renewable sources are used, then the optimization is achieved by a higher percentage, adding to the fact that greenhouse gases (GHGs) are reduced in the process. The global trend of renewable energy usage has been low, and therefore there is a growing need to have more exploration of the renewable sources. In the year 2018, about 181 GW was the amount of power installed globally, 100 GW

solar PV, which was 55% of the renewable power sources installed, the others are 28% wind power, and 11% hydro power [1]. This is still not sufficient going by the global consumption of electric energy according to British Petroleum (BP) report, citing that per hour, we need 26614.8TWh [2].

We can be hopeful that the trend of investment in renewable energy globally is on the increase with solar being the leading, then wind as shown in figure 1. That from 2010 to 2019, there has been over US\$2.5 Trillion worth of investment in renewable energy. The 2019 report released by the United Nations Global Climate Action Summit dubbed The Global Trend in Renewable Investment, the investment has quadrupled the one of 2009 (which was 414 GW), to slightly over 1650 GW by the close of this decade [3]. This growth has also been encouraged by the lower prices of the renewables.

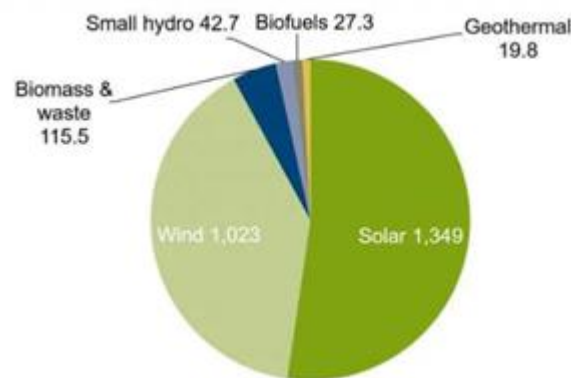


Figure 1: Global investment in renewable sources of energy [3]

These energy sources can be integrated into the existing electricity system, or can they? Achieving this is not an easy affair, because for integration to occur, there must be reliability of the power system, efficiency issue must be dealt with, the cost of integration, storage of these generated energy, among other issues. This paper deals with the current renewable sources, in Turkish Republic of Northern Cypress (TRNC) and finding the possible ways, challenges and what needs to be done to achieve the integration of renewable energy sources. The first point is looking into the current renewable sources in that country, the energy storage facilities, especially when there is intermittent of the sources, and challenges faced, and finally possibility of integration of the system. In the discussion, the focus shall be on solar (photovoltaic, and concentrated solar power), wind and biogas. When the renewable energy sources are integrated with the traditional energy sources, there shall be an improvement of reliability of the power system, and this will be enhanced further when appropriate storage systems of energy are incorporated, this becomes important when the weather conditions changes.

2 Literature Review

2.1 Integration of renewable sources in the grid

Many countries foster sustainability of energy and low emission of GHGs by embracing the technology of renewable energy, and so they have different targets for their electric supplies. Solar and wind are variable sources than the traditional methods of electric generation, and therefore their production of energy is not constant, so this calls for planning the power system to accommodate those facts. Integration of power to the grid, is a way of delivering to the grid a variable renewable energy (VRE) in an efficient way. While integrating the VRE, there must a consideration of the cost at the same time increasing stability of the system and reliability. There are changes in the power system globally, which is caused by the upsurge of available low-cost variable renewable energy, the advanced technology which involves digitalization and the opportunity in electrification brought by high growth rate. For a power system to be referred to as flexible, it must possess the capability of maintaining uninterrupted service while there are large swings in supply and demand. Power system also, must be flexible for it to cope with the unexpected emergencies like plant and power outages. System integration of VRE can be implemented when four things are considered that are different, based on the support of the system flexibility, identification of the challenges and apply suitable measures that supports the integration of the VRE [4]. They are:

Generation of new renewable energy – when planning to invest in a generation of a new VRE, targets and incentives must be aligned with the consideration of grid integration. Policy makers or regulators of a country can make targets that drives innovations that supports clean energy. Also, they can establish rewarding schemes that are geared towards those of generate power through renewables, like wind or solar. These factors encourage investments in green energy technology at the same time avert negative effects of integration.

- New transmission – when there is a target to have VRE capacity increased, then the grid must be expanded and modified to allow the power system to be connected to a high-quality renewable source, which remotely work from the available transmission networks.
- The system flexibility must be increased – sources that are flexible in operation are important when the renewable sources are connected to the grid. Flexibility encompasses market practices and the procedures of operation. Also, the response demand and means of storage of the electric power are among the consideration in a flexible system.
- Future planning for a higher capacity of renewable energy – when planning a power system, demand is usually given highest priority, and so this involves expanding the system's capacity to cater for the expected demand. This factor is tied to flexibility is that when a higher capacity of VRE generation is employed in a power system, then the planning involved must include flexibility in the power system [5].

3 Case study

3.1 Grid integration in Turkish Republic of Northern Cyprus (TRNC)

Cyprus island comes third after Sicily and Sardinia in terms of surface area, which amounts to 9,251 km², which 3,355 km² belongs to TRNC and the remaining belongs to Cypriot Administration (GCA) [6]. The island mostly depends on oil for its economy, and this makes renewable sources like solar, wind, geothermal, biofuels etc. to have less usage. This has gotten the administration and policy makers worried because of high carbon emissions [7]. That is why there is the urge to transform the resources of energy to 100% renewable to meet the EU target of having a zero emission by the year 2050 [8].

There is a huge potential of solar energy in TRNC, as far as renewable energy, especially solar energy harnessing in Europe, TRNC has the best solar irradiation to obtain a higher electrical energy [9]. Even with this, it has only installed 403.2 MW of renewable energy and of this only 1.2 MW of solar is installed (see table 1) [10]. However, TRNC an island country and therefore the grid power is sensitive to the production of electricity that comes from renewable sources of energy, majorly solar and wind. The only problem in this area is intermittency, where sometimes the weather conditions reduces production to zero. This is what drives the country to integration of the power system to cater for the lost power. The grid in TRNC is limited to respond to sudden changes in the production of power and as a result power outage are rampant. As a response to this, the power grid of the island needs to be connected to a much bigger power grid, which is interconnection between grids that means integration is necessary.

Table 1: Total Installed power capacity in TRNC as of the 2nd half of 2019 [11]

Location	Type of Technology	Number and Size of Units	Fuel	Total Installed Capacity
Teknecik	Steam Turbine	2 × 60 MW	Heavy fuel oil	120 MW
Teknecik	Gas Turbine	20 MW + 10 MW	Diesel	30 MW
Teknecik	Diesel Generator	8 × 17.5 MW	Diesel	140 MW
Dikmen	Gas Turbine	20 MW	Diesel	20 MW
Kalecik	Diesel Generator	8 × 17 MW	Diesel	136 MW
Kalecik	Steam Turbine	6 MW	Heavy fuel oil	6 MW
Serhat	Solar	1.2 MW	-	1.2 MW
Total				453.2 MW
Total without Gas Turbines				403.2 MW

3.2 Actions that needs to be taken

The ambition is that by 2050 TRNC achieves 100% renewable energy usage, the timeline from 2020 is sufficient for the island to do the necessary installation and have its citizens transition to a new way of life, including having Electric Vehicles (EV) on the roads. This means solar and wind mostly, and a small capacity of biogas. For the country to achieve 100% renewable transition, there must be some guidelines and some transformation to be carried through. Now there is a need to integrate renewable with the existing grid system. Here, we are going to look at the solar irradiation and wind power and see how much can be harnessed from the existing resources that are available presently.

Solar

Solar PV is the best and cheaper way of tapping electric energy around the world, since during the day light is everywhere. TRNC is regarded as one of the countries in Europe with the highest solar radiation, where the sun shines for more than 300 days in a year, the average irradiation is about $2,000 \text{ Wh/m}^2$ on a surface that is tilted to around 27.57° [12]. In the lowlands of TRNC, the sunshine duration is between 5.5 hours to around 12.5 hours in the winter and summer, respectively. If for instance, just 0.05% of the land is taken and used for solar, assuming the capacity of solar PV are the same, and there is a uniform amount of solar irradiation experienced. That means we shall have around $1,677,500 \text{ m}^2$ and with 2000 Wh/m^2 (which is 2000 watts in an hour for every square metre) means that there shall be about 335.50 GWh/m^2 of power produced annually. In a year there 300 days of sunshine, that is what gives us about 335.5 GW of power can be produced in one hour yearly if just about 0.05% of the land capacity in TRNC is used. Assume a loss of 70% of the ideal power produced, or an efficiency of about 30%, which is produced annually. This with a country of around 320,475 [13], that alone might not suffice going by the growing demand of power and population.

Another system that this can be integrated with is the Solar Concentrated power (CSP). The mode of operation of this type, is by use of reflected light by mirrors or collectors and concentrated at one place where there is water. This concentrated power produces heat which is used for thermal energy which can be stored and later used in the production of electric power.



Figure 2: A typical concentrated solar power plant (CSP)

Depending on the amount of electricity that needs to be produced, the plant can be occupying a large area. For the sun radiation capacity of TRNC, this plant can be installed in around three areas, Serhatkoy being one of them where sun radiation is significant. The country just needs an area of around $551.47\text{m}^2 \times 800$ collectors, this translates to around $450,000\text{ m}^2$, with a mean efficiency of the collector per year (which depends on the annual direct radiation) of 67%, an annual solar hour of 1600 hours/year, about 482 GWh. When the temperature is heated to 550°C , and a storage capacity is used around 3000MWh [13].

Wind

Wind turbines work well whenever there is a lot of air movement, which is the wind speed, like the seashores around beaches and in hilly places. The second factor that policy makers needs to have in mind is the wind direction, then lastly, how the wind changes with the height of the ground (this gives an idea of how wind speed measurement scales with interpolation of the height of the turbine hub) [14].

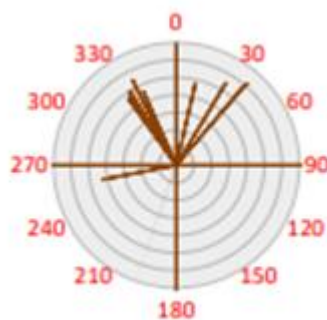
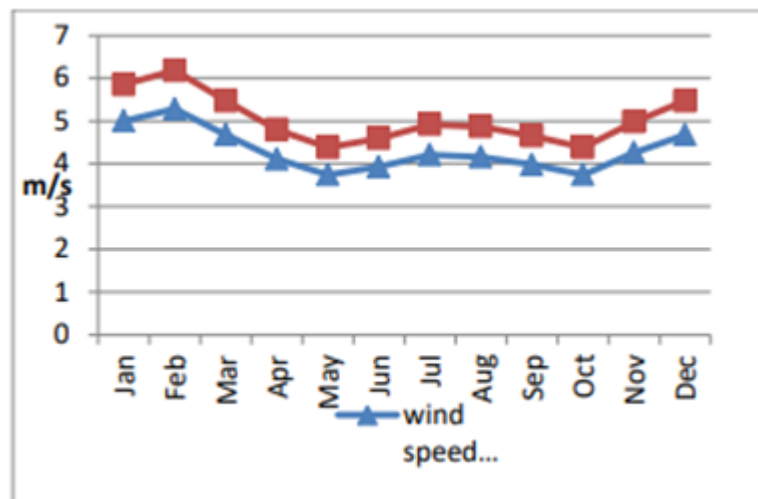


Figure 3: The graph showing wind speed of TRNC from January to December and wind rose diagram [15].

The wind can be harnessed from the north-western direction than the northern side according to the wind rose diagram. The wind speed in those areas are between 4m/s to 6m/s. which according to the wind turbine selection in table 2, it is estimated that one turbine of 3 blades can produce about 1.3kW

Table 2: Table showing specs of a wind turbine [15].

Type	3 blade, horizontal axix
Cut-in speed	3m/s
Cut-out speed	11m/s
Survival wind speed	45m/s
Rated power output	1.3kW
Swept area	6.8m ²
Blade diameter	2.9m

When looking at the capacity of the power produced by solar, wind energy capacity can fill in the rest of the power.

4 Conclusion

For the country to embrace 100% renewable power production to its people, there is a need to have a lot of power produced by solar. Solar has the highest capacity of producing a lot of power and wind can just supplement, in case of intermittency. The government also needs to invest in storage facility, the large batteries for storing power produced by solar, and for CSP, the storage tanks can suffice and maintain the temperature at about 250°C. The country's industries need to focus on the bio energy. There is a need to improve the model of consumption to the facilities used in the industries. In the transport sector, the government can start importing vehicles that are fuel efficient at the moment and when the renewable plants are up and running and are seen to be producing surplus, then EV importation needs to take effect. With electric vehicles competing with the Fuel-Cell Vehicles (FCV), there is a projection that by 2030, there might be several FCV on the roads. FCVs are vehicles that are running on hydrogen gas conversion. Lastly, on biomass production, which there are debates whether they really curb CO₂ emission or not (Woody, 2017), needs to be used for industrial heating and domestic.

References

1. A Zervos, A. & Adib, R., 2019. RENEWABLES 2019: GLOBAL STATUS REPORT, Athens: REN21.
2. Dudley, B., 2019. BP Statistical Review of World Energy, London: BP.
3. UN Global Climate Action Summit, 2019. Global Trends in Renewable Energy Investment, Geneva: UN.
4. IEA, 2019. System integration of renewables Decarbonising while meeting growing demand. [Online] Available at: <https://www.iea.org/topics/system-integration-of-renewables> [Accessed 17 January 2020].
5. Cochran, J. & Katz, J., 2015. Integrating Variable Renewable Energy into the Grid: Key Issues, s.l.: National Renewable Energy Laboratory.
6. Kıbrıs, K., Cumhuriyeti, T., Devlet, B. & Örgütü, P., 2018. Turkish Republic of Northern Cyprus Prime Ministry Planning Organization. [Online] Available at: <http://www.devplan.org/2017%20EKO-SOS-GOR.pdf> [Accessed 18 January 2020].
7. Özden, M. Ö., 2019. TURKEY - CYPRUS ISLAND INTERCONNECTOR AS AN ENERGY POLICY FOR TURKEY. [Online] Available at: <http://turkishpolicy.com/blog/36/turkey-cyprus-island-interconnector-as-an-energy-policy-for-turkey> [Accessed 19 January 2020].
8. European Commission, 2018. The Commission calls for a climate neutral Europe by 2050. [Online] Available at: http://europa.eu/rapid/press-release_IP-18-6543_en.htm [Accessed 18 January 2020].
9. Middle East Technical University, 2019. Investigating Renewable Energy Integration into the TRNC Power System. [Online] Available at: <https://ncc.metu.edu.tr/announcement/campus-funded-project1> [Accessed 18 January 2020].
10. Kurumu, E. & Türk, K., 2019. Cyprus Turkish Electricity Institution: KKTC'de Elektrik Üretim Santralleri: Electricity Production Power Plants in GCA. [Online] Available at: <https://www.kibtek.com/uretim/> [Accessed 19 January 2020].
11. KIB-TEK, 2018. Total power installation in TRNC by the second half of 2018. [Online] Available at: <https://www.mdpi.com/2071-1050/11/3/593/htm#B2-sustainability-11-00593> [Accessed 19 January 2020].
12. Abbasoglu, S., 2017. Techno-Economic and Environmental Analysis of Photovoltaic Power Plants in Northern Cyprus. Energy Education Science and Technology Part A: Energy Science and Research Volume 28(1), pp. 357-368.
13. Abbasoglu, S. & Okoye, C., 2018. Empirical investigation of fixed and dual axis tracking Photovoltaic system installations in Turkish Republic of Northern Cyprus. Journal of Asian Scientific Research, 3(5), pp. 440-453.
14. McGowan, J. G., Manwell, J. F. & Rogers, A. L., 2016. Wind Energy Explained: Theory, design and application. Second ed. s.l.:s.n.
15. Abdullahi, I., Muhammed, G. & Aliyu, A., 2017. Installation Of 2MW Wind Power Plant in Northern Cyprus: Technical, Economical and Environmental Analysis. INTERNATIONAL JOURNAL OF SCIENTIFIC & TECHNOLOGY RESEARCH, 6(11), p. 2.

Multivariate Based Modelling of Solar Energy Growth: A Discussion of Relevant Factors Influencing African Solar Energy Development

Humphrey Adun¹, Michael Adedeji¹, Tonderai Ruwa¹, and Mustafa Dagbasi¹

¹ Cyprus International University, Energy systems engineering, North Cyprus

Abstract. Renewable energy integration into the global energy mix has grown over the years in most countries, though in varying proportions. Solar energy due to its highly abundant nature is the most utilized form of renewable energy in the world. The current energy mix in Africa is not a proper reflection of the energy endowments of the continent. The integration of renewable energy resources into the energy mix on the continent varies from country to country. Undoubtedly, the integration of renewable energy into the energy mix in Africa is on the rise, with immense potentials for the development of solar energy on the continent. Hence, this study employs the use of multivariate regression in modeling the trend of solar energy growth in 15 African countries by analyzing five decision variables suspected to aid its growth. The African countries covered in this study are; South Africa, Egypt, Morocco, Algeria, Uganda, Mauritius, Kenya, Nigeria, Mauritania, Tunisia, Angola, Tanzania, Cape Verde, Rwanda, and Mozambique. The independent variables considered for the study are their; renewable energy policies, energy consumption, carbon emissions, population, and gross domestic product (GDP). In order to perform a detailed and more precise study, the countries are divided into three groups, with each group presenting countries with similar solar energy growth. A sensitivity analysis is also performed to ascertain the robustness of each model to the variables considered. The results of the study show that the variables that affect solar energy growth on the continent vary based on the geographical location of each country. The results also indicate that the three most dominant factors aiding solar energy growth amongst the countries considered in this study are their carbon emissions, energy consumption, and GDP.

Keywords: Energy, artificial neural network, solar energy growth, modelling, carbon emission, energy consumption.

1 Introduction

Given the global consensus on tackling the environmental issues of climate change and global warming, which is majorly caused by the production of energy with fossil fuels, the development of renewable energy has become critical in energy matter at local and international levels. According to the United Nations, Africa is highly vul-

nerable to the effects of climatic change due to its high dependence on fossil fuels for energy generation, population growth and inflexibility to change. The deployment of renewable energy in African energy mix has been on the steady rise, as a means to cut down on the reliance on fossil fuels, and this is aided by the immense renewable energy resource available on the African continent [1]. The geographical location of Africa gives it the natural RE endowment.

However, despite the rich renewable energy resources in Africa and the increase in RE production, the continent is still characterized by insufficient electricity and the lack of access to basic electricity infrastructure to meet growing energy demands [2]. Most of the countries in Africa are heavily reliant on non-renewable energy resources for electricity production. Oil and gas are predominant energy resources for energy production in North Africa. The Sub-Saharan region is also reliant on fossil fuels, accounting for about 70%-90% of primary energy supply [3]. Hence, coal, oil and natural gas are used to meet the fast-growing demand for energy on the continent [4]. Despite the dominating use of these conventional sources for electricity generation, most of these countries on the continent are still considered as energy poor. According to [5], 69% of the African population make use of biomass for cooking.

Considering that easy access to electricity and modern energy sources play a crucial role in economic growth and sustainable development, the continent of Africa has been subjected to under-development and poverty [6]. Figure 1 shows the access to electricity in the African countries considered in this study, as the data is retrieved from [5]. Some significant benefit, in case of RE utilization, is the electrification of rural African, job creation, economic growth and energy security [4]. According to the statistics published by the National Renewable Energy Laboratory (NREL), the demand for renewable energy has continued to rise since the year of 2010. Among renewables, solar energy is an inexhaustible and pollution-free energy resource that plays a remarkable role in providing energy in a sustainable way. Many countries have tapped into solar energy production for meeting rising energy demands as it bears no risk of environmental pollution [7], hence solar energy can be seen as alternative energy source that could be used to increase the electricity share in the African continent.

Certain parameters such as technical expertise and policies may pose a limitation towards utilizing solar energy in certain regions and countries. For instance, the lack of technical expertise on renewable energy production makes it unrealistic to project the incorporation of renewable energy into the energy mix of Namibia despite the fact that Namibia has about 100 times more energy production potential (from solar energy) than its current energy consumption [8]. The share of solar energy to the global electricity production has increased over the years [9]. Cumulative installed capacity of solar PV increased from 127MW in 2009 to 1334MW in 2014, which represents % growth. South Africa leads the continent in solar PV production, haven added 780MW between 2013 and 2014 [10].

This study attempts to bridge the gap in literature on energy solar energy developed countries across different regions on the African continent; by emphasizing on key parameters that could potentially impact on solar energy production development, through data aggregation, modelling and sensitivity analysis.

In this study, the solar energy growth in Africa, between the period of 2000 and 2014, is considered. Considering the fact that the accuracy of this study is reliant on the use of appropriate data, the study is carried out using the time gap of 14 years with 2014 being the end time frame because of the unavailability of sufficient data for later years. Investigating the effects of different parameters (gross domestic product, policies, energy consumption, carbon emissions, and population) on growth constitute the main focus of this study. These parameters are then used to develop a model; in order to understand their effects on the growth level of solar energy in the countries after which future predictions and suggestions are made concerning solar energy growth in these regions.

This study is structured as follows: Section 2 briefly discusses the state of energy situation in Africa, and the general growth in some countries. Section 3 provides the details of the methodology, mainly describing the divisions of the top solar energy countries in Africa and the parameters used in the modelling. Section 4 presents the results of the developed simulation model. Finally, Section 5 briefly comments on the results and future projections of solar energy growth in the countries considered in this study.

2. Current Status of Solar Energy in Africa

Kaygusuz [11], stated that the rapid population growth is stated as the major reason for the exponential growth of energy demand in Africa and other developing countries. The study further claimed that Africa will experience medium growth in energy consumption, in which the major consumption comes from biomass

Investments in renewable energy in terms of technical development and research is the doorway towards increasing the share of renewable energy production in Africa. Solar energy represents a viable renewable energy option in Africa due to its decentralised nature and its immense availability [8]. Also, putting into consideration cost, solar energy technologies also stand out as a more attractive renewable energy option to African countries, as there have been a steady fall in the cost of solar technologies [7]. Solar energy is less prone to supply uncertainty as it is the most abundant renewable energy resource in Africa; For instance, the Sub Saharan and North Africa regions are richly endowed with great solar energy potential [12]. However, sub Saharan is still in the dark while North Africa is on the verge of exporting solar energy to the Europe [13].

3. Methodology

In this study, linear programming modelling is utilized in investigating solar energy growth in selected African countries. Linear programming is used in maximizing or minimizing a linear function, having some constraints. Its applications span diverse field of study; telecommunications, construction, thermal science, medicine, and

many others [14]. In this study, the linear programming is used in finding the optimum parameters.

In the modelling procedure, the difference in solar growth between 2000 and 2014 is implemented as the independent variable. The dependent variables that are used in modelling the solar energy growth are; number of policies, carbon emissions, Gross Domestic Product (GDP), energy consumption, and solar radiation. The dependent variables are retrieved from the database of dependable sources, and this will be discussed in details in the subsequent sections. The solar energy installed capacity level for each country of analysis was retrieved from the IRENA database. The difference between the installed capacity in 2014 and 2000 refers to the “solar growth” in this study. 15 African countries were studied and divided into three sections based on the level of their solar energy growth for the 14 years. The sectional divisions have five countries each, and this is made based on similar growth rate across 2000-2014. Section 3.1 will give more explanation on the sorting of the countries considered, section 3.2 explains in clarity, the parameters utilized in the modelling, section 3.3 gives a summary of the modelling technique, and section 4 gives the result from the simulation modelling

3.1. Country categorization

For the purpose of this paper, the countries will be grouped as; *Developed* (Section A), *moderately developed* (Section B) and *Less developed* (Section C) countries. Section A countries are; Egypt, Morocco, Algeria, Uganda and South Africa. Section B countries include; Mauritius, Kenya, Nigeria, Mauritania, Tunisia. Section C countries cover; Angola, Tanzania, Cape Verde, Rwanda and Mozambique. The countries are grouped based on their individual solar energy production. The first group consisting of 5 countries are those whose solar energy installed capacity within the 14 years considered ranges between 20-914MW, in same vein, Section B countries range between 15MW-18MW and Section C countries are between 7MW-12MW. It should be noted that there are other countries in Africa that had an increase in installed capacity of solar energy growth within the period considered in this study. However, the growth levels (<1MW) were too minimal to be considered in this study, as they affected the modelling result due to the significant difference in value as compared with the other countries considered. The table 1 shows the solar growth between 2000 and 2014 of the countries considered in this study.

Table 7. Solar energy growth

Sections	Countries	Solar Energy production		
		2000	2014	Growth
Group A (20-914MW)	South Africa	8	922	914
	Egypt	0	35	35
	Morocco	7	40	33
	Algeria	2	28	26
	Uganda	0	20	20
	Mauritius	0	18	18
Group B (15-18MW)	Kenya	4	22	18
	Nigeria	0	16	
	Mauritania	0	15	15
	Tunisia	0	15	15
Group C (7-12MW)	Angola	0	12	12
	Tanzania	0	11	11
	Cape Verde	0	9	9
	Rwanda	0	9	9
	Mozambique	0	7	7

The largest growth of solar energy in Africa between 2000 and 2014 occurred in South Africa with a growth margin of 914MW.

3.2. Modelling

The model used is the multiple regression method. The model equation employed is:

$$P = a * X_1^b + c * X_2^d + e * X_3^f + g * X_4^h + i * X_5^j + k \quad (1)$$

Where P represents the solar energy growth estimation, X_1 represents carbon emission, X_2 represents GDP per capita, X_3 represents population, X_4 represents no. of policies and X_5 represents energy consumption. The weights; a, b, c, d, e, f, g, h, i are obtained from the MATLAB simulation results. The percentage error $e_{(\%)}$ is also calculated as the percentage difference between the real solar growth and the predicted growth of each country in each categorization.

The significance of the relationship between the solar growth and the parameters is shown by the root mean square value. Root mean square error is a measure of the deviation of the predicted values to the observed values. In calculating the total root mean square, the equation format used is shown in Equation (2).

$$\text{Total RMSE} = \sqrt{\frac{\sum_{i=1}^n (\check{y}_i - y_i)^2}{n}} \quad (2)$$

Where \check{y}_i represents the observed value. In this study, the observed values are the solar growth of the countries considered. y_i Represent the predicted values, which is the predicted solar energy growth calculated using the model equation given in equation 1

$$\text{Total RMSE} = \text{qrt}(\text{mean}((\text{solar energy growth} - \text{prediction})^2)) \quad (3)$$

The total RMSE value is minimized to obtain the optimum combination of variables (factors). The optimum model equation is then used in the sensitivity analysis to make prediction of solar growth upon percentage increment of 10% to 50% of the variables used in the simulation model. This is presented in the prediction analysis section.

The MATLAB Rb17 is used in carrying out the simulation modelling and sensitivity analysis.

3.3. Results and Discussion

In this section, the modelling results of the different sections of the country categorization are presented. The final model equation, which is the Predicted solar growth, from the simulation is also presented

Modelling Results of Section A Countries

The table 2 is a representation of the results of the study done for section A countries showing their predicted growth.

Table 2: Predicted growth of section A Countries

Countries	Real Growth	P (1)	e (%) (1)
South Africa	914	819.457	10.343
Egypt	35	187.889	-436.827
Morocco	33	22.553	31.657
Algeria	26	163.535	-528.981
Uganda	20	-1.839	109.194
RMSE		101.875	
$\bar{e}_{(%)}$			-162.922

$$P = 0.008X_1^{2.45} + 0.249X_2^{0.21} + 1.130X_3^{-0.091} - 0.061X_4^{-0.359} - 1.958X_5^{0.316} + 5.595 \quad (6)$$

Table 2 shows a very high percentage error; thus, the model did not work well. A possible explanation for this is the disparity in the growth of solar energy in South

Africa which is way higher than the others in the section. This model is then carried out without South Africa in the country mix and the result is shown in table 3.

Table 3: Predicted growth of developed countries

Countries	Real Growth	P (1)	e (%) (1)
Egypt	35	32.96	5.54
Morocco	33	27.30	18.00
Algeria	26	33.66	-28.96
Uganda	20	19.45	1.76
RMSE		4.92	
$\bar{e}_{(%)}$			-0.91

$$P=4.22X_1^{0.36} + 0.45X_2^{0.16} + 1.37X_3^{-2.2} + 0.29X_4^{0.21} + 4.34X_5^{0.14} + 2.14 \quad (7)$$

Equation 7 shows the result of the model without the inclusion of South Africa. The equation is constructed using the values derived from the optimization result and inputted in the model equation as shown in equation 1.

Modelling Results of Section B Countries

A similar analysis is done for section B countries as was done for section A countries and a table of the results is shown in table 4.

Table 4: Predicted growth of Section B countries

Countries	Real Growth	P (1)	e (%) (1)	P (final)	e (%) (final)
Mauritius	18	18.50	-2.77	19.43	-7.98
Kenya	18	13.50	25.00	15.74	12.52
Nigeria	16	23.50	46.87	19.47	-21.72
Mauritania	15	11.68	22.13	15.01	-0.07
Tunisia	15	17.14	14.28	19.15	-27.66
RMSE			3.26		
$\bar{e}_{(%)}$					-8.98

$$P=2.80X_1^{0.274} + 0.34X_2^{0.156} + 1.38X_3^{-3.073} + 1.23X_4^{0.2365} + 3.67X_5^{0.21435} + 1.59 \quad (8)$$

Equation 8 shows the optimal result for the optimization iterations. The iteration was done severally until the final optimization point is derived. The values derived are inputted into the model equation as shown in equation 1.

Modelling Results of Section C Countries

A similar analysis is done for section C countries as was done for section A and B countries and the table of the results is shown in table 5.

Table 5: Predicted growth of less countries

Coun-tries	Real Growth	<i>P</i> (1)	<i>e</i> _(%) (1)	<i>P</i> (final)	<i>e</i> _(%) (fi-nal)
Angola	12	11.60	3.25	11.75	2.08
Tanzania	11	10.73	2.39	10.81	1.69
Cape Verde	9	11.30	25.59	9.59	-6.66
Rwanda	9	9.03	-2.67	9.32	-5.93
Mozam-bique	7	8.48	21.23	7.33	-4.81
RMSE			0.41		
$\bar{e}_{(%)}$					-2.72

$$P=0.92X_1^{0.13} + 2.56X_2^{0.20} + 5.43X_3^{-0.63} - 2.28X_4^{0.68} + 0.64X_5^{0.007} - 0.76 \quad (9)$$

Equation 9 shows the optimal result for the optimization iterations. The iteration was done severally until the final optimization point is derived. The values derived are inputted into the model equation as shown in equation 9.

3.4 Prediction Analysis

The equation derived from the model is used in making predictions of future solar energy situations upon increments of the factors stated. The increment used was between 10% and 50%. The decision variable which causes the most prominent increase in solar energy is deemed as the factor with most effect on solar energy growth in that country.

Section A Countries

The percentage increase of 10% to 50% for each of the countries in the section A was done. The most significant effect was seen in carbon emission increment. This is shown in the figure 8. A sensitivity analysis is also investigated for all the factors considered in order to determine the parameter that would have most effect on the growth of solar energy.

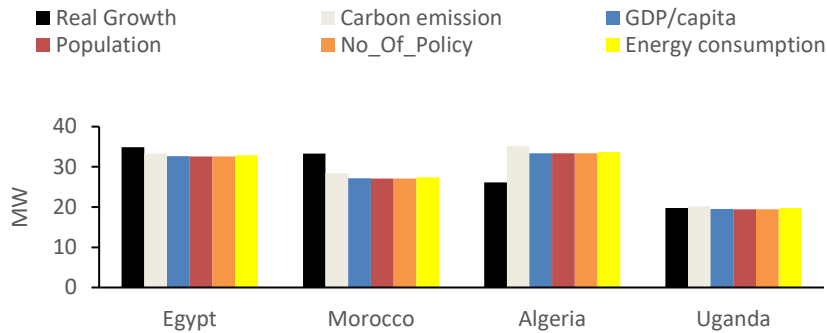


Fig.1. Predicted growth for de *Section A Countries*(All factors)

From the prediction analysis using the optimum model, it is seen from figure 1 that carbon emission has the most significant effect on the production of solar energy in this categorized region of Africa. This is not to say that the other factors do not contribute to the solar energy development, however, the model proofs that renewable energy policies are enacted basically due to reduction of greenhouse gases in the region.

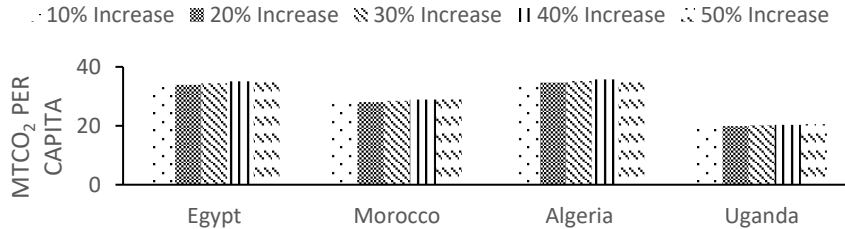


Fig.2. Predicted growth for Section A Countries (carbon emission)

It is seen from figure 2 that fossil fuel usage will still be a major source of energy production in this countries, as increasing carbon emission is modelled from 10% to 50%, however, this trend will cause more solar energy projects to be installed. This result is backed up by literature, as Morocco where about 90% of the energy production comes from imported Oil, recently commissioned the largest solar project in the world; the NOOR project. Carbon emission is one of the issues been considered for mitigation. A study by [15] agrees that solar energy is slowly coming up to solve issues regarding reducing carbon emissions and the author also explained that the severity of CO₂ emissions intensity on the economic activities, need to reduce by 85% between 2015 and 2050. Carbon emission has a significant influence on the growth of solar energy because of the ability of the renewable energy to de-carbonize

energy which is a key aspect of climate change mitigation [16]. This is one of the many reasons why solar energy is being considered

Section B countries

Upon carrying out the predictions for all the factors to check their impact on the possible solar energy growth, energy consumption proves to cause the most significant growth in the section B countries.

The same method is applied for the other parameters as done for the section B countries.

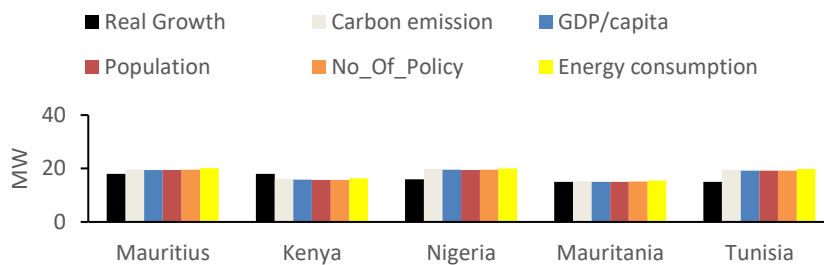


Fig.3. Predicted growth for *Section B countries*(All factors)

From the figure 3, it is seen that the major influencer of solar energy development in the countries is energy consumption. Nigeria, for instance is one of the most populous countries in Africa, and the high energy demand of the population is a significant factor for solar energy development in the country.

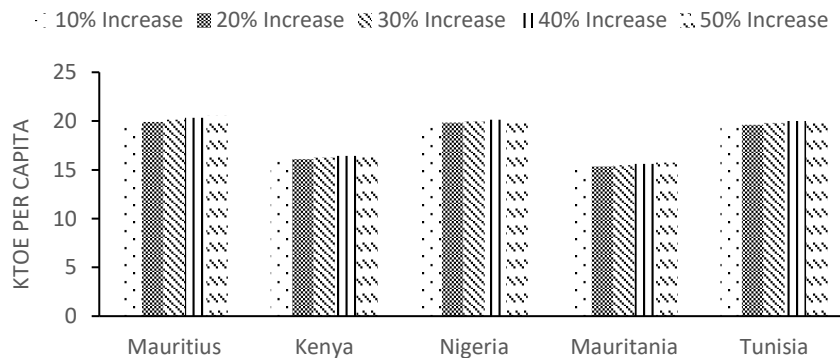


Fig.4. Predicted growth for *Section B countries* (Energy consumption)

From figure 4, it is seen that increasing energy demand in the countries in this sectional categorization will cause more solar energy development. A previous study agrees with this research outcome that the demand for solar energy is increasing and

as such, investments required for this renewable energy are increasing too[17]. This ultimately results to the growth of solar energy. Another study by [18] showed that solar energy development among other renewable contributes is influenced by energy consumption (demand). Solar energy is experiencing an increase in consumption as countries have come to recognize the negative impacts of burning fossil fuels and this has resulted to increased competition. On the other hand, [19] stated clearly that the increase in demand for solar energy has resulted to the decline in the GDP of countries that export and produce fossil fuel.

Section C countries

Having carried out the predictions for the 10% to 50% increase in each of the parameters considered, GDP showed the most significant effect for each increment.

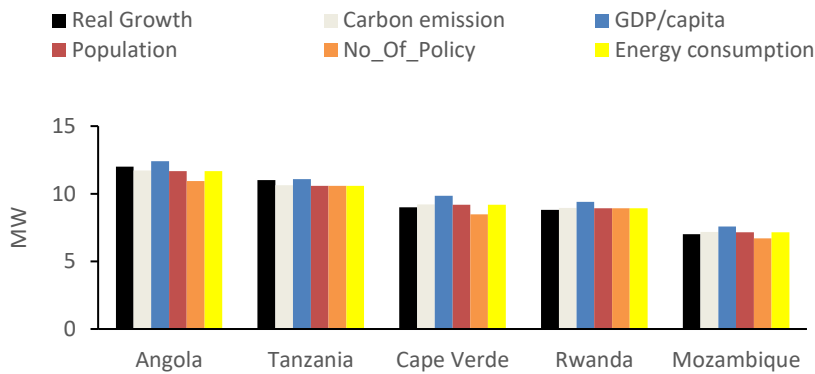


Fig.5. Predicted growth for *Section C countries*(All factors)

The figure 5 shows that the increase in the economy of the countries in this section represent the most significant effect on solar energy development.

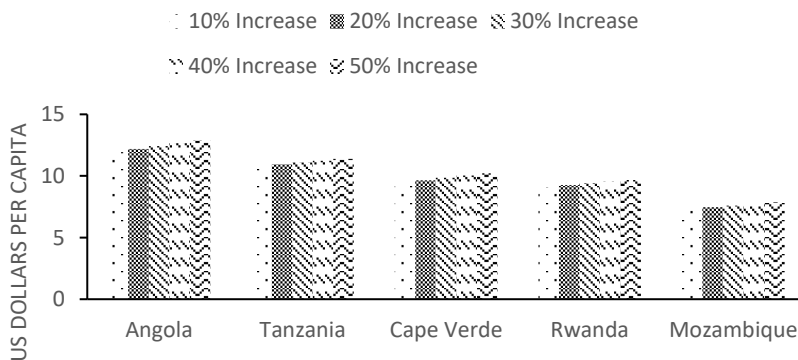


Fig.6. Predicted growth for *Section C countries*(GDP)

Figure 6 shows that as the GDP increases, there will be more energy development. A previous research emphasized on that increased GDP will have an effect on solar energy development [20]. [21] also mentioned that increased GDP (economic growth) influences solar energy development and the solar energy in turn helps to boost the economy through its increasing investments and increasing global production of solar panels. Investing in solar energy also contributes to the economy and it also encourages energy security and easy energy access for economies in Africa [22]. An increased GDP will make it possible for solar energy production, creating a good market value and also make it accessible to those who demand it.

4. Conclusion

The diffusion of solar energy in the African countries has grown steadily over the years, however, there is an uneven trend of this growth. This is despite the fact that solar energy resource is abundant throughout the countries within the continent. Within the scope of the findings of this study, it was suggested that there are several factors that could have aided the growth of solar energy in the solar developed countries as compared to the many other African countries that are still heavily reliant on fossil fuels and biomass for energy generation.

The possible factors studied alongside the solar energy growth between 2000 and 2014 are carbon emission, energy consumption, GDP, renewable energy policies, and population. The result shows that different factors aid solar growth in both the different solar developed classifications and each country. Carbon emission is the most significant factor that has aided solar energy production amongst the developed African countries. Predictions show that Algeria would experience steadier solar energy growth in the coming years. Amongst the moderately developed region, energy consumption is the driving force for the solar energy growth between the times period considered. While in the less developed countries, increase in GDP was the spurring factors towards solar energy growth. Predictions thus projects that as GDP increases in the countries in this section (Angola, Tanzania, Cape Verde, Rwanda and Mozambique), the solar energy production would also increase

References

1. M. Y. Suberu, M. W. Mustafa, N. Bashir, N. A. Muhamad, and A. S. Mokhtar, "Power sector renewable energy integration for expanding access to electricity in sub-Saharan Africa," *Renew. Sustain. Energy Rev.*, vol. 25, pp. 630–642, 2013.
2. I. M. Bugaje, "Renewable energy for sustainable development in Africa: A review," *Renew. Sustain. Energy Rev.*, vol. 10, no. 6, pp. 603–612, 2006.
3. S. Karekezi, "Poverty and energy in Africa - A brief review," *Energy Policy*, vol. 30, no. 11–12, pp. 915–919, 2002.
4. T. Beiter, Philipp Elchinger, Michael Tian, "U.S Department of Energy: 2016 Renewable Energy Data Book," pp. 1–132, 2016.
5. REN 21, *Global Status Report*. 2017.
6. G. Black, M. A. T. Black, D. Solan, and D. Shropshire, "Carbon free energy development and the role of small modular reactors: A review and decision framework for deployment in developing countries," *Renew. Sustain. Energy Rev.*, vol. 43, pp. 83–94, 2015.
7. M. E. Flowers, M. K. Smith, A. W. Parsekian, D. S. Boyuk, J. K. McGrath, and L. Yates, "Climate impacts on the cost of solar energy," *Energy Policy*, vol. 94, pp. 264–273, 2016.
8. U. Deichmann, C. Meisner, S. Murray, and D. Wheeler, "The economics of renewable energy expansion in rural Sub-Saharan Africa," *Energy Policy*, vol. 39, no. 1, pp. 215–227, 2011.
9. R. Prävãlie, C. Patriche, and G. Bandoc, "Spatial assessment of solar energy potential at global scale. A geographical approach," *J. Clean. Prod.*, vol. 209, pp. 692–721, 2019.
10. IRENA, *Roadmap For A Renewable Energy Future*. 2015.
11. K. Kaygusuz, "Energy for sustainable development: A case of developing countries," *Renew. Sustain. Energy Rev.*, vol. 16, no. 2, pp. 1116–1126, 2012.
12. C. Brunet, O. Savadogo, P. Baptiste, and M. A. Bouchard, "Shedding some light on photovoltaic solar energy in Africa – A literature review," *Renew. Sustain. Energy Rev.*, vol. 96, no. August, pp. 325–342, 2018.
13. C. Kost, B. Pfluger, W. Eichhammer, and M. Ragwitz, "Fruitful symbiosis: Why an export bundled with wind energy is the most feasible option for North African concentrated solar power," *Energy Policy*, vol. 39, no. 11, pp. 7136–7145, 2011.
14. Y. M. R. Aboelmagd, "Linear programming applications in construction sites," *Alexandria Eng. J.*, vol. 57, no. 4, pp. 4177–4187, 2018.
15. Staffell, I., Scamman, D., Abad, A. V., Balcombe, P., Dodds, P. E., Ekins, P., ... & Ward, K. R. (2019). The role of hydrogen and fuel cells in the global energy system. *Energy & Environmental Science*, 12(2), 463-491.
16. Sepulveda, N. A., Jenkins, J. D., de Sisternes, F. J., & Lester, R. K. (2018). The role of firm low-carbon electricity resources in deep decarbonization of power generation. *Joule*, 2(11), 2403-2420.
17. Gielen, D., Boshell, F., Saygin, D., Bazilian, M. D., Wagner, N., & Gorini, R. (2019). The role of renewable energy in the global energy transformation. *Energy Strategy Reviews*, 24, 38-50
18. Sharvini, S. R., Noor, Z. Z., Chong, C. S., Stringer, L. C., & Yusuf, R. O. (2018). Energy consumption trends and their linkages with renewable energy policies in East and South-east Asian countries: Challenges and opportunities. *Sustainable Environment Research*, 28(6), 257-266.
19. Ritchie, H., & Roser, M. (2017). Fossil fuels. *Our World in Data*.

20. Ntanos, S., Skordoulis, M., Kyriakopoulos, G., Arabatzis, G., Chalikias, M., Galatsidas, S., ... & Katsarou, A. (2018). Renewable energy and economic growth: Evidence from European countries. *Sustainability*, 10(8), 2626.
21. Liu, W. (2016). Is renewable energy effective in promoting local economic development? The case of China. *Journal of Renewable and Sustainable Energy*, 8(2), 025903.
22. Energy, W. (2014). The Socio-economic Benefits of Solar and Wind Energy.

The Evolution of Feed in Tariff Mechanism Towards Feed in Premium Mechanism

Mustafa Anıl Akkaya¹, Murat Onuk²

¹EPIAŞ

²Business Administration Department, Faculty of Economics and Administrative Sciences/Yeditepe University

Kayışdağı Cd. No:326A, 34755 Ataşehir/İstanbul

manil.akkaya@epias.com.tr
murat.onuk@yeditepe.edu.tr

Abstract. In this study, two important policies used by governments for the deployment of renewable energy will be compared. These policies are feed in tariff guarantee and feed in premium. YEKDEM, a policy based on feed in tariff is implemented in Turkey. In Europe, the feed in premium mechanism has taken over the feed in tariff mechanism recently. In this context, the development, advantages, disadvantages of these two policies will be discussed and explained what should be done by giving examples from Europe to implement a feed in premium based system instead of YEKDEM, which still remains unclear how it will continue after 2020

Keywords: Feed-in-tariff, feed-in-premium, renewable energy, strategies for financing renewable energy.

1 Introduction

Renewable energy has increased in the world in 2000s due to the international treaties such as the Paris Agreement and the Kyoto Protocol, and the countries' desire to get rid of dependence on fossil fuel resources. The policies developed by states on this issue undoubtedly have taken an important place for this deployment. The most important of these policies is the feed in tariff mechanism and this mechanism has been used in more than 50 countries. The mechanism of supporting renewable energy resources in Turkey (YEKDEM) is a kind of this policy. In recent years, payments made to renewable energy plants through the feed in tariff mechanism have started to be reduced in most countries where this policy is preferred. In fact, due to the wholesale electricity price distorting effect of the feed in tariff in Europe, this policy has

gradually begun to be replaced by the feed in premium [1]. Therefore, the practices in Europe will be explained the rest of the paper. Some recommendations will be given inspired of implementations in Europe, using some empirical data that relevant to current policy YEKDEM for Turkey

2 Comparison of Feed in Tariff and Feed in Premium

Feed in tariff is an energy supply policy that focuses on supporting the development of new renewable energy projects by offering long-term purchasing agreements for renewable energy sales [2,3,4]. The feed in premium policy is a mechanism where electricity generated from renewable energy sources is sold from the spot electricity markets and renewable energy producers receive premiums at the spot electricity price. [4,5].

Technology, installed power, quality of the source or the location of the project are taken consideration determining incentive price in feed in tariff mechanism. In addition to the payment made with the feed in tariff, a bonus payment can made for the restrengthening of the power plants or the development of innovative technologies [4]. In addition, there are ancillary design elements such as predetermined tariff discounts, sensitive tariff discounts, tariff discounts according to inflation, high tariff payment at high electricity demand hours [4,6,7].

In determining the incentive price with feed in premium, there are payment designs according to fixed price or floating price. In fixed price design, payment is made according to the determination of a fixed floor and cap depending on the spot electricity markets [5]. Sliding premium guarantee payment can be designed in four different ways [4]. The first design is to set cap and floor in the total premium amount. In other words, when the spot electricity prices fall below the determined floor price, the premium amount to be paid increases; no premium payment is made when the spot electricity price exceeds the cap price to be determined [4]. Putting floor and cap on the total payment amount which is the second design is a way of ensuring that the revenues under the premium price option remain within a sufficient range to encourage investors while securing the hedging benefit of renewable energy sources as electricity prices increase [4]. The third designed is spot market gap model. In this design, the difference between the average price in the spot electricity market and the minimum payment guarantee level is paid. If the spot electricity market average is below the minimum payment guarantee, no premium will be paid in any way [4]. The fourth design is the premium guarantee prices being determined as a percentage of spot electricity prices. This means that premium guarantee payments can suddenly rise and fall in response to market price trends [8]

3 The Evolution of Feed in Tariff Mechanism Towards Feed in Premium Mechanism in EU Countries

The commission working document on renewable energy support mechanisms published as of 2013 November includes first time in EU level that emphasizes that the feed in tariff should be replaced with the feed in premium [1]. Accordingly, countries implemented feed in tariff policy such as Germany, France, England, Austria, Belgium, Czechia, Hungary, Ireland, Luxembourg and Greece reduce the fixed tariff guarantee with formulas that are dependent on variables such as source type and inflation [10,11]. Feed in premium implementations are detailed below.

3.1 Implementation of Feed in Premium in EU Countries

The main support mechanism has been feed in premium in France with 2015/932 numbered law the enacted in August 2015. Due to the nature of this mechanism, a bonus payment is made to renewable power plants that cost more than the prices in the electricity market. In the mechanism in France, premium tariffs are determined either by direct guaranteed contracts or by the tender process [11]. Onshore wind power plants with an installed capacity not exceeding 3 MW, offshore wind power plants with an installed power not exceeding 6 MW, hydroelectric power plants with an installed power not exceeding 1 MW, biomass power plants that only use domestic waste, biogas power plants that installed power of 500 KW and 12 MW that used methanization of urban or industrial sewage, biogas power plants that installed power of 500 KW and 12 MW that provides fuel from harmless garbage tanks benefited from direct guaranteed contracts. In addition to these, geothermal wells shall be located in the same geothermal site for geothermal power plants benefited from direct guaranteed contracts. However project developers of geothermal power plants have to apply for supporting mechanism before starting the installation if they benefited from direct guaranteed contracts [10]. In the payment design, depending on the type of power plant source and the technology used, the management premium is added to the difference between the reference tariff defined by the French regulator every year and the price of electricity in the wholesale market.

Reference tariffs can be reduced by 30% to 60% with a formula based on annual inflation [10]. The feed in premium policy can be implemented both within the tenders and on a direct market basis in Germany. Tenders are only valid for projects of a certain size. Unlike in France, the reference tariff is calculated monthly, not annually in Germany. Monthly generation values of renewable power plants are used in determining the reference tariff. Reference tariffs range from 8.91-12.70 Eurocent / kWh for solar energy, 4.66-8.38 Eurocent / kWh for onshore wind power plants, 1.4-3.9 Eurocent / kWh for offshore wind power plants, 25-25.2 Eurocent / kWh for geothermal power plants, 3.47-12.40 Eurocent / kWh for hydroelectric power plants and 5.71-13.22 Eurocent / kWh for biomass power plants. Reference tariff levels can be changed through laws or reduced based on newly established capacities in the relevant resource type [10]. Renewable energy support mechanisms are managed by the Electricity Services Directorate (Gestore dei Servizi Energetici, GSE) in Italy. Elec-

tricity generated from renewable energy resources will be sold to the markets or to the Electrical Services Directorate. Thus, the Directorate of Electric Services will act as a mediator between the producer and the market. Producers can decide whether they want a guaranteed minimum price or a market price. In case the market price is higher than the guaranteed minimum price, the producers will receive annual payments. This mechanism is the feed in premium system in Italy (ritiro dedicato). Solar power plants with an installed power of up to 100 kW, hydroelectric power plants with an installed power of up to 500 kW, and those with an installed power of up to 1 MW for all remaining renewable plants benefit from this mechanism [10]. Denmark is one of the EU countries that promote renewable energy generation through feed in premium. Renewable power plants receive a sliding bonus above the market price. There are two types of premium guarantee incentives. One of the both is maximum bonus payments and when maximum bonus paid, the sum of the given bonus and market price will not exceed a legal maximum value determined depending on the connection date of a particular facility and the energy source used. The second type of premium guarantee is the guaranteed bonus. In some cases, renewable power plants are given a guaranteed bonus at the market price. Incentives given in such cases are not defined by law. For example, the guaranteed bonus for onshore wind farms is 0.25 DKK / kWh, the maximum bonus is 0.58 DKK / kWh. If the onshore wind farm belongs to a supplier company, the maximum bonus is 0.33 DKK / kWh [11] Apart from these countries, other countries where premium tariff levels are determined by a regulator from European Union countries are Belgium, Bulgaria, Czechia, Greece, Hungary, Luxembourg [12].

4 Empirical Indicators Relevant with Yekdem Implemented in Turkey

4.1 YEKDEM and Market Clearing Price

The Law Amending the Law on the Use of Renewable Energy Resources for Electricity Generation was enacted and published in the Official Gazette No. 27809 dated 8/01/2011. This law is known as the Renewable Energy Law No. 6094. Feed in tariff system, which is still used today, and a mechanism with bonus payments for power plants with domestic components, has been established with this law. Hydroelectric power plants, whose reservoir area of less than 15 km², wind power plants solar power plants biomass power plants and geothermal power plants will be utilized tariff guaranteed payments, in case these power plants put into service between 18.05.2005 and 31.12.2015. Later, this mechanism was extended for renewable power plants that were put into operation between 2016 and 2020 by amending the relevant article of the law. Fixed tariff guarantee prices applied since the enactment of Law No. 6094 are \$ 13.3 / MWh for solar and biomass, \$ 10.5 / MWh for geothermal, and \$ 7.3 / MWh for hydroelectricity and wind [13]. When the feed in tariff mechanism is implemented through this law, it is based on payment basis according to the metering data of the

renewable power plant until May 1, 2016. Later, this payment design was associated with market clearing price and renewable power plants were designed to repay this overpayment if it received a payment above the market clearing price [14]. This situation can be considered as the first step to premium guarantees in Turkey and is the first attempt to prevent distortion in the markets. However, when the 32,160 hours between May 1, 2016 and December 31, 2019 were analyzed, it was observed that market clearing price was below the lowest incentive price that is \$ 7.3 / MWh in 31.866 hours. This change is meaningless due to market design. Because these power plants sell the electricity they generate to the spot markets and receive advance payments. Therefore, there is an incentive restriction only when market clearing price is above the incentive price. These hours are quite low as indicated in the graph below.

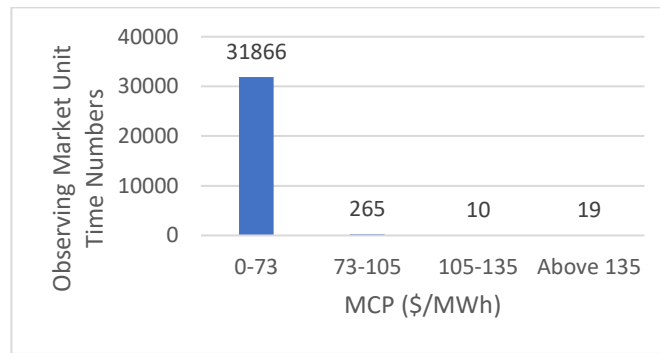


Figure 1: Comparison of Market Clearing Price and Incentive Price [15]

4.2 YEKDEM and Market Situation

In order to discover the effect of YEKDEM on the market, the behavior of YEKDEM participants was observed in the day ahead market operated by EPIAŞ and where the reference price of electricity determined. In these observations covering the first 12 months of 2019, hourly average 9,823 MWh price independent offer was supplied. Price-independent sales offer is preferred that by market participants who do not want to reflect their marginal cost to the electricity market and want to trade with market clearing price. It is estimated that the plants benefiting from YEKDEM act in this way. The final daily production plan reported to TEİAŞ as a result of the transaction made by the YEKDEM power plants in the day ahead market for the first 12 months of 2019 through the EPIAŞ transparency platform was filtered by source type to support this idea. The results support our prediction. The hourly average value final daily production plan of the power plants benefiting from YEKDEM in these 12 months is 7.429 MWh.

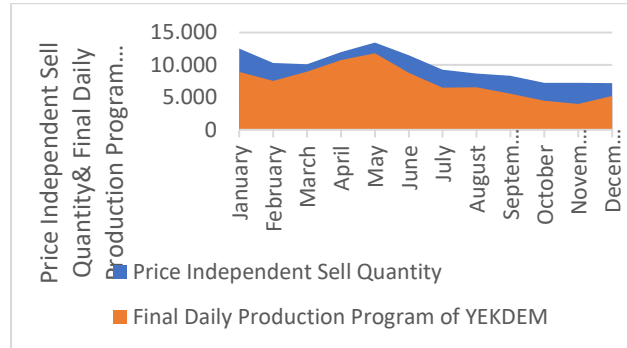


Figure 2: Price Independent Sell Quantity & Final Daily Production Program of YEKDEM [15]

5 Conclusion

Credit debt situation resources type, importance of power plant's location etc. are taken consideration and created a scale according to these variables. After determination of this scheme fixed guarantee payments should be reduced gradually to rules that determined with this scheme. These schemes can be valid situation for power plants benefiting from YEKDEM. Apart from this premium guarantee scheme mechanism should be established in which variables such as resource type, technology, inflation, electricity demand, and project location are taken into account for new investments.

References

1. European Commission. (2013). *European Commission guidance for the design of renewables support schemes*. 1–29. Retrieved from http://ec.europa.eu/energy/sites/ener/files/com_2013_public_intervention_swd04_en.pdf
2. Mendonça, M. (2007). *Feed-in Tariffs: Accelerating the Deployment of Renewable Energy*. London: EarthScan.
3. Lipp, J. (2007). Lessons for effective renewable electricity policy from Denmark, Germany and the United Kingdom. *Energy Policy*, 35(11), 5481–5495. <https://doi.org/10.1016/j.enpol.2007.05.015>
4. Couture, T. D., Cory, K., & Williams, E. (2010). *A Policymaker's Guide to Feed-in Tariff Policy Design*. Office, (July). Retrieved from <http://www.nrel.gov/docs/fy10osti/44849.pdf>
5. Energypedia (t.y) Access Adress: [https://energypedia.info/wiki/Feed-in_Premiums_\(FIP\)](https://energypedia.info/wiki/Feed-in_Premiums_(FIP))
6. Couture, T., & Gagnon, Y. (2010). An analysis of feed-in tariff remuneration models: Implications for renewable energy investment. *Energy Policy*, 38(2), 955–965. <https://doi.org/10.1016/j.enpol.2009.10.047>
7. Klein, A., Merkel, E., Pfluger, B., Held, A., Ragwitz, M., Resch, G. (2010). *Evaluation of different feed-in tariff design options*, Ministry for the Environment, Nature Conservation and Nuclear Safety. (October).
8. del Río González, P. (2008). Ten years of renewable electricity policies in Spain: An analysis of successive feed-in tariff reforms. *Energy Policy*, 36(8), 2917–2929. <https://doi.org/10.1016/j.enpol.2008.03.025>
9. EEG. (2017). *Renewable energy sources act*. (July). Retrieved from <http://www.iwr.de/re/iwr/info0005e.html>
10. Res Legal (n.d). Access Adress: <http://www.res-legal.eu>
11. Banja, M., Jégard, M, Monforti-Ferrario F., D. J.-F., & Taylor N., Motola V., S. R. (2017). *Renewables in the EU: an overview of support schemes and measures*. <https://doi.org/10.2760/69943>
12. Council of European Energy Regulators. (2018). *Status Review of Renewable Support Schemes in Europe for 2016 and 2017 | Public report*. (December), 126. Retrieved from <http://eur-lex.europa.eu/legal->
13. Yenilenebilir Enerji Kaynaklarının Elektrik Enerjisi Üretimi Amaçlı Kullanımına İlişkin Kanunda Değişiklik Yapılmasına Dair Kanun. (2010, December 29).Resmi Gazete. (Sayı:27809). Access Adress: <https://www.resmigazete.gov.tr/eskiler/2011/01/20110108-3.htm>
14. Yenilenebilir Enerji Kaynaklarının Belgelendirilmesi ve Değerlendirilmesine İlişkin Yönetmelikte Değişiklik Yapılmasına İlişkin Yönetmelik. (2016,29 April). Resmi Gazete. Sayı (29698). Access Adress: <https://www.resmigazete.gov.tr/eskiler/2016/04/20160429-8.htm>
15. EPIAŞ. (n.d). Access Adress: <https://seffaflik.epias.com.tr/transparency/uretim/planlama/kgup.xhtml>

The Effect of Molasses Concentration on Voltage Generation

Tuba Artan Onat

Niğde Ömer Halisdemir University, Faculty of Science and Arts, Department of Biotechnology, Niğde

tubaartan@ohu.edu.tr tubaartanonat@gmail.com

Abstract. Two-chambered MFC was used for experiments and the connection between anode and cathode compartments was made by a salt bridge. The electrodes were made of carbon rods. The anode chamber was filled with molasses medium and the cathode chamber was contained 50 mM $K_4[Fe(CN)_6]$. The molasses was added at 50 mL/L, 100 mL/L, 150 mL/L and 300 mL/L concentrations. The inoculum was taken from Akkaya Lake, which was the main drainage dam for domestic wastewater in Niğde. The MFC was operated in fed-batch mode at 25°C and 100 rpm and the system was monitored with a Fluke 8846A multimeter at 20 minutes interval. The COD removal of molasses medium determined as Δ COD. The columbic efficiency calculated by current and COD removal values. The results were showed the voltage generation of microbial consortia in MFC from 400 hours to 592 hours. The voltage generation is similar for 50 and 100 mL/L and 150 and 300 mL/L molasses concentrations. On the other hand, the COD removal efficiency values were different and that was affected by the bioelectricity production of MFC. The most effective molasses concentration was determined as 50 mL/L due to columbic efficiency and COD removal values.

Keywords: Biomass, Microbial fuel cells, Molasses, Voltage generation

1. Introduction

The global population increased in steady and consistent values that resulted in drastically rising fossil fuel usage also, wastewater augmentation and pollution. The recognition of renewable energy caused by increased public requirements and unbalanced usage of energy. The main issue in today's world is the replacement of fossil fuels with renewable energy sources. The interest of fuel cells technology as a new source of renewable energy rises in nowadays [1-6].

Microorganisms enzymes should use for energy production from different substrates in biological fuel cells. Microbial Fuel Cells (MFCs) is one of the major categories of the biological fuel cell. In MFCs, microorganisms convert the chemical energy, which found in the organic matter in wastewater, to the direct electricity.

Thereby, high-organic wastewater treatment and simultaneous electricity generation should be made by MFC technologies and different substrates eg. food processing wastes would be useful as organic source [4, 7-11].

Industrial wastewaters are significant pollution issues due to the high Chemical Oxygen Demand (COD) and nitrogen values, which have detrimental effects on the ecosystem. The MFC reactors could be used for COD removal as 99% in primary sludge in 1-5 days' anaerobic incubation period. The manufacture of food process (starch, sugar, dairy or brewery) products involves a large amount of water usage, consequently resulting in large quantities of wastewater and different wastes. These wastewaters should be used as substrates for electricity generation in MFCs [3, 12-17]. Molasses, which has high COD values, low pH, strong odor and the dark brown color, is one of the most pollutants in sugar processing industries [1, 4, 18-23].

This study is about the effect of molasses concentration on voltage generation, current and power density values that were determined as a function of microbial community growth at 30 days incubation period.

2. Material and Method

2.1. MFC Setup

Two-chambered MFC made from glass cylinder and total volume of MFC is 0.75 L. The volumes of anode and cathode compartments are 300 mL. The anode and cathode compartments connected with the salt bridge was prepared with straight glass cylinder which has 150 mL volume and filled with 5% agar-agar and 1 M KCl solution used due to inexpensive option [24]. The electrodes were made of carbon rods 0.8 cm in diameter and 10 cm long. The surface area of the electrodes was 7.1296 cm². In order to fill the anode chamber with molasses medium sparged with nitrogen for 30 minutes. Experimental MFCs use chemical oxidizers because of this the catholyte solution prepared with 50 mM [K₃Fe(CN)₆] and aerated [2, 3, 16].

2.2. Inoculum and Medium

The medium and catholyte solution prepared with 50 mM phosphate buffer solution (PBS) was prepared with 2.452 gr/L NaH₂PO₄ and 4.576 gr/L Na₂HPO₄ and 0.13 gr/L KCl added for conductivity. The molasses medium used for bacterial growth at anode chamber was prepared with PBS and 1.0 gr/L (NH₄)₂SO₄ and 0.5 gr/L KH₂PO₄ added to the medium. Molasses added at 50 mL/L, 100 mL/L, 150 mL/L, and 300 mL/L concentrations as a carbon source to medium. The pH value of medium settled to 7.0 with 0.1 M H₂SO₄ and 0.1 M NaOH [25-27]. The anode chamber fed with molasses media at 48 hours period for support to bacterial growth in the incubation period and the experiments conducted at 25°C in a temperature-controlled shaker. The inoculum was taken from Akkaya Dam, which was the main drainage dam for domestic wastewater in Niğde. The collected samples were stored at 4°C before COD and

optical density (OD) analyses. COD values determined with standard COD measurement method [14, 23] and the OD values were determined with at 600 nm [20].

2.3. Data acquisition and measurements

The MFC was operated in fed-batch mode at 25°C and 100 rpm in a temperature and shaker controlled-incubator and the system was monitored with a Fluke 8846A multimeter at 20 minutes interval. The circuit completed with a 10 Ω resistor, which applied by multimeter to determine the power generation as a function of load. Current (I) was calculated according to Ohm's law with resistance (R) from the voltage (V) and normalized by the surface area of the anode. Besides, Power (P) was calculated with $P=IV$ formula and normalized with total MFC volume. The coulombic efficiency calculated by integrating the measured current to relative to the theoretical current based on the consumed molasses and normalized with volume [15, 24].

The COD removal of molasses medium determined as ΔCOD ($C_o\text{COD} - \text{CCOD}$). Removal rate of COD was determined the given formula(1) [25]:

$$\text{Removal of COD \%} = [(C_o\text{COD} - \text{CCOD})/C_o\text{COD}] * 100 \quad (1)$$

The coulombic efficiency calculated with given formula (2):

$$CE = \frac{M \int_0^t I dt}{n v F \Delta\text{COD}} \quad (2)$$

Where M is the molecular weight of oxygen, I is the current, F is the faraday's constant, n=4 is the number of electrons exchanged per mole of oxygen and v is the anolyte volume [15, 23, 26].

3. Results and Discussion

The concentration and biodegradability of the organic matter and temperature of wastewater and the absence of toxic chemicals will be affected by the success of MFC applications directly[26]. H-shape systems are used to determination of basic parameters of MFCs and in this work, used that system. The amount of molasses in the anode chamber fed with the 48 hours intermittent period while maintaining a certain level of microbial growth is regularly and consistently for high output voltage level. The MFC was incubated for 30 days at 25 °C to monitor microbial growth and voltage generation. The voltage values of the MFC were recorded at 20 minutes intervals during the whole incubation period.

3.1. The effect of molasses concentration on voltage generation

The produced voltage values of MFC were equilibrated at 20 days of incubation period and this situation is coherent with literature (Catal et. al., 2008; Haddadi et. al., 2014; Taşkan, 2016). Fig. 1 was showed the voltage generation of microbial consortia

in MFC at 50, 100, 150 and 300 mL/L molasses concentrations from 400 hours (approximately 20 days of incubation) to 592 hours (approximately 30 days of incubation). It is clear from the graph the voltage generation at 50 and 100 mL molasses concentrations were higher than 150 and 300 mL molasses concentrations. The voltage values were recorded at the beginning and at the end of feeding cycles in 20-30 days incubation period was shown in Table 1. The voltage generation of anodic compartments were 0.380 V, 0.380 V, 0.260 V and 0.280 V for 50, 100, 150 and 300 mL/L molasses concentration sequentially.

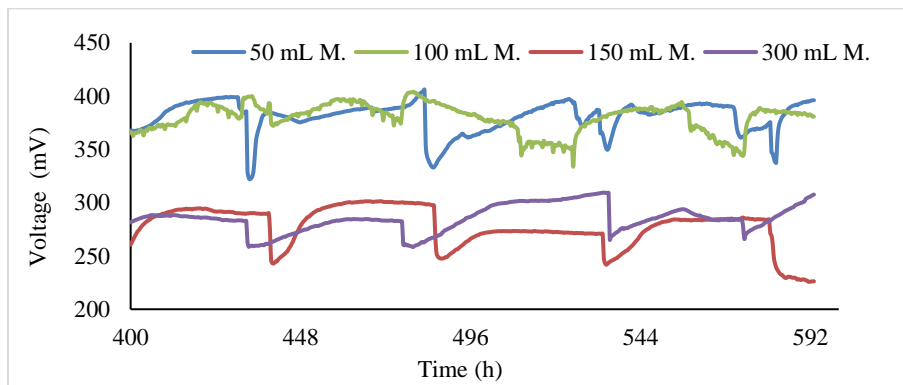


Fig. 1. The voltage generation of MFC with different molasses concentrations at 20-30 days of incubation period.

Table 1. The voltage values of MFC with different concentrations of molasses concentration at feeding cycles at 20-30 days incubation period.

Molasses Conc.	1. cycle		2. cycle		3. cycle		4. cycle		5. cycle	
	After Feeding (V)	Before Feeding (V)	After Feeding (V)	Before Feeding (V)	After Feeding (V)	Before Feeding (V)	After Feeding (V)	Before Feeding (V)	After Feeding (V)	Before Feeding (V)
50 mL	0.367 8	0.382 5	0.383 8	0.395 6	0.396 4	0.397 3	0.397 0	0.385 4	0.375 2	0.39 61
100 mL	0.366 1	0.380 6	0.380 4	0.374 3	0.384 4	0.333 7	0.351 5	0.344 0	0.348 1	0.38 08
150 mL	0.260 7	0.289 5	0.289 7	0.297 6	0.297 4	0.243 7	0.244 5	0.284 1	0.284 2	0.22 62
300 mL	0.281 6	0.282 8	0.263 1	0.282 1	0.260 7	0.309 1	0.265 3	0.283 8	0.277 3	0.30 76

3.2. Current and Power Densities of MFC

The current, power, current density (I_{dens} , mA/cm²) and power density (P_{dens} , mW/cm³) were calculated with the given formulas at the data acquisition section above and the results were given in Table 2 and Fig. 2 a-b. The calculated I_{dens} and P_{dens} values were determined at approximately constant values that were the maximum values of current and power density at feeding cycles. The current densities were determined as 3.1×10^{-3} mA/cm² for 50 mL/L and 100 mL/L concentrations, 2.3×10^{-3} mA/cm² for 150 and 300 mL/L molasses concentrations sequentially at feeding periods of incubation. The power densities were calculated as 22 mW/cm³ for 50 and 100 mL/L, and 12 mW/cm³ for 150 and 300 mL/L molasses concentration at feeding periods of incubation.

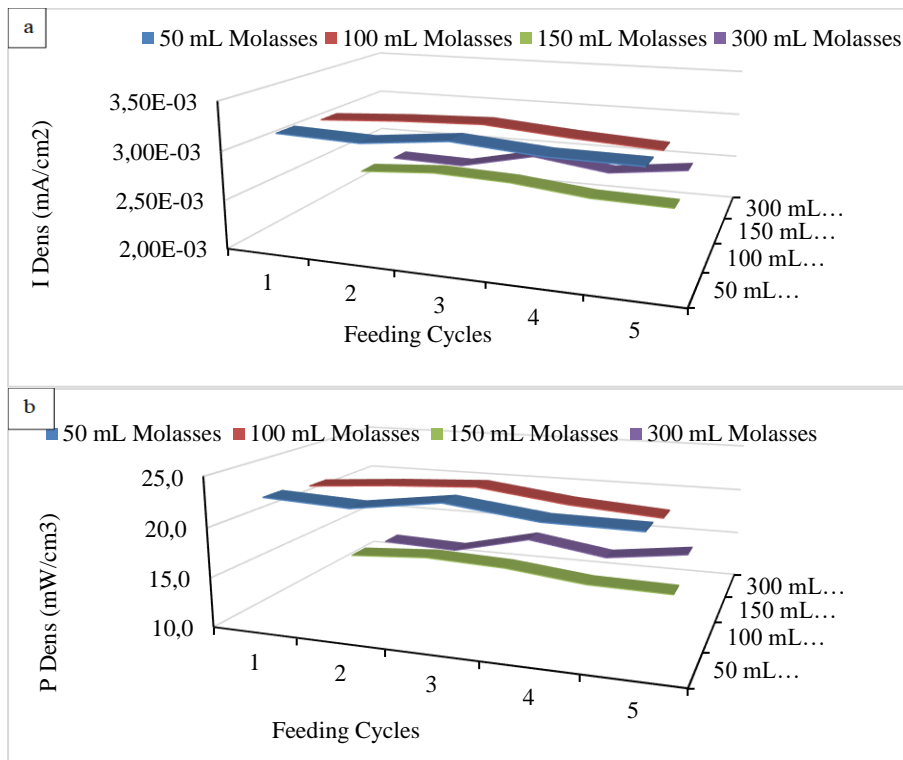


Fig. 2. a) The current density of MFC at feeding cycles of 20-30 days incubation period b) The power density of MFC at feeding cycles of 20-30 days incubation period

Table 2. The current density and power density values of different molasses concentrations at feeding cycles of 20-30 days incubation period

Molasses Conc.	1. cycle		2. cycle		3. cycle		4. cycle		5. cycle	
	<i>I_{dens}</i>	<i>P_{dens}</i>	<i>I_{dens}</i>	<i>P_{dens}</i>	<i>I_{dens}</i>	<i>P_{dens}</i>	<i>I_{dens}</i>	<i>P_{dens}</i>	<i>I_{dens}</i>	<i>P_{dens}</i>
50 mL	3.16E-03	22.766	3.13E-03	22.357	3.22E-03	23.554	3.15E-03	22.510	3.14E-03	22.414
100 mL	3.12E-03	22.201	3.17E-03	22.846	3.20E-03	23.311	3.13E-03	22.230	3.08E-03	21.613
150 mL	2.33E-03	12.398	2.39E-03	12.969	2.36E-03	12.635	2.27E-03	11.685	2.25E-03	11.539
300 mL	2.28E-03	11.874	2.26E-03	11.571	2.45E-03	13.675	2.33E-03	12.340	2.44E-03	13.517

3.3. The coulombic efficiency of MFC

Initial COD values were determined as 10.81, 13.84, 31.15, 50.59 g/L respectively, for increasing molasses (50, 100, 150, 300 mL/L) concentrations. In the fed-batch MFC system, COD removal was detected merely at 50 mL/L molasses concentration, therefore coulombic activity was calculated at this concentration. The COD change (ΔCOD) and the coulombic activity calculated from COD change (ΔCOD) are shown in Fig. 3 at five feeding cycles at 20-30 days incubation period for used MFC system in this work.

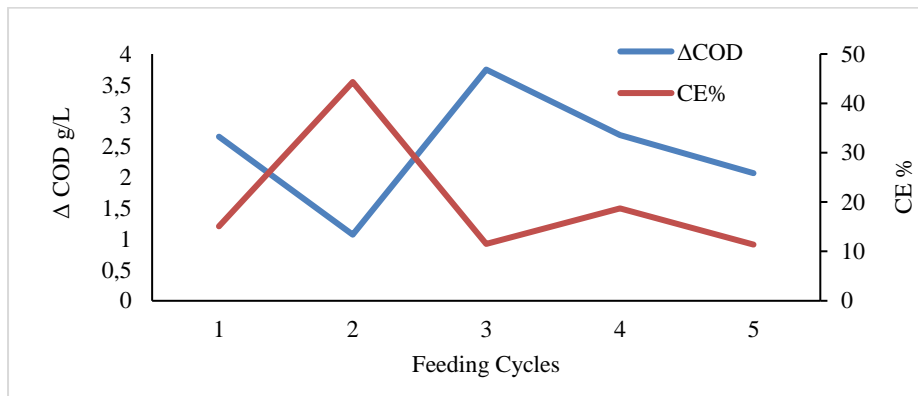


Fig. 3. The ΔCOD and CE% graph of MFC with 50 mL/L molasses concentration at 20-30 days incubation period.

In the 20-30 day incubation period, ΔCOD values were determined as 2.66, 1.07, 3.75, 2.69 and 2.07 g/L, at the feeding intervals respectively. The coulombic activity values calculated with the formula given above; were calculated as 15.12%, 44.33%, 11.51%, 18.74%, and 11.39%, sequentially. According to this, it was determined that the CE% increased with the decrease of ΔCOD and the increase of ΔCOD decreased the CE%. Therefore, there was an inverse relationship between ΔCOD and CE% values.

The two-chambered MFC was run with four different molasses concentrations and it was clear from the results the higher molasses concentrations were reduced the voltage generation and coulombic efficiency. The molasses concentrations were increased due to the addition of the molasses with fresh medium and the microbial culture could not reduce the molasses concentrations and COD values at higher levels. The COD values of molasses was reduced only at 50 mL concentration (Fig. 4).

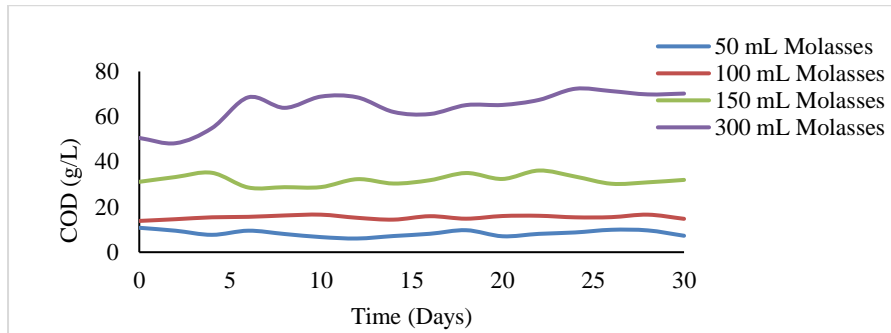


Fig. 4. The COD values of four different molasses concentrations at 30-day incubation period in two-chambered MFC.

The optical density of microbial biomass was determined as a function of 30-days incubation period at four different molasses concentration. The optical density was balanced as 1.00 absorbance approximately at 15 days of incubation period in different concentrations of molasses (Fig. 5). After 15 days incubation period the microbial community balanced and the voltage generation and current density and power density came up to similar ratio for different molasses concentrations.

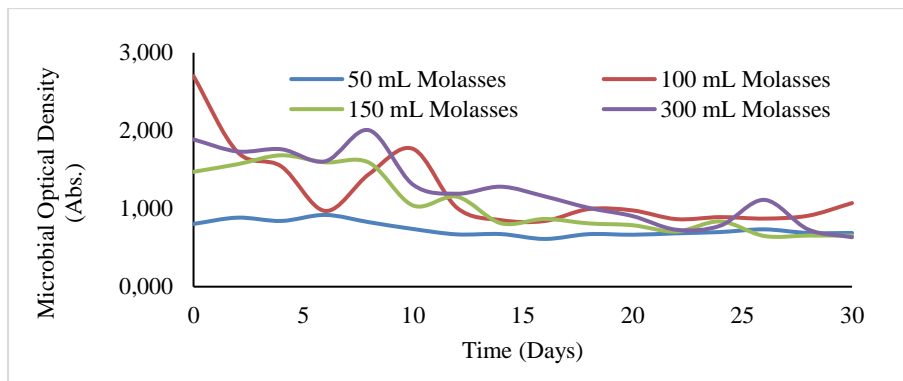


Fig. 5. The microbial density at MFC at different molasses concentrations at 30-days incubation period.

4. Conclusion

The voltage in microbial fuel cells is formed by transferring the electrons released by the microorganism in the biochemical reactions of the organic matter to the cathode through a circuit over the anode electrode. It is compatible with the literature that adaptation to the microbial community at the anode chamber of MFC in the incubation period. The COD value of the medium is one of the important factors affecting voltage production, current, and power density. It has been determined that the in-

crease in chemical oxygen demand also increases electricity production. On the other hand, the increased molasses concentration reduces the effect of the microbial community due to the high COD value. Considering the voltage generation, current, and power density, and columbic efficiency values of the microbial community collected from sediment of the Akkaya Dam is considered that 50 mL / L molasses concentration can be used in electricity production.

Acknowledgements

The author would like to acknowledge to the Niğde Ömer Halisdemir University BAGEP (FEB 2015/27) for financial support.

References

1. Daniel D. K., Mankidy B. D., Ambarish K., Manogari R.: Construction and operation of a microbial fuel cell for electricity generation from wastewater. *International Journal of Hydrogen Energy*, 34, 7555 – 7560 (2009).
2. Samrot, A. V., Senthilkumar, P., Pavankumar, K., Akilandeswari, G.C., Rajalakshmi, N., Dhathathreyan, K.S.: Electricity generation by *Enterobacter cloacae* SU-1 in mediatorless microbial fuel cell. *International Journal of Hydrogen Energy* 35, 7723-7729 (2010).
3. Herrero-Hernandez, E., Smith, T.J., Akid, R.: Electricity generation from wastewaters with starch as carbon source using a mediatorless microbial fuel cell. *Biosensors and Bioelectronics*, 39, 194–198 (2013).
4. Sawasdee V., Pisutpaisal N.: Simultaneous pollution treatment and electricity generation of tannery wastewater in air-cathode single chamber MFC. *International Journal of Hydrogen Energy* Volume 41, Issue 35, 21, Pages 15632-15637 (2016).
5. Xia C., Zhang D., Pedrycz W., Zhu Y., Guo Y.: Models for Microbial Fuel Cells: A critical review. *Journal of Power Sources* 373, 119–131 (2018).
6. Fernández-Marchante C. M., Asensio Y., León L. F., Villaseñor J., Cañizares P., Lobato J., Rodrigo M. A.: Thermally-treated algal suspensions as fuel for microbial fuel cells, *Journal of Electroanalytical Chemistry* 814, 77–82 (2018).
7. Rabaey, K., Clauwaert, P., Aelterman, P. and Verstraete, W.: Tubular microbial fuel cells for efficient electricity generation. *Environmental Science & Technology* 39(20), 8077-8082 (2005).
8. Larrosa-Guerrero A., Scott K., Head I.M., Mateo F., Ginesta A., Godinez C.: Effect of temperature on the performance of microbial fuel cells. *Fuel* 89, 3985–3994 (2010).
9. Afsham N., Roshandel R., Yaghmaei S., Vajihinejad V., Sherafatmand M.: Bioelectricity Generation in a Soil Microbial Fuel Cell with Biocathode Denitrification. *Energy Sources, Part A: Recovery, Utilization, and Environmental Effects* 37:19, 2092-2098 (2015).
10. Fangzhou, D., Beizhen, X., Wenbo, D., Boyang, J., Kun, D., Hong, L.: Continuous flowing membraneless microbial fuel cells with separated electrode chambers, *Bioresource Technology* 102, 8914–8920, (2011)
11. He W., Zhang X., Liu J., Zhu X., Feng Y., Logan B. E.: Microbial fuel cells with an integrated spacer and separate anode and cathode modules, *Environ. Sci.: Water Res. Technol.*, 2, 186 (2016).

12. Rodrigo M. A., Canizares P., Lobato J., Paz R., Sáez C., Linares, J. J.: Production of electricity from the treatment of urban waste water using a microbial fuel cell, *Journal of Power Sources* 169(1), 198-204, (2007).
13. Çatal, T., Li, K., Bermek, H., Liu, H.: Electricity production from twelve monosaccharides using microbial fuel cells, *Journal of Power Sources*, 175, 196–200, (2008).
14. Huang L., Zeng R. J., Angelidaki I.: Electricity production from xylose using a mediator-less microbial fuel cell, *Bioresource Technology* 99, 4178–4184, (2008).
15. Lu, N., Zhou, S., Zhuang, L., Zhang, J., Ni. J.: Electricity generation from starch processing wastewater using microbial fuel cell technology, *Biochemical Engineering Journal* 43, 246–251, (2009).
16. Futamata H., Bretschger O., Cheung A., Kan J., Owen R., Neelson K.H.: Adaptation of soil microbes during establishment of microbial fuel cell consortium fed with lactate *Journal of Bioscience and Bioengineering* Vol. 115 No. 1, 58-63, (2013).
17. Mansoorian, H. J., Mahvi, A. H., Jafari, A. J., Amin, M. M., Rajabizadeh, A. and Khanjani, N.: Bioelectricity generation using two chamber microbial fuel cell treating wastewater from food processing, *Enzyme and Microbial Technology* 52(6), 352-357, (2013).
18. Sirianuntapiboon S., Phothilangka P., Ohnomo S.: Decolorization of molasses wastewater by a strain No.BP103 of acetogenic bacteria, *Bioresource Technology*, 92, 31 – 39, (2004).
19. Tondee, T., Sirianuntapiboon, S. and Ohmomo, S.: Decolorization of molasses wastewater by yeast strain, *Issatchenkia orientalis* No. SF9-246, *Bioresource Technology* 99(13), 5511-5519, (2008).
20. Wang ., Li B., Zeng Q., Liu H.: Antioxidant and free radical scavenging activities of pigments extracted from molasses alcohol wastewater, *Food Chemistry*, 107, 1198-1204, (2008).
21. Deval, A. and Dikshit, A. K.: Construction, working and standardization of microbial fuel cell, *APCBEE Procedia* 5, 59-63, (2013).
22. Satyawali Y., Balakrishnan M.: Wastewater treatment in molasses-based alcohol distilleries for COD and color removal: A review, *Journal of Environmental Management*, 86, 481-497, (2008).
23. Zhang X., He W., Ren L., Stager J., Evans P. J., Logan B. E.: COD removal characteristics in air-cathode microbial fuel cells *Bioresource Technology*, 176, 23–31, (2015).
24. Min Li X., Cheng K. Y., Selvam A., Wong J. W.C.: Bioelectricity production from acidic food waste leachate using microbial fuel cells: Effect of microbial inocula, *Process Biochemistry*, 48, 283–288, (2013).
25. Dönmez G.: Bioaccumulation of the reactive textile dyes by *Candida tropicalis* growing in molasses medium, *Enzyme and Microbiol. Technology*, 30, 363 – 366, (2001).
26. Logan B. E., Hamelers B., Rozendal R., Schroder U., Keller J., Fregua S., Aelterman P., Verstraete W., Rabaey K.: *Microbial Fuel Cells: Methodology and Technology*, *Environmental Science & Technology*, Vol. 40, no. 17, 5181 – 5192, (2006).
27. Mohan, S. V., Saravanan, R., Raghavulu, S. V., Mohanakrishna, G. and Sarma, P. N.: Bioelectricity production from wastewater treatment in dual chambered microbial fuel cell (MFC) using selectively enriched mixed microflora: effect of catholyte, *Bioresource Technology* 99(3), 596-603, (2008).

The Wind Farm Design Optimizing for Pendik Sabiha Gokcen Region

Ali Şahin¹, Tanay Sıdkı Uyar¹

¹ Mechanical Engineering Department/ Marmara University
Kadıköy-Istanbul, 34722, Turkey

n.sahinali@gmail.com tanayuyar@marmara.edu.tr

Abstract. With the increasing population growth, our atmosphere and environment have been damaged by fossil fuels for many years, and may reduce these damages and reduce losses to zero with the idea of 100% renewable energy. For this reason, the demand for renewable energy has increased recently and the studies are increasing. Wind energy-based studies are also leading in renewable energy studies. In this study, made the calculation of the electricity incomes and the installation expenses of a turbine to be established in the area with the support of the softwares before wind turbine installation is carried out on a designated area in Pendik-Sabiha Gokcen Airport region. These studies have been tried to analyze whether the income and expenses to be provided to the municipality of the region will be useful or not at the end of the study.

Keywords: Wind Energy, Wind Power Plant, Renewable Energy, Energy Modelling, Sabiha Gokcen

1 Introduction

Energy has become the most needed issue with the growth of the industry. Especially in recent years, the energy needs of all societies are increasing. And as it is known, the level of development of the countries is directly proportional to the amount of electricity they produce.

In these periods of increasing demand for energy, efforts are being made to convert the energy resources used from fossil fuels to renewable energy sources and, if possible, to 100% renewable energy sources. These studies have started to yield results in recent years.

Many countries are seriously advancing their 100% renewable energy efforts in order to reach their own independent energy sources and energy sources that will not harm the nature. The governments of the world come together and set policies and conduct standardization studies in line with the analysis. One of the leading sources in this 100% renewable energy project is wind power. The use of wind energy has increased recently and its technology is developing rapidly. Wind-generated energy cost (COE) can compete with traditional power plants in many parts of the world.

Wind energy is widely used in other countries, especially in the USA, Germany, Spain, Denmark and India. For instance, while wind energy investments in Europe were 52% in 2017, wind energy received the largest share of new renewable energy financing in 2018 with around 63%.

Currently there is an installed wind power capacity of 370 GW in the world and now a total of 128.8 GW has been installed in the European Union. As a result of this evolution, the design process is becoming more complex in terms of significant energy capacity, which often requires the installation of hundreds of wind turbines (WTs) in a limited space. Therefore, it is not easy to choose a wind turbine installation area. In order to select this area, all climatological information, topographic structure and surrounding houses, high buildings, trees and similar windbreak structures should be determined. [1]

In this study, necessary calculations and estimations for wind turbine installation have been carried out in order to help the increase of wind energy rapidly and to solve the energy demand problems of the regions. These calculations were carried out for Sabiha Gokcen Airport, which belongs to Pendik Municipality. During the study, the necessary climatological information was obtained from the meteorological measurement stations, the coordinates of the region were specified in the calculation program and the necessary geographical calculations were made and the last data of the region were revealed. By integrating these data, the wind turbine cost is also taken into account and it is determined that the region meets the electricity required, and if the region accepts the initial investment cost, it is considered appropriate to install these turbines in the region.

2 Proposed Method

According to geographical coordinates system, the mathematical position of Sabiha Gokcen Region 40,897700 northern latitudes and 29,303300 east longitudes. Sabiha Gokcen is located in the Anatolian Side of Istanbul and Pendik province. The average altitude is about 95 m. After the data of that region was taken from Directorate General of Meteorology; the Windsim software program is used to define the climatology data of that place for simulation and calculation. 2 Wind Turbines are determined for that region to supply electricity to that region. Vestas V-90 model is preferred and the rated power is 2MW for each turbine according to Table 1.

Table 8. The technical specifications of Vestas V90 model Turbine [7]

Technical Specifications	
Operational Data	
Rated Power	2,000 kW/2,200 kW
Cut-in wind speed	4 m/s
Cut-out wind speed	25 m/s
Re cut-in wind speed	23 m/s
Wind class	IEC IIA;IEC S
Operating temp. range standard turbine	-20 °C to 40 °C
Operating temp. range low temperature Turbine	-30 °C to 40 °C
Sound Power	
Maximum	104 dB* *Noise modes available
Rotor	
Rotor diameter	90 m
Swept area	6,362 m ²
Air brake	Full blade feathering with 3 pitch cylinders
Electrical	
Frequency	50/60 Hz
Generator type	4-pole(50 Hz)/6-pole(60 Hz)doubly fed generator, slip rings

And realistic input values have been considered as Table 2. The programs need also the values for each minute in a season.

Table 2. The wind values according to each month [2]

Turkish Republic Ministry of Agriculture and Forestry Directorate General of Meteorology													
Wind Data of Istanbul Sabiha Gokcen Airport Latitude 40.8977 Longitude 29.3033 Height: 99m													
Data	Jan	Feb	Mar	Apr	May	June	July	Aug	Sep	Dec	Oct	Nov	Average Year
Wind Speed m/s	3.2	3.5	3.3	3.2	3.3	3.5	4.1	4.1	3.5	3.3	3.0	3.0	3.4
Max Wind Speed m/s	24.7	22.1	24.7	30.4	31.9	22.6	22.1	20.6	29.8	23.1	23.7	25.7	31.9
Wind Dir.	W	SW	SSW	WSW	S	SW	E	NE	W	NNE	S	WSW	S

3 Designing The Wind Turbine via Windsim Software

After made the climatology calculation different types visual outputs are obtained for area from the program. There are 3 models to show the area as Terrain Model, Roughness Model and Map from Satellite with the Wind Turbine that we used for the project.

3.1 Terrain Model

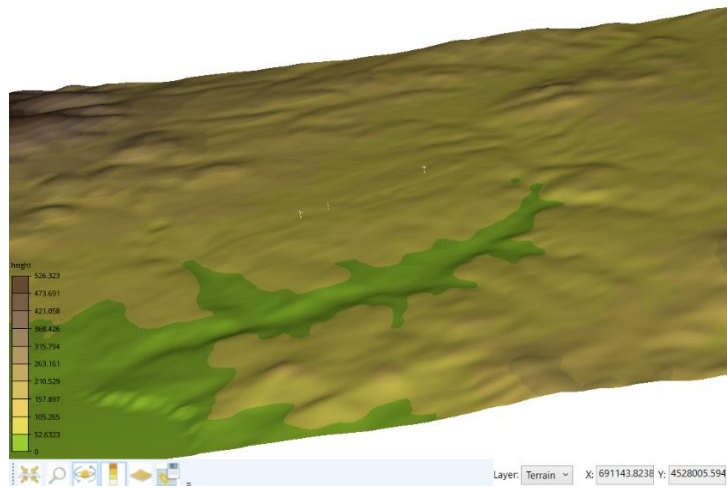


Fig. 1. The terrain model is shown for the selected region

3.2 Roughness Model

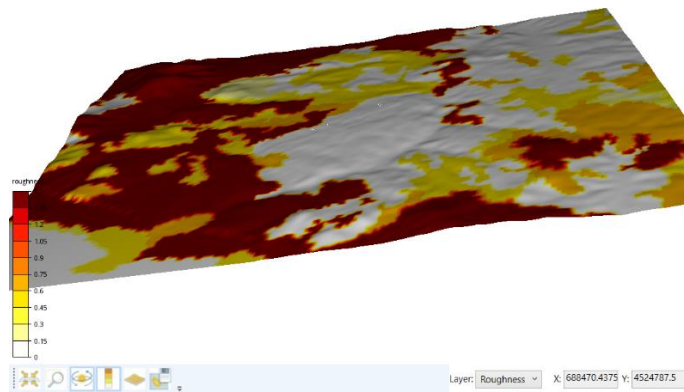


Fig. 2. Wind Turbines are seems on the roughness calculation of area.

3.3 Map from Satellite

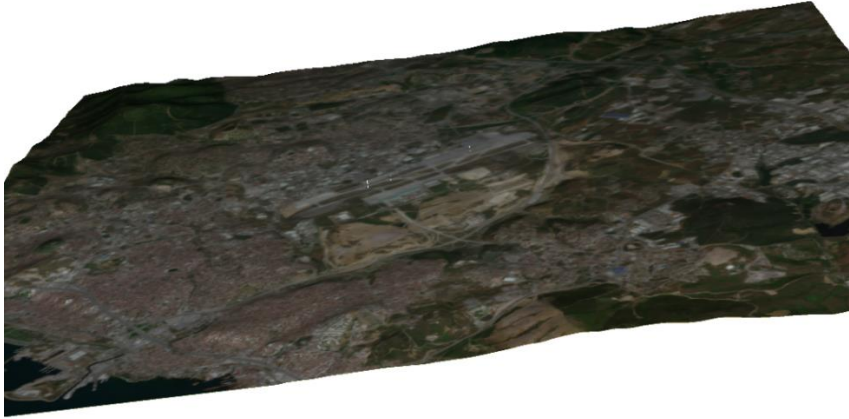


Fig. 3. Wind turbines are seemed more realistic in the real area.

On the all images that is obtained from the program wind turbines can be seem. The selected coordinates of turbines and measuring point are seem easily with that option from program.

After these calculations and obtaining the images about that selected coordinates, the climatology calculation is as proceed to next step shown with more details on the 2nd part of the software program.

3.4 Simulation

3D modeling of the area to be worked on is the first operation to achieve a result related to the calculation of flow areas. As can be seen in Fig. 4, the related study is carried out using the Terrain module. Not many changes and additions are made on the incoming map by default. As the specified area becomes more precise, the calculated and predicted distributions appear more intensely and clearly. The detailed area selected is located in the middle of the default area. Dimensions are integrated by creating a relationship between the area in the middle and the assumed area. And as a result of the transactions, the data used to determine the detailed area is stored. [5]

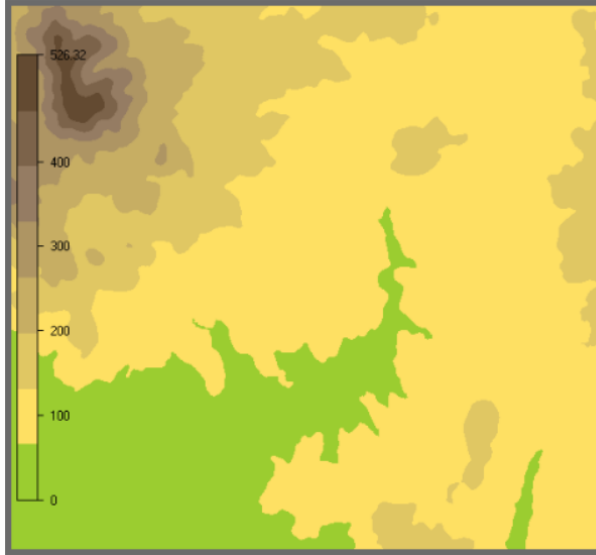


Fig. 4. Digital Terrain Model

When finish the modeling of the terrain about the location on the simulation side the wind fields must be defined. (Fig. 5.) The Reynolds equations, aka Reynolds Mean Navier-Stokes (RANS), determine the wind areas needed in the project.

The model applied for turbulence closure is the k-epsilon model. Since the equations used in the calculation process are not linear, the processes applied for the solution should be repeated with iterations to achieve more precise results. The solution is gradually dissolved by iteration, starting from the initial conditions, which are the predicted estimates, until a combined solution is obtained.

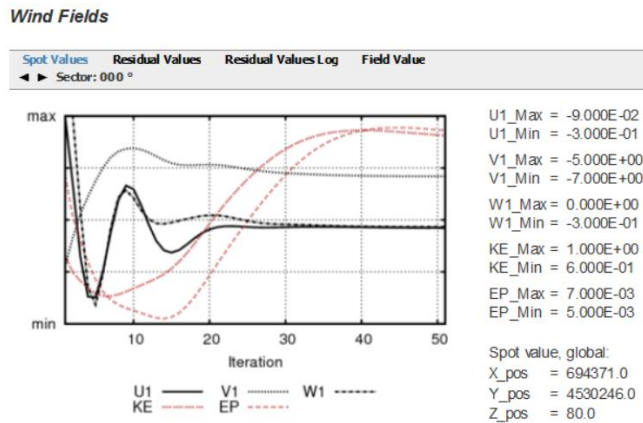
Solved flow variables:

The Pressure (P1)

The Velocity components (U1,V1,W1)

The kinetic energy of turbulent (KE)

The dissipation rate of turbulent (EP)



The convergence of the wind field simulations is evaluated by inspection of the spot and residual values for the velocity components (U1,V1,W1), the turbulent kinetic energy (KE) and its dissipation rate (EP) or the turbulent frequency (OMEG). All variables are scaled according to the min and max values given on the right side. A convergence criteria is set via properties panel so that the simulation stops automatically when the residuals fall below this convergence criteria. A (C) is then displayed in the column (S) of Table 2. In case the solution has not yet converged after the maximum amount of iterations a (-) is displayed. In case of divergence a (D) is displayed.

Fig. 5. The Wind Fields Calculation [4]

3.5 Placing The Wind Turbines

To explain this module of the program, the placing module is used to apply the climatological data obtained first and then transferred to the program. In order to enrich the visuals obtained, the selected objects can also be placed on the land. The fact that realistic objects are located on 3D terrain makes the work more visually understandable. (Fig. 6.)

When calculating the placement of turbines, the program takes into account the Hub curve, Rotor diameter, Rotation speed, Wind direction for the Power curve; Coordinate system, X and Y position for the position; Noise map height, Background noise, Noise at height, Slimming coefficient.

Sound pressure levels resulting from different wind turbines and ultimately background sound pressure levels are calculated according to the decibel formula. [3]

$$Lp(x,y) = 10 \text{ Log}10 (\Sigma 10^{0.1 Lpi} + 10^{0.1 Lpbg}) \quad (5)$$

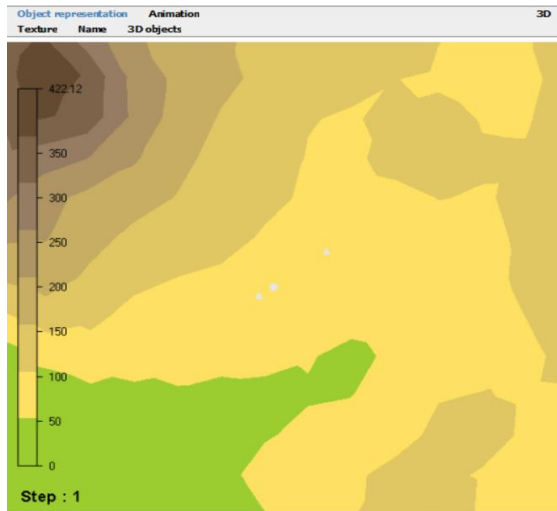


Fig 1. Digital terrain model with objects ▲ Wind turbine ● Climatology station

Wind data from the climatology station(s) is used in calibration of the wind resources, and in the energy calculations. The position of the climatology station is also used as reference point when presenting normalized results, as the speed-ups.

Fig. 6. Result of the objects' calculation

Another module is the wind source module, this module helps to classify the regions to be calculated and used. For the determined areas to be areas with high wind speed, they classify these areas according to the speed and magnitude of the wind. In this way, estimated energy production of the selected area can be also obtained. The example can be seen in Fig 07.

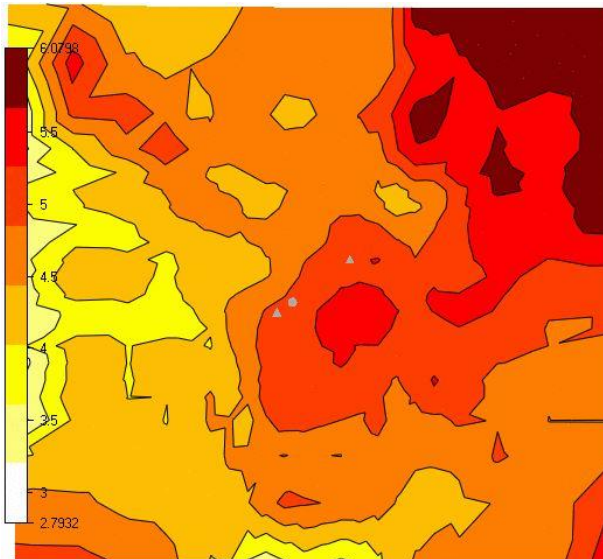


Fig. 7. Wind Resources Example of sector interpolation [6]

And the resulting of wind speed depend on wind turbines locations can be obtained as seems below outputs from software program. And the location might be analyzed about the right place or not. But if the values take consider the choosen place is seems a right place to create a turbine plant. (Fig. 8) [8]

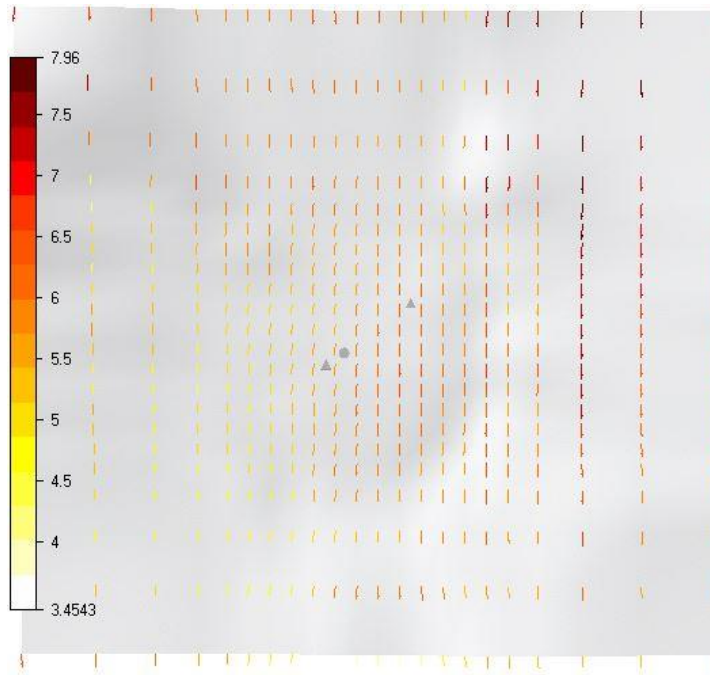


Fig. 8. Wind Speeds Results

As a result, after these simulations and calculations the energy summary table can be observed as seem below example (Table 9) The all parameters that is important to design any plant are noticed at the summary energy production table.

Table 9. Energy Production Table

Name	Power (kW)	Hub height (m)	Density (kg/m ³)	Wind Speed (m/s)	Power density (W/m ²)	Gross AEP (MWh/y)	Wake loss (%)	Full load hours (h)
Wecs1	2000	80	1.225	5.72	208.0	4469	-	2234.5
Wecs2	2000	80	1.225	5.51	182.8	4031.3	-	2015.7
All	4000	-	-	-	-	8500.3	-	2125.1
Mean	-	-	1.225	5.61	195.5	-	-	-
Reference production at climatology position: Sabiha_10m								
ref	2000	80	1.225	5.56	188.4	4135.5	-	2067.8
ref	2000	10	1.225	4.61	99.7	2277.9	-	1138.9

4 Conclusion

The estimation can complete with using that parameters of data and software program. And now the result is shown easily after that report for the case when the people from that region want to use turbines. And also that calculation can recalculate for the more than 2 turbines according to demand.

If we consider the Sabiha-Gokcen Region consumption of any houses is approximately 2100MW with a year. And the selected turbines can produce about 35.000 MW with a year, so they can supply the electricity for a hometown. Also power plant, production will always return to profit in the remaining years.

References

1. Renewables 2019 Global Status Report. Ren21
2. Turkish Republic Ministry of Agriculture and Forestry Directorate General of Meteorology Wind Values
3. Katul, G.G., Mahrt, L., Poggi, D. & Sanz, C. "ONE- AND TWO-EQUATION MODELS FOR CANOPY TURBULENCE." *Boundary-Layer Meteorology*, Kluwer Academic Publishers, No.113, pp81-109, 2004
4. Yap, C. J. "Turbulent Heat and Momentum Transfer in Recirculating and Impinging Flows." PhD Thesis, Faculty of Technology, University of Manchester, United Kingdom, 1987.
5. SRTM Worldwide Elevation Data (3-arc-second resolution)
6. CORINE Land Cover Europe 2006 (100 m resolution)
7. https://www.vestas.com/en/products/2-mw-platform/v90-2_0_mw#!related-products
8. Larsen, C. G. "A Simple Wake Calculation Procedure." Risø-M-2760, 1988.(<http://www.risoe.dk/rispubl/VEA/veapdf/ris-m-2760.pdf>)